The Synthesis, Detection and Repair of Nucleotides Containing the 8-Nitroguanine Modification

Thesis submitted in accordance with the requirements of the University of Liverpool for the degree of Doctor in Philosophy

By

Katie Jane Alexander

September 2014

Abstract

There is accumulating evidence that reactive nitrogen species derived from nitric oxide metabolism are involved in cancer as they are able to damage DNA largely through oxidation or nitration of the guanine base. The 8-nitroguanine lesion is increasingly associated with cancers that result from chronic inflammation; however due to its instability, very little is known about this base modification. Consequently this thesis focuses upon establishing methods to detect and quantify the lesion and investigate enzymes potentially involved in repair systems directed against 8-nitroguanine in DNA.

The approach outlined in this thesis utilises ribonucleoside analogues of the lesion which sufficiently stabilised the labile glycosidic bond. The 8-nitroguanine nucleosides were prepared prior to incorporation into the oligodeoxynucleotide sequences using the traditional 3'- to 5'-solid-phase phosphoramidite chemistry. A number of oligodeoxynucleotides of varying lengths containing a single modification, and dinucleotides containing two modifications were prepared.

A variety of reactions of the 8-nitroguanine base both in nucleosides and oligodeoxynucleotides have been investigated. Studies revealed a different pattern of alkylation for the modified base when compared to results reported in the literature for the natural nucleoside. Thus demonstrating the dramatic effect that nitration has on the intrinsic reactivity of the nucleoside. In view of the susceptibility of nitro group to reaction with thiol nucleophiles, displacement of the nitro group from within nucleosides and oligodeoxynucleotides has been achieved. In particular a fluorescent nucleophile has been developed which stabilises the lesion and could enable direct detection of the levels of 8-nitroguanine in DNA.

Using a variety of substrates prepared in this thesis, detection of the 8-nitroguanine base in oligodeoxynucleotides has been investigated using surface enhanced Raman spectroscopy in collaboration with Professor Steven Bell at Queen's University, Belfast. The unique absorption profile of the 8-nitroguanine derivatives allows for signals exclusively associated with the lesion to be identified using this highly sensitive technique.

The synthesis of 8-nitroguanosine triphosphate was investigated using a number of different approaches. Although the initial aim was not successful, the principles for the phosphorylation of a nucleoside have been shown. The problems encountered were attributed to the conformational constraints of the molecule.

Contents

Acknowledgements

Firstly I would like to express my deepest gratitude to my supervisor Professor Rick Cosstick; your guidance, encouragement and patience throughout both the high and low points of the past four years has been invaluable. I wouldn't have got this far without your unfailing optimism and confidence in me (even when I didn't have any myself). The support you have given me has been above and beyond what is expected; I really couldn't have hoped for a better supervisor.

Additional thanks are given to the following: Susan Dick and Professor Steven Bell in Belfast for the work performed on the SERS analysis of nucleosides and oligonucleotides, Ben Libberton and Professor Andy Bates in biological sciences for the studies of DNA replication on templates containing the 8-nitroguanine base, Professor Aidan Doherty in Sussex for the preliminary studies on the enzymatic repair of the lesion, my secondary supervisor Dr. Ian O'Neil and the technical staff at the University of Liverpool.

I would like to thank Dr. Inder Bhamra for his help and patience and remaining a constant source of wisdom to me even after leaving the University. I'll never know how you manage to have a solution for everything that goes wrong! I would also like to thank former group member Dr. James Gaynor for his help and advice particularly in my final two years.

To the past and present members of the Cosstick and Carnell groups, thank you for making my time in Lab 1.84 entertaining. I am particularly thankful to Lee, (my colleague) Vicky and Katy for keeping me (mostly) sane with frequent tea breaks and being so understanding about all my eccentricities.

I would like to thank my dad for his unwavering support, love and encouragement. Dad your belief in me has encouraged me to pursue my dreams; you are my parent, my friend and my inspiration. To my little big sister Louise, you are there for me no matter what and I appreciate your help and advice more than you know.

Finally James, I don't know where I would be without you. You've encouraged me and supported me throughout my PhD and made the hard times seem not so bad after all. You've looked interested when I talked to you about my work, even though you say you only understand every other word. For everything you have done for me I am eternally grateful.

Abbreviations

A	Adenine
Ac_2O	Acetic anhydride
AcOH	Acetic acid
AIBN	Azobisisobutyronitrile
amu	Atomic mass unit
AMV-RT	Avian myeloblastosis virus reverse transcriptase
ap	Apparent
ATP	Adenosine triphosphate
BER	Base excision repair
BH_4	Tetrahydrobiopterin
BHT	Butylated hydroxytoluene
br	Broad
$Br\text{-}H_2O$	Bromine water
C	Cytosine
CaM	Calmodulin
cGMP	Cyclic guanosine monophosphate
CHC	Chronic hepatitis C
COSY	Correlation spectroscopy
CPG	Controlled pore glass
d	Doublet
DAMPs	Damage associated molecular patterns
DCM	Dichloromethane
dd	Double doublet
ddd	Double double doublet
DEPT	Distortionless enhancement by polarisation transfer
DFT	Density functional theory
Dimer 8	G*G* (G* = 2'-*O*-methylguanosine)
Dimer 9	G**G** (G** = 8-nitro-2'-*O*-methylguanosine)
DIPEA	*N,N*-Diisopropylethylamine
DMAP	4-Dimethylaminopyridine
DMF	Dimethylformamide
DMSO	Dimethyl sulfoxide

DMT	4,4'-Dimethoxytriphenylmethyl
DMTCl	4,4'-Dimethoxytriphenylmethyl chloride
DMTr	4,4'-Dimethoxytriphenylmethyl
DNA	Deoxyribonucleic acid
dq	Double quartet
dt	Double triplet
EDRF	Endothelium-derived relaxing factor
eNOS	Endothelial nitric oxide synthase
ESMS	Electrospray mass spectrometry
Et_2O	Diethyl ether
Et_3N	Triethylamine
EtOAc	Ethyl acetate
EtOH	Ethanol
ETT	5-Ethylthio-1*H*-tetrazole
FAD	Flavin adenine dinucleotide
FMN	Flavin mononucleotide
G	Guanine
GTP	Guanosine triphosphate
H. pylori	*Helicobacter pylori*
HBTU	*N,N,N',N'*-Tetramethyl-*O*-(1*H*-benzotriazol-1-yl)uronium hexafluorophosphate
HCC	Hepatocellular carcinoma
HCV	Hepatitis C virus
HMBC	Heteronuclear multiple bond correlation
HOBt	1-Hydroxybenzotriazole hydrate
HOMO	Highest occupied molecular orbital
HPLC	High performance liquid chromatography
HRMS	High-resolution mass spectometry
HSQC	Heteronuclear single quantum coherence
IARC	The International Agency for Research on Cancer
IE	Ion exchange
iNOS	Inducible nitric oxide synthase
^{i}PrOH	Propan-2-ol

IUPAC-IUB	International Union of Pure and Applied Chemistry - International Union of Biochemistry
J	Coupling constant
L-Arg	L-Arginine
LCAA	Long chain alkyl amine
L-Cit	L-Citrulline
LUMO	Lowest unoccupied molecular orbital
m	Multiplet
m/z	Mass to charge ratio
MeCN	Acetonitrile
MeOD	Methanol-d_4
MeOH	Methanol
NADPH	Nicotinamide adenine dinucleotide phosphate
NBS	*N*-Bromosuccinimide
NC-IUB	Nomenclature Committee of the International Union of Biochemistry
NF-κB	Nuclear factor kappa B
NMR	Nuclear magnetic resonance
nNOS	Neuronal nitric oxide synthase
NOS	Nitric oxide synthase
o	*ortho*
OGG1	8-Oxoguanine glycosylase
OMe	Methoxy
*o*QMP	*ortho*-Quinone methide precursor
p	*para*
PAMPs	Pathogen associated molecular patterns
PG	Protecting group
$PO(OMe)_3$	Trimethyl phosphate
ppm	Parts per million
Pro-Cys	Boc-Cys-OEt
PRRs	Pattern recognition receptors
*p*TsOH	*para*-Toluenesulfonic acid
PyBOP	Benzotriazol-1-yl-oxytripyrrolidinophosphonium hexafluorophosphate
q	Quartet

RF	Retention Factor
RNA	Ribonucleic acid
RP-HPLC	Reverse phase high performance liquid chromatography
s	Singlet
SERRS	Surface-enhanced resonance Raman scattering
SERS	Surface-enhanced Raman scattering
Site 1	GCGTACG**CATGCG (G** = 8-nitro-2'-*O*-methylguanosine)
Site 1 control	GCGTACG*CATGCG (G* = 2'-*O*-methylguanosine)
Site 1, adduct 1	GCGTACG$^{(glut)}$CATGCG (glut = glutathione)
Site 1, adduct 2	GCGTACG$^{(fluor)}$CATGCG (fluor = fluorescent thiol)
Site 1, adduct 3	GCGTACG$^{(Pro\text{-}Cys)}$CATGCG
Site 2	5'-d(GCGCAACGCAATTAATGTG**AGTTAGCTCACTCATTAG)-3' (G** = 8-nitro-2'-O-methylguanosine)
Site 2 control	5'-d(GCGCAACGCAATTAATGTG*AGTTAGCTCACTCATTAG)-3' (G* = 2'-*O*-methylguanosine)
Site 2, adduct 3	5'-d(GCGCAACGCAATTAATGTG$^{(Pro\text{-}Cys)}$AGTTAGCTCACTCATTAG)-3'
Site 3	5'-d(GTGACTGGG**AAAACCCTGGCGTTACCC)-3' (G** = 8-nitro-2'-*O*-methylguanosine)
Site 3 control	5'-d(GTGACTGGG*AAAACCCTGGCGTTACCC)-3' (G*= 2'-*O*-methylguanosine)
Site 3, adduct 3	5'-d(GTGACTGGG$^{(Pro\text{-}Cys)}$AAAACCCTGGCGTTACCC)-3'
S_N1	Unimolecular nucleophilic substitution
S_N2	Biomolecular nucleophilic substitution
SOD	Superoxide dimutase
T	Thymine
t	tert
t	Triplet
TBAF	Tetrabutylammonium fluoride
TBDMS	*tert*-Butyldimethylsilyl
TBDMSCl	*tert*-Butyldimethylsilyl chloride
^{t}Bu	*tert*-Butyl
TCA	Trichloroacetic acid
TEAA	Triethylammonium acetate

TEAB	Triethylammonium bicarbonate
THF	Tetrahydrofuran
TLC	Thin-layer chromatography
T_m	thermal melting temperature
TMP	Trimethylphosphate
TMS	Tetramethylsilane
TRIS	Tris(hydroxymethyl) aminomethane
Trityl	Triphenylmethane
U	Uracil
UV	Ultraviolet

This thesis is dedicated to the memory of my mum

Kay Glynis Alexander

Chapter 1

Introduction

1 Introduction

1.1 A brief history of DNA

The history of DNA began in 1869 when Friedrich Miescher became the first person to isolate a substance later to be recognised as the hereditary material[1]. Due to the localisation of the substance in the nucleus Miescher termed the compound 'nuclein', this later became known as a nucleic acid which was found to more accurately describe the nature of the compound[2]. Interest in DNA was renewed in the 1940s when Avery, MacLeod and McCarthy demonstrated that DNA is the carrier of genetic information[3]. In the following years, a number of research efforts revealed important details about the structure of DNA which provided the foundation from which Watson and Crick derived the three dimensional structure. Noteworthy contributions include; Chargaff's revelation that the proportion of adenine in a nucleic acid was equal to the proportion of thymine and likewise, the proportions of guanine and cytosine were equivalent[4] and the crucially important X-ray crystallography work by Rosalind Franklin and Maurice Wilkins that determined DNA has a regularly repeating helical structure[5,6]. The molecular structure of DNA was deciphered in 1953 by James Watson and Francis Crick[7,8], who along with Wilkins received the Nobel prize for chemistry in 1962 for their ground breaking discovery. The discovery that hereditary information was contained in DNA and with the molecular structure now known, interest in how it could be faithfully replicated was a key question. A decade later in the 1960s, Holley, Khorana and Nirenberg cracked the genetic code[9].

The knowledge provided by these pioneers in nucleic acid research, has led to continued advances in the understanding of the human genome; the complete sequence of which was published in 2001[10]. Examining the structure of DNA and how it functions has unlocked an interesting and important area of research and led the study and development of therapeutics and diagnostics for many diseases.

1.2 Composition of nucleotides

Knowledge of the structural features of nucleic acids is vital in understanding their biological function. In order to explore the structures derived from DNA damage and their significance, it is first appropriate to discuss the nomenclature, principles and key features which define nucleic acids.

The features defining the primary structure of DNA are ultimately responsible for its secondary, tertiary and quaternary structure. DNA is a linear polymer which encodes information through a series of monomers called nucleotides. A nucleotide is a repeating unit which is comprised of three distinct components: the sugar, the heterocyclic base and the phosphate group.

The heterocyclic base is attached to the pentose sugar at the anomeric position *via* a β glycosidic bond; this condensation product is characterised as a nucleoside. Nucleosides polymerise by the formation of a phosphate ester upon phosphorylation of one of the hydroxyl groups of the pentose sugar. The bases are not involved in the polymerisations; hence the chain is held together by a sugar – phosphate backbone from which the bases extend[11]. The sugar – phosphate backbone acts as a constraint on the conformational space that is accessible to the base pairs[2].

1.3 The sugar

In both RNA and DNA a pentose sugar which has been locked into a five membered furanose ring conformation is present. One of the two inherent structural variations between DNA and RNA is the substitution of a hydrogen atom with a hydroxyl group at the second carbon in the ring. In DNA the pentose sugar is 2-deoxy-D-ribose, whereas in RNA it is D-ribose. The numbering system for the sugar atoms is noted in Figure 1.1, with these being distinguished from those of the base atoms by a prime.

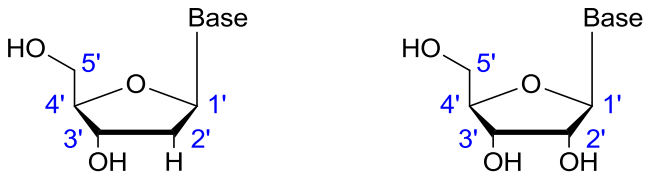

Figure 1.1: The pentose sugar numbering scheme for DNA (left) and RNA (right).

The distinctly different behaviour of the 2'-deoxyribose and ribose systems reveals information of critical importance to the global structure of nucleic acids and their biological function. Due to energetically unfavourable eclipsing interactions of adjacent bonds, the atoms in the five membered furanose ring cannot adopt a planar structure[12]. Puckering of the system reduces the steric conflict experienced due to eclipsed groups. The puckering of the ribose ring gives rise to two main structural conformations, the envelope (E) and the twist (T). In the envelope conformation one atom is displaced from the plane formed by the other four atoms. In the twist conformation two adjacent atoms are displaced from the plane formed by the other three atoms; one is above, one is below the plane[13].

The pucker is described in terms of which atom in the ribose ring is displaced furthest out of plane. Conformations in which the atom displaced furthest from the plane resides on the same side as both the C5' and the heterocyclic base are termed *endo*. When in the opposite orientation the conformation is termed *exo*[14].

In general, there are two principle low energy conformations which best alleviate steric conflict observed for all 2'-deoxyribose and ribose sugars: C3'-*endo* and C2'-*endo* (Figure 1.2). The terms 'North' (N) and 'South' (S) are often used to describe the C3'-*endo* and C2'-*endo* conformations respectively. While this terminology refers to their geographic positions on the pseudorotational cycle[15], the notation is also representative of the shape of the chain of 4 carbon atoms in the ring.

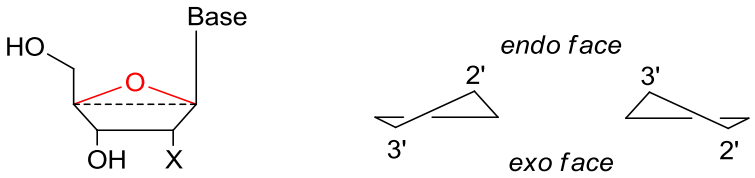

Figure 1.2: C1'-O4'-C4' shown in red (left) are in plane perpendicular to the paper. Simplified versions of the two principle sugar puckers C3'-*endo* (centre) and C2'-*endo* (right) are also shown. Note X = H or OH.

The substitution of the hydrogen at the C2' position in deoxyribose with a hydroxyl group in ribose accounts for the difference in preferred puckering modes of DNA and RNA. Interconversion between the various conformations of the sugar, known as pseudorotation, is possible due to the energy barrier separating the two preferred conformers being less than 20 kJ mol^{-1} [16]. However the presence of substituents on both the *endo* and the *exo* face introduce a potential energy barrier that can oppose free pseudorotation.

The position of the equilibrium between the two preferred conformational states is determined by stabilising stereoelectronic effects, the strongest of which arise from gauche interactions (60º dihedral angles). The gauche interaction is the tendency of X-C-C-Y containing systems, where X and Y are electronegative groups, to adopt a gauche conformation. In sugars, the stabilisation is as a result of the donation of electron density from a C-H bonding orbital to an adjacent C-O antibonding orbital; this can only be achieved when the bonds are in an antiperiplanar orientation[17]. There are several gauche interactions in the 2'-deoxyribose and ribose systems. 2'-Deoxyribose has two gauche interactions, the most important of which is O4'-C4'-C3'-O3', while ribose has three additional gauche interactions most importantly O4'-C1'-C2'-O2' (Figure 1.3).

Figure 1.3: A Newman projection of C2'-*endo* and C3'-*endo* gauche interactions.

The second and relatively weaker stabilising stereoelectronic effect which plays a role in determining the preferred conformational state of the sugar is an anomeric interaction[18]. The anomeric effect is applicable to chemical systems C-X-C-Y, where X has at least one set of lone pair electrons and Y is an electronegative atom. It describes the tendency of the lone pair on O4' to orient antiperiplanar to the antibonding orbital of the C-Y bond. This geometry allows orbital interactions in which the lone pair on O4' can donate into the antibonding orbital which is energetically favourable (Figure 1.4)[17].

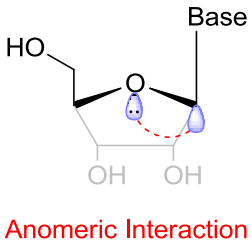

Figure 1.4: Showing the anomeric interaction highlighted in red.

The structurally asymmetric 2'-deoxyribose ring exhibits a preference for the C2'-*endo* conformation over the C3'-*endo* conformation. This preference is due to the gauche effect of the O4'-C4'-C3'-O3' fragment, which is stronger than the anomeric effect. Therefore the dominating gauche interaction drives the pseudorotational equilibrium towards S type conformations[19].

In ribose however, the presence of a hydroxyl group in the 2'-position changes the situation. The additional gauche interaction from the O4'-C1'-C2'-O2' counteracts the stabilisation provided by the O4'-C4'-C3'-O3' fragment. Therefore based on gauche interactions alone there would be no preference for either the C2'-*endo* or C3'-*endo* conformation. The conformational behaviour can therefore be attributed to the anomeric effect in this complex system. The extra stabilisation provided by the anomeric effect, in which a pseudo-axial heterocyclic base

conformation is preferred, means that the O4'-C4'-C3'-O3' gauche interaction predominates and the C3'-*endo* conformation is preferred[20].

1.4 The heterocyclic base

The heterocyclic base forms the distinguishing component of nucleosides. There are five bases which occur naturally, three of which are common to both DNA and RNA: adenine (A), cytosine (C) and guanine (G). Thymine (T) and uracil (U), differing only by the absence of a methyl substituent, are found in DNA and RNA respectively. These bases can be categorised into two groups based on their structure: purines and pyrimidines. The purines, consisting of A and G are bicyclic molecules, whereas the pyrimidines consisting of C, T and U are smaller monocyclic structures. The chemical structure and numbering system for the bases according to the IUPAC-IUB[21] are shown in Figure 1.5. Groups appended to the ring are given the same number as the position to which they are linked.

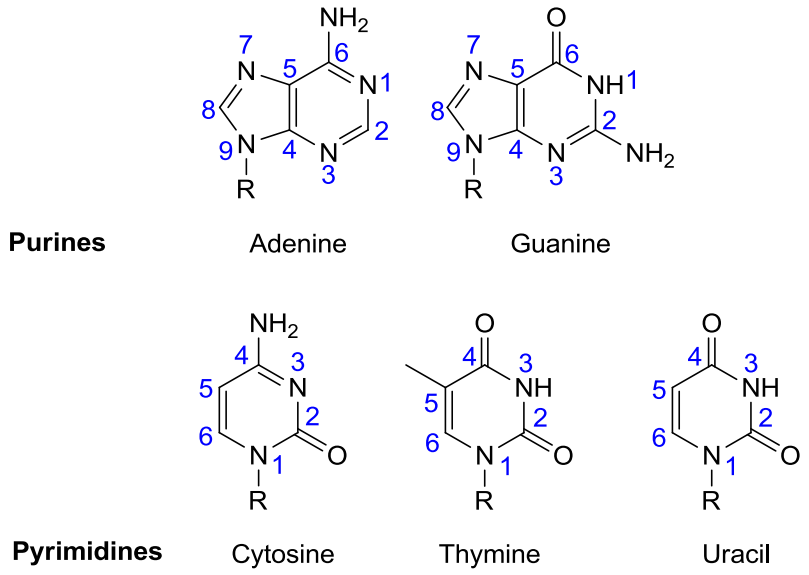

Figure 1.5: The heterocyclic base numbering scheme for purines and pyrimidines.

In relation to the sugar moiety, the base effectively lies in a perpendicular plane and approximately bisects the O4'-C1'-C2' angle[2]. The base can adopt one of two main orientations about the glycosidic bond (Figure 1.6). The most stable and consequently most prevalent of these is the *anti* conformation. This describes the situation where the main bulk of the base is orientated away from the sugar ring; this reduces the steric hindrance and interactions which may occur between the CO and NH groups in positions 1, 2 and 6 of the purine ring (or 2 and 3 of the pyrimidine ring) and the sugar. In the alternative *syn* conformation, the position of the glycosidic bond is such that the base in oriented above the

sugar ring which can result in unfavourable steric interactions. While the *syn* conformation is less commonly observed as it tends to be somewhat higher in energy, it affords a more compact nucleoside which may be of biological importance[22].

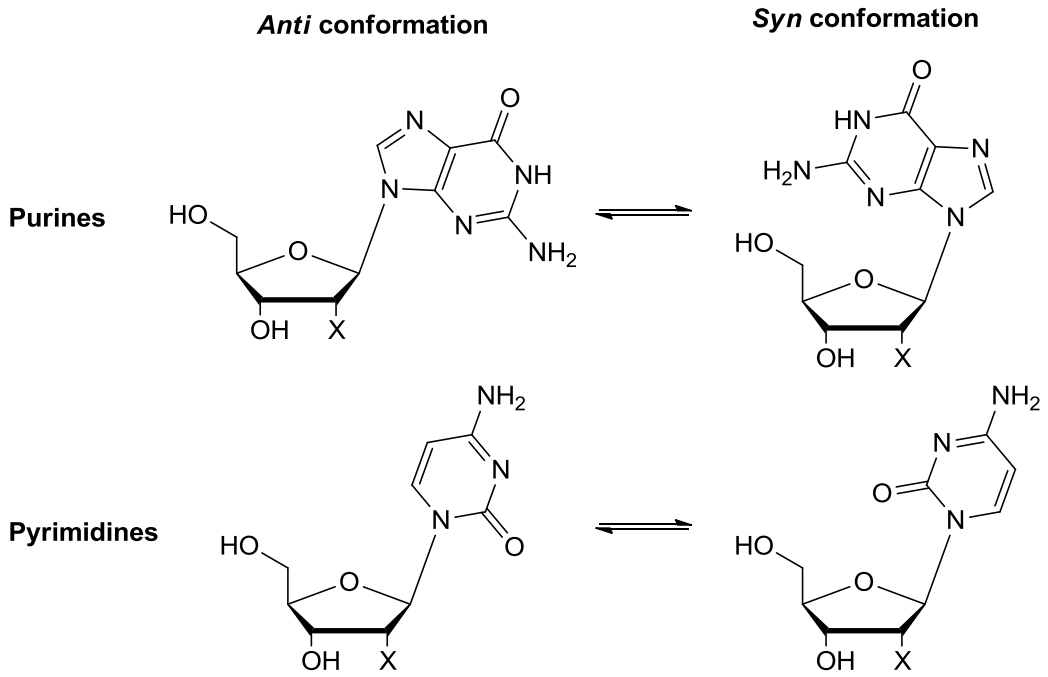

Figure 1.6: *Anti* (left) and *syn* (right) nucleoside conformations. Note X = H or OH.

The higher energy *syn* conformation can be stabilised by internal hydrogen bonding between the sugar and the base; this is often accompanied by changes in the sugar pucker. The barrier between the *anti* and *syn* conformations in deoxyribonucleosides is found to be less than 42 kJ mol^{-1} and tends to be lower with purines than with pyrimidines[23].

It has been shown that in certain cases guanine preferentially adopts the *syn* conformation. This is probably as a result of the formation of a hydrogen bond between the N2 amino group and the 5'-phosphate; however other stabilising interactions have been suggested[23]. This characteristic of guanine can result in formation of unusual structures in G rich sequences, such as in G-quadruplexes.

Substitutions at the C8 position of a purine base can also result in destabilisation of the *anti* conformation causing the base to preferentially adopt the *syn* conformation[24]. For example, replacing the C8 hydrogen in guanine with a bromine atom, forming 8-bromoguanosine, prevents the close packing relationship with the C2' hydrogen[25]. Additionally the steric influence of the bromine atom limits free rotation around the glycosidic bond therefore the *syn* conformation is maintained; as confirmed by X-ray crystallography[26].

This finding is significant as the conformational preference of nucleosides and thus base pairing can be affected by introducing steric hindrance and hydrogen-bonding interactions to a nucleotide. There are various other situations in which the *syn* conformation is favoured that will be discussed in more detail later in the chapter.

1.5 Base pairing

The structure of DNA determined by Watson and Crick describes the pairing of bases, which is a crucial feature in storing, directly copying and transforming genetic information. Therefore the most common base pairing model encountered in nature is known as Watson-Crick base pairing; which was founded on the idea that adenine pairs to thymine and guanine to cytosine. This not only takes into account Chargaff's rule, but also the structural parameters of the double-helix determined by X-ray crystallography.

Naturally occurring bases present predominantly in their keto and amino tautomeric forms; this is an important requirement in the correct recognition of their respective base pairing partner. The hydrogen bonding involved in forming base pairs can be considered as an electrostatic interaction between an acidic proton and a good electron donor and play a key role in stabilising the secondary structure of DNA. The sp^2 hybridized lone electron pairs on both the oxygen and nitrogen atoms of the base act as hydrogen bond acceptors, while the NH groups are good hydrogen bond donors. The average strength of these hydrogen bonds is between 6 – 10 kJ mol^{-1} [2].

Each base pair consists of one purine and one pyrimidine. Adenine is always coupled with thymine in DNA and uracil in RNA *via* the formation of two hydrogen bonds. Guanine is always coupled with cytosine in both DNA and RNA forming three hydrogen bonds, making this base pair more thermodynamically stable[2,7,27]. Accordingly, these are known as complementary base pairs. The two pairing arrangements have similar overall shapes and fit specific geometric requirements, so that any sequence could be accommodated within the same double-helix framework. This accounts for the fact that although the Watson-Crick A:T(U) base pair is not favoured energetically like the G:C base pair, it is still the preferred conformation due to the steric constraints of the sugar phosphate backbone[14].

Karst Hoogsteen reported an alternative hydrogen bonding arrangement, based on a crystal structure, in which A and T formed a base pair that had a different geometry to that previously reported. Similarly, an alternative base pairing geometry can form between G and C using this

arrangement. Hoogsteen base pairs require rotation of the base about the glycosidic bond in order to utilise the *syn* face of the purine for hydrogen bonding with the *anti* face of the pyrimidine[28]. The Hoogsteen G:C base pair differs from that of Watson-Crick as, not only is the N7 imidazole nitrogen used in hydrogen bond formation, but the cytosine base requires protonation and only 2 hydrogen bonds are formed. Consequently the chemical properties of the heterocyclic bases in this model are significantly different to that of the Watson-Crick base pairing.

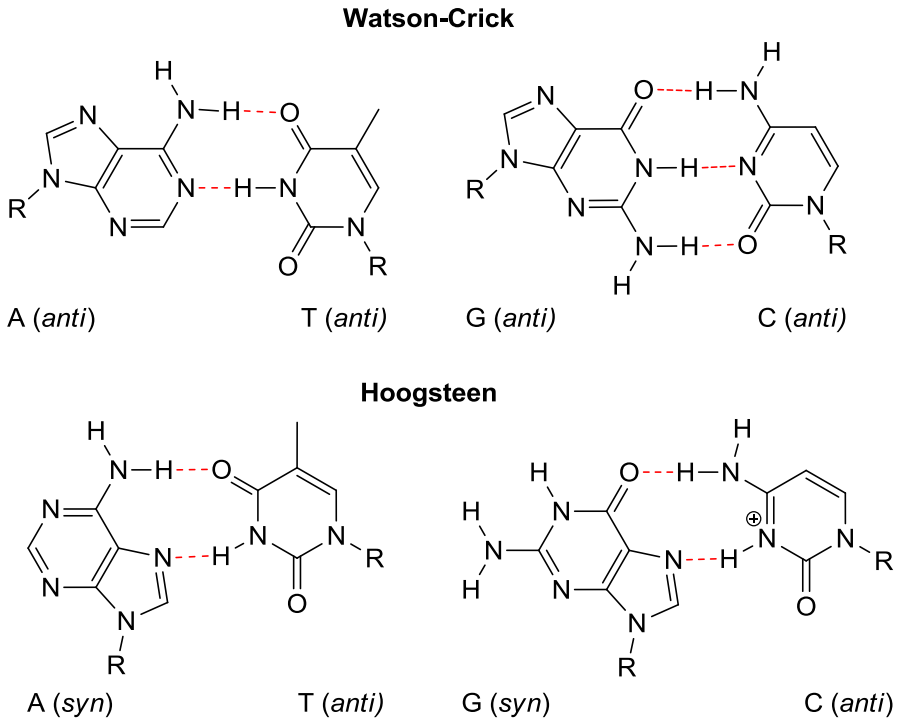

Figure 1.7: Watson-Crick (top) and Hoogsteen base paring (bottom).

Hoogsteen base pairing expands the structural and functional versatility of DNA and RNA and these hydrogen bonding arrangements are often found in multi stranded structures[29].

1.6 The double-helix

The original structure of DNA, proposed by Watson and Crick in 1953 consists of two right-handed polynucleotide strands that are coiled about the same axis[7,8]. Using X-ray crystallography data, it was determined that the helical structure repeats every 10 residues and the space occupied by each nucleotide in the sequence is 3.4Å. The hydrophilic sugar phosphate backbone is positioned on the outside of the helix and the heterocyclic bases project inward toward the hydrophobic centre so that they can interact with one another. The negatively charged phosphate groups of the backbone are mutually repulsive and contribute to

the rigidity of the molecule[30]. The two strands are arranged in an anti-parallel orientation; this relates to the 5'-end of one strand aligning with the 3'-end of the other strand.

While the formation of DNA duplexes is strongly favoured by the formation of numerous bonding interactions, entropically the process is unfavourable due to restrictions being applied to the otherwise flexible backbone[31]. The entropic consideration is an aspect of molecular biology which is unavoidable. This unfavourable interaction is overcome as DNA polymerases pre-organise the molecule into the conformation necessary for DNA synthesis[32].

The structure of the DNA duplex is governed by a balance of non-covalent interactions in polar solvents. The hydrogen bonding between complementary bases discussed previously is one of the three important interactions which stabilise the double-helical structure. The major contributor to duplex stability is base stacking interactions between adjacent base pairs[33,34]. The main principles which contribute to the π-π interactions between planar DNA bases are; van der Waals dispersive forces (permanent dipole/induced dipole and induced dipole/induced dipole interactions), the permanent electrostatic effects of interacting dipoles and the entropically favoured exclusion of water from the hydrophobic interior of the duplex. The strength of the base stacking interaction is dependent on the base sequence. Purines stack more strongly than pyrimidines presumably due to the larger surface area and greater polarisabilty[31]. Additionally, the stabilisation conferred by solvent interactions between water molecules and the hydrophobic sugar phosphate backbone plays a role in the overall duplex stability.

Double-helical nucleic acids exhibit two characteristic grooves known as the major and the minor grooves. As the names suggest the grooves are asymmetrical. These grooves are a result of spaces that are present between the sugar phosphate backbones of each polynucleotide strand[2]. Potential hydrogen-bond donor and acceptor atoms line both the major and minor grooves; therefore these regions have the potential to interact selectively with proteins[31].

1.7 Structural polymorphism

DNA occurs in three major structural forms: A-DNA, B-DNA and Z-DNA. This structural polymorphism is dependent on its environment and occasionally its primary structure. Table 1.1 lists some of the key defining structural parameters of the three forms of DNA helices[35].

Parameter	A-DNA	B-DNA	Z-DNA
Helical Sense	Right handed	Right handed	Left handed
Residues per turn	11	10	12
Axial rise (Å)	2.9	3.4	3.7
Helical pitch (Å)	24.6	33.2	45.6
Base tilt (º)	20	-6	7
Twist angle (º)	32.7	36	-30
Helix diameter (Å)	23	20	18
Sugar pucker	C3'-*endo*	C2'-*endo*	C3'-*endo(syn)*

Table 1.1: Structural parameters of DNA Helicies[2,35].

B-DNA is the most common form and adopts the structure as first described by Watson and Crick. B-DNA is a right handed helix and it is the predominating form under physiological conditions. It has an elongated structure with a helical diameter of 20Å. The helix features a wide major groove with a diameter of 11.7Å (depth of 8.5Å) and a narrow minor groove measuring 5.7Å in width (depth of 7.5Å). A-DNA, also a right handed helix, is a broader more compact form with a helical diameter of 23Å. The major groove of A-DNA is comparatively slim with a width of 2.7Å but is far deeper than the in B-DNA with a depth of 13.5Å; naturally the minor groove is wide (11Å) and shallow (2.8Å) to accommodate for this[2,36,37].

Water is crucial to the conformation and hence biological functions of double-helical DNA. Research has shown that the number of water molecules per nucleotide must be greater than 20 for B-DNA to be stable[38]. This explains why this structure is favoured under standard hydrated physiological conditions. Upon dehydration A-DNA is formed. The A-DNA structure is found in RNA irrespective of the environment and in DNA/RNA hybrids[39].

Many of the structural differences between B-DNA and A-DNA arise from the different conformation adopted by the deoxyribose sugar. Within B-DNA duplexes a C2'-*endo* pucker is adopted, whereas in A-DNA, the sugar conformation is generally restricted to the C3'-*endo* orientation. Consequently this conformation is favoured by RNA duplexes as additional stabilisation is gained by an intra-strand hydrogen bond between the O4' of one nucleotide and the 2'-hydroxyl group on the next nucleotide in the sequence. This accounts for A-DNA forming a wider and flatter helix[2].

The placement of each base pair with respect to the helical axis presents another major structural variation between A-DNA and B-DNA. In B-DNA, the base-pairs are essentially perpendicular the helical axis, but in A-DNA, they are displaced away from the central axis and closer to the major groove[30,37]. The base pairs are positioned 4.5Å away from the central axis which leaves a hollow cylindrical core 3Å in diameter. In addition, a positive tilt of 20º allows a van der Waals separation of 3.4Å to be maintained[2].

In 1979 a third, infrequently observed form of DNA was discovered when Rich *et al.* solved the structure of the hexamer dCGCGCG[40]. While the structure was in the antiparallel arrangement and held together by Watson and Crick base pairs, the fragment formed a left handed (Z-DNA) helix[41]. Z-DNA is thinner with an 18Å helical diameter and is more elongated in comparison to B-DNA. There is only one narrow, deep groove present in the structure which is equivalent to the minor groove in B-DNA; the major groove is not discernible[37,42]. The repeating unit in Z DNA is a dinucleotide which is in further contrast to A- and B-DNA in which the repeating unit is a mononucleotide[43].

It is known that the formation of Z-DNA is highly composition and base sequence dependent, generally being confined to alternating purine and pyrimidine sequences[43]. The purine bases are rotated about their glycosidic bond so that the base assumes the *syn* conformation while the pyrimidine bases remain in the *anti* conformation[30]. The alternating sugar pucker conformation in Z-DNA is unusual as purine nucleosides adopt the C3'-*endo* conformation found in A-DNA. This results in a duplex containing C3'-*endo*/*syn* purines followed by a C2'-*endo*/*anti* pyrimidines[12].

Furthermore, these characteristics cause the phosphate backbone of the molecule to adopt a zig-zag arrangement, affording it the name Z-DNA. This arrangement of the duplex backbone causes some of the phosphate groups to be positioned closer together than in B-DNA; therefore there is greater electrostatic repulsion between them. Consequently, Z-DNA is highly stabilized by high salt concentrations[35].

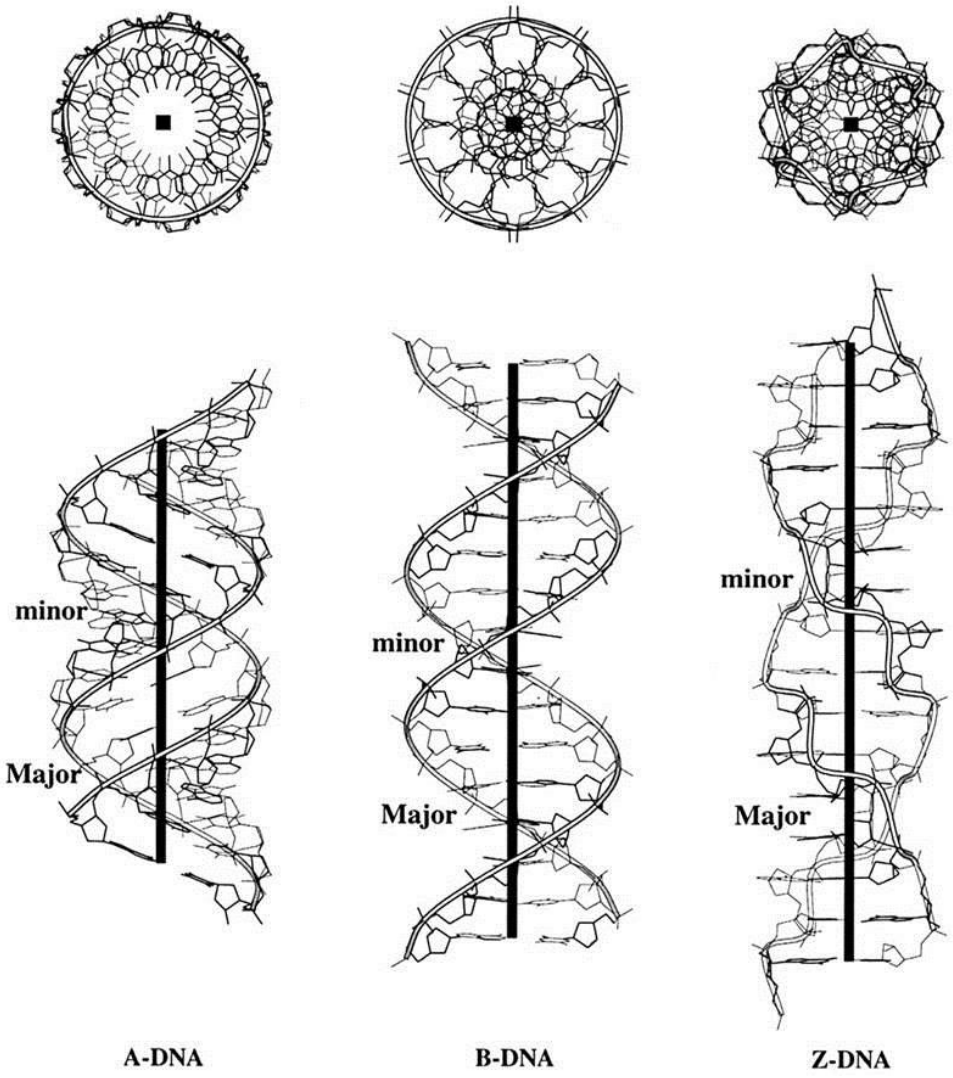

Figure 1.8: A-, B- and Z-DNA forms showing a view down the helical axis (top) and a side view of the helix (bottom). Helical diagrams adapted from reference 44[44].

1.8 Higher order structures

The formation of DNA secondary structures requires specific sequence arrangements[45]. In the case of G-quadruplexes which are of interest to the scope of this thesis, the presence of a suitable cation also plays an important role in the stabilisation of the structure.

In this unusual structure, four guanine bases form a co-planar array due to the formation of Hoogsteen type bonds[46]. In this arrangement each base acts as both a hydrogen bond donor and acceptor forming a total of 8 hydrogen bonds; represented in Figure 1.9 by dashed lines. This structure is known as a G-tetrad, the building block for the formation of G-quadruplexes. These tetrad units are stacked upon each other to form a stable G-quadruplex structure[47]; in general the stability increases with the number of units[48]. Formation and stability of G-

quadruplexes is dependent on the presence of a monovalent chelating cation (typically Na^+ or K^+). The carbonyl oxygen atoms create a strong negative electrostatic potential in the centre of the tetrad. Cations positioned in this channel reduces the electronic repulsion between these atoms and overall stabilises the structure[45,49].

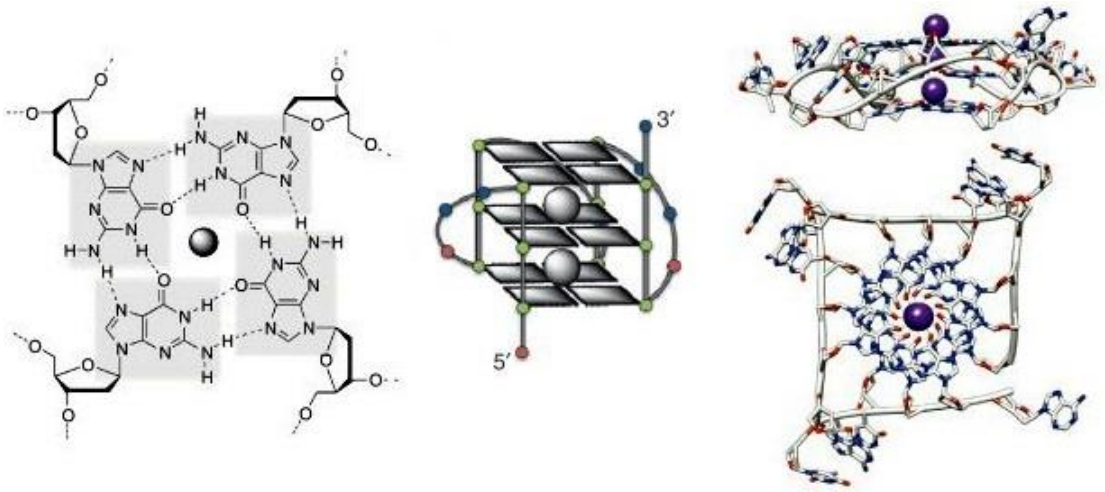

Figure 1.9: Structure of guanine tetrads (left), schematic representation of an intramolecular quadruplex motif (middle) and side and top view showing the position of the K^+ ions in a human telomeric quadruplex (right) adapted from reference 46[46].

G-quadruplexes can form when four guanine rich sequences, containing two or more guanine residues each are in close proximity to one another[45]. This can either be due to intramolecular interactions within the same strand or intermolecular association between two or four different strands[30,49]. The quadruplexes are held together by three connecting loops arising from the mixed-sequence nucleotides between the guanine residues; these are not usually involved in the tetrads themselves[48,49].

It has been identified by computational methods, that based on G-rich patterns in the human genome, there are theoretically 376,000 sequences with the potential to form G-quadruplex structures[48]. Recent investigations have quantitatively shown the presence of G-quadruplexes and their stability in human genomic DNA using a highly specific DNA G-quadruplex antibody[50]. The large number of potential sites, the unique arrangement and the presence in important regions of the genome, means that G-quadruplexes are an attractive target for therapeutic treatments.

Telomeres are non-coding sequences that appear at the ends of chromosomes and their role is to provide genomic stability and protection against gene erosion during cell division[51].

Telomeric DNA contains thousands of tandem repeats of the sequence d(TTAGGG). It contains a 3'-single-stranded overhang of 100–200 nucleotides which can fold into a G-quadruplex. Each replication results in shortening of the telomere by 50–200 bases[51,52]. DNA has a finite replicating capacity which is governed by a critical shortening of telomeric DNA; this causes cell death[53]. Telomerase is a reverse transcriptase which is responsible for maintaining the length of telomeres, hence making the cells that express the enzyme immortal. Telomerase is expressed in 80-90% of tumour cells[47,51]. The capability of telomeric DNA to form G-quadruplexes inhibits telomerase by locking the sequence into an inactive conformation that is no longer recognised by the enzyme[47]. This means that the telomeres are not inappropriately elongated and therefore the cell cannot become immortal. Consequently the development of small molecules capable of stabilising the telomeric G-quadruplex is a promising target for anti-cancer therapy[54].

G-quadruplexes are also highly prevalent in human gene promoter regions and are in this respect an emerging therapeutic target[55]. Their existence in the promoter region of oncogenes has recently been confirmed using both a G-quadruplex DNA cross-linking strategy[56] and a G-quadruplex specific probe[57]. Pharmacological manipulation of these structures may prove to be valuable for transcriptional repression of oncogenes and therefore suppression of the resultant oncoproteins.

The biological properties of DNA are closely associated with its structure and alteration to the structure of the nucleotides, which might for example be caused by chemical modification, can interfere with the process of replication and transcription, leading to mutations. This thesis is largely concerned with a naturally occurring chemical modification of DNA that is caused by reactive nitrogen species that are associated with inflammation. It is therefore necessary to consider how these reactive species are generated and how they affect DNA.

1.9 The physiology of inflammation

To understand the underlying mechanisms involved in inflammation related carcinogenesis, it is helpful to first give a brief overview of the normal tissue response to injury. Inflammation is an adaptive response to any damaging condition which threatens the integrity of cellular homeostasis[58]. The mechanism can often be diverse in terms of the cell types and inflammatory mediators but essentially elicits the same response. Despite this complexity, the generic inflammatory pathway can be categorised into four key components: inducers, sensors, mediators and effectors (Figure 1.10)[59].

Inducers of inflammation can be classified as either exogenous or endogenous. An example of an exogenous inducer is pathogen associated molecular patterns (PAMPs)[60]. PAMPs are specific structural components of invading microbial species that are not found in the host organism, but are essential for the pathogens physiology[61]. Endogenous inducers of inflammation are known as damage associated molecular patterns (DAMPs). These are the signals which are produced by the host in response to stressed, damaged or otherwise malfunctioning tissues[59].

Tissue-resident macrophages, dendritic cells and mast cells are classed as inflammatory sensors. These cells express transmembrane pattern recognition receptors (PRRs) which are capable of recognising and responding to PAMPs and DAMPs[62]. There are various types of PRRs, but they all possess common characteristics. PRR induced signalling ultimately results in the activation of transcriptions factors responsible for gene expression and the recruitment and synthesis of a broad range of inflammatory mediators. The nature of both the inducer and sensor are responsible for the different combinations and amounts of mediators produced by a given trigger[62].

Mediators of systemic inflammation can be classified with regards to their biochemical properties into seven groups: cytokines, chemokines, vasoactive amines, vasoactive peptides, anapylatoxins, lipid mediators and proteolytic enzymes[59]. The effect of the mediators is to locally elicit a physiological response; the tissue affected is known as the effector. Consequently, there is an increased blood supply at the site of inflammation and increased vascular permeability allowing for the recruitment of more important secretory cells (*e.g.* neutrophils, monocytes and macrophages), promotion of angiogenesis and production of reactive species designed to inactivate, destroy or remove an irritant[63].

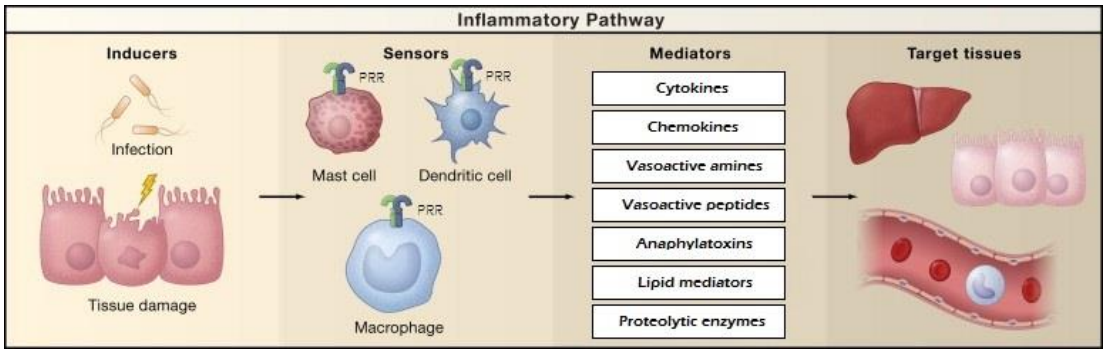

Figure 1.10: Inflammatory Pathway Components adapted from reference 64[64].

One mechanism by which the host signals to recruit mediators of the inflammatory response is through the activation of nuclear factor kappa B (NF-κB). It is well documented that NF-κB is rapidly activated through the PRR signalling pathway by a large range of PAMPs and DAMPs[65]. In the cytoplasm NF-κB exists in an inactive form which is regulated by IκB (inhibitor of NF-κB). Upstream signalling pathways activate a kinase enzyme which phosphorylates IκB thereby targeting it for degradation. The destruction of IκB releases NF-κB allowing it to translocate to the nucleus where it binds to the promoter regions of target genes and upregulates their transcription[66,67].These genes encode a broad range of proteins including pro inflammatory cytokines, chemokines, cellular inhibitors of apoptosis, inducible nitric oxide synthase and negative regulators of NF-κB to name a few[68,69].

Acute inflammation is short lived and self-limiting[63]. A successful inflammatory response eliminates the pathogen and the host subsequently undergoes a resolution and repair phase[59]. Although there are many processes involved in the resolution of inflammation, macrophages are the key mediator. During the repair phase both tissue resident and recruited macrophages shift from producing pro-inflammatory cytokines to the expression of anti-inflammatory mediators such as lipoxins and resolvins. Lipoxins inhibit the recruitment of anti-microbial cells such as neutrophils and instead promotes the infiltration of monocytes that ingest and clear cellular debris in order for the cell to return to homeostasis[67,70].

In summary, inflammation is the body's normal response to cellular injury; it is designed to protect from further damage, remove irritants and repair the affected tissues. However, this coordinated response occurs at the expense of normal cellular functions such as growth and reproduction. This is an unavoidable consequence of restoring homeostasis and since acute inflammation is generally short lived, in these circumstances, it does not cause detrimental effects to the host[62,64].

Acute inflammation is a tightly regulated process with a limited duration and magnitude; it has an integral resolution phase where the normal tissue architecture is restored[71]. However acute inflammation does not always resolve. Defects in the negative regulatory mechanisms result in the persistent activation of immune cells leading to the development of chronic inflammation. This persistent activation may be due to failure of the immune cells to remove the stimulus or events, such as genetic alterations, which maintain the inflammatory microenvironment preventing the onset of the resolution phase. The characteristics associated with chronic inflammation include; tissue remodelling, angiogenesis, promotion of growth and increased

cellular turnover[67,72]. These features contribute to the pathologic potential which accompanies chronic inflammation.

1.10 Role of nitric oxide synthase in infection

One of the mechanisms by which immune cells attempt to combat infection is by generating cytotoxic species such as nitric oxide (NO)[73]. This reactive nitrogen species has a multifaceted role in the human body; it plays a vital role in diverse biological processes, but can simultaneously act as a causative agent[74]. The role nitric oxide plays is dependent on the environment and which isoform of nitric oxide synthase catalyses its production[75].

There are three isoforms of the enzyme nitric oxide synthase, named according to the tissue type in which they were first described or their expression: the endothelial form (eNOS), the neuronal form (nNOS) and the inducible form (iNOS)[75,76]. The three isoforms are encoded by different genes but they display between 51-67% sequence homology[75,77,78]. The isoforms differ in their localisation, regulatory mechanisms, catalytic properties and the level of NO they produce.

All NOSs are homodimers in their active form, comprising oxygenase and reductase domains. Various activities of these domains can be likened to those of the cytochrome p450 enzymes[79]. Calmodulin is required for the enzymatic activity and acts as an essential third subunit for all isoforms[80]. Additional requirements include the substrates molecular oxygen (O_2) and L-arginine, the cofactors nicotinamide adenine dinucleotide phosphate (NADPH), flavins and tetrahydrobiopterin (BH_4) and the presence of an iron protoporphyrin IX (haem) group[75,81].

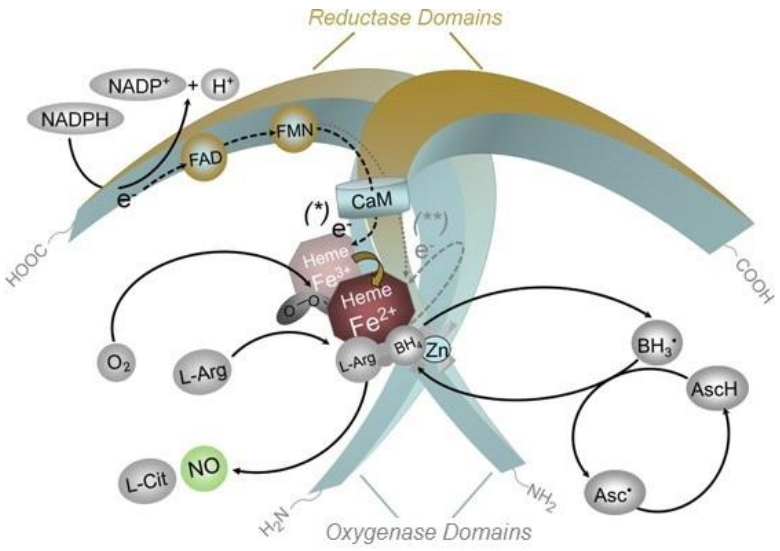

Figure 1.11: Generalised structure and function of NOS adapted from reference 82[82].

In the presence of the essential cofactor and substrates, electrons are donated by NADPH to the reductase domain. These electrons are then transferred *via* the flavins, FAD and FMN to the oxygenase domain. The two domains are linked by a calmodulin (CaM) recognition site, without the presence of which the enzyme is inactive. In the oxygenase domain, the electrons interact with the haem and BH_4 at the active site to reduce molecular oxygen and oxidise L-arginine (L-Arg) to generate L-citrulline (L-Cit) and nitric oxide (NO) as products[79,82]. This process is summarised in Figure 1.11.

Two of the isoforms, nNOS and eNOS are constitutively expressed and their activation is in response to increases in intracellular calcium (Ca^{2+}) concentration. The increased concentration of Ca^{2+} induces the binding of the essential third calmodulin subunit and therefore leads to a transient increase in the production of NO. In contrast, the activity of iNOS is calcium concentration independent, as calmodulin binds to iNOS with high affinity even in at very low cellular Ca^{2+} concentrations[82]. iNOS expression and hence NO production, is principally controlled by the upregulation of transcription of the enzyme in response to immunoactivation; rationalising the nomenclature 'inducible'. Typically, the iNOS enzyme synthesises NO continually, providing there are sufficient levels of L-arginine and other cofactors, until the enzyme is degraded[75,77,81].

The conversion of the substrate L-arginine to L-citrulline and NO is carried out *via* the two-step process shown in Scheme 1.1. The initial oxidation of arginine in the first step generates the intermediate *N*-hydroxyarginine, this is then further oxidised to give L-citrulline and NO[76,83].

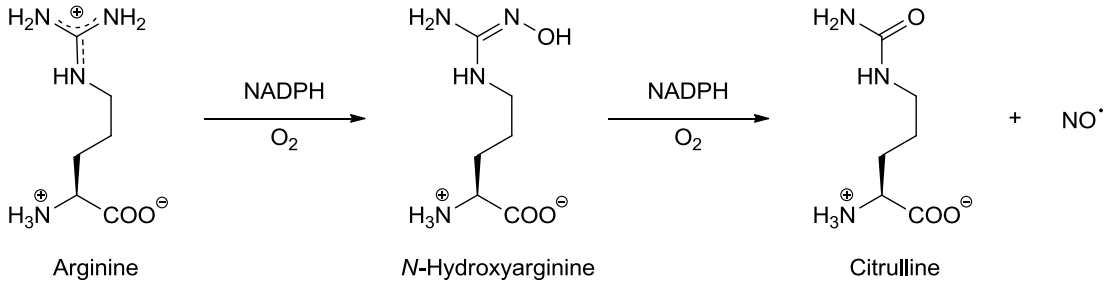

Scheme 1.1: Oxidation of L-Arginine to NO and Citrulline catalysed by NOS.

There are a number of mechanisms proposed for the transformation carried out at the active site of the NOS enzyme shown in Scheme 1.1, however many of these present conflicting views[83–85]. The most recent mechanism proposed is shown below. In the first step (Scheme 1.2[86]), the terminal oxygen of the peroxo species hydrogen bonds to L-arginine and a water

molecule. Heterolytic cleavage of the peroxy bond leads to the release of a water molecule and the formation of an oxy-ferryl species. This species then provides the oxygen atom for the formation of *N*-hydroxy-L-arginine[85].

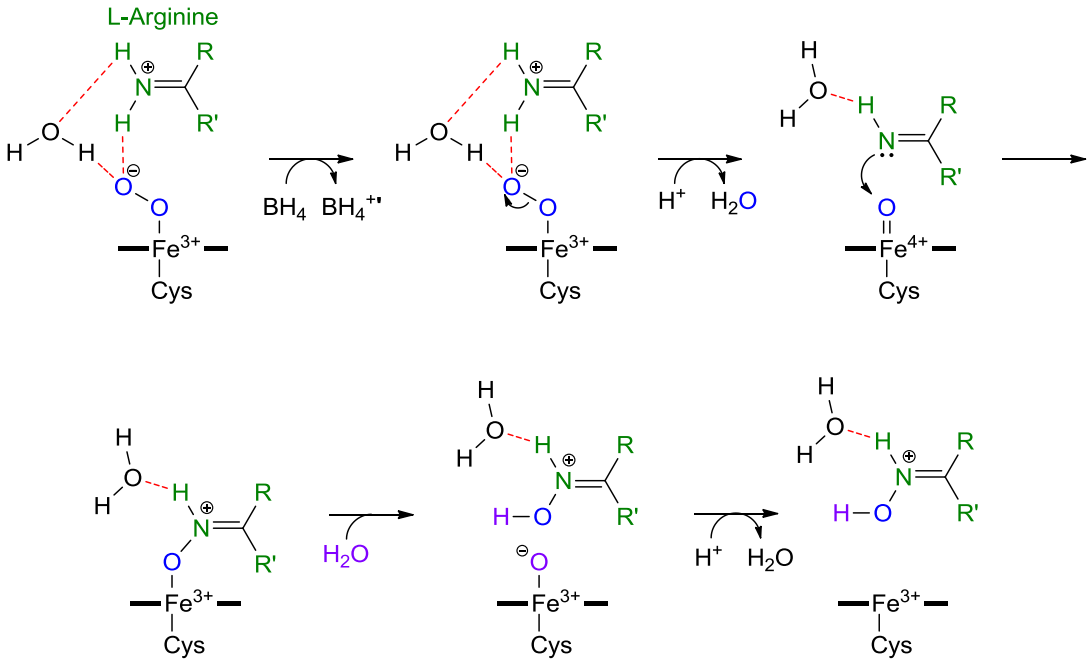

Scheme 1.2: Proposed mechanism for the first oxidation step.

In the second step of the mechanism (Scheme 1.3[86]) the enzyme binds molecular oxygen and owing to the hydrogen bonding arrangement the terminal oxygen adds in to the substrate to give the ferric bound peroxo species. Subsequently a bond rearrangement generates citrulline and an additional electron transfer produces NO and water[86].

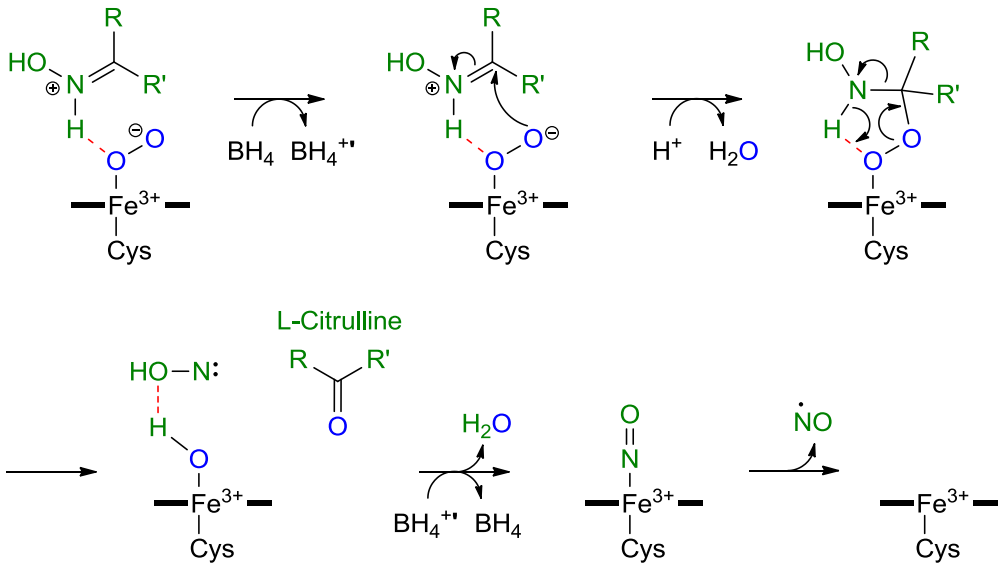

Scheme 1.3: Proposed mechanism for the second oxidation step.

1.11 Nitric oxide and its biological function

In 1987 Ignarro *et al.* and Palmer *et al.* simultaneously identified the small molecule that diffuses between cells and relaxes smooth muscle tissue, originally called endothelium derived relaxing factor (EDRF), was in fact NO[87,88]. In order to discuss the physiological outcomes produced by NO it is first necessary to consider its chemistry. NO has 11 valence electrons; this mean that the highest occupied molecular orbital of the molecule contains an unpaired electron. Consequently NO is an uncharged, radical species. Due to its small size and electrical neutrality, NO is free to diffuse through cell membranes and perform its role as an intracellular signalling molecule[89]. NO is relatively stable although it reacts with other radical species in favour of the formation of covalent bonds. However, dimerization of NO does not occur readily as it is unfavourable entropically[90,91]. The movement of NO within the human body is diffusion controlled. It has a half-life of several seconds and its actions are relatively long range[92]. The distance that NO can diffuse from its releasing cell is between 100-200μm and it has a high diffusion coefficient of 3300$\mu m^2 s^{-1}$ [93].

Although endogenous NO was originally recognised as a mediator of smooth muscle relaxation, it is now known that NO plays a diverse range of functions within the human body. The role NO plays is dependent on its environment and which enzyme catalyses its production. One of the primary substrates for NO is the enzyme soluble guanylate cyclase. NO binds to the haem cofactor in guanylate cyclase stimulating conformational changes which activate the catalytic domain of the enzyme. The active site catalyses the cyclisation of guanosine triphosphate (GTP) to form guanosine-3',5'-cyclic monophosphate (cGMP). This then initiates cGMP mediated signalling cascades resulting in physiological changes within the target cells[92,94]. In the immune system, macrophages produce NO from iNOS in response to pro-inflammatory cytokines and other mediators (*e.g.* NF-κB) as part of the inflammatory response[95]. In these circumstances NO can act as an antimicrobial or cytotoxic agent and its production is a mechanism by which the host fights infection.

NO produced in the endothelium is responsible for smooth muscle relaxation and hence vasodilation, it inhibits platelet aggregation, prevents adhesion of neutrophils and platelets to endothelial cells and plays a role in angiogenesis. In the autonomic nervous system, neuronal NO acts as a non-adrenergic non-cholinergic neurotransmitter[96,97]. In general at lower concentrations (<1μM) the direct effects of NO itself predominate; this includes the effects produced by eNOS and nNOS as they typically produce low amounts of NO for short periods

of time. At higher concentrations (>1μM) such as that produced by iNOS, indirect and cytotoxic effects are exhibited, these will be discussed in more detail later in the chapter[98].

The role of NO in the human body is multidimensional. It can exhibit distinctly different and often opposing actions in similar environments. For example, in acute inflammation NO is an essential part of the host defence however in chronic inflammation it can be potentially toxic; although these effects are predominantly mediated indirectly *via* oxidation products rather than directly by NO itself[90].

1.12 Peroxynitrite

A large proportion of the indirect effects of NO are mediated by the formation of peroxynitrite ($ONOO^-$). The main route of its formation is the reaction between NO and superoxide. Superoxide is generated by a number of endogenous mechanisms; one of which is in immune cells *(e.g.* neutrophils) during a process known as an oxidative or respiratory burst. This can be defined as the increased oxygen consumption of immune cells during host defence. It has been established that the increase in oxygen consumption is a consequence of the activity of the enzyme NADPH oxidase. The active enzyme generates superoxide by catalysing the NADPH-dependent reduction of molecular oxygen shown in Scheme 1.4[99,100].

Scheme 1.4: Generation of superoxide.

Under normal physiological conditions, the levels of superoxide are kept low by the enzyme superoxide dismutase (SOD). The enzyme prevents the formation of a build-up of superoxide by conversion to oxygen and hydrogen peroxide[101]. However, in chronic inflammation, the simultaneous production of superoxide and high levels of NO can lead to the preferential formation of the powerful oxidant peroxynitrite.

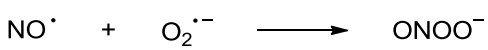

Scheme 1.5: Generation of peroxynitrite.

The reaction is thermodynamically very favourable due to the formation of a covalent bond from two radical species; it is therefore irreversible. There are various different rate constants quoted for the reaction shown in Scheme 1.5, the most common of which is 6.7×10^9 $M^{-1}s^{-1}$ [102]. In comparison, the decomposition of superoxide by superoxide dismutase has a rate constant of ~2×10^9 $M^{-1}s^{-1}$ [90,103]. Consequently, in chronic inflammation the localisation and

concentration of NO is such that it is able to compete with endogenous superoxide dismutase for superoxide in order for the generation of peroxynitrite to predominate.

Oxidative and nitrative damage caused by peroxynitrite can be attributed to one of three mechanisms. Firstly peroxynitrite itself can be toxic; it can react with electron rich groups readily oxidising both free and protein bound sulfhydryl groups[104]. It can irreversibly inactivate protein tyrosine phosphatase[105], which is responsible for the regulation of signalling pathways that underlie an extensive range of fundamental physiological processes[106]. Additionally it induces oxidative inactivation of enzymes containing a thiolate center such as alcohol dehydrogenase[107].

Although peroxynitrite can itself be toxic, a large proportion of the deleterious effects observed are caused by secondary reaction products. These can vary depending on the local environment and the pH. Under physiological conditions peroxynitrite can be protonated (pK_a 6.8) to form peroxynitrous acid, which rapidly decays with a half-life of approximately 1s at 37°C[108]. The decomposition products of peroxynitrous acid can be either inactive metabolites or toxic radicals which can participate in secondary reactions resulting in oxidative and nitrative damage.

Peroxynitrous acid undergoes isomerisation adopting either the *cis*- or the *trans*-conformation (Scheme 1.6), this is due to the partial double bond between the nitrogen atom and the first peroxide oxygen[109]. While the *cis*-isomer is more stable due to hydrogen bonding, the labile *trans*-isomer is significantly more reactive[110]. In the *trans*-conformation, the peroxo bond is lengthened, making the molecule susceptible to degradation at this position[111,112]. Peroxynitrous acid can undergo molecular rearrangement to form nitrate but can also undergo homolytic decomposition of the peroxo bond to form highly reactive hydroxyl and nitrogen dioxide radicals in a parallel reaction (Scheme 1.6).

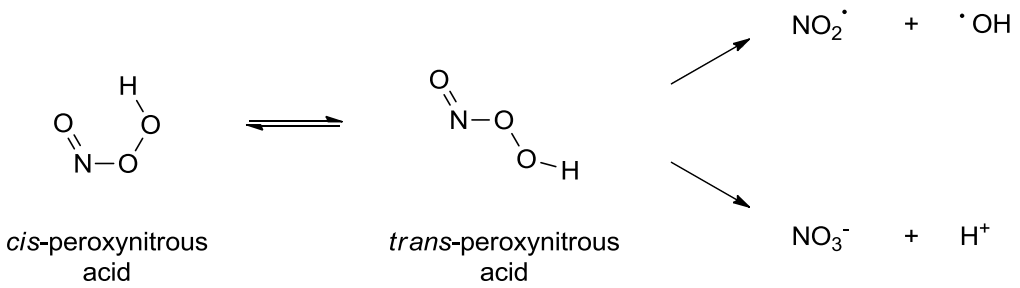

Scheme 1.6: The reactivity of peroxynitrous acid.

Despite extensive research into the chemistry of peroxynitrous acid decomposition no consensus has emerged on its mechanism. Whilst some research supports the radical pair decomposition mechanism,[113–115] others dispute it[103]. Further research in this area is necessary to provide unambiguous evidence to support either conclusion.

Finally, the reaction of peroxynitrite with carbon dioxide can lead to toxic radical formation. The intracellular concentration of carbon dioxide is approximately 1mM, which is approximately 10,000 times greater than the concentration of hydrogen ions, making it the most important modulator of peroxynitrite activity[102]. The peroxynitre anion reacts with carbon dioxide at a rate of 5.8 x 10^4 $M^{-1}s^{-1}$ under physiological conditions to form the nitrosoperoxycarbonate anion (Scheme 1.7)[116,117]. The nitrosoperoxycarbonate anion is highly unstable and rapidly homolysis of the weak peroxo bond to form carbonate and nitrogen dioxide radicals[118].

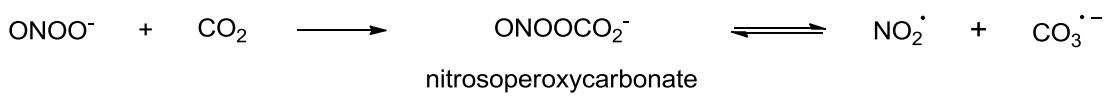

Scheme 1.7: Formation of carbonate and nitrogen dioxide radicals.

The production of reactive oxygen and nitrogen species is a vital defence mechanism by which immune cells fight invading pathogens. However, peroxynitrite generated during chronic inflammation represents a major threat to the cellular components. The sustained high levels often results in damage to host nucleic acids, lipids, proteins and carbohydrates. Damage can be caused directly by peroxynitrite or indirectly by radical mediated nitration reactions, highlighting the multifaceted role played by NO in the human body. The inflammatory process triggered by infection or irritant can initiate cellular transformations that promote the development of cancer[119].

1.13 DNA damage caused by peroxynitrite

Prolonged exposure of nucleic acids to reactive oxygen and nitrogen species generates various base modifications. This damage can lead to the initiation and advancement of mutagenesis and chromosomal instability[120]. Initial investigations into the oxidation of DNA were focused on the formation of strand breaks, however, now it is recognised that the formation of base adducts can have deleterious effects on cellular function and survival[121]. Relative to the other DNA bases, guanine represents the major target for oxidation by chemical

mediators of inflammation. This is attributed to it having the lowest oxidation potential (E_{ox} = 1.29 V vs. standard hydrogen electrode)[122,123].

A range of chemical and biological agents are capable of abstracting an electron from guanine. This one-electron oxidation can lead to a number of nitrated and oxidised DNA adducts shown in Figure 1.12.

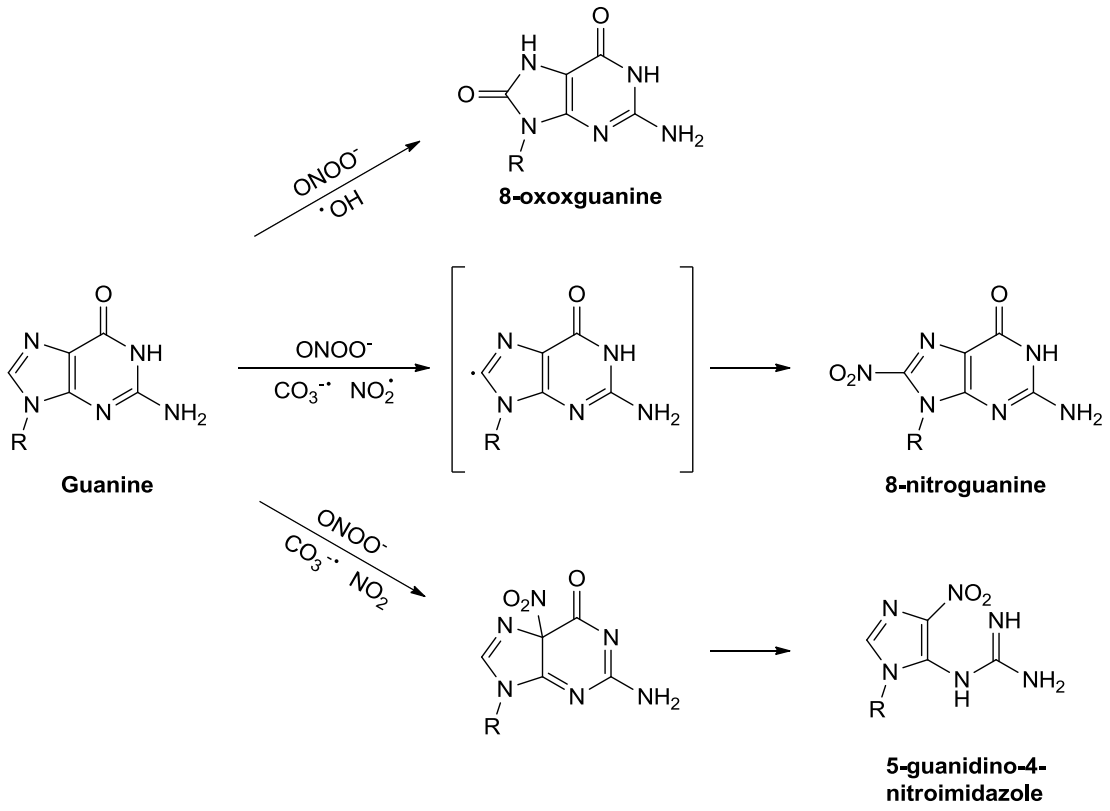

Figure 1.12: Oxidative and nitrative damage to guanine[116].

The content of the DNA sequence is also responsible for modulating the oxidation potential of guanine. There is evidence to show that the 5'-guanine of stacked sequences containing consecutive guanines oxidises more easily than an individual guanine in a sequence; hence, the reactivity of a guanine base in a run of guanines is significantly influenced by the surrounding nucleotides. Abstraction of one electron from a guanine base will induce electron transfer from the subsequent guanine base. Consequently, a radical cation introduced to DNA will migrate to the lowest energy site (if the radical is not trapped first by oxidising agents)[124–126].

1.14 The link between inflammation and cancer

The observation by Rudolf Virchow in 1863 that leukocytes were present within cancerous lesions, provided the first link between inflammation and cancer[95,127]. The hypothesis that an inflammation promotes a cellular environment that that drives the initiation and development of carcinogenesis is now well documented. The tumour microenvironment is comprised of a complex system of cells. Inflammatory cells and their mediators have been found to comprise a key component of most, if not all tumours, irrespective of their cause for development[69].

The inflammatory cells provide an attractive environment for tumour growth[63]. They activate pro-tumourigenic processes leading to; the release of growth and survival factors, the promotion of angiogenesis, the facilitation of invasion and the increased production of reactive oxygen and nitrogen species that are known to induce DNA damage. These processes, among others, act as part of a positive amplification loop that attract additional cells in order to sustain the tumour microenvironment (Figure 1.13)[127].

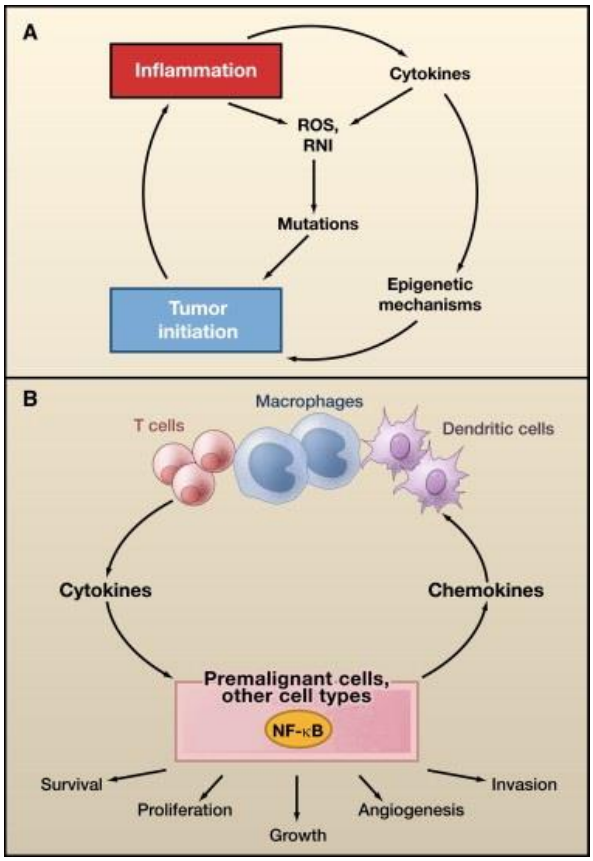

Figure 1.13: Role of inflammation in tumour initiation (A) and promotion (B), adapted from reference 127[127].

The link between inflammation and cancer is mediated by two converging pathways: the extrinsic and the intrinsic. In the extrinsic pathway, pre-existing chronic inflammatory conditions and their associated microenvironments initiate cancer development[69]. Specific inflammatory conditions which can precede carcinogenesis at certain sites will be discussed later in the chapter. The intrinsic pathway is associated with tumours of which the cause is unrelated to any underlying inflammatory conditions[128]. In this pathway, cells that have undergone genetic alteration secrete inflammatory mediators and therefore create their own inflammatory microenvironment[129]. Regardless of which pathway elicits the inflammatory response, ultimately the outcome is the same.

In 2000 the six hallmarks of cancer were defined as; self-sufficiency in growth signals, insensitivity to anti-growth signals, evasion of apoptosis, unlimited replicative potential, ability to stimulate angiogenesis, capability for tissue invasion and metastasis[128,130]. The evidence that the inflammatory microenvironment is a key component in the development of cancer suggests that this may represent the seventh hallmark of cancer[128,131].

Cause	**Inflammatory Condition**	**Associated Cancer**
Heliobacter pylori	Gastritis	Gastric cancer
Gut pathogens	Inflammatory bowel disease	Colorectal cancer
Tobacco smoke	Bronchitis	Bronchial lung cancer
Hepatitis C virus	Hepatitis	Hepatocellular carcinoma
Bacteria, gall bladder stones	Cholecystitis	Gall bladder cancer
Tobacco, genetics, alcohol	Pancreatitis	Pancreatic cancer
Epstein-Barr virus	Mononucleosis	Burkitts lymphoma
Ultraviolet light	Sunburn	Melanoma
Asbestos fibres	Asbestosis	Mesothelioma
Gram-uropathogens	Schistosomiasis (Biharzia)	Bladder cancer
Gastric acid, alcohol, tobacco	Esophagitis	Esophageal adenocarcinoma

Table 1.2: Inflammatory conditions and the related cancer adapted from reference 129[129].

Evidence suggests that more than 25% of human cancers are attributable to chronic inflammation where DNA damage resulting from chronic inflammation is believed to be the mechanism[120,129,132,133]. In many of these cases the continued presence of an infection, bacteria or irritant in the affected tissue is the causative agent. A summary of inflammatory and pathogenic conditions that are considered to be associated with malignant transformation is

shown in Table 1.2[129]. The strongest association of chronic inflammation with malignant diseases is in colon carcinogenesis arising in individuals with inflammatory bowel diseases. Hepatitis C infection in the liver predisposes to liver carcinoma, whereas chronic *Helicobacter pylori* (*H. Pylori*) infection is the world's leading cause of stomach cancer[63].

1.15 Inflammation associated cancers and DNA damage

Since its discovery in 1983[134], *H. pylori* has been recognised as the major cause of chronic gastritis and the development of gastric carcinoma. In 1994 the International Agency for Research on Cancer considered there to be significant evidence for the classification of *H. pylori* as a type I carcinogen in humans[135]. *H. pylori* is a spiral gram-negative bacterium which colonises in the stomach and is known to infect more than half of the world's population[136]. It is considered to be the most common factor leading to infection related cancers and 5% of all people infected will go on to develop gastric cancer[120]. In 2012 gastric cancer was reported by the International Agency for Research on Cancer (IARC) as the 5th most prevalent cancer worldwide with the 3rd highest mortality[137].

H. pylori infection elicits an inflammatory response, as previously discussed; this is responsible for the production of inflammatory mediators, the upregulation of expression of iNOS and the production of reactive oxygen and nitrogen species. However, the immune system is not able to eliminate the bacteria which results in a sustained presence of inflammatory mediators leading to the development of continuous and progressive chronic inflammation[138]. This chronic inflammatory state exposes DNA to consistently high concentrations of cytotoxic agents which is recognised to play an important role in the initiation and progression of gastric cancer[136].

H. pylori has various mechanisms to evade host defence; a number of these are summarised in Figure 1.14. In order to be able to survive in the stomach, the bacteria produce the enzyme urease to catalyse the hydrolysis of urea to carbon dioxide and ammonia which neutralises the surrounding gastric acid[138,139]. NO irreversibly inhibits the respiration of *H. pylori*; in fact *in vitro* studies suggest that NO is capable of killing the bacteria. However this is not the case *in vivo, H. pylori* generates superoxide radicals which rapidly react with NO to form peroxynitrite. While peroxynitrite produces similar effects to NO and irreversibly inactivates the respiration of the bacteria, due to the actions of urease, it preferentially reacts with carbon dioxide which is in consistently high concentration in the surrounding area. It is suggested that formation of the nitrosoperoxycarbonate anion inhibits the bactericidal activity of peroxynitrite but as described

previously can decompose to free radical species which cause damage to surrounding gastric epithelium[138,140,141]. In clinical studies, both 8-nitroguanine and 8-oxoguanine have been observed in the nuclei and cytoplasm of gastric epithelial cells of *H. pylori* infected patients. Treatment and eradication of the infection lead to dramatically decreased levels of these DNA adducts[142,143].

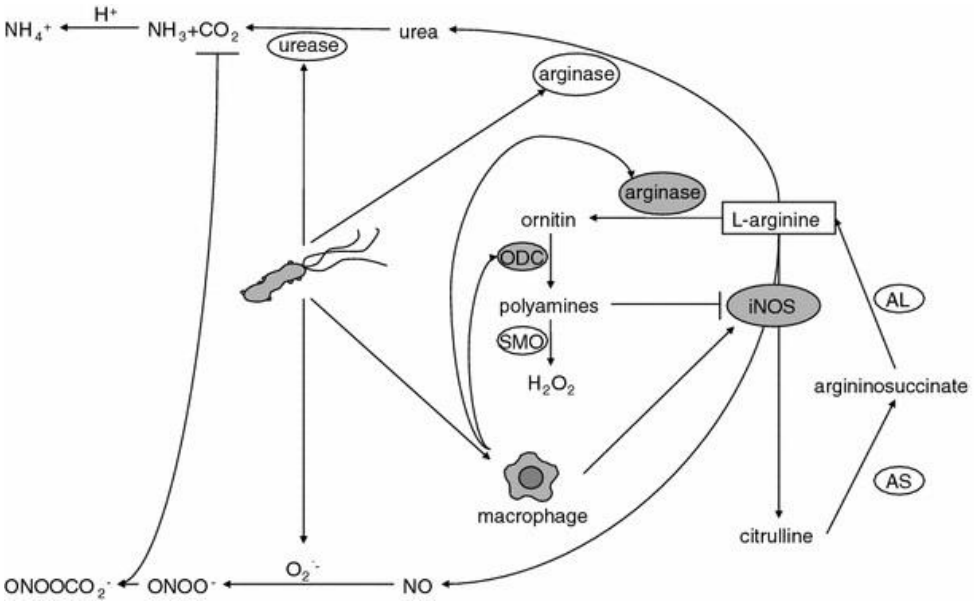

Figure 1.14: The defence mechanisms against oxidative stress taken from reference 138[138].

Based on the GLOBOCAN 2012 estimates, liver cancer is the sixth most frequently diagnosed cancer, and is the second leading cause of cancer-related deaths worldwide[137]. Hepatocellular carcinoma (HCC) is the most common primary liver cancer, accounting for between 70-85% of cases[144]. Infection with the Hepatitis C virus (HCV) is a significant predisposing factor in the development of HCC. While the pathogenic mechanism underlying the evolution from HCV to HCC is not well defined, the multistage progression is summarised below.

In between 70-80% of individuals infected with HCV, the acute phase is asymptomatic despite triggering an immune mediated inflammatory response. While 15-25% of patients will clear the infection, in the vast majority of cases, the disease will become chronic. Chronic hepatitis C (CHC) is characterised by the presence of HCV RNA in the blood 6 months after the onset of the acute infection[145]. Failure of the immune response to clear the infection leads to chronic inflammation; 20-40% of individuals develop liver cirrhosis and 4-6% progress to HCC after 10-40 years of infection. HCV is a single stranded RNA virus that does not integrate into the host genome, therefore the chronic inflammatory environment it elicits is considered a major contributing factor to the development of carcinogenesis[144].

The reactive oxygen and nitrogen species released from activated immune cells as a consequence of chronic inflammation can interact with nucleic acids leading to mutations and malignant transformation[143,146]. To determine the extent of DNA damage resulting from HCV, the formation of the DNA adducts 8-nitroguanine and 8-oxoguanine in the liver of patients with CHC before and after treatment has been analysed. Both 8-nitroguanine and 8-oxguanine formation was apparent in the nucleus of hepatocytes in patients with CHC. The number of hepatocytes identified containing the DNA adducts increased with the degree of inflammation of the liver. Furthermore, upon treatment, the accumulation of 8-nitroguanine and 8-oxoguanine base modifications in the liver decreased[147]. Together these findings support the conclusion that oxidative and nitrative DNA damage are an important contributing factor to HCV associated HCC.

Cigarette smoking is a well-established risk factor in cancer development. The precise mechanisms for this transformation remain to be defined, however the connection between lung cancer, tobacco smoke and inflammation are unquestioned. Lung cancer is the leading cause of cancer related deaths worldwide[137]. It has been estimated that cigarette smoking can be attributed to 90% of lung cancer incidence in men and 70 to 80% in women[148]. Approximately 5000 chemical compounds are released during the combustion of tobacco[149]. These chemicals have cytotoxic, mutagenic and carcinogenic properties.

Continued exposure to cigarette smoke can foster an environment that induces chronic inflammation which can lead to carcinogenesis. The gas phase of cigarette smoke contains high concentrations of nitric oxide; estimated figures range from 300-600µg per cigarette[150–152]. This exogenous source of nitric oxide can directly, or as a consequence of secondary reaction products, lead to oxidative and nitrative DNA damage. In addition, the components of cigarette smoke are known to activate several inflammatory signalling cascades, including the NF-κB pathway. As previously discussed, this transcription factor is responsible for the expression of inflammatory genes, the release of a number of inflammatory mediators and ultimately the production of reactive oxygen and nitrogen species[153,154]. These converging pathways both result in the formation of DNA adducts and contribute to the pathogenesis of lung cancer.

Various studies have been carried out to quantify the oxidative and nitrative products of DNA damage caused by cigarette smoke. Smoking has been shown to greatly increase the amount of 8-nitroguanine found in urine by between 6-69 fold when compared to non-smokers. The increase in the levels of 8-oxodeoxyguanosine was modest in comparison with amounts

between 9-50% higher[155]. Hsieh *et al.* determined the levels of 8-nitroguanine in DNA extracted from peripheral lymphocyte of tobacco smokers and compared the results to that of non-smoking healthy controls. The DNA from the healthy control volunteers contained trace levels of the DNA adduct, whereas the levels were significantly higher in cigarette smokers[116,151].

1.16 8-Oxoguanine

It has been estimated that approximately 20,000 mutagenic lesion are formed in each mammalian cell per day[156]. Exposure to reactive oxygen and nitrogen species is considered to be major factor contributing to DNA damage. However the high fidelity of DNA replication is maintained by a combination of proofreading and repair mechanisms.

One of the most abundant and extensively studied oxidative DNA lesions is 8-oxoguanine. By its chemical incorporation into DNA, it has been possible to gain in depth information about this lesion and how it may be a factor in carcinogenesis. The formation of 8-oxoguanine was first reported in 1984 as a result of the treatment of DNA with ascorbic acid[157]. *In vivo* the addition of a hydroxyl radical to the C8 position of guanine forms a radical adduct which can be oxidised to yield 8-oxoguanine[158]. The additional presence of a carbonyl group at the C8 position and a hydrogen atom at the N7 position significantly changes the bases properties with respect to guanine and alters the efficiency and fidelity of transcription. 8-Oxoguanine can adopt a number of different tautomeric structures; the predominant forms are shown in Figure 1.15. Computational methods suggest that in the aqueous phase the keto form is the most stable tautomer and hence it is most likely that this species contributes to the mutagenesis of 8-oxoguanine[159]. The estimated daily level of 8-oxoguanine formed is approximately 10^3 lesions per cell in tissues at homeostasis; however this can be as high as 10^5 lesions per cell in cancerous tissues[160].

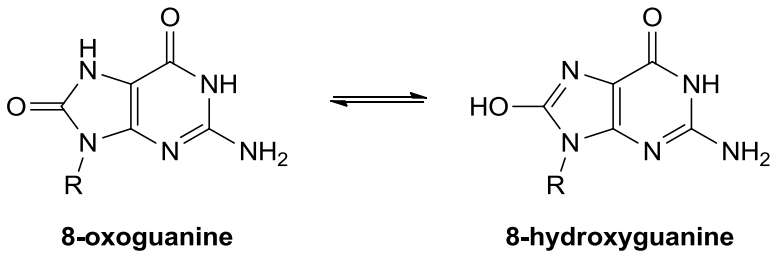

Figure 1.15: Keto-enol tautomerisation of 8-oxoguanine.

The primary structural basis for the mutagenicity of 8-oxoguanine is its ability to form base pairs with both cytosine and adenine. This requires rotation of the base about the glycosidic bond relative to the sugar moiety. The oxygen atom at the C8 position can result in destabilisation of the *anti*-conformation causing the base to preferentially adopt a *syn* orientation[24]. This can be attributed to the steric clash between the C8 substituent and the sugar-phosphate backbone; the *syn*-conformation best alleviates these unfavourable steric interactions[161]. The conformation of the 8-oxoguanine glycosidic bond in DNA is dependent on its base pairing partner which is determined by the polymerase replicating the DNA.

While 8-oxoguanine can form a stable Watson-Crick base pair with cytosine, it can pair with comparable stability to adenine[162]. When pairing to cytosine, 8-oxoguanine adopts the unfavourable *anti* conformation. Despite forming three hydrogen bonds this base pair is destabilised in comparison to the corresponding natural G:C base pair. The protonated nitrogen in the N7 of position of 8-oxoguanine creates an additional hydrogen bond donor. Consequently in the *syn* orientation, 8-oxoguanine can functionally mimic thymine and form a Hoogsteen base pair with adenine. If cytosine is incorporated opposite the lesion, complementary base pairing is maintained ensuring faithful DNA replication and therefore there is no mutation as a result of oxidative DNA damage. Conversely, if adenine is incorporated opposite 8-oxoguanine in subsequent DNA replication the lesion would be recognised as a thymine instead of guanine; this is known as a G→T transversion. These seeming small changes to the DNA sequence can cause mutagenesis[24,163,164].

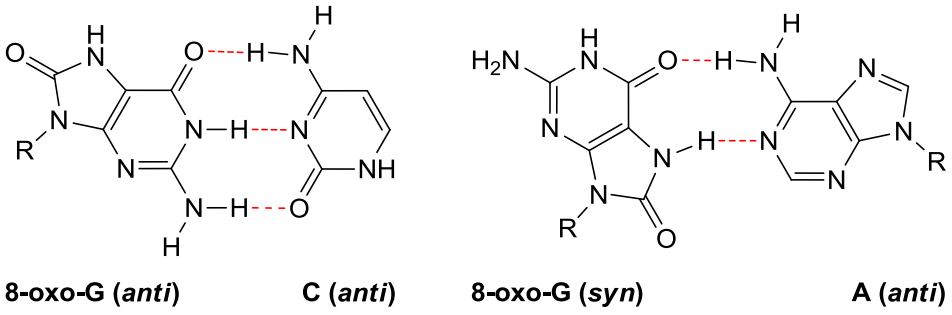

Figure 1.16: Base pairing of 8-oxoguanine.

The defence mechanisms against mutagenesis caused by 8-oxoguanine have been extensively studied. Three key enzymes have been identified that reduce the mutagenic potential of 8-oxoguanine. These fall into two categories, those that prevent the incorporation of the oxidised nucleotide into DNA and those that are involved in the repair of the lesion[165].

The accuracy of the recognition and repair processes plays a critical role in determining the consequences of oxidative DNA damage.

MutT (hMTH1 in humans) is responsible for preventing the misincorporation of 8-oxoguanine nucleotides opposite adenine by DNA and RNA polymerases. The enzyme is a triphosphatase that hydrolyses 8-oxo-dGTP in the nucleotide pool to the corresponding monophosphate and pyrophosphate, thus eliminating it as a potential DNA synthesis precursor[166]. The structural basis for this specificity is the presence of a hydrogen bond between the N7 hydrogen and an oxygen atom in the substrate binding site of the enzyme. Additionally, 8-oxoguanine is discriminated from guanine nucleotides by the *syn* conformation of the glycosidic bond which is preferential for the 8-oxoguanine mononucleotide. MutT exhibits high substrate specificity for 8-oxoguanine nucleotides, although it is known to hydrolyse several other oxidised purine nucleosides[167].

8-Oxoguanine can be repaired by the base excision repair (BER) pathway; this can be initiated by DNA glycosylate/β-lyase OGG1. This enzyme is responsible for the removal of 8-oxoguanine from DNA when it is paired opposite cytosine, in order to restore the G:C base pair and to ensure faithful replication in subsequent DNA synthesis. OGG1 can recognise and bind to 8-oxoguanine while it is stacked within the double-helix[165]. Initially hydrogen bond formation between the 8-oxoguanine base and the enzyme destabilise the base pairing with cytosine. This promotes rotation of the modified base into the active site of the enzyme; both the extruded base and the double-helix are stabilised by key residues of the protein. The hydrolysis of the glycosidic bond is catalysed by the enzyme to leave an apurinic site in the DNA[168].

The OGG1 enzyme possesses a high degree of substrate specificity. When guanine is located in the active site of the enzyme, despite being positioned in approximately the same position as 8-oxoguanine, OGG1 does not catalyse base excision[169]. OGG1 is the enzyme primarily responsible for repairing 8-oxoG once it has been formed in, or been incorporated into DNA. However, if for some reason OGG1 does not remove the lesion, a second enzyme excises the mispaired adenine base in order to promote incorporation of the correct base pair.

The enzyme adenine DNA glycosylase, known and MutY in bacteria and hMYH in humans is responsible for removing an inappropriately paired adenine base from DNA if replication has already taken place. The enzyme recognises the mismatch by an extensive array of hydrogen bonds which engage every face of the 8-oxoguanine base. An important factor in this

recognition is the unique C-terminal domain of MutY, without which the enzyme cannot discriminate for the mismatch of adenine with 8-oxoguanine[170]. The enzyme rotates the base out of the helix by inducing bending and distortion. The extruded adenine base is inserted into the binding site in the catalytic domain of the enzyme. MutY then removes the base *via* hydrolysis of the glycosidic bond[163,171]. As previously mentioned, to mispair with adenine, the glycosidic bond of 8-oxoguanine adopts the *syn* conformation. Interestingly crystal structures of the bound MutY-DNA complex show that 8-oxoguanine is rotated about the glycosidic bond into the *anti* orientation. This rotation would cause a unfavourable steric interaction providing the driving force to expel adenine from the helix[170].

Subsequent steps involve further processing by various different proteins in the base excision repair pathway (AP endonuclease, DNA polymerase, DNA ligase). This corrects the DNA sequence by template-directed insertion of nucleotides to restore the original G:C pair[166]. Mutations in any of the genes in DNA repair pathway play an important role in the development of carcinogenesis[172]. Despite the actions of these repair enzymes, some oxidatively damaged bases remain unrepaired. These can potentially be detected by DNA polymerases during replication.

DNA synthesis opposite 8-oxoguanine is problematic because the lesion can evade proofreading mechanisms which can lead to mutagenesis. Two of the many mechanisms by which it can avoid detection are detailed below. To facilitate base pairing between 8-oxoguanine and cytosine, the DNA strand adopts a kinked configuration. This prevents unfavourable steric interactions between the C8 substituent of 8-oxoguanine and the sugar phosphate backbone, but induces a conformational change in the enzyme. Distortion of the active site functions to identify mismatched base pairs and suspends DNA replication. When paired to adenine, 8-oxoguanine adopts the sterically favoured *syn* conformation. In this orientation, the mismatch geometrically resembles that of a conventional Watson-Crick base pair. Therefore the 8-oxoguanine adenine base pair is able to occupy the active site without distorting the protein thus evading this method of error detection[173,174].

High fidelity polymerase enzymes consist of a number of key sites that consecutive bases occupy. After incorporation, the new base pair moves to a post-insertion site where hydrogen bonds are formed between residues on the enzyme and universal hydrogen bond acceptors in the minor groove of the DNA. Failure to form these hydrogen bonds leads to recognition of the mismatched base pair which stalls the polymerase. When 8-oxoguanine adopts the *syn*

conformation, the C8 substituent is projected into the minor groove of the helix. The oxygen atom acts as a hydrogen bond acceptor and effectively mimics the N3 of an undamaged purine in the *anti*-configuration. Consequently, it provides feedback to the enzyme concerning the geometry of the minor groove. As the oxidative damage enables 8-oxoguanine to interact appropriately with these donors, the lesion does not trigger proofreading functions and is considered as an undamaged nucleoside[175].

Much of what is known about 8-oxoguanine has been established by chemically incorporating the modification into DNA; it has been possible to gain in depth information about how the lesion may be a factor in carcinogenesis. This includes details of how the modification influences the structure of the DNA duplex, how the lesion is recognised in vivo and which enzymes are involved in its repair.

1.17 8-Oxoguanine as a biomarker of disease

The National Institutes of Health define a biomarker as 'a characteristic that is objectively measured and evaluated as an indicator of normal biological processes, pathogenic processes, or pharmacologic responses to a therapeutic intervention'[176]. Biomarkers are used for the early detection of a disease before the development of clinical symptoms. They are based on the concept that accumulation of a particular precursor is directly proportional to mutagenic potential[177]. Ideally the marker must be detectable in samples from easily accessible proxy tissues[178]. Understanding the relationship between measurable biological molecules or processes and how they influence the development of diseases plays an important role in rational drug design.

The presence of 8-oxoguanine is often exploited as a cellular biomarker to indicate the extent of oxidative stress and the potential for carcinogenesis. It is relatively easily formed, is mutagenic and is measurable by a variety of methods[179]. Validated biomarkers of oxidative DNA damage such as 8-oxoguanine, could provide an approach to early detection and prevention strategies for diseases associated with oxidative stress[180].

1.18 8-Nitroguanine

8-Nitroguanine is readily identified following damage by reactive oxygen and nitrogen species and is of particular interest with regard to this thesis. In order to gain a comprehensive understanding of how this lesion can be a factor in carcinogenesis it is essential to be able to

synthesise and examine oligonucleotides containing the modification; however, until recently this was not been possible.

8-Nitrodeoxyguanosine (8-NO_2-dG) undergoes rapid hydrolysis of the glycosidic bond to give the free 8-nitroguanine base, leaving an abasic site in the DNA (Scheme 1.8). Under physiological conditions 8-nitrodeoxyguanosine has a half-life of 1-4 hours[126,181]. However it has been found that 8-nitroguanine in RNA is significantly more stable with only 5% depurination occurring within 6 hours[182]. The increased stability can be attributed to the additional C2' hydroxyl group characteristic of the ribose sugar. The hydroxyl group destabilises the oxonium ion intermediate making the hydrolysis process less favourable.

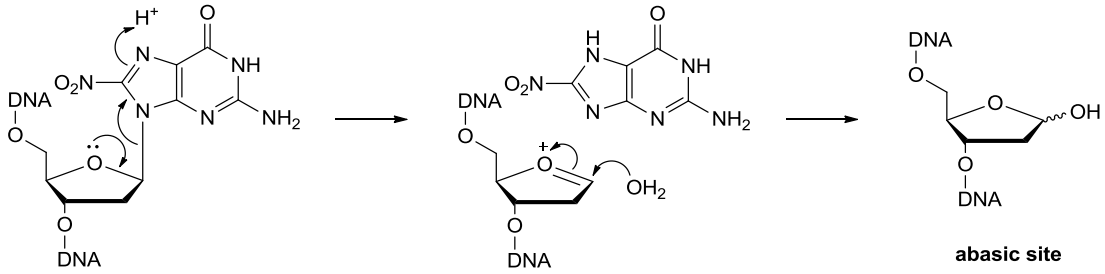

Scheme 1.8: Hydrolysis of the glycosidic bond.

8-Nitrodeoxyguanosine has been shown to have a high miscoding frequency. This may be due to the lesion itself causing miscoding or its ability to form apurinic sites in DNA[183]. Abasic sites are one of the most frequently encountered DNA lesions, they are generated *via* a number of mechanisms and their mutagenic effects have been extensively studied[184,185]. Abasic sites are predominantly recognised by the enzyme AP endonuclease[186]. The AP endonuclease initiates a repair cascade involving a concerted effort of the enzymes in the base excision repair pathway. Briefly, after recognition of the lesion, the proteins excise the damaged nucleotides and subsequently replace the damaged moiety with an undamaged nucleotide which restores the original DNA sequence[185–187].

Abasic sites that remain undetected challenge DNA polymerases to incorporate a nucleotide without a template strand to copy. These lesions are known to inhibit the progress of high fidelity DNA polymerases responsible for catalysing the majority of DNA synthesis[175]. In order to bypass the abasic site, the sequential actions of two error prone DNA polymerases are required. The enzymes Pol δ and Rev1 are involved in the insertion of a nucleotide opposite an abasic site; however these DNA polymerase cannot catalyse translesion synthesis. DNA

polymerase ζ is required in order to extend from nucleosides incorporated opposite the lesion[188,189].

Translesion synthesis favours the incorporation of adenine opposite the abasic site leading to G→T transversions; this preference is known as the 'A rule' of mutagenicity[188]. It has been suggested that adenine is incorporated opposite an abasic site as this does not confer any distortion to the double-helical structure of B-DNA[188]. Additionally the melting temperature of the duplex containing this base pair is the same as that of a T:A base pair in the same duplex[190]. The use of error prone polymerases in this bypass mechanism, may contribute further to extensive point mutations[191].

Interestingly, it has been reported that 8-nitroguanine nucleosides and nucleotides can be directly involved in the generation of oxidative stress; this provides an alternative mechanism by which the lesion can lead to mutagenesis[192]. As described previously, NOS utilises NADPH as an electron donor to facilitate the production of nitric oxide. In the presence of 8-nitroguanine, the electron transfer can become disorganised causing 8-nitroguanosine to be reduced forming an 8-nitroguanosine radical (Figure 1.17)[193]. This electron is then transferred to molecular oxygen in a redox cycling reaction which reforms 8-nitroguanosine and generates superoxide[116]. This process is pathophysiologically significant because superoxide and its secondary reaction products, such as peroxynitrite, can lead to further cellular damage which can contribute to carcinogenesis.

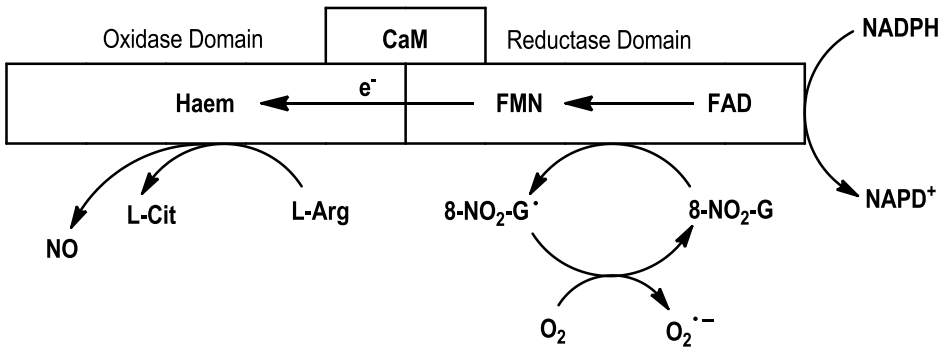

Figure 1.17: Mechanism of superoxide production stimulated by 8-nitroguanosine. Adapted from reference 193[193]

A large proportion of what is currently known about the 8-nitroguanine lesion has been recently established by Bhamra *et al.* However, the miscoding properties of 8-nitroguanine were previously explored by Suzuki *et al.* An oligonucleotide was prepared by photochemical synthesis which contained a single 8-nitrodeoxyguanosine residue.

The oligodeoxynucleotide containing the 8-nitroguanine lesion was then used as template in primer extension reactions in order to study polymerisation past the 8-nitroguanine base. This involved treatment of the photochemically nitrated oligodeoxynucleotide, primed with a 5'-labelled short complementary sequence, with variable amounts of DNA polymerases α, β, η and κ in the presence of four deoxyribonucleotide triphosphates. Synthesis catalysed by polymerases α and β was blocked to a certain extent, one base prior to, or opposite the 8-nitroguanine residue. Of the polymerases that were able to extend past the lesion, cytosine was preferentially incorporated opposite 8-nitroguanine, nevertheless misincorporation of both adenine and guanine was observed. Extension of the primers past the lesion by polymerases η and κ was more efficient, but exhibited a high miscoding frequency and broad miscoding specificity. Direct incorporations of adenine and cytosine were observed along with less significant amounts of guanine and cytosine; in addition one and two base deletions were detected[183].

The evidence presented by Suzuki *et al.* suggests that 8-nitroguanine can be mispaired with adenine in mammalian cells, directly inducing a G→T transversion. They propose that adenine is incorporated opposite the lesion by forming complementary hydrogen bonds with the Hoogsteen face of 8-nitroguanine in the *syn* conformation. However the experiments were conducted using a template-primer system that readily releases the 8-nitroguanine base, so it is also possible the polymerases are in fact placing adenine opposite an abasic site which cause the same transversion mutation[187,194].

The scope of this procedure is limited by a number of factors. Firstly this method is not suitable for preparing oligodeoxynucleotides which contain more than one guanine base. Secondly, the yield of the oligodeoxynucleotides containing the photochemically nitrated nucleoside was only ~3% of the initial concentration[195]. Furthermore, the deoxyribose sugar moiety renders the lesion highly susceptible to hydrolysis of the glycosidic bond. Despite some structural information being obtained using oligomers synthesised by this procedure, the extremely low yields and instability meant this was not the ideal method to determine the physicochemical properties of the lesion.

As chemically incorporating 8-nitrodeoxyguanosine into oligonucleotides is impractical, generation of a suitable hydrolytically stable mimic of this nucleotide was required to explore the chemical and biological effect of the modification. The approach established by Bhamra *et*

al. in the first phase of the project utilised a 2'-*O*-methyl analogue of 8-nitroguanine that could be chemically incorporated into oligodeoxynucleotides.

The synthesis of 8-nitroguanosine and its 2'-fluoro and 5'-azido analogues, considered suitable for biochemical research, has been described by Saito *et al.* The hydrolytic stability of these analogues was assessed and half-lives of 72 and 4.5 days were established for the 2'-fluoro and 5'-azido derivatives respectively[196]. Using this methodology, it was envisioned that the use of an electronegative 2'-*O*-methyl substituent would stabilise the labile glycosidic bond and hence minimise depurination to allow for chemical incorporation into oligodeoxynucleotides.

2'-*O*-Methyl nucleosides have been extensively investigated in comparison to the ribonucleoside and other 2'-modified analogues. Introducing a 2'-*O*-methyl substituent to the nucleoside has a significant effect on the conformation of the sugar. As mentioned previously, the substitution of the hydrogen at the C2' position with a hydroxyl group accounts for the difference in preferred puckering modes of DNA and RNA. Hence, in addition to stabilising the glycosidic bond, substitution with an electronegative group at the 2'-position shows a strong preference to adopt the C3'-*endo* conformation of RNA[197]. The conformational bias imposed on the sugar pucker by the 2'-substituent is relative to the electronegativity of the substituent[197–199].

Replacement of the 2'-hydrogen by a fluorine atom may be considered a more suitable mimic as it does not cause significant steric perturbations to the shape of the molecule. However, despite the 2'-fluoro nucleosides being isoteric to their DNA equivalents, the electronegativity of the substituent would cause these derivatives to adopt a sugar conformation that is increasingly detached from the of the C2'-*endo* conformation of DNA[194,198].

The 2'-*O*-methyl analogue was readily available and its use is advantageous in that the 2'-position of the nucleoside does not require additional protection. The incorporation of a 2'-*O*-methyl substituent allowed for analysis of the chemical and biological properties of the stabilised 8-nitroguanine analogue to be obtained.

The physicochemical data previously obtained by Bhamra *et al.* confirms that 8-nitro-2'-*O*-methylguanosine adopts a *syn* conformation about the glycosidic bond. The evidence for this comes from characteristic shifts in the NMR spectrum of the nucleoside upon adopting the *syn* conformation[200,201]. A significant upfield shift in the 2'-carbon signal of 8-nitro-2'-*O*-methylguanosine was exhibited with respect to the unmodified 2'-*O*-methylguanosine.

Furthermore a downfield shift in the signals corresponding to H2', C1', C3' and C4' were also observed. Analogous data was obtained for 8-bromo-2'-*O*-methylguanosine, which is known to adopt the *syn* conformation, and this was consistent with that of the nitro analogue (Table 1.3)[194]. It has been proposed that the upfield shift of the C2' signal is a consequence of the proximity of the lone pair of electrons on the N3 atoms with the C-H bond at the C2' position[200]. The downfield shift observed for the signal corresponding to the H1' proton is seemingly a feature which is unique to the 8-nitroguanine analogues. The spatial orientation of the H1' proton in relation to the nitro group in the *syn* conformation is proposed to be the basis for this[194].

Nucleoside	H1'	H2'	C1'	C2'	C3'	C4'
2'-O-Me-G	5.82	4.28	85.85	82.73	68.66	84.32
8-Br-2'-O-Me-G	5.79	4.78	88.01	79.79	69.27	86.67
8-NO_2-2'-O-Me-G	6.32	4.68	89.12	80.88	69.55	86.20

Table 1.3: NMR data for studies on the conformation of 8-nitro-2'-*O*-methylguanosine, taken from reference 194[194]

The pK_a of the atoms in a nucleic acid can be used as a measure to determine how it will interact with and behave towards other molecules. The strength of the hydrogen bonds which are formed between complementary base pairs can be correlated to the relative pK_a values of the donor and acceptor atoms of the bases. When modifications lead to deviations in the pK_a of a nucleobase, the bonding geometry and base pairing properties are altered accordingly. Hence, this may be an indication of the potential mutagenicity of a lesion[202–204].

Nucleosides containing the 8-nitroguanine modification have a distinctive UV absorption at approximately 390nm. This enabled the determination of the pK_a for the deprotonation of N1 by analysing the changes in this UV absorption as a function of pH. pK_a values of 8.4 and 8.3 were calculated for 8-nitroguanosine and 8-nitro-2'-*O*-methylguanosine respectively. The data establishes that the nucleosides containing the 8-nitro moiety are significantly more acidic than guanosine and 2'-*O*-methylguanosine which have pK_a values of 9.4 and 9.5 respectively. These results reflect the electron withdrawing capacity of the nitro group[194].

An accurate indication of oligodeoxynucleotide stability can be obtained by measuring the UV absorbance of a DNA duplex at regular intervals as a function of increasing temperature. Upon the formation of a duplex, base stacking is accompanied by a reduction in the absorbance when compared to the corresponding unhybridised strands. The interaction between the π

electrons on neighbouring bases reduces the transition dipoles, hence reducing the ability of the system to absorb light. This results in a reduced UV absorbance of the duplex, which upon dissociation of the two strands is reversed. The thermal melting temperature (T_m) is the temperature at which 50% of the mixture exists as a single stand and 50% exists in the duplex formation[2,205].

Thermal melting studies of duplexes containing the stabilised 8-nitroguanine analogue were performed. The formation of a number of duplexes in which each of the DNA nucleobases are paired with the modified base allows for information on the base pairing preferences to be obtained. The results indicated that there is significant destabilisation of the duplex upon pairing 8-nitroguanine with cytosine. The base pair formed between 8-nitroguanine and a guanine base appears to form the most stable duplex on the basis of it having the highest T_m temperature. However, it is likely that *in vivo* DNA polymerases would discriminate against this pairing due to the poor geometric fit within the helical structure. The 8-nitro moiety seemingly had no effect on the stability of the pairing with adenine or thymine[194].

Further to this, primer extension studies were performed to examine the mutagenic potential of the lesion. Two different polymerases were studied; the polymerase AMV-RT, chosen due to its ability to extend past the 2'-*O*-methyl modification and DNA polymerase β, chosen to provide a direct comparison to previously published results. AMV-RT paired deoxycytidine predominantly opposite the 8-nitro-2'-*O*-methylguanosine analogue, forming a fully extended product. Conversely polymerase β preferentially inserted deoxyadenosine as opposed to deoxycytidine in a ratio of 2:1 and the primers were not fully extended. Extension past the lesion was significantly impaired in both cases. Although the 2'-*O*-methyl substituent may be a factor in this, control experiments established that it did not significantly affect the specificity of the enzyme[194].

While the conclusions drawn from primer extension reactions with polymerase β were in agreement with those previously stated by Suzuki *et al.*[183], the level of incorporation opposite the lesion was not. There are a number of aspects of the systems that may be responsible for the difference seen between the two studies including: the model of the lesion, the pH and the primer extension reaction construct.

The use of running start and standing start reactions can be used to determine the efficiencies and specificities of nucleotide insertion opposite a lesion with respect to a particular DNA polymerase. A standing start, used by Bhamra *et al.*, is defined as a reaction where the first

nucleotide to be incorporated is opposite the position of interest on the template strand. In comparison, Suzuki *et al.* utilised a running start primer extension which requires the polymerase to incorporate one or more nucleotides prior to reaching the position of interest[206]. Both primer template systems have their own merits, but might account for the observed variations.

As previously shown for abasic sites, the sequential actions of more than one polymerase can be required to insert a nucleotide opposite a lesion. Therefore, using this reasoning, it is possible that bypass of the 8-nitroguanine lesion could efficiently be carried out *in vivo* by one or more of the other 14 DNA polymerases the human genome encodes[207].

Overall these findings demonstrate the potential value of further investigation into recognition and repair of this lesion. Oligodeoxynucleotides containing the 8-nitroguanine modification are not widely prepared and studied due to the inherent difficulty in their preparation. Recent results from Bhamra *et al.* have enabled the incorporation of a suitable model of 8-nitrodeoxyguanosine into chemically synthesised DNA. In terms of sugar conformation, the 2'-*O*-methyl analogue populates a configuration closer to that of RNA as opposed to DNA. Nevertheless this is considered a suitable mimic for the scope of this thesis. Not only may 8-nitroguanine function as an endogenous mutagen, but it may also serve as a biomarker for inflammation related carcinogenesis. 8-Nitroguanine is already considered a marker for inflammation and nitrative stress[147], but as the link between sustained production of reactive nitrogen species and the initiation and progression of cancer is strengthened, it is possible that the lesion itself could be exploited as a biomarker for inflammation related cancers.

1.19 Projects aims

It is clear that the 8-nitroguanine lesion plays an important role in mutagenesis, carcinogenesis and is also associated with a poor prognosis of the cancer[191]. To obtain a more detailed understanding of these effects, it is apparent that new and sensitive methods are required to detect the lesion. A major aim of this thesis is to study the reactions of the 8-nitroguanine modification to understand how it differs from guanine and to develop new methods for its detection. Additionally this work initiates studies aimed at investigating whether mechanisms exist to repair this lesion.

More specifically the following studies have been undertaken:

- Synthesis of oligodeoxynucleotides containing the 8-nitroguanine modification (Chapter 2).
- Reactions of 8-nitroguanine nucleosides and oligodeoxynucleotides (Chapter 3).
- Detection of the 8-nitroguanine lesion using surface enhanced (resonance) Raman spectroscopy (Chapter 4).
- Studies towards the synthesis of 8-nitroguanosine triphosphate to investigate repair by MutT (Chapter 5).

Chapter 2

Results and Discussion 1:

Synthesis of oligodeoxynucleotides containing the 8-nitroguanine modification

2 Result and Discussion 1

2.1 Proposed route for the synthesis of 8-nitroguanine nucleosides

Prior to the start of this project in 2010, Saito had developed a simple method for the nitration of guanosine nucleosides[196]. This method was subsequently adapted by a postdoctoral worker (Dr. I. Bhamra) within our research group to prepare 8-nitro-2'-*O*-methylguanosine phosphoramidite for incorporation into oligodeoxynucleotides[194]. The initial part of this project was to repeat the preparation of this monomer, with the additional aim of trying to optimise the critical nitration step which proceeded in low yield. The work in this chapter is based on the generation of 8-nitroguanine nucleosides derived from 2'-*O*-methylribose, but it has also been applied to the corresponding ribose derivative (Chapter 3).

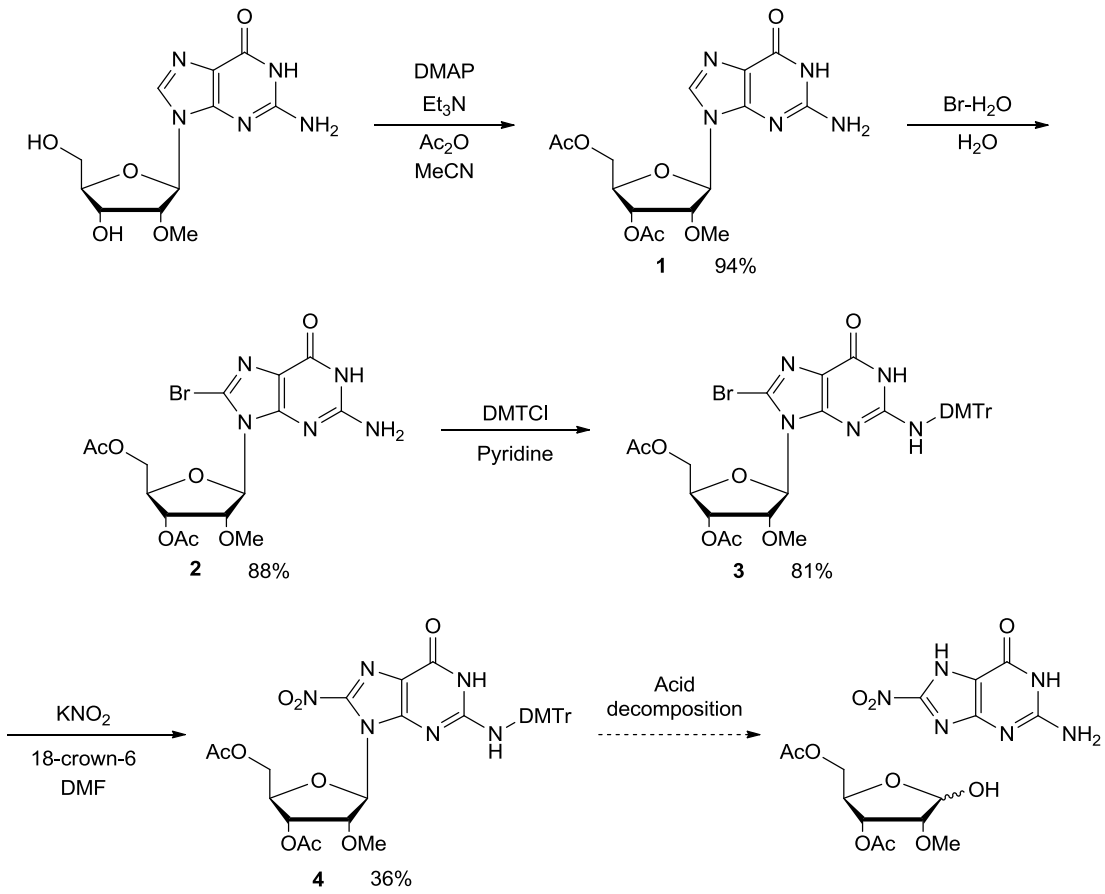

Scheme 2.1: Synthetic route to 8-nitro-2'-*O*-methylguanosine.

The individual steps for the synthesis of 8-nitro-2'-*O*-methylguanosine are shown in Scheme 2.1 and will now be discussed individually. The first step in the scheme is protection of the hydroxyl groups of the sugar component. Protection of these groups was necessary to prevent

unwanted side reactions from occurring and to ensure selective reaction at the C8 position in subsequent steps.

The acetyl protecting group was considered appropriate for this because it is removed under basic conditions. As alluded to in Chapter 1, the nitro group greatly increases the lability of the glycosidic bond[181]. Despite the extra stabilisation provided by the 2'-*O*-methyl group, under acidic conditions the glycosidic bond remains susceptible to hydrolysis. Therefore exposure to acidic conditions must be kept to a minimum in order to produce a sufficient quantity of the nitrated nucleoside.

Reaction of 2'-*O*-methylguanosine with triethylamine and acetic anhydride in the presence of a 4-dimethylaminopyridine (DMAP) catalyst generated the acetyl protected nucleoside in a 94% yield. DMAP acts as a nucleophilic catalyst increasing the rate of the esterification reaction[208]. Analysis of the product by ^{1}H NMR spectroscopy confirmed the addition of the acetyl protecting groups due to the presence of two singlets at 2.07 and 2.13 ppm corresponding to the CH_3 groups.

Following this, an electrophilic bromination reaction was carried out at the C8 position. Treatment of the acetylated 2'-*O*-methylguanosine with saturated bromine water formed the desired compound (**2**) in a yield of 88%. Evidence for the formation of the 8-bromo derivative included the disappearance of the peak corresponding to H8 at 7.98 ppm in the ^{1}H NMR. Additionally mass spectrometry demonstrated an isotopic pattern corresponding to the incorporation of a bromine atom into the molecule.

The exocyclic amine moiety *N2* was then protected using dimethoxytrityl chloride (DMTCl) to give the fully protected nucleoside (**3**) in an 81% yield. Using a DMT protecting group has the advantage of greatly improving the solubility of the nucleoside in a range of organic solvents as prior to this step the compound was incredibly insoluble. The reaction was particularly sensitive to the presence of water, as it can quench the DMT cation formed during the S_N1 reaction; therefore to ensure complete conversion the reaction was carried out under stringent anhydrous conditions. The use of anhydrous pyridine as the solvent not only ensured the exclusion of water from the reaction it also acts as an acid scavenger so any HCl generated *in situ* was neutralised. Diagnostic peaks in the ^{1}H NMR spectrum of the *N2*-DMT nucleoside are a peak at 3.71-3.72 corresponding to the six methoxy protons and the appearance of aromatic protons at 6.90-7.14 ppm.

Largely the synthesis proceeded as reported and isolated yields were typical of those stated previously[196]. However the yields produced during the conversion of the 8-bromo analogue (**3**) to the 8-nitro analogue (**4**) were not in agreement with those stated by Saito *et al*. The reaction was carried out using a large excess of both 18-crown-6 and potassium nitrite, in DMF and was heated at 100°C for 6 hours. The high temperature is necessary to solubilise the potassium nitrite.

Crown ethers are recognised as chelating agents[209,210]. Ion-dipole interactions form between a cation and the oxygen atoms of the polyether ring generating a stable complex. The size of the cavity is an important factor in determining which cations are complexed; 18-crown-6 is selective for potassium cations (or cations of a similar size)[209]. Hence, 18-crown-6 is capable of chelating the K^+ cation from the ionic salt KNO_2 thereby improving the nucleophilicity of the NO_2^- anion.

The reaction was monitored by reverse phase (RP) high performance liquid chromatography (HPLC) in order to closely follow the conversion to the nitro compound; this also enabled us to limit the production of decomposition products, formed under the harsh conditions, by stopping the reaction when these became significant. Analysis of the major decomposition products identified the detritylated and the depurinated species. The UV absorption of the 8-nitroguanine base provides an efficient method for identifying whether the nitro functionality has been incorporated into a molecule. In contrast to the starting material, introduction of the nitro group gives the nucleoside a unique UV absorption at ~400nm; therefore it is possible to change the detection wavelength on the HPLC so that only molecules containing the 8-nitroguanine base are seen. This proved useful not only in identifying the product but also in monitoring the level of unwanted depurination which gives 8-nitoguanine as a by-product under the harsh conditions.

Initially, consistently low yields of ~20% were achieved for the nitrated nucleoside and it was apparent that optimisation of the reaction was necessary. However, due to uncertainty regarding the mechanism by which the reaction proceeds, identifying conditions to improve the yield or elucidate the reaction mechanism have proved problematic. Although the reaction *in vivo* with peroxynitrite and its secondary reaction products are thought to proceed *via* a radical based mechanism, it is not clear whether this is the case for the reaction with KNO_2. It is possible that the reaction could alternatively occur *via* an addition-elimination type mechanism (Figure 2.1).

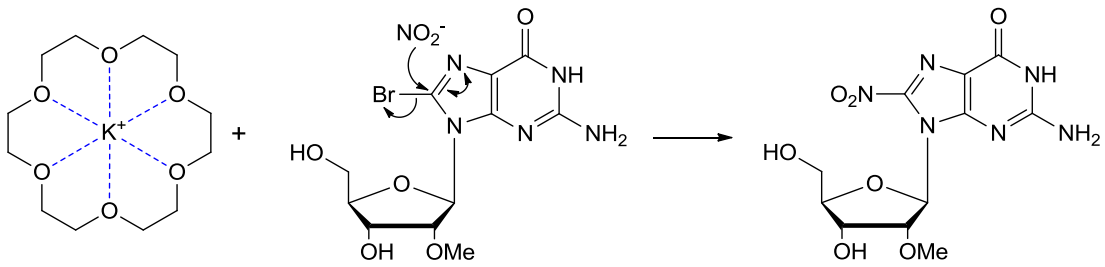

Figure 2.1: Addition-elimination type reaction to form 8-nitroguanine.

The first attempts to optimise the reaction conditions involved varying the reaction period and solvent. In addition to those previously examined by Saito *et al.*, which used DMF and MeCN, the high boiling point solvent DMSO was investigated. The use of a polar aprotic solvent was required to facilitate solvation of the cation, leaving the anion free to readily react with the nucleoside. While acetonitrile generated very low yields of the nitrated nucleosides, DMF and DMSO both produced yields comparable to those previously achieved (~20%). Owing to the fact that DMSO has a higher boiling point and its removal was more problematic during purification, DMF was chosen as the most favourable solvent.

In an attempt to determine whether the nitration proceeds *via* a radical or nucleophilic pathway, a radical initiator, azobisisobutyronitrile (AIBN), was added to the reaction. It was apparent that the radical initiator had no effect on the reaction rate or yield. This suggests that synthetically, a radical mechanism is not in operation as if this was the case there would have been a significant improvement in the reaction. However additional mechanistic investigation would be required to provide unambiguous proof of this. Further failed optimisation attempts have included; the use of an alternative source of nitrite (sodium nitrite and tetrabutylammonium nitrite), addressing the necessity of anhydrous conditions and an inert atmosphere and varying the number of equivalents of each reagent used.

Efforts to optimise the reaction by varying the concentration illustrated that the reaction shows a high concentration dependence. The optimal concentration was found to be 0.01mM of the nucleoside achieving an improved yield of 36%. This suggests that there may be competing pathways in operation reducing the amount of the desired product generated.

Speculating upon possible causes for the consistently low yields, it was considered that the bromide ion displaced during the reaction could theoretically undergo a further addition-elimination reaction on the nitro compound to regenerate the starting nucleoside. This would account for the absence of by-products formed during the reaction. In order to investigate this,

silver (I) salts ($AgNO_3$) were added to small scale reactions. The silver would sequester the free bromide ion from the reaction mixture thus eliminate the competing reaction pathway. However in the presence of the silver salts the yields were essentially unchanged suggesting that displacement of the nitro group by bromide was not a significant reaction.

Unfortunately no further improvement on the 36% yield for the formation of the nitrated nucleoside could be obtained. Despite the yield being low, it was considered acceptable as it was possible to recover a significant amount of starting material which could be recycled and thereby generate a sufficient quantity of the desired product.

The absence of protons close to the site of nitration resulted in a ^{1}H NMR spectra similar to that of the 8-bromo nucleoside, with the only significant difference being the downfield shift in the H1 proton. This is a consequence of the close proximity of the nitro group in the preferred *syn* conformation of the nucleoside. Confirmation of the incorporation of the nitro group is evident in the ^{13}C NMR as the peak corresponding to C8 shifts from 121.60ppm to 151.80ppm from the starting material to product respectively[194]. Furthermore, mass spectrometry indicated the presence of one isotope with an accurate mass consistent with that of the nitrated nucleoside.

2.2 Manipulation of the protecting groups

The fully protected 8-nitroguanine nucleosides are common intermediates which required further modification depending on the requirements of the project. One application is the incorporation into oligodeoxynucleotides. In order to prepare the nucleoside, manipulation of the protecting groups was necessary (Scheme 2.2).

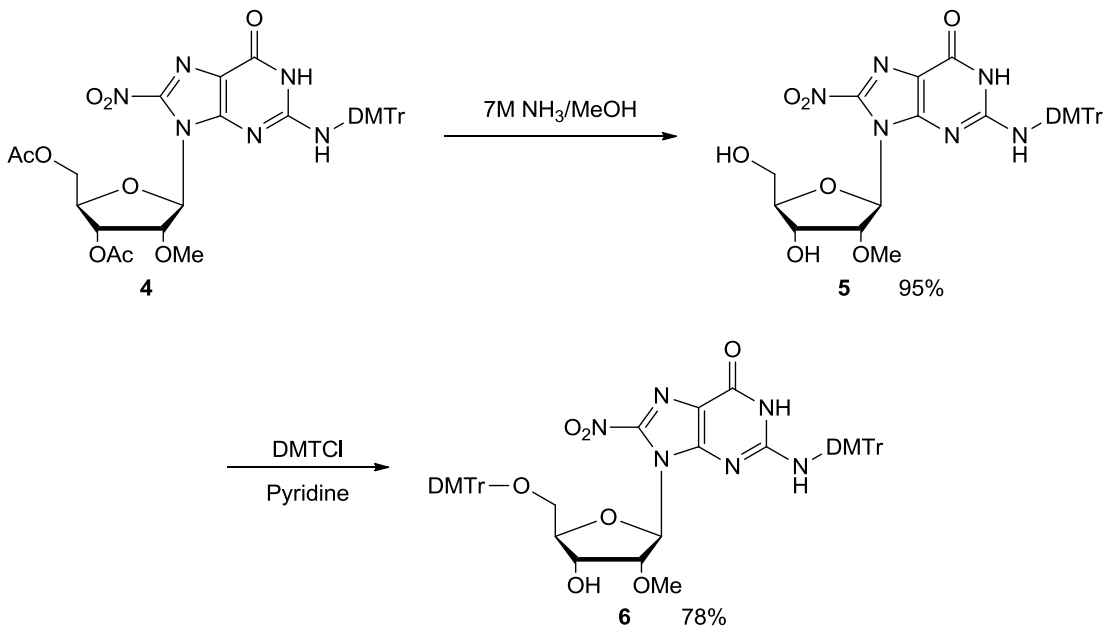

Scheme 2.2: Synthetic route for the generation of 5'-*O,N2*-bis-dimethoxytrityl-8-nitro-2'-*O*-methylguanosine.

Typical for acetyl protecting groups, deprotection was carried out using methanolic ammonia which reacts with the ester (**4**) to form acetamide and the unprotected alcohol (**5**). Despite the reaction taking several days, the method is appropriate as it does not cause decomposition of the nucleoside. Removal of the excess base followed by purification by flash column chromatography afforded *N2*-dimethoxytrityl-8-nitro-2'-*O*-methylguanosine (**5**) in a nearly quantitative yield (95%). Confirmation of the deprotection was seen in the ^{1}H NMR spectra due to the disappearance of the peaks at 2.09 and 2.05ppm corresponding to the CH_3 group of the methyl esters.

Protection at the 5'-hydroxyl group was then required; firstly, to ensure selective reaction at the 3'-hydroxyl group in subsequent steps and secondly, they are the desired substrates for solid-phase synthesis which will be discussed later in the chapter. Selective protection of the primary 5'-hydroxyl group over the secondary 3'-hydroxyl group of nucleoside was achieved using DMTCl in anhydrous pyridine. The reaction proceeds *via* an S_N1 mechanism. The predominance of the 5'-isomer is attributed to the steric bulk of the DMT cation and the greater nucleophilicity of the primary 5'-hydroxyl group.

Whilst substitution is favoured at the 5'-position, the formation of small amounts of the di-substituted nucleoside was observed. This was kept to a minimum by using a reduced number of molar equivalents of DMTCl and performing the reaction under moderate dilution.

Purification of the crude material by flash column chromatography afforded the 5'-*O,N2*-bis-dimethoxytrityl-8-nitro-2'-*O*-methylguanosine (**6**) in a 78% yield. Addition of the second DMT protecting group was confirmed by a twofold increase in the integration of the peaks resulting from the trityl moiety.

2.3 Synthesis of the 8-nitroguanine phosphoramidite

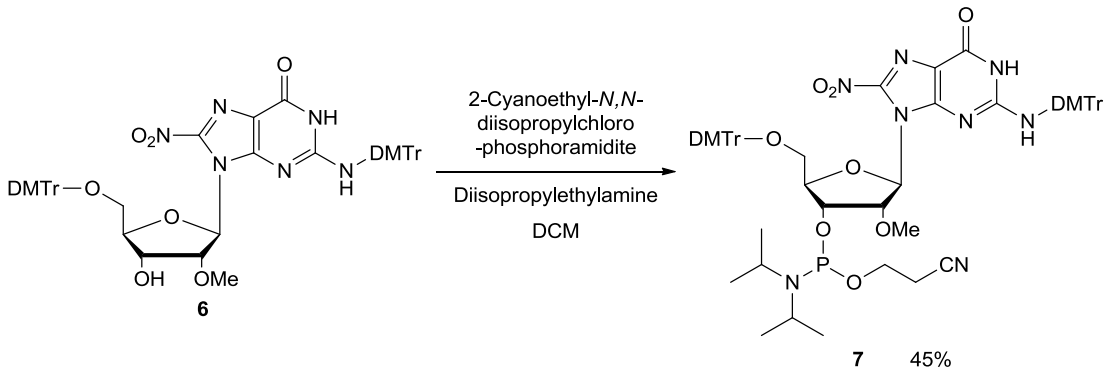

Scheme 2.3: Formation of the 8-nitro-2'-*O*-methylguanosine phosphoramidite.

Since the 5'-hydroxyl group is a more effective nucleophile than the secondary 3'-hydroxyl group, the phosphite group is best placed on the 3'-position to ensure efficient coupling during DNA synthesis. Following manipulation of the protecting groups, the suitably protected nucleoside underwent functionalization with 2-cyanoethyl-*N,N*-diisopropylchlorophosphoramidite in the presence of a non-nucleophilic base *N,N*-diisopropylethylamine to afford the phosphoramidite required for incorporation of the modification into oligodeoxynucleotides.

The phosphitylation reaction proved difficult for a number of reasons. Firstly, monitoring the phosphitylation reaction was problematic. The retention factor (R_f) for both the starting material and the product were identical in various solvents, as a result the only indication that the reaction was proceeding was a slight colour change on developing the TLC plate with the *p*-anisaldehyde stain. Secondly, the product was extremely sensitive to both oxidation and hydrolysis; however, exposure to these conditions was required in order to isolate the compound. Purification was carried out quickly and carefully under a nitrogen atmosphere to prevent decomposition of the phosphoramidite. Together these factors account for the low yield (45%).

The phosphorus atom in the phosphoramidite assumes a tetrahedral geometry, on account of it having three different substituents and a lone pair. Therefore due to the chiral centre, the phosphoramidite is generated as a mixture of two diastereoisomers. Both diastereoisomers were suitable for DNA synthesis since upon oxidation of the P(III) compound to the P(V) compound and subsequent deprotection of the 2-cyanoethyl group, the presence of two non-bridging oxygens causes the phosphorus atom to become achiral. Conveniently this meant that separation of the two diastereoisomer was not necessary.

Despite the factors complicating the synthesis and isolation of the phosphoramidite (**7**), the diastereoisomers were recovered in a reasonable yield (45%). Although ^{1}H NMR could only be tentatively assigned, the appearance of aliphatic protons corresponding to the isopropyl amine and 2-cyanoethyl moieties was evident. Analysis by ^{31}P NMR confirmed formation of the phosphoramidites as two distinct peaks at 152.06ppm and 150.57ppm corresponding to each diastereoisomer were identified.

2.4 Introduction to solid-phase synthesis

The solid-phase synthesis of nucleic acids is an automated method in which monomers are sequentially coupled to growing oligonucleotide sequence which is bound to a solid-support. The principle of solid-phase chemical synthesis was first developed by Bruce Merrifield in 1963 which later (1984) earned him a Nobel Prize. The concept involved the tethering of the final amino acid in a peptide to a solid-support, followed by the sequential covalent linkage of the relevant amino acids to the fixed terminus. This elegant method allowed for reagents to be washed away from the resin following each synthetic step and upon completion of the sequence, the polypeptide was readily detached from the solid-support[211,212]. It was apparent that this solid-phase technique could be applicable to monomeric units other than amino acids; consequently the technique was adapted for the generation of oligonucleotides.

Although various methodologies have been developed for the preparation of oligonucleotides; the phosphoramidite approach (Figure 2.2) is currently the most widely applied[213,214]. Phosphoramidite chemistry was first established by Beaucage and Caruthers in 1981[215], based upon the phosphite-triester approach originally developed by Lestinger and Ogilvie[216,217]. The subtle exchange of a chloride leaving group for an amine functionality was fundamental in the development of the rapid, robust and efficient means by which oligonucleotides are prepared today.

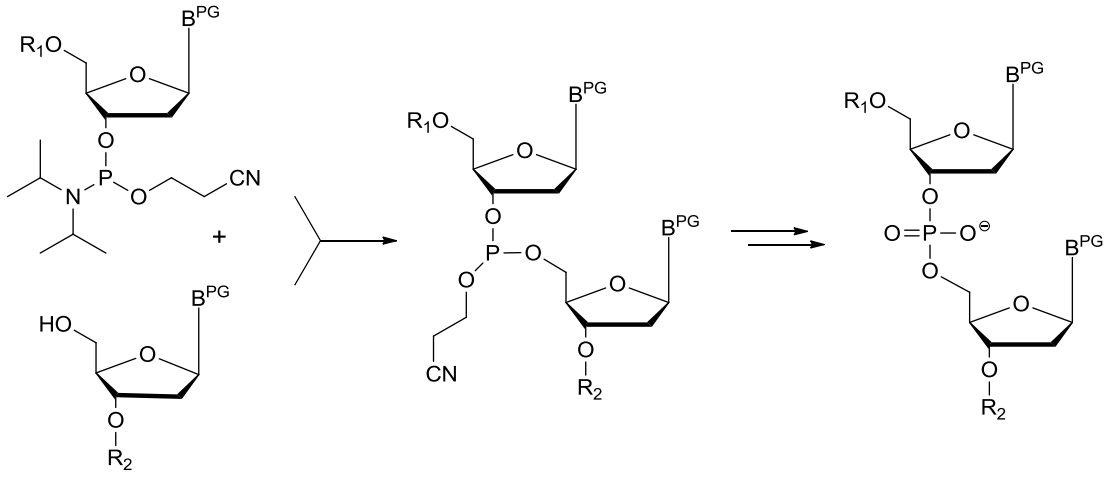

Figure 2.2: The generic phosphoramidite route to oligodeoxynucleotides.

Using this methodology, activated phosphoramidites are sequentially coupled to a growing oligonucleotide chain that is tethered to an insoluble support. In contrast to enzymatic DNA synthesis, chain elongation occurs in 3'- to 5'-direction. Therefore the oligonucleotide is bound to the solid-support *via* the 3'-terminal residue. Reverse oligonucleotide synthesis, that is, in a 5'- to 3'-direction can also be achieved; however this approach has not been utilised to the same extent[218,219].

2.5 Protecting groups

In 1961 Khorana *et al.* introduced the concept of a protecting group scheme which allowed for the selective removal of a particular group, at a given time, to facilitate sequential oligonucleotide synthesis; this concept is still used today[220,221]. The reactions utilised in DNA synthesis must take into consideration the high sensitivity of nucleic acids to a wide range of chemical reagents; therefore mild reaction conditions are required. A number of key criteria must be met for a protecting group to be compatible with DNA synthesis including; compatibility with reagents used during solid-phase synthesis, commercial availability and enhancing the solubility of the nucleoside.

All nucleophilic moieties that are not directly involved in the coupling require suitable protection, to ensure that only the desired oligonucleotide product is generated. These include; the exocyclic amino groups of the heterocyclic bases, the 5'-hydroxyl group and the phosphoryl oxygen of phosphoramidite moiety. Since all standard nucleosides are 2'-deoxyribose sugars and the 2'-*O*-methyl substituent present on the modified nucleoside is permanently protected

and the therefore does not require additional protection, it is not necessary for the scope of this thesis to discuss protection of the 2'-hydroxyl group.

2.5.1 Exocyclic amine nucleobase protecting groups

The nucleobase protecting groups must be retained throughout assembly of the complete oligonucleotide as the residues are susceptible to reactions with electrophilic reagents. It is therefore appropriate to use base labile protecting groups since cleavage of the full length oligonucleotide from the solid-support is performed under basic conditions at the end of the synthesis.

With the exception of thymine, which lacks an exocyclic amine functionality, all the other nucleobases require protection. In addition to preventing reactions from occurring at these positions, protection can be advantageous in enhancing the solubility of the nucleosides.

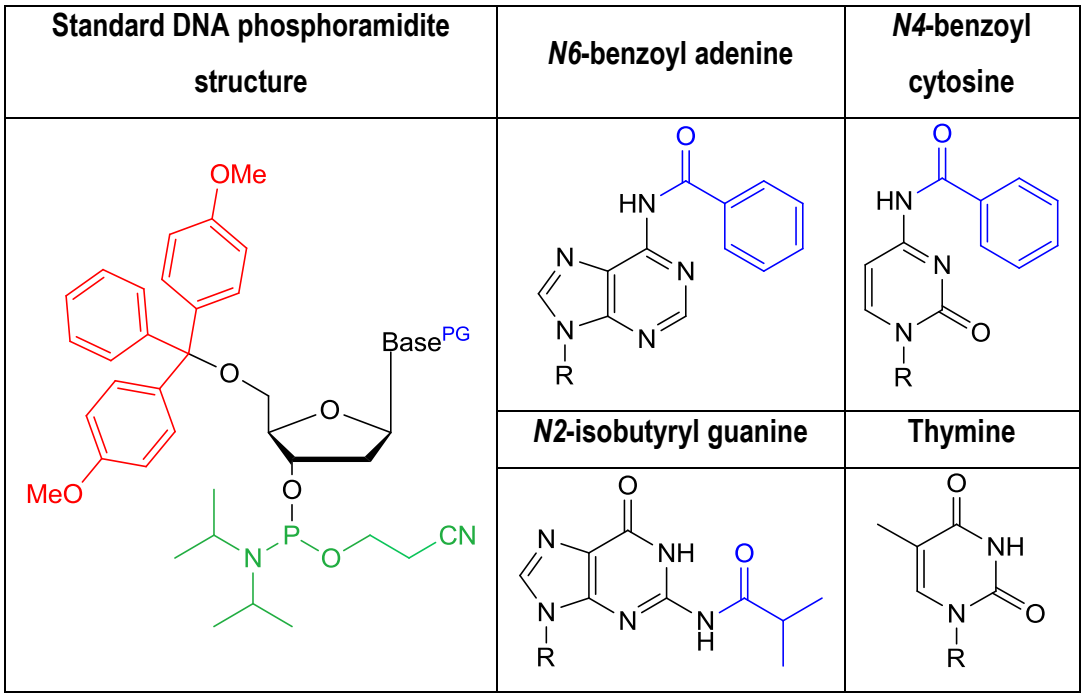

Figure 2.3: General structure of the phosphoramidites utilised during oligodeoxynucleotide synthesis (left) and the exocyclic amine protecting group for each nucleobase (right). Note PG = protecting group.

The classically protected DNA nucleoside phosphoramidites utilised in all oligodeoxynucleotide syntheses outlined in this thesis are show in Figure 2.3. A benzoyl group is used to protect adenine and cytosine while an isobutyryl group is used to protect guanine[215]. Alternative protection schemes involving *N4*-acetyl-2'-deoxycytidine and *N2*-dimethylformamidine-2'-deoxyguanosine phosphoramidites are now widely used when modifications render oligodeoxynucleotides unable to withstand strongly basic conditions[214]. These protecting

groups are removed readily under conditions milder than those employed for the standard protecting groups. However for the scope of this thesis the use of these more labile protecting groups was not necessary.

It was established in the first phase of this project conducted by Dr. I. Bhamra that the reactivity of the guanine base is significantly reduced by the incorporation of a nitro group at the C8 position. Consequently, permanent protection of the exocyclic amine group was considered not to be necessary. The DMT group retained at the N2 position was sufficient to enhance the solubility of the nucleoside; although it was undoubtedly removed during the subsequent detritylation steps of DNA synthesis[194].

2.5.2 5'-Hydroxy protecting group

During solid-phase synthesis, the removal of the 5'-hydroxyl protecting group is required prior to the introduction of the subsequent nucleoside in the sequence. This sequential removal of protecting groups is the basis upon which the formation of unwanted by-products is avoided during oligodeoxynucleotide synthesis. As the solid-support and nucleobase protecting groups must be retained throughout assembly of the complete oligonucleotide, it is essential that the temporary protecting group on the 5'-position of the nucleoside is orthogonal to this.

The classical triphenylmethyl (trityl) protecting group was largely unsuitable for the synthesis of oligodeoxynucleotides due to its cleavage conditions being sufficient to cause significant hydrolysis of the glycosidic bond of the acid labile purine nucleosides after repeated cycles of DNA synthesis. To avoid the use of strong acids for an extended period of time alternative trityl protecting groups were investigated. Introduction of a *p*-methoxy group to the trityl chlorides resulted in an increased rate of reaction and improved hydrolysis conditions acceptable for the use with DNA. Therefore, Smith *et al.* proposed the use of the DMT protecting group which combines good general stability with easy removal under mild acid conditions[221,222].

The dimethoxytrityl ether cleaves readily under acidic conditions as it forms a highly stabilised carbocation. The electron donating *p*-methoxy substituent increases the acid lability of the protecting group by offering higher resonance stabilisation to the carbocation formed during cleavage[222]. In addition to achieving high yields, retention of the DMT group during RP-HPLC purification ensures that failure sequences are well separated from the full length product. The DMT cation has a distinctive colour, which can be exploited as a diagnostic tool for measuring coupling efficiencies. Efficiencies of each cycle of nucleoside addition can be approximated by measuring the absorbance of the detritylation eluent and comparing it to that of the previous

step. The cation has a high extinction coefficient; consequently accurate measurements quantifying low concentrations of the species can be obtained. Nevertheless, these spectrophotometric methods can only be used as a guide for assessing coupling efficiencies and will be discussed in more detail later in the chapter. Interestingly, the distinctive colours of a range of triarylmethyl protecting groups have been exploited by Caruthers *et al.* in a colour-coded method to confirm the sequence of synthetic oligonucleotides[223].

2.5.3 Phosphite protecting group

A protecting group is also required for the anionic site of the oligodeoxynucleotide backbone; a variety of protecting groups have been evaluated for this purpose. During the 1980's a methyl ester protecting group was used in solid-phase oligonucleotide syntheses. Evidence that the protecting group could cause small amounts of methylation at the N3 position of thymine, in addition to its unpleasant deprotection conditions lead to the development of an alternative protection scheme[224]. Tenner first described the 2-cyanoethyl group as a protecting group for phosphates in 1961[225] and it was used by Letsinger and Ogilvie in early phosphotriester coupling reactions[226]. However, it was not until it was reintroduced by Sinha *et al.* and used in conjunction with the phosphoramidite approach, that this protecting group became the preferred choice for oligonucleotide synthesis[224].

The 2-cyanoethyl protecting group is compatible with solid-phase synthesis conditions and is conveniently removed under mild alkaline conditions, alongside the other permanent nucleobase protecting groups after generation of the full length oligonucleotide. As a consequence of the electron withdrawing 2-cyanoethyl protecting group, the phosphorus centre of the phosphite triester is rendered highly electrophilic. Therefore, reaction with the 5'-hydroxyl group of the support bound nucleoside is favourable.

Although in large scale syntheses, alkylation of the thymine base during ammonolysis has been detected[227], it is not normally considered to be a significant problem for small scale reactions. Therefore cleavage from the support and deprotection can be performed using standard deprotection conditions without modification of the thymine residues in DNA.

2.5.4 Solid-support and Linker

The use of an appropriate solid-support is a consideration in efficient oligonucleotide synthesis. Many solid-supports have been developed; of these, controlled-pore glass (CPG) and polystyrene are the most prevalent. The support is held in a small synthesis 'column' that acts

as the reaction vessel, the dimensions of which can vary considerably dependant on the scale of the synthesis.

The solid-support utilised for the DNA synthesis described in this thesis was a 500Å CPG consisting of deep pores and channels where the protected oligonucleotide is attached. The CPG provides a unique composition with a uniform pore size, which does not swell in organic solvents. Thus excess reagents can be efficiently rinsed from the column to avoid interference in subsequent steps of the synthesis. The rigidity of the support allows high flow rates of solvent and reagents.

CPG supports can be defined by the diameter of their pores, which range from 500Å to 3000Å. Oligonucleotide assembly is strictly limited by the pore size; therefore, a larger pore size is required for the synthesis of a longer length oligonucleotide. The use of a support in which the pore diameter is too small, risks blockage and a reduction in the diffusion of the reagents through the matrix as the synthesis proceeds. Steric considerations factor in the loading density of the CPG. A loading within a narrow range of 30-60µmol g^{-1} is maintained to avoid crowding between chains and to achieve suitable coupling efficiencies[2]. The typical loading of the CPG can differ depending on the batch, consequently yield can vary accordingly.

For the work described in this thesis, oligodeoxynucleotides greater than two units in length were prepared from supports purchased with the 3'-terminal residue pre-attached to the CPG support. The preparation of oligonucleotides which contain a modified nucleoside at the 3'-terminus require the use of an alternative, so called universal support which can accommodate this. As this is applicable to the dinucleotides prepared in this thesis, universal supports will be discussed in more detail where appropriate.

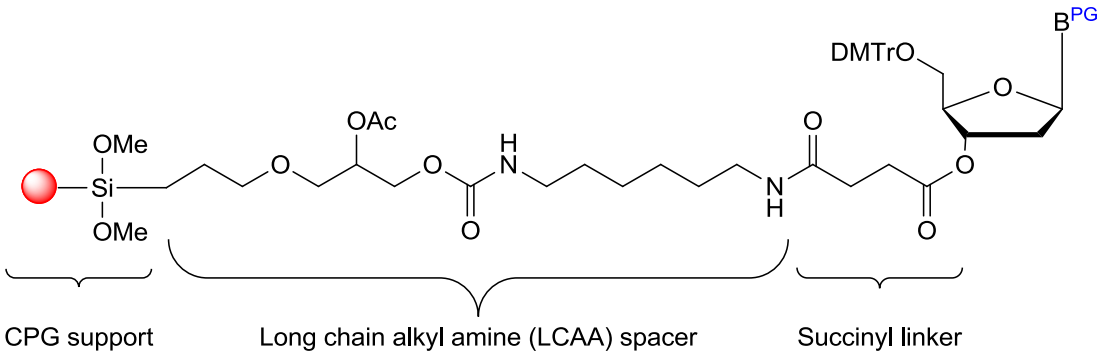

Figure 2.4: The solid-support consisting of the 3'-nucleoside connected to the CPG *via* a succinyl linker and a long chain spacer. Note PG = protecting group.

The linker and spacer between the matrix and the functionalised 3'-terminal nucleoside have been extensively researched. Primarily to optimise the spacer length and chemical structure of silica based solid-supports. In this case, the CPG support was functionalised with a long chain alkyl amine (LCAA) and a succinyl linker as shown in Figure 2.4[228]. Upon complete assembly of the full length oligodeoxynucleotide, it can be readily released from the solid-support and eluted from the column.

2.5.5 Reaction scheme for solid-phase DNA synthesis

A general reaction scheme for solid-phase synthesis is presented in Figure 2.5.

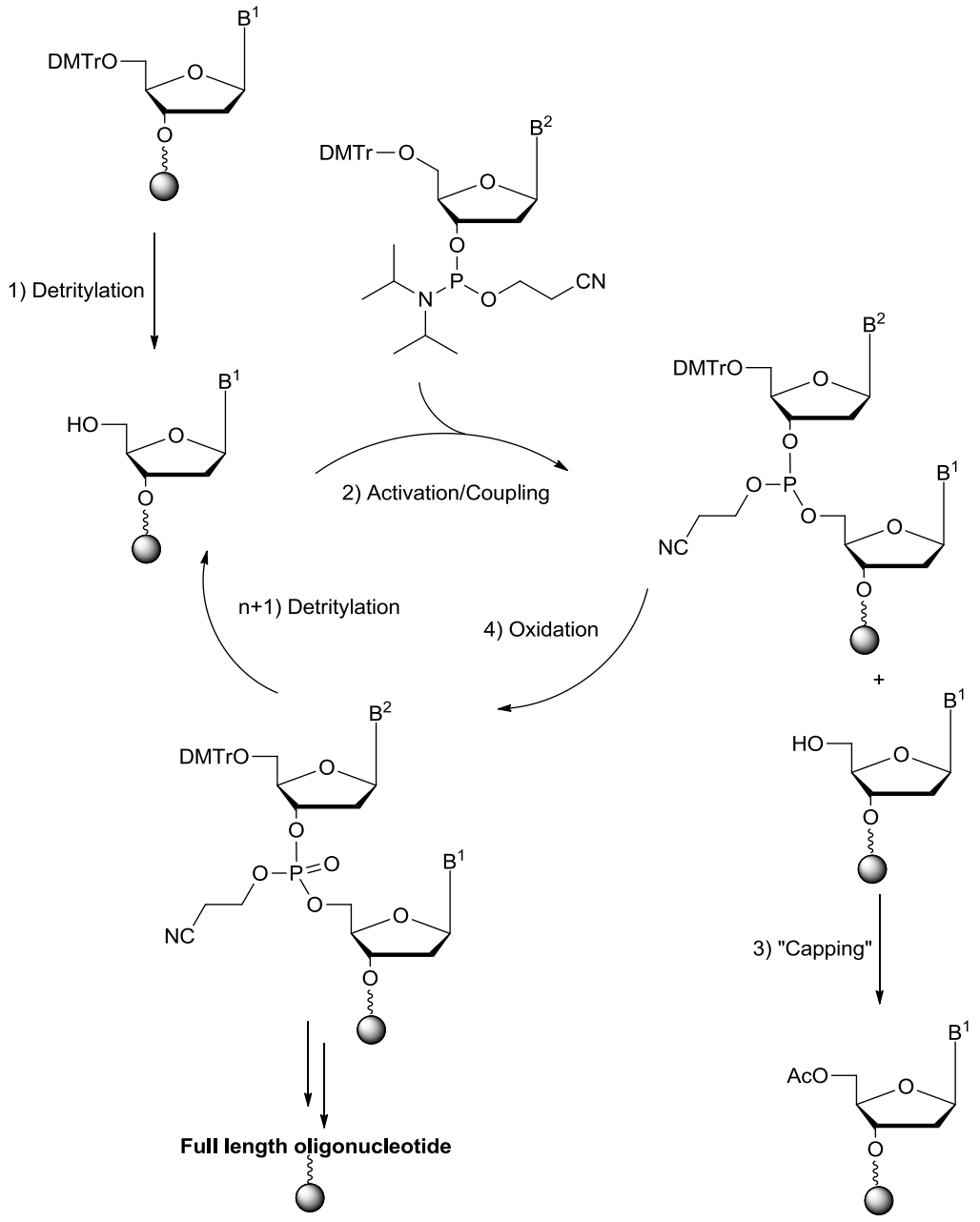

Figure 2.5: The solid-phase synthesis of oligodeoxynucleotides *via* the phosphoramidite approach.

Step 1: Detritylation

Detritylation (also known as deblocking) of the 5'-hydroxyl group of the terminal nucleoside bound to the solid-support is carried out under relatively mild conditions due to the lability of the activated DMT groups to weak acid. Treatment with 3% trichlororacetic acid (TCA) in dichloromethane (DCM) is suitably acidic to afford the free 5'-hydroxyl group. The reaction proceeds rapidly which is valuable in minimising depurination of acid labile nucleosides.

Step 2: Activation and Coupling

The coupling reaction can effectively be described as the substitution of the amine functionality of the phosphoramidite with the 5'-terminal hydroxyl group of the solid-support bound nucleoside; however the mechanism for this transformation is more complex. The phosphoramidite which corresponds to the second residue in the oligonucleotide sequence requires activation prior to its incorporation.

Efficient activators are required to act as an acid to protonate the diisopropylamino group of the phosphoramidite, a good nucleophile to ensure rapid conversion to the activated intermediate and finally a good leaving group to enable the formation of the phosphite triester. Furthermore, the pK_a of the acid is required to be high enough to ensure that it does not prematurely remove the DMT group from the phosphoramidite reagent, yet still acidic enough in order to assist in the activation of the phosphoramidite. Typically, tetrazole based activators are used for this purpose[229].

The originally used 1*H*-tetrazole has been increasingly replaced by alternative activators which exhibit improved coupling efficiencies and generate greater oligodeoxynucleotide yields. One of the most commonly used tetrazole based activators is 5-ethylthio-1*H*-tetrazole (ETT) and it has been used exclusively in the solid-phase synthesis outlined in this thesis.

ETT has lower pK_a (4.28) than that of 1*H*-tetrazole (4.89)[230], as a consequence of the electron withdrawing group at the C5 position. The higher acidity of the activator renders it a better proton donor, thus generation of the active intermediate is more readily achieved leading to an increased rate of reaction. The efficiency of activation can additionally be improved with an activator solution of a higher concentration. It is therefore important that the activator does not have a low solubility in acetonitrile as this can lead to crystallisation in the DNA synthesiser at low temperatures, as can occur for 1*H*-tetrazole. Accordingly the higher solubility of ETT in acetonitrile is advantageous in improving the efficiency of the synthesis[229].

Step 3: Capping

While the efficiency of the coupling step is very high (99%), it has a finite failure rate. Consequently, there will be a small number (typically 0.1 to 1% abundance) of unreacted 5'-hydroxyl groups of the solid-support bound nucleoside. If these were to remain exposed, they would be available to participate in the successive coupling step. The resulting oligodeoxynucleotide would lack one nucleoside relative to the full length oligodeoxynucleotide; thus corresponding to a deletion mutation. As these deletion mutations would accumulate following each coupling reaction, upon completion of the synthesis a complex mixture of oligodeoxynucleotides would be obtained.

To prevent this, unreacted 5'-hydroxyl groups are acetylated using a mixture of acetic anhydride and *N*-methylimidazole in tetrahydrofuran and pyridine. This capping procedure serves to permanently block these positions to avoid further reactions in successive coupling reactions.

Step 4: Oxidation

The last step in the synthetic cycle involves oxidation of the phosphite triester to form a pentavalent phosphate triester, a protected precursor to the phosphate linkage between neighbouring nucleosides in an oligodeoxynucleotide. The phosphite triester is fairly unstable and susceptible to cleavage by acid, therefore it is necessary to stabilise the backbone prior to the following TCA detritylation step. This is achieved using a solution of iodine in THF in the presence of water acting as an oxygen donor and pyridine acting as a base. The conditions are mild to avoid the unwanted oxidation of the nucleobases.

Following oxidation, the synthetic cycle relating to the addition of one nucleotide to the sequence is completed. Steps 1 to 4 are repeated for each nucleotide in the sequence.

2.6 Synthesis of oligodeoxynucleotides containing 8-nitroguanine

The detailed protocol for the synthesis of oligodeoxynucleotides containing 8-nitro-2'-*O*-methylguanosine is presented in the experimental section. However the essential alterations for inclusion of this modification are as follows:

- The concentration of the 8-nitro-2'-*O*-methylguanosine phosphoramidite was increased from 0.1M to 0.12M.
- The coupling time was increased from 30 to 70 seconds.

- Removal of the final DMT group, following RP-HPLC purification used 20% acetic acid in distilled water rather than the typical 80% acetic acid solution.

All oligodeoxynucleotides were prepared with the final DMT group retained (DMT-on) in order to facilitate purification by RP-HPLC.

2.7 Oligodeoxynucleotides synthesised

Overall six different oligodeoxynucleotides were successfully prepared; these are shown in Table 2.1. The site 1 oligodeoxynucleotide is a 13mer containing a centrally placed 8-nitroguanine base and also contains all four natural nucleobases. It was originally prepared by Bhamra *et al.* to study the base pairing preferences of 8-nitroguanine[194], but was prepared in this study to investigate the reactivity of the 8-nitroguanine base in oligodeoxynucleotides. Chemical modifications of the site 1 sequences are described in detail in the Chapter 3. The site 2 and site 3 oligodeoxynucleotides were prepared primarily as examples of longer oligodeoxynucleotides containing the 8-nitroguanine modification. These sequences also correspond to parts of the *lac* operon and were used to study *in vivo* replication and repair of the 8-nitroguanine lesion (see future work). Control sequences containing 2'-*O*-methylguanosine were also prepared.

Oligodeoxynucleotide	Sequence
Site 1 control	d(GCGTAC**G***CATGCG)
Site 1	d(GCGTAC**G****CATGCG)
Site 2 control	5'-d(GCGCAACGCAATTAATGT**G***AGTTAGCTCACTCATTAG)-3'
Site 2	5'-d(GCGCAACGCAATTAATGT**G****AGTTAGCTCACTCATTAG)-3'
Site 3 control	5'-d(GTGACTGG**G***AAAACCCTGGCGTTACCC)-3'
Site 3	5'-d(GTGACTGG**G****AAAACCCTGGCGTTACCC)-3'

Table 2.1: Showing the six different oligodeoxynucleotides synthesised. Note that the G residues highlighted in red correspond to the modified 8-nitro-2'-*O*-methylguanosine and the G* residues highlighted in blue correspond to 2'-*O*-methylguanosine.**

The trityl traces recorded for site 1 and site 3 sequences are shown in Figure 2.6. These demonstrate the high overall coupling efficiencies achieved for the synthesis of the oligodeoxynucleotides. Despite there being two trityl groups on the modified monomer, the peak corresponding to the incorporation of this nucleoside is similar to that of the preceding

coupling. This is likely due to the slow release of the DMT group from the N2 position over subsequent detritylation steps of DNA synthesis.

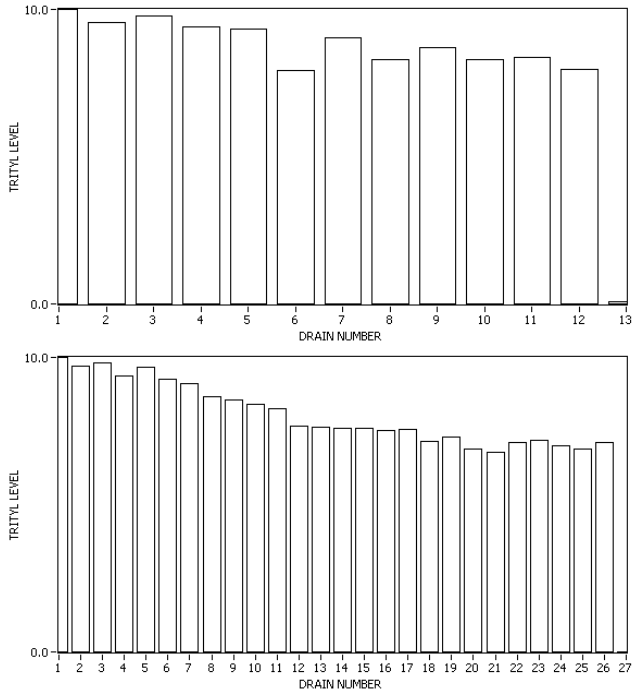

Figure 2.6: Trityl traces obtained during spectrophotometric analysis of the detritylation solutions of a 13mer (site 1) containing one 8-nitroguanine modification at position 7 (top) and a 27mer (site 3) containing one 8-nitroguanine modification at position 9 (bottom). Note that the 5'-terminal trityl group is not removed so no absorbance is recorded for the final residue. For sequences see Table 2.1.

2.7.1 Standard post synthetic deprotection and purification

Upon completion of the synthesis, the full length oligodeoxynucleotide remained attached to the CPG solid-support by the 3'-terminal nucleoside and the 5'-hydroxyl group was protected with a DMT group. Furthermore, the exocyclic amine base protecting groups and phosphate protecting groups were retained. Complete deprotection is necessary to isolate the pure oligodeoxynucleotide. This is carried out using a stepwise approach.

The first step involved treatment with ammonium hydroxide at 55°C. This resulted in cleavage of the succinyl linker thus detaching the oligodeoxynucleotide from the solid-support. Under these conditions all base labile protecting groups were also removed. The aqueous solution was then evaporated and the oligonucleotide was subsequently purified by RP-HPLC using a C18 column. This technique separates molecules according to their hydrophobicity and polarity. The oligodeoxynucleotides were bound to the hydrophobic matrix in an aqueous triethylammonium bicarbonate (TEAB) buffer and eluted from the column using an increasing

gradient of acetonitrile. The retained 5'-terminal DMT group serves as a lipophilic 'handle' for purification. The hydrophobicity of the 5'-DMT group, only present on the desired oligodeoxynucleotides, allowed for convenient isolation and separation from the capped failure sequences which have much shorter retention times by comparison (Figure 2.7).

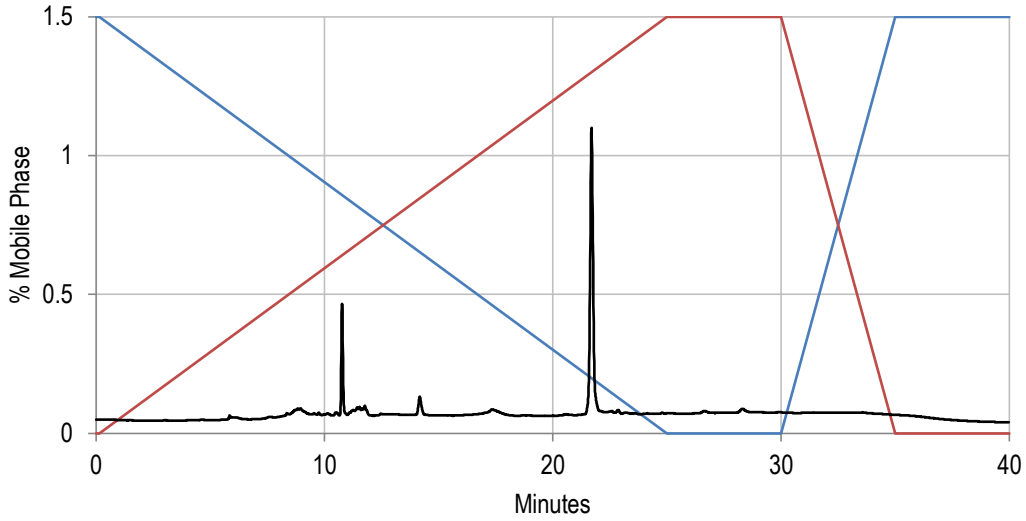

Figure 2.7: Analytical RP-HPLC trace obtained for crude site 1 sequence which contains one 8-nitroguanine modification. Peaks at ~11 minutes correspond to failure sequences and the peak at 21.69 minutes corresponds to the full length DMT protected site 1 sequence (Control method 0-100, page 139).

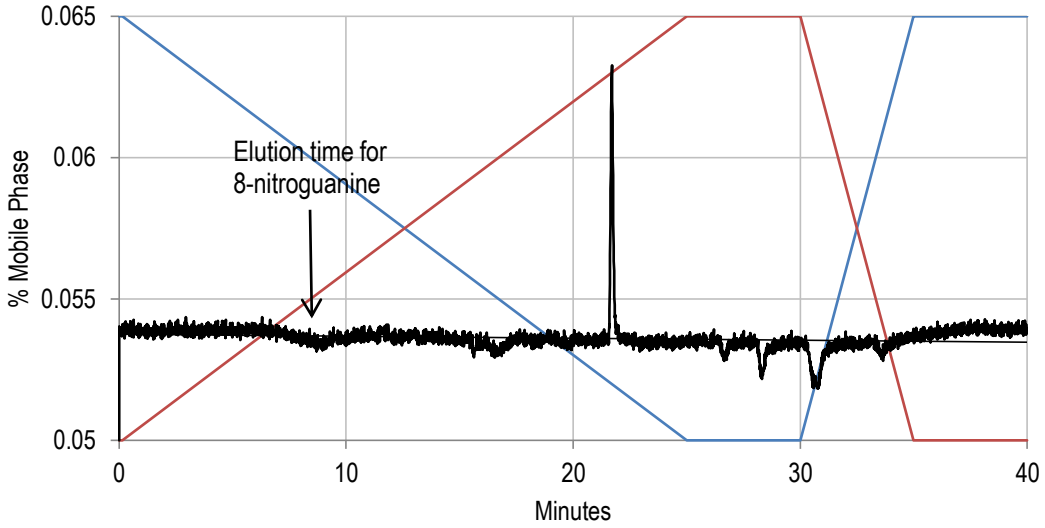

Figure 2.8: The analytical RP-HPLC trace recorded for the crude site 1 sequence at 350 nm where only 8-nitroguanine derivatives have a significant absorbance. Arrow marks the position where 8-nitroguanine would elute (Control method 0-100, page 139).

As mentioned previously, the distinctive UV absorption of the 8-nitroguanine base at approximately 400nm provided us with a unique method for identifying whether it has been incorporated into any molecule. This unique method of identification was utilised to determine whether the 8-nitroguanine modification had been successfully incorporated into the oligonucleotide (Figure 2.8). Moreover, this proved valuable as a means to establish whether depurination had occurred releasing the 8-nitroguanine base. Figure 2.8 shows the RP-HPLC trace of the crude site 1 sequence recorded at 350nm. It shows only a single peak corresponding to the product and there is no peak at 8.40 minutes corresponding to the elution position of the 8-nitroguanine base.

Treatment of the purified 'DMT-on' sequence with aqueous 20% acetic acid afforded the detritylated oligodeoxynucleotides. This deprotection step was deliberately kept short (20 minutes) to minimise the possibility of depurination. To avoid prolonged exposure to acidic conditions the solution was neutralised with triethylamine. Therefore, in contrast to oligodeoxynucleotides which are comparatively stable in acid and can be purified at this stage by extraction with ethyl acetate, those containing an 8-nitroguanine modification required further RP-HPLC purification as a desalting step.

Following the final RP-HPLC purification, the TEAB buffer salts were removed by repeated evaporation of the eluted oligodeoxynucleotides with water. The resulting oligodeoxynucleotides were analysed by RP-HPLC to ensure that they were recovered in satisfactory purity (<90%) and were thus suitable for the use in subsequent applications (Figures 2.9 and 2.10).

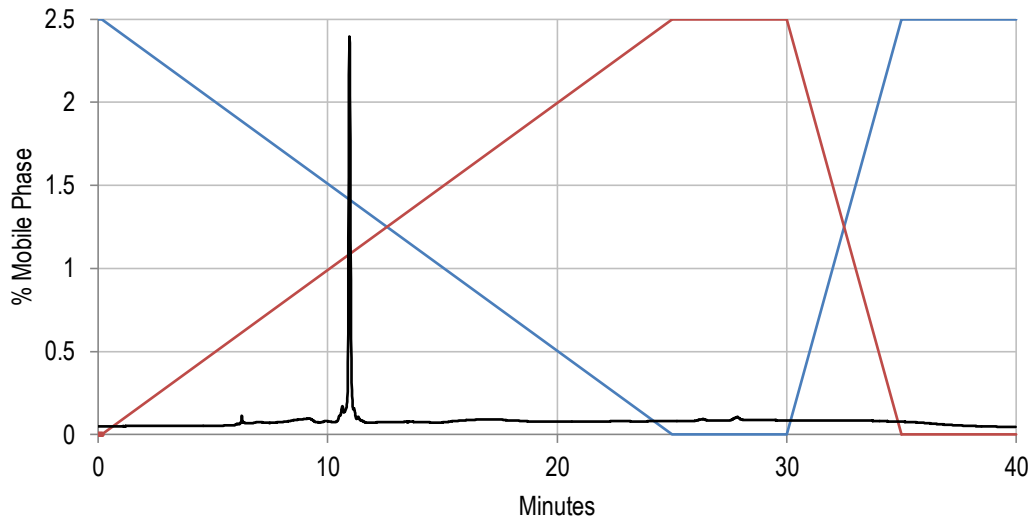

Figure 2.9: Analytical RP-HPLC trace obtained for the purified site 1 oligodeoxynucleotide containing one 8-nitroguanine modification (Control method 0-100, page 139).

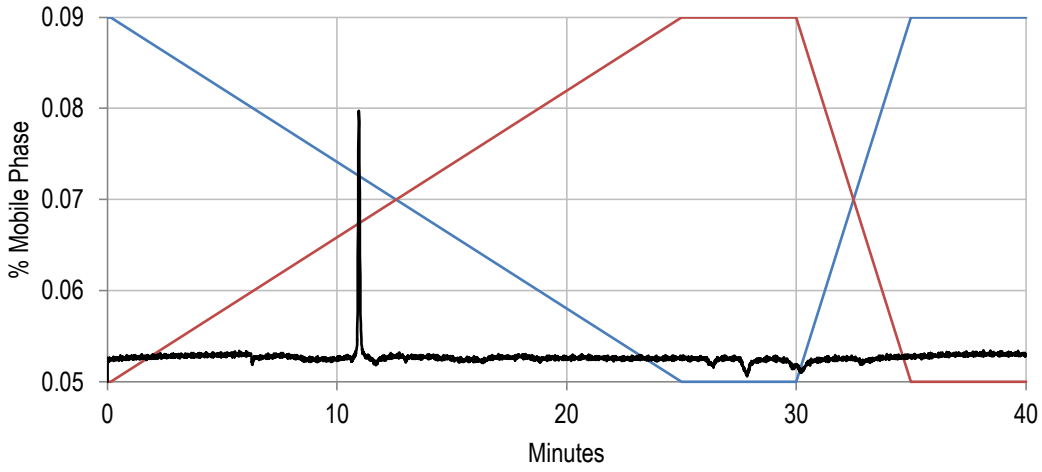

Figure 2.10: The analytical RP-HPLC trace recorded for the purified site 1 at 350nm showing the absorbance corresponding to the 8-nitroguanine residue within the oligodeoxynucleotide (Control method 0-100, page 139).

2.7.2 Yields and characterisation of oligodeoxynucleotides

Since the typical loading of the CPG solid-support is in the range of 30-60µmol g^{-1} the exact quantity of oligodeoxynucleotide being produced for a given batch of columns can vary. Therefore the yields calculated for oligodeoxynucleotide synthesis is an approximation rather than accurate calculation. For this approximation, it was assumed that each reactor column had 1µmol of the 3'-terminal nucleoside. Providing each coupling reaction was quantitative, theoretically the full length oligodeoxynucleotide would be produced in a 1µmol scale.

			Average masses	
Oligodeoxynucleotide	**OD_{260} units**	**Yield (%)**	**Theoretical**	**Experimental**
Site 1 control	31.65	26	3975.7066	3975.6844[a]
Site 1	39.02	32	4050.7025	4050.6133[a]
Site 2 control	25.72	7	nd	nd
Site 2	66.60	18	nd	nd
Site 3 control	51.04	20	8311.42	8314.74[b]
Site 3	29.21	11	8460.31[c]	8460.64[b]

Table 2.2: Showing the OD_{260} units, approximate yields (%) and average theoretical and experimental masses for the oligodeoxynucleotides synthesised. Note, nd = not determined, [a] determined by electrospray ionisation, [b] determined by MALDI and [c] corresponds to (M-4H)+3Na+K. For sequences see table 2.1.

As the length of the oligodeoxynucleotide sequences increased, the yield of the full length product was generally lower. This can be attributed in part to the limitations of the chemistry. Even with a 99% coupling efficiency for each addition, the cumulative effect of a 1% failure rate can be significant, particularly for long oligodeoxynucleotides. Consequently, the relative proportion of failure sequences increases according to the length of the oligodeoxynucleotide.

Regardless of the quantity of the crude material produced in the synthesis, the yield was dramatically reduced during deprotection and purification. Additionally, the increased processing required in the purification of oligodeoxynucleotides containing the 8-nitroguanine modification was detrimental to the yields, however this was unavoidable. The yields were calculated based on extinction coefficients for the oligodeoxynucleotides (see experimental section). The yields obtained for synthesis of the modified oligonucleotides is comparable to those that are unmodified, thus it was concluded that the synthetic mimic did not significantly affect the overall synthesis.

The principle technique for the characterisation of oligodeoxynucleotides was negative mode electrospray mass spectrometry (ESMS). This method has limitations since a molecular weight of the parent free acid oligodeoxynucleotide, in which all of all the phosphate groups are protonated, cannot be directly obtained. Multiple phosphoryl protons are removed during ionisation and as a result a series of multi-charged ions were observed for the mass to charge ratio (m/z). It was possible to determine experimental m/z values for multi-charged ions fitting the formula $[M-nH]^{n-}$, where M represents the free acid of the oligodeoxynucleotide and n is the

number of charges. Using these values it was possible to determine an average experimental m/z value of the parent free acid.

The molecular weights of the 27mer site 3 oligodeoxynucleotides were determined by MALDI and gave masses consistent with the products. The presence of the 8-nitroguanine base in both the site 2 and site 3 oligodeoxynucleotides was also confirmed by the absorption at 350nm in their HPLC traces.

2.8 Synthesis of dinucleotides

Oligonucleotide syntheses are generally carried out utilising CPG solid-supports to which the 3'-nucleoside has been pre-attached. This is appropriate for oligonucleotides containing a standard nucleobase at the 3'-terminus. However the preparation of oligonucleotides which comprise a modified nucleoside at the 3'-terminus require the use of an alternative support.

The synthesis of the first universal support for the construction of oligodeoxynucleotides was published by Gough *et al* in 1983. This approach was based upon utilising a terminal uridine residue which was removed during treatment with Pb^{2+} once the synthesis had been completed[231]. Since their discovery many alternative universal supports have been described in the literature[232–234]; a number of these are commercially available. The supports can either be nucleoside derived or non-nucleosidic; the majority of which incorporate a 5 membered ring similar to the ribose moiety of nucleosides as in Figure 2.11.

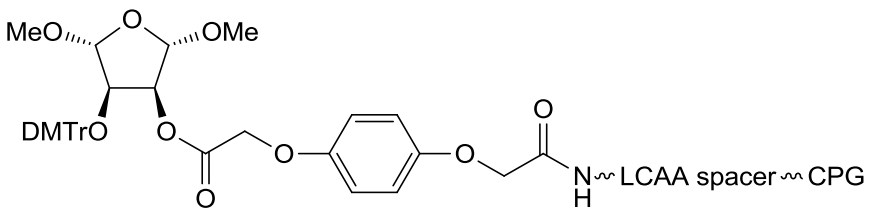

Figure 2.11: The universal solid-support attached to the CPG *via* a hydroquinone-*O,O'*-diacetic acid linker and a long chain alkyl amine (LCAA) spacer.

In this approach the 3'-nucleoside is added during the first coupling reaction; however this generates an undesired phosphate linkage between this nucleoside and the universal support. This undesired phosphate group is conveniently removed alongside the other protecting groups following generation of the full length oligonucleotide during post synthetic processing. For use in studies investigating detection of the 8-nitroguanine lesion using SERS (Chapter 4), the synthesis of a dinucleotide (dimer) containing two 8-nitro-2'-*O*-methylguanosine modifications and the corresponding unmodified 2'-*O*-methylguanosine dimer were required

(structures shown in Figure 2.12). The universal support utilised for this synthesis was that developed by Pon *et al.* (Figure 2.11). It is readily available, and compatible with the established phosphoramidite chemistry[235]. A DMT group is incorporated at the site of elongation to enable real-time coupling efficiency measurements.

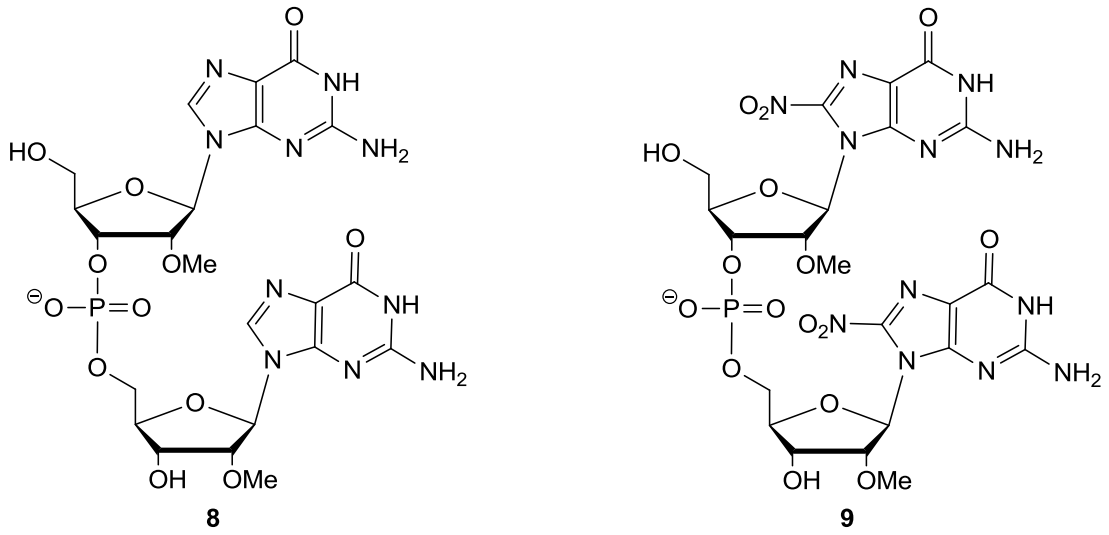

Figure 2.12: The dinucleotide species required for SERS detection studies.

The synthesis was largely carried out as described previously (Chapter 2, Section 6) when using the 3'-functionalised support. Only minor adjustments of the conditions were required in order to adapt the procedure for the universal support. Since the support was non-nucleosidic, an initial extended detritylation step was performed in order to ensure that complete detritylation of the support was achieved prior to the first synthetic cycle. Upon completion of the synthesis, the dimer remained connected to the universal solid-support and the 5'-hydroxyl group was protected with a DMT group. Post synthetic deprotection was achieved using a solution of concentrated aqueous ammonia and methylamine heated to 55°C for 17 hours which

In the case of the unmodified dimer (**8**) purification with the 5'-DMT group still attached to the dimer proceeded as expected affording the desired product in an excellent yield of 68% based on the loading of the resin. The dimer was analysed using RP-HPLC establishing the purity of the recovered sample to be 97%. Characterisation by negative mode ESMS provided conformation of the generation of the dimer; a mass of 655.1617 was observed compared to the calculated mass of 655.1626 (Table 2.3).

			Average masses	
Dimer	**OD_{260} units**	**Yield (%)**	**Theoretical**	**Experimental**
8	14.65	68	655.1626	655.1617
9	0.97	4	745.1327	745.1313

Table 2.3: Showing the OD_{260} units, approximate yields (%) and average theoretical and experimental masses for the dimers synthesised.

Isolation of the 8-nitro-2'-*O*-methylguanosine dimer (**9**) however was somewhat problematic. The crude 5'-DMT protected dimer was analysed by RP-HPLC following post synthetic deprotection; however there was no peak in the chromatograph representative of what we thought at this stage was the bis-DMT protected dimer. This was unexpected as the coupling efficiencies measured using the online spectrophotometer present in the DNA synthesiser, suggested that the coupling reactions has proceeded in a good yield.

Thus aside from the nitro group, which is hydrolytically stable under basic conditions, the only variation between the two systems is the additional DMT protecting groups on the *N2* position of the modified bases (Figure 2.13).

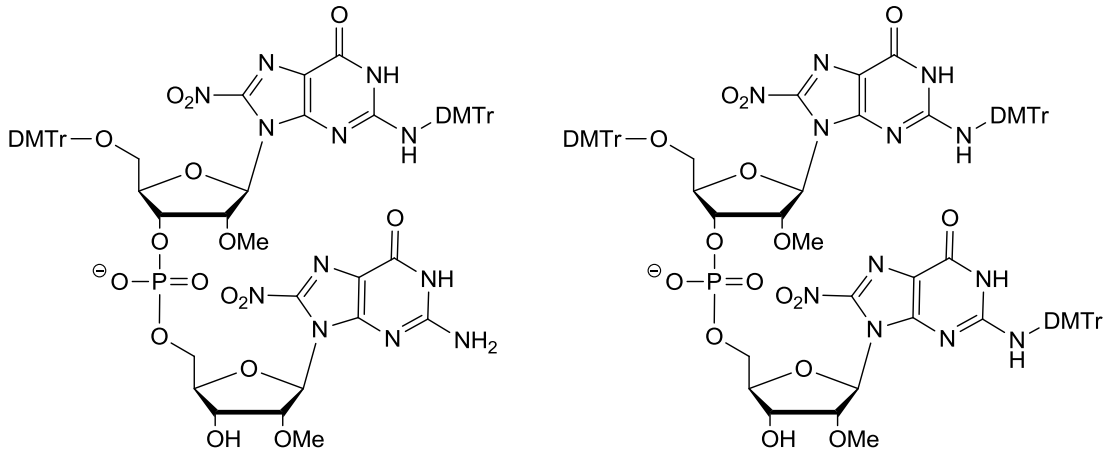

Figure 2.13: Showing the structures of the bis- and tris-DMT dimers prior to purification.

It was anticipated that the DMT group on the 3'-nucleoside would be removed during the subsequent detritylation step, leaving a bis-DMT protected species which would elute in the HPLC conditions utilised. However subsequent review of the literature revealed that removal of trityl groups from primary amines requires stronger acidic conditions or extended reaction times[236]. Therefore it was most likely that the crude product was the tris-DMT dimer and the

inability to purify the modified dimer using RP-HPLC was attributed to the extreme lipophilicity of the molecule. It was envisaged that had the DNA sequence been longer, the DMT groups on the 8-nitroguanine base would have been removed during successive detritylation steps, as was apparent for the longer oligodeoxynucleotides previously synthesised.

In order to obtain a sample suitable for purification, following cleavage from the universal support, the crude DMT protected dimer was exposed to conditions analogous to those which the longer oligodeoxynucleotides underwent during the DNA synthesis. The modified dimer was treated three times with a 3% TCA solution prior to purification in order to generate the fully detritylated dimer (**9**) which was sufficiently polar to be eluted by RP-HPLC. Unfortunately, due to the extra steps necessary to purify the 8-nitro-2'-*O*-methylguanosine dimer, the yield for the reaction was lower than expected (4%). Nevertheless, characterisation using negative mode ESMS confirmed generation of the desired product; an accurate mass of 745.1313 was obtained compared to the calculated mass of 745.1327 (Table 2.3).

2.9 Conclusion

A fully protected 8-nitro-2'-*O*-methyguanosine derivative was successfully prepared in solution *via* a four step procedure. Although the hydrolytically stable analogue was generated using this methodology, there is obvious scope for improvement. The nitration reaction remains relatively low yielding despite numerous optimisation attempts and perhaps a thorough investigation of palladium catalysed coupling reactions would give rise to a more efficient method of nitration[237]. Nevertheless, the devised route provided sufficient quantities and purities of the compound for the purposes of this thesis. This synthetic pathway was also reproduced starting from the readily available ribose sugar derivative. At this point, the synthesis diverges into two distinct pathways dependant on whether the monomer or oligodeoxynucleotide is appropriate for the prospective application.

Following manipulation of the protecting groups, a phosphoramidite was prepared that was suitable for the incorporation into DNA. Oligodeoxynucleotides 13, 27 and 37 residues in length were generated by the application of a solid-phase synthesis protocol previously developed for the 2'-*O*-methyl analogues. In total, three unmodified and three modified oligodeoxynucleotide strands were prepared using a 3'-functionalised solid-support. Additionally a dinucleotide containing two 8-nitro-2'-*O*-methylguanosine modifications and the corresponding unmodified 2'-*O*-methylguanosine dimer were prepared. These sequences are suitable for the use in the chemical and biological applications described in the following chapters.

Chapter 3

Results and Discussion 2:

Reactions of 8-nitroguanine nucleosides and oligodeoxynucleotides

3 Results and Discussion 2

3.1 Substrates for studying the reactions of 8-nitroguanine

This chapter describes studies on the reactions of the 8-nitroguanine base in both nucleoside and oligodeoxynucleotide substrates. Whilst the synthesis of 8-nitro-2'-*O*-methylguanosine derivatives were described in the previous chapter, because of the relative expense of the methylated starting material, it was decided that 8-nitroguanosine would be used for these studies. This was considered appropriate as like the 2'-*O*-methyl derivative, it is also relatively stable to depurination due to the additional hydroxyl group destabilising the oxonium ion intermediate and making the hydrolysis process less favourable.

The synthesis of 8-nitroguanosine and some of its partially protected derivatives is shown in Scheme 3.1. This route is analogous to that previously described in Chapter 2 Section 1 for the 2'-*O*-methyl derivative. The reaction conditions and product yields were comparable to those in the 8-nitro-2'-*O*-methylguanosine synthesis. Thus a fully protected derivative of 8-nitroguanosine (**13**) was prepared in an overall yield of 22% from guanosine (Scheme 3.1). For the studies described in this chapter it was also necessary to prepare the triacetylated derivative of 8-nitroguanosine (**14**) and the fully deprotected 8-nitroguanosine (**15**). These were obtained using standard deprotection conditions and the yields and reaction conditions are shown in Scheme 3.1.

Additionally, a sample of the 8-nitroguanine base (**16**) was required for the use as a standard to monitor depurination; this was most readily prepared *via* treatment of **13** with 1M HCl at 60ºC. Upon complete depurination, the solution was neutralised using 1M NaOH; care was taken to maintain a pH greater than 7 to avoid the formation of salts. Filtration of the resulting precipitate afforded the 8-nitroguanine base as an orange solid in a 79% yield. The success of the depurination reaction was confirmed by the absence of peaks corresponding to the carbon atoms in the ribose sugar in the ^{13}C NMR.

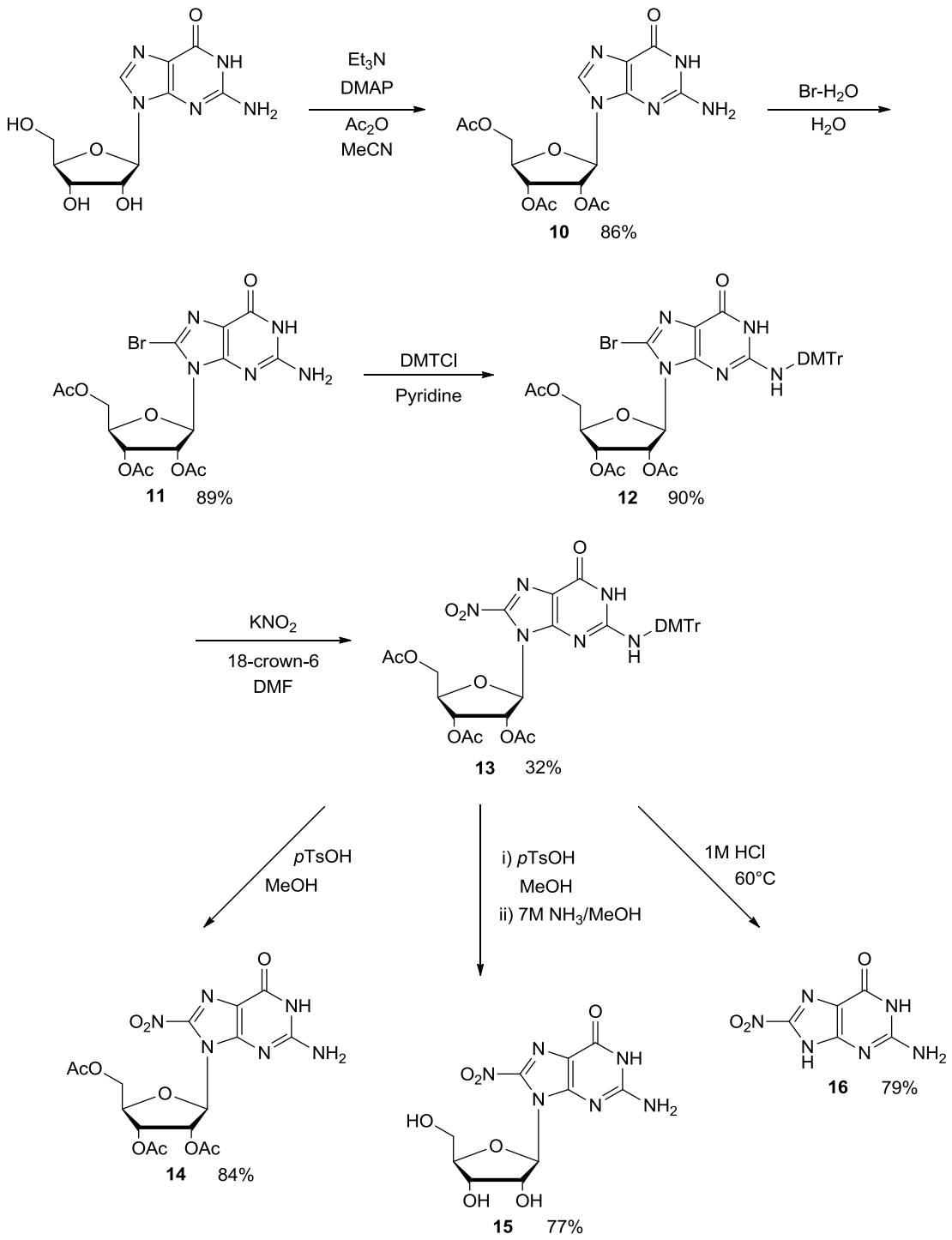

Scheme 3.1: Synthetic route to 8-nitroguanosine analogues.

3.2 Alkylation of 8-nitroguanine

Before discussing the alkylation reactions performed on 8-nitroguanine nucleosides it is necessary to briefly review this area. The most nucleophilic sites of the DNA bases have previously been identified[238,239]. Given that the nitrated nucleoside demonstrates a significantly

reduced reactivity towards electrophiles due to the electron withdrawing nature of the nitro group, it is reasonable to assume that these would not be in agreement with 8-nitroguanine.

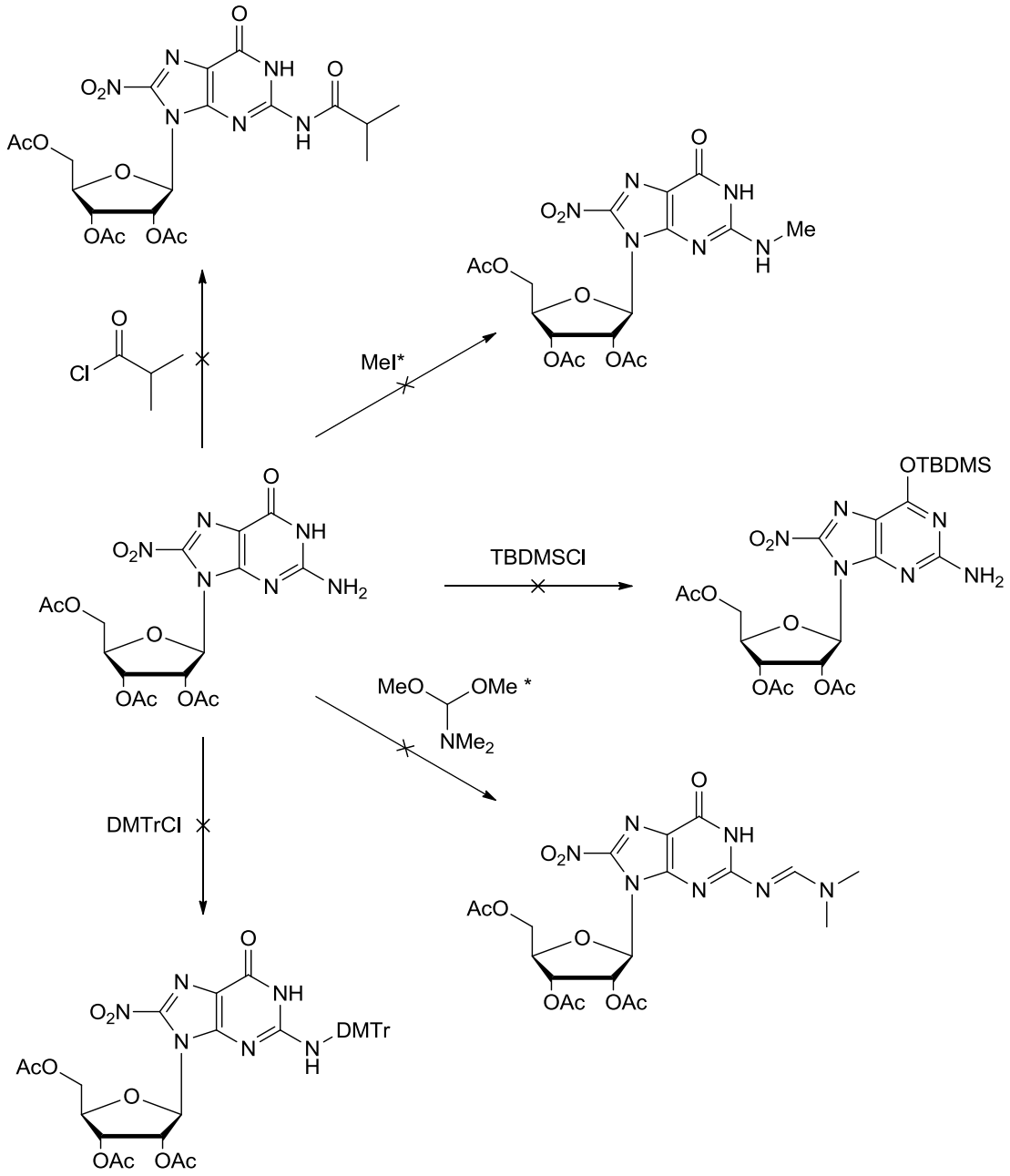

Figure 3.1: Failed attempts to derivatise the nucleobase after nitration. * These reactions were attempted by Dr I. Bhamra.

To illustrate this point, a series of reactions are shown in Figure 3.1 which can be carried out successfully using guanine nucleosides, however prove to be unsuccessful when performed on 8-nitroguanosine. Attempts to introduce any of the customary protecting groups, namely acetyl, methyl, silyl and formamidine groups and notably efforts to reinstate the trityl group after

nitration were ineffective. This failure to derivatise the base demonstrates the extent to which the reactivity is reduced by the nitro group. The intrinsic reactivity of the 8-nitroguanine nucleoside is of interest in order to gain a comprehensive understanding of the molecular basis by which the lesion reacts synthetically and *in vivo*.

Alkylating agents are a class of strongly electrophilic species that can react with the nucleophilic sites of nucleic acids. A wide range of compounds have been used and studied as DNA alkylating agents since the use of cytotoxic 'mustard gas' during World War I and World War II. It was the delayed biological effects of exposure to low doses of these agents, in particular, the inhibition of cell division, that led nitrogen mustards to be evaluated as antitumor agents[240]. This demonstrates the multifaceted role that alkylating agents can play in mutagenesis; while they are known to induce cancer, they can also be utilised as a treatment. Alkylating agents react with the nucleobases to generate a variety of covalent adducts that vary in complexity and regiochemistry. Comprehensive structural characterisation of these adducts provides vital information on the types of DNA lesions that can be formed by alkylating agents[241].

In order to explore the behaviour of the 8-nitroguanine base, it is first appropriate to discuss some general principles of chemical reactivity. The terms 'hard' and 'soft' are often used to describe the varying reactivities of a molecule. Oxygen is considered a 'hard' nucleophile and its reactions are governed by charges and electrostatic effects. Nitrogen atoms are considered to be 'softer' nucleophiles than oxygen and are dominated by orbital overlap between the HOMO of the nucleophile and the LUMO of the electrophile. Electrophiles can also be defined in terms of their 'hard' or 'soft' nature. 'Hard' electrophiles are generally charged species or those which contain dipoles while soft electrophiles are dominated by orbital interactions. Typically hard nucleophiles prefer to react with hard electrophiles and likewise soft nucleophiles with soft electrophiles[17]. Therefore it is reasonable that the reactivities of the various nucleophilic sites of the nucleobases differ accordingly.

These concepts are consistent with results determined previously for the alkylation of nucleosides. For example, hard electrophiles such as those generated by *N*-alkyl-*N*-nitrosourea react *via* S_N1 like processes forming adducts at the electronegative oxygen atoms. Whereas soft electrophiles such as dimethyl sulfate and methyl iodide react *via* S_N2 like processes to modify the nitrogen nucleophiles[239,242–244].

Quinone methides are a class of DNA alkylating agents, structurally related to quinones, which appear often in both chemistry and biology. Of the three possible isomers, *para* (1,4) and *ortho* (1,2) quinone methides are the most commonly utilised. Essentially a quinone methide is a formally neutral benzylic carbocation, whereby electron donation from the oxygen substituent in the *para* or *ortho* position contributes towards resonance stabilisation (Figure 3.2). This results in molecules that are highly reactive and formally undergo reactions as a Michael acceptor. *Meta* (1,3) substituted ortho quinone methides are comparatively unstable as there is no orbital interaction between the meta oxygen and the substituents on the aromatic ring[245,246].

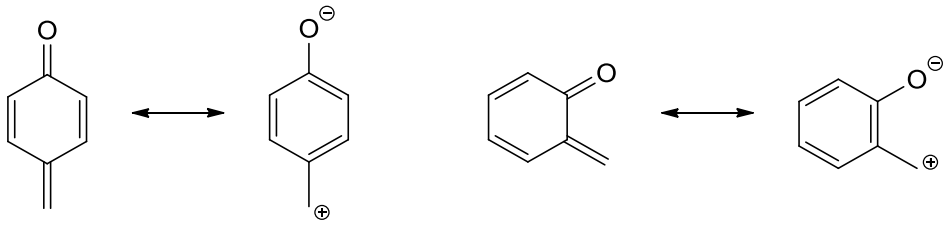

Figure 3.2: Resonance stabilisation of *para* (left) and *ortho* (right) quinone methide.

The extensive conjugation of quinone methides generates a benzylic carbon which is highly electron deficient making it extremely susceptible to nucleophilic attack; hence it is an attractive compound for investigating the properties of the seemingly inert 8-nitroguanine base. The reactions between guanine and various quinone methides have been extensively studied previously[244], it is therefore of interest to be able to compare these results to those obtained with the modified nucleoside.

In order to characterise the nucleophilicity of 8-nitroguanine and evaluate the broader implications of these results, the reactions of two quinone methides were examined.

3.3 Synthesis of a *para* quinone methide adduct of 8-nitroguanine

The applications of quinone methides are largely limited to reactions in which the activated species is generated *in situ* from a precursor[247]. The intrinsic reactivity of a quinone methide, that is its propensity to rapidly undergo exocyclic nucleophilic attack, prevents the synthesis and isolation of the unstable species prior to reaction. Quinone methides can be stabilised to varying degrees by the attachment of bulky groups at the positions *ortho* to the quinone oxygen; thus producing a diverse range of molecules with broad reactivities. The presence of large, hydrophobic alkyl substituents, such as *tert* butyl groups at the 2- and 6-positions, effectively prevents solvent interactions with the carbonyl oxygen. Consequently the oxidised

quinone methide exists predominantly in the uncharged form and whilst it can still undergo the addition of nucleophiles, it is significantly more stable[244,247,248].

Initial efforts were targeted towards the generation and characterisation of an adduct from the reaction between 8-nitro-2',3',5'-tri-*O*-acetylguanosine (**14**) and a *para* quinone methide derivative. All of the hydroxyl groups on the sugar remained protected throughout the alkylation studies in order to prevent competing reactions at these positions and aid in purification.

Scheme 3.2 shows the oxidation of the 2,6-disubstituted phenol, butylated hydroxytoluene (BHT), with a large excess of silver oxide (Ag_2O) to produce the corresponding quinone methide[244]. Following filtration, the *para* quinone methide derivative was reacted directly with the partially protected 8-nitroguanosine (**14**) in DMF at 37°C (Scheme 3.2). The reaction was monitored closely by TLC and RP-HPLC; after 1 hour all the starting material had been consumed. Purification by flash column chromatography generated a single product (**17**) in a 68% yield.

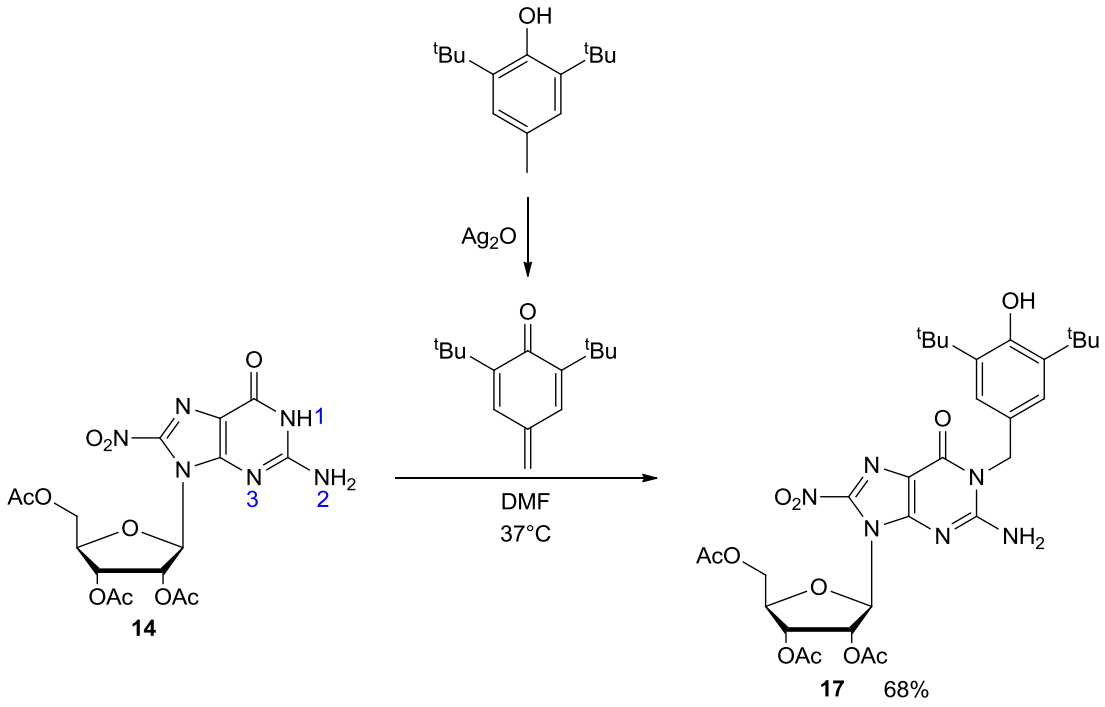

Scheme 3.2: *Para* quinone methide adduct formation. Note, the numbering system of the nitrogen atoms in the guanine base is shown in blue.

The nucleophilic addition of the nucleoside to the electron deficient benzylic carbon of the *para* quinone methide is formally a Michael addition. However, the reaction is significantly different to a typical Michael addition as the reaction restores the aromatic stability of the

cyclohexadiene ring. Re-establishing the aromaticity of the phenol is thermodynamically favourable and therefore drives the reaction[245].

Structural assignments for the alkylated species have not been trivial and have relied principally on the interpretation of NMR chemical shifts and their comparison with those values previously determined. The literature example whereby deoxyguanosine is alkylated by a *para* quinone methide results in the formation predominantly of the *N2* adduct (Scheme 3.3). Minor products as a result of alkylation of the *N1* and *N7* positions were additionally observed; though the *N7* adduct was unstable and subsequently depurinated to form the guanine derivative[244].

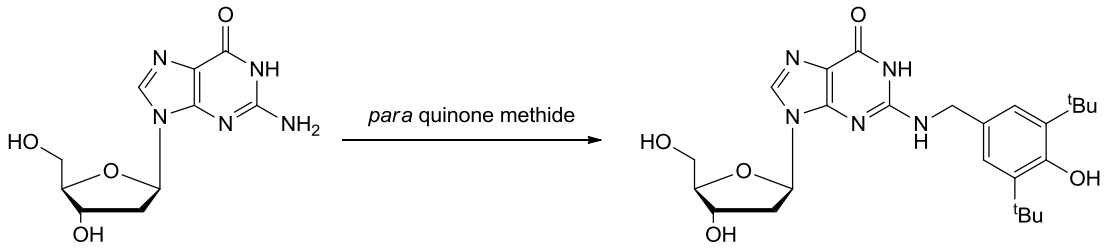

Scheme 3.3: Showing the literature example of the alkylation of deoxyguanosine with *para* quinone methide[244].

Interestingly, upon evaluation of reaction with the nitrated guanosine derivative (**14**) there was considerably evidence to suggest that the *N1* product is exclusively formed. The HPLC data and mass spectrometry both confirmed the conversion to a single mono-alkylated product, although using these techniques it was not possible to determine which of the competing nucleophilic sites of 8-nitroguanine had been modified.

Structural characterisation was achieved using 1D and 2D NMR studies. The resonance of the protons and carbon at the benzylic position are highly sensitive to the site by which they are attached to the nucleoside[244]. Therefore it was necessary initially to ascertain which signals were associated with the CH_2 group at the benzylic position. This was determined using distortionless enhancement by polarization transfer (DEPT), correlation spectroscopy (COSY) and heteronuclear single quantum coherence (HSQC) experiments.

Two CH_2 peaks were identified in the ^1H NMR spectrum corresponding to the C5' and the benzylic carbon resonance. By utilising HSQC and COSY experiments it was then possible to identify the associated protons. HSQC correlates protons with the heteronuclei through which they are directly attached to; therefore this experiment determined which proton signals were

related to both of the CH_2 groups in the molecule. This was followed by analysis of the acquired COSY spectra. The cross peaks indicate couplings between neighbouring protons, therefore the isolated benzylic protons at 5.11ppm are easily identified. These key assignments enabled complete characterisation of the 8-nitroguanosine adduct.

The benzylic resonance in the ^{13}C NMR at 45.64ppm is characteristic of a carbon-nitrogen bond; this is supported since a chemical shift of approximately 70ppm would be expected should the benzylic carbon have been attached to an oxygen atom. From the ^{1}H NMR it was possible to determine which nitrogen atom was alkylated. Acquisition of the spectra in a non-protic solvent indicated the absence of the signal corresponding to the *N1* proton resonance which was present in the starting material at 11.34ppm. Additionally, the broad peak at 6.06ppm corresponding to the *N2* signal integrated to 2 protons. These observations confirm that alkylation occurred at the *N1* position. This assignment was strengthened as when compared to the *N2* alkylated product from the literature reported reaction between deoxyguanosine and *para* quinone methide these observations were reversed; the peak at 10.35ppm associated to the *N1* proton was present and the signal associated with the *N2* protons integrated to 1[244].

The pK_a values for deprotonation of the *N1* position of 8-nitroguanosine and guanosine have previously been calculated to be 8.4 and 9.5 respectively[194]. This increased acidity reflects the electron withdrawing capacity of the nitro group. Therefore alkylation occurring exclusively at the *N1* position could be attributed to the influence the nitro substituent has on the reactivity of the modified base.

3.4 Synthesis of an *ortho* quinone methide adduct of 8-nitroguanine

Following these interesting results, we focused upon characterisation of the products generated from the reaction of the partially protected 8-nitroguanosine (**14**) with *ortho* quinone methide. The simplest and most efficient route to form the alkylating agent was using the procedure devised by Rokita *et al.* for an *ortho* quinone methide precursor (*o*-QMP)[243,249]. The *o*-QMP was based on an *ortho* cresol derivative in which the hydroxyl group is protected as a silyl ether and functionalised with a bromine leaving group at the benzylic position.

The silyl group is frequently used for the protection of alcohol moieties due to the ease of which it is removed by nucleophilic attack of a fluoride anion. The best nucleophiles with

regards to silicon are charged and highly electronegative, therefore efficient and selective removal can be achieved due to the strong affinity of silicon for fluorine[17].

The synthetic pathway followed to obtain the *o*-QMP is shown in Scheme 3.4. The silyl ether was prepared by treatment of *ortho* cresol with *tert*-butyldimethylsilyl chloride (TBDMSCl) in the presence of a weak base and nucleophilic catalyst, imidazole. The product (**18**) was isolated in a 97% yield by partitioning the reaction mixture between DCM and sodium hydrogen carbonate ($NaHCO_3$) to remove excess reagents. Successful silylation was confirmed by ^1H NMR spectroscopy through the appearance of characteristic peaks corresponding to the 6 methyl protons and 9 *tert*-butyl protons at 0.20ppm and 1.00ppm respectively.

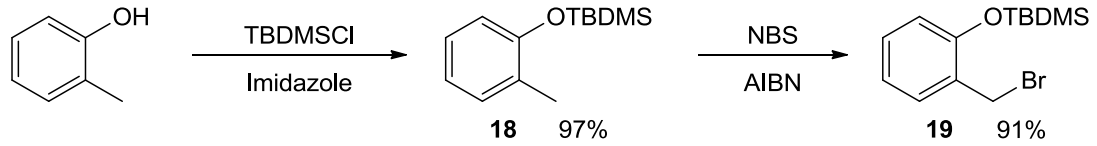

Scheme 3.4: Synthetic pathway towards *o*-QMP.

The next step in the synthesis was functionalisation of the benzylic position with a bromine leaving group. A radical halogenation reaction was carried out using *N*-bromosuccinimide (NBS) in the presence of AIBN a radical initiator[250]. The resulting resonance stabilised benzylic radical then reacts in a radical chain mechanism ultimately generating the bromo methyl derivative. Purification by flash column chromatography afforded the desired product as a colourless oil in a 91% yield. Mass spectrometry clearly demonstrated the presence of a bromine atom as the peak representing the molecular ion consists of two molecular ions differing by 2 amu.

The reaction with the 8-nitroguanine nucleoside was initiated by the *in situ* activation of the *o*-QMP using potassium fluoride[239]. Nucleophilic attack of the fluoride anion at silicon atom leads to a pentacoordinate intermediate; this is permitted as the orbitals of silicon do not have to conform to same geometric constraints as carbon centres[17]. Subsequent elimination of the bromide ion generates the activated *ortho* quinone methide (Scheme 3.5).

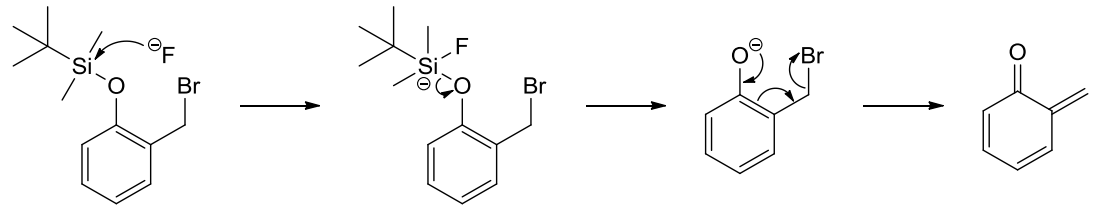

Scheme 3.5: Mechanism for the generation of the activated *ortho* quinone methide.

Initially, a small scale reaction between the nucleoside and *ortho* quinone methide was performed and monitored closely by TLC and RP-HPLC. There was significant evidence to suggest that two nucleoside derived products were formed. As previously discussed, the introduction of a nitro group at the C8 position of guanine nucleosides shifts the UV spectrum towards longer wavelengths. Therefore these distinctive UV properties can be exploited to monitor the production of alkylated 8-nitroguanine derivatives. The polarities of the two new species varied as was evident from their different retention times on RP-HPLC of 16.55 and 17.58 minutes, suggesting that more than one alkylation reaction may have occurred. Taking into account both the lipophilic and hydrophilic functionalities of the molecule it is reasonable to assume that a higher order alkylated species would be significantly less polar than the mono-alkylated species and have a longer retention time on RP-HPLC.

In order to isolate a suitable quantity of the two products and clarify the effect of varying the number of equivalents of *o*-QMP, optimisation of the reaction conditions was necessary. Consequently, a number of small-scale test reactions were carried out. The time dependent profiles produced for the adducts formed upon varying the number of equivalents of *ortho* qunione methide in the reaction are shown in Figure 3.3.

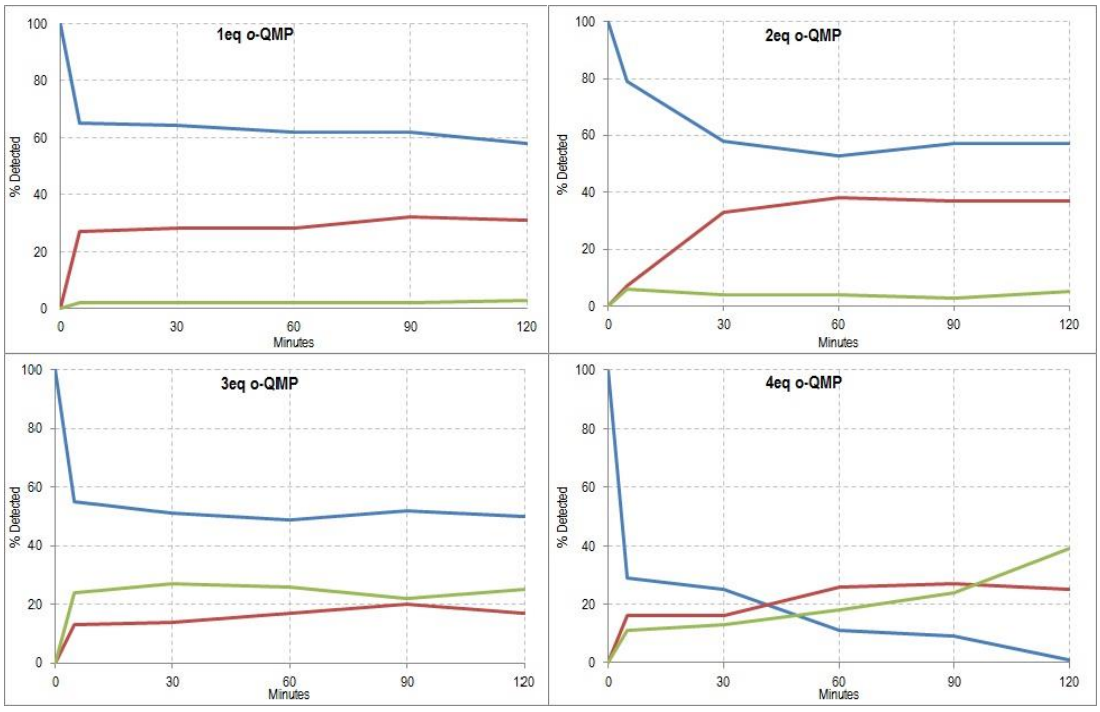

Figure 3.3: Showing the time dependent profile of 8-nitroguanine alkylation with variation of the number of equivalents of *o*-QMP. Note, starting material (retention time = 6.47 minutes) is represented by a blue line, the more polar species (retention time = 16.55 minutes) with a red line and the less polar (retention time = 17.58 minutes) with a green line (Control method 65/35B, page 141).

Whilst the greatest yield of the most polar product was obtained using 2 equivalents of *o*-QMP, these conditions only generated 4% of the less polar species. Therefore in order to maximise production of both species the reaction was carried out using 4 equivalents of *o*-QMP as this generated an even distribution of both products. Purification of the crude material by flash column chromatography isolated the less polar (**21**) and more polar species (**20**) in yields of 27% and 40%, respectively. The generation of a higher order alkylated nucleoside (**21**) was confirmed as both mass spectrometry and various NMR experiments identified that the two products generated were the mono- and di-substituted species.

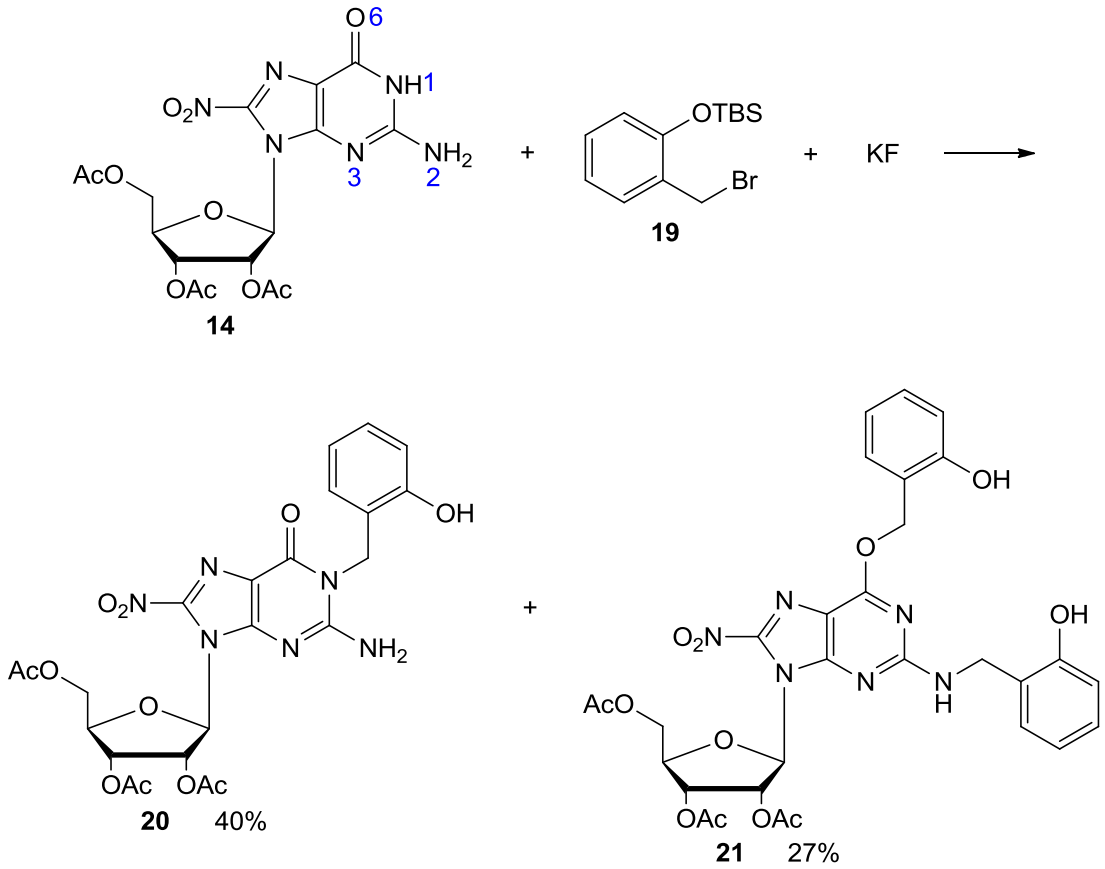

Scheme 3.6: Formation of *ortho* quinone methide adducts. Note, the numbering system of the oxygen and nitrogen atoms in the guanine base is shown in blue.

For the mono-alkylated product (**20**), nucleophilic attack of the *ortho* quinone methide occurred exclusively at the *N1* position. Structural characterisation for this compound was achieved using 1D and 2D NMR; the results were consistent with those determined for the *N1*-(*para* quinone methide)-8-nitroguanosine derivative.

In contrast to the mono-alkylated species, DEPT experiments detected three CH_2 resonances for the di-alkylated species (**21**). Previous analysis enabled us to unambiguously assign the

C5'-nuclei; therefore the resultant signal at 63.59ppm was discounted. The remaining two signals had chemical shifts of 67.25ppm and 39.89ppm in the ^{13}C NMR spectrum; these resonances are characteristic of a benzylic carbon-oxygen bond and a benzylic carbon-nitrogen bond and therefore indicates that *O6* is one of the alkylation sites[242,251]. Since oxygen is more electronegative than nitrogen, the carbon-oxygen bond is more polarised, that is the oxygen atoms draws the electrons in the bond away from the benzylic carbon more effectively than nitrogen. The change in the distribution of electrons causes the benzylic carbon to be less shielded from the applied external magnetic field and therefore resonates at higher frequencies than the corresponding carbon-nitrogen bond[17].

With regard to the second alkylation site on nitrogen, alkylation at the *N1* position seemed unlikely as this would generate unfavourable steric interactions with the substituent present in the *O6* position. Moreover, substitutions at the *N3* and *N7* positions can be disregarded as they would result in unstable nucleosides that depurinate readily at room temperature[242]. Convincing evidence was obtained to support these conclusions. ^{1}H NMR spectra recorded in a non-protic solvent revealed the presence of a single *NH* signal which integrated to one proton. This is consistent with the structure of the *O6,N2* di-alkylated species as the product exists as the *enol* tautomer and therefore there is no proton present at the *N1* position.

The assumption that the *N1* alkylated species would not be able to undergo further alkylation reactions due to steric factors was confirmed by subjecting the mono-alkylated species to a second reaction with *ortho* quinone methide. The reaction was monitored closely by RP-HPLC; while a less polar nucleoside derived polar was briefly observed it rapidly decomposed back to the mono-alkylated species. This suggested that the species was unstable and therefore its formation unfavourable. Taking this evidence into account the di-alkylated species was assigned as *O6*,*N2*-bis-alkylated product (**21**).

3.5 Conclusion

This represents the first example of the generation of an *O6,N2* di-alkylated guanosine derivative using *ortho* quinone methide The literature example whereby deoxyguanosine is alkylated by *ortho* quinone methide results in the formation of the both the *N2* and *N1* substituted adducts[239,242]. Though there is computational evidence to suggest that alkylation at the *O6* position of 9-methylguanine (as a model for deoxyguanosine and guanosine) is as a result of kinetic control and modification of the *N2* position is generated by thermodynamic equilibrations, there is not synthetic evidence to support this[252]. These results demonstrated

the dramatic effect nitration has on the intrinsic reactivity of the nucleoside. It was proposed that di-alkylation was not observed when using the *para* quinone methide species as due to the size of the alkylating agent, steric interactions resulting from additional alkylation would cause this process to be unfavourable thus preventing the formation of higher order alkylated species.

3.6 Identification of the 8-nitroguanine lesion using a sulfur nucleophiles

8-Nitroguanine serves as a biomarker for exposure to inflammation and nitrative stress; it may also have the potential to identify associated carcinogenesis. At present there is no method that is capable of detecting the levels of 8-nitroguanine in DNA. This is a consequence of the susceptibility of the glycosidic bond to hydrolysis following nitration which results in release of the 8-nitroguanine base, and the formation of an abasic site in the DNA. Abasic sites arise under a variety of circumstances, so it is not possible to distinguish those caused by nitrative DNA damage.

Currently, the most efficient method to quantify production of the lesion entails determination of the levels of free 8-nitroguanine in biological fluids[151,155]. Unfortunately using these analytical methods it is not possible to identify whether the 8-nitroguanine detected is formed in the nucleotide pool, in RNA or in DNA. Therefore our aim was to generate a method to stabilise the lesion within DNA in order to minimise depurination and enable its detection *via* a sensitive technique such as fluorescence. Such a technique would potentially provide a method to quantify the steady state levels of this lesion in DNA.

Fluorescence is one of the many different luminescence processes by which molecules emit light. When a molecule is predisposed to absorb electromagnetic energy it is known as a fluorophore. Fluorescence can be defined as the light emitted during the rapid relaxation of a fluorophore following excitation by light of a specific wavelength[253,254].

Fluorescent nucleosides that have been reported to date are as a result of various modifications that range from covalently attaching a fluorescent moiety to the molecule, to directly altering the structure of the nucleobase itself to generate a fluorescent analogue; this typically results in minimal perturbation of the natural structure[255]. As the 8-nitroguanine lesion is non-fluorescent, labelling the nucleoside with an extrinsic fluorophore would introduce the desired characteristics.

It is essential that the fluorescent analogue demonstrates the specificity to covalently bind to and hence detect the 8-nitroguanine modification, differentiating it from the naturally occurring nucleosides. For this purpose, a thiol nucleophile was investigated. Evidence suggests that the nitro group is reactive towards sulfur nucleophiles. *Saito et al.* have previously described the reaction of an endogenous 8-nitroguanine derivative with proteinous thiols, thus providing the basis for this approach[196]. Research very recently published by Fuchi *et al.* demonstrated the

covalent capture of 8-nitroguanosine, facilitated by the formation of multiple hydrogen bonds, using thiol containing recognition molecules[256]. The electron donating nature of the thioether substituent is favourable as it stabilises the lesion by increasing the electron density of the nucleoside through an inductive donating effect.

The chemical nature and the length of the linker between the fluorescent molecule and the nucleoside are of high importance as they can dramatically influence the accessibility and the binding of the fluorophore. Due to the simplicity and versatility of the approach, amide bonds were chosen to connect the fluorophore to the nucleophilic thiol.

3.7 Glutathione displacement reactions

In order to obtain proof of principle, prior to the development of a fluorescent analogue, the potential of the concept was verified using glutathione. Glutathione is tripeptide, comprising of glutamic acid, cysteine, and glycine residues[257] (Scheme 3.7).

As the reaction will inevitably be carried out under physiological conditions when analysing DNA, it is advantageous to develop a protocol compatible with these conditions from the offset. However, at this early stage in development, stabilising the labile glycosidic bond in aqueous solution prior to its displacement takes precedence over an entirely accurate representation of physiological conditions. Consequently the use of a basic 0.1M TRIS HCl (pH 9) buffer was considered appropriate.

The thiol displacement reaction was performed by treating 8-nitroguanosine (**15**) with a five-fold excess of glutathione at 37ºC. RP-HPLC was used as a tool to monitor the reaction. Due to uncertainty as to which peak in the HPLC trace corresponded to the desired product, our aim was to measure the disappearance of 8-nitroguanosine. Additionally this approach was valuable in determining the extent of depurination as the 8-nitroguanine base appears as an additional peak (retention time = 9.62 minutes) when the chromatograph is recorded at 350nm. Upon a 97% conversion of the starting material (retention time = 12.9 minutes), the aqueous solution was then evaporated and the product was isolated by RP-HPLC. The new product had a shorter retention time (10.34 minutes) than the starting material which was consistent with the greater polarity of the glutathione substituent. The purified product was isolated in a 61% yield as an off white solid.

Incorporation of glutathione and displacement of the nitro group was confirmed by mass spectrometry, though this did not establish through which atom the adduct was covalently

attached. Complete characterisation of the product was critical as glutathione has a number of nucleophilic sites with the potential to displace the nitro group, or preferentially functionalise an alternative position of the unprotected nucleoside. Therefore, in order to unambiguously determine the structure, 1D and 2D NMR experiments were required.

As the C8 carbon is not directly connected to a proton, the structure of the adduct could not be confirmed using short-range heteronuclear correlation. Therefore a heteronuclear multiple bond correlation (HMBC) experiment was performed. This technique is used to study ^{2}J and ^{3}J connectivity between carbon (or other heteroatom) and hydrogen atoms; direct ^{1}J correlations are supressed.

Analysis of the ^{1}H-^{13}C HMBC contour map showed that there was a correlation between the C8 of guanosine and the CH_2 group adjacent to the sulfur atom. This established that it is the sulfur atom of glutathione acting as a nucleophile to displace the nitro group *via* an addition-elimination type mechanism, thus confirming the reactivity of the nitrated nucleoside to thiols (Scheme 3.7).

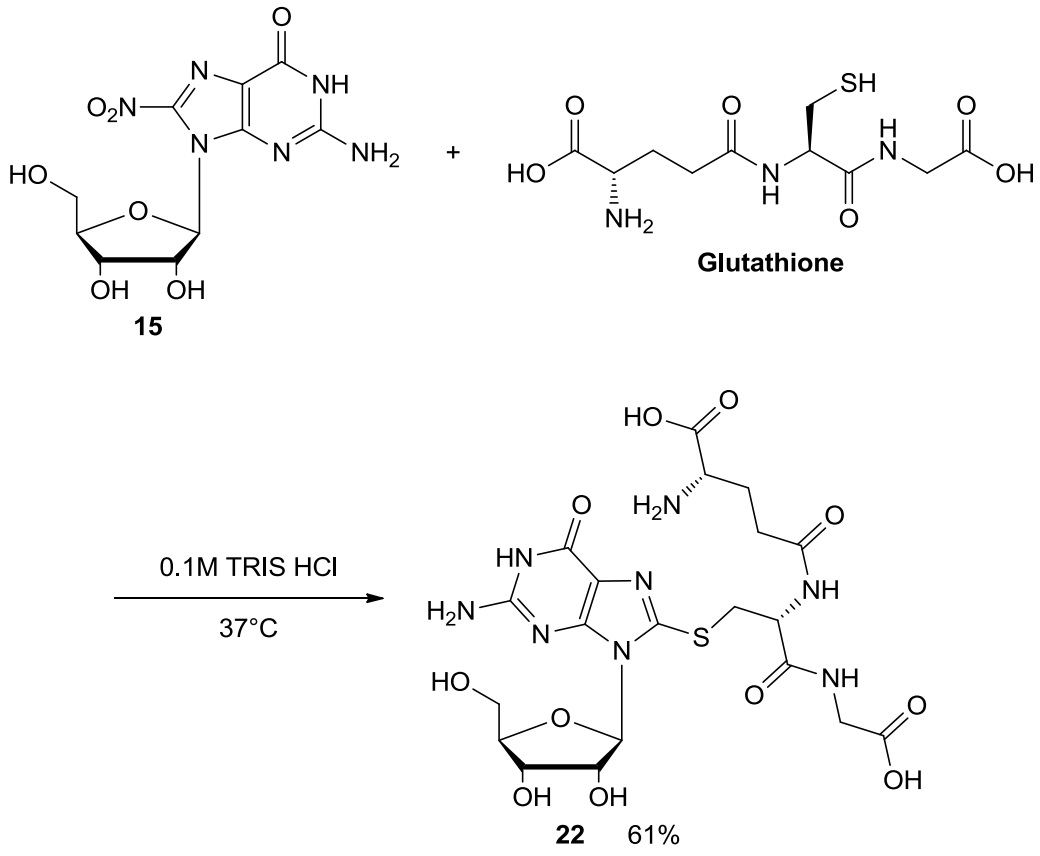

Scheme 3.7: Formation of the C8 glutathione adduct of guanosine.

The next aim was to investigate this reaction using the site 1 oligodeoxynucleotide which contains the 8-nitroguanine base. This would give a better indication as to how applicable this reaction would be to detect this lesion in DNA samples. In preparation, it was decided to prepare the glutathione adduct of 8-nitro-2'-*O*-methylguanosine (**24**) as this would be a useful standard if it proved necessary to characterise the product oligodeoxynucleotides by enzymatic digestion. Given the relative expense of 2'-*O*-methylguanosine and the poor yields of the nitration step, it was decided to prepare the glutathione adduct (**24**) from 8-bromo-2'-*O*-methylguanosine (Scheme 3.8).

The glutathione adduct was prepared by treating 8-bromo-2'-*O*-methylguanosine (**23**) with 5 equivalents of glutathione in a 0.1M TEAB buffer (pH 7.5) at 37°C (Scheme 3.8). The use of TEAB was appropriate as this is a more volatile buffer which can easily be removed and 8-bromoguanosine is not susceptible to depurination therefore more basic conditions were not necessary. The reaction was monitored and the product purified using RP-HPLC. The increased reaction time required and modest yield of 21% demonstrated the greatly reduced susceptibility of the bromo derivative to undergo nucleophilic displacement with a sulfur nucleophile when compared to 8-nitroguanosine.

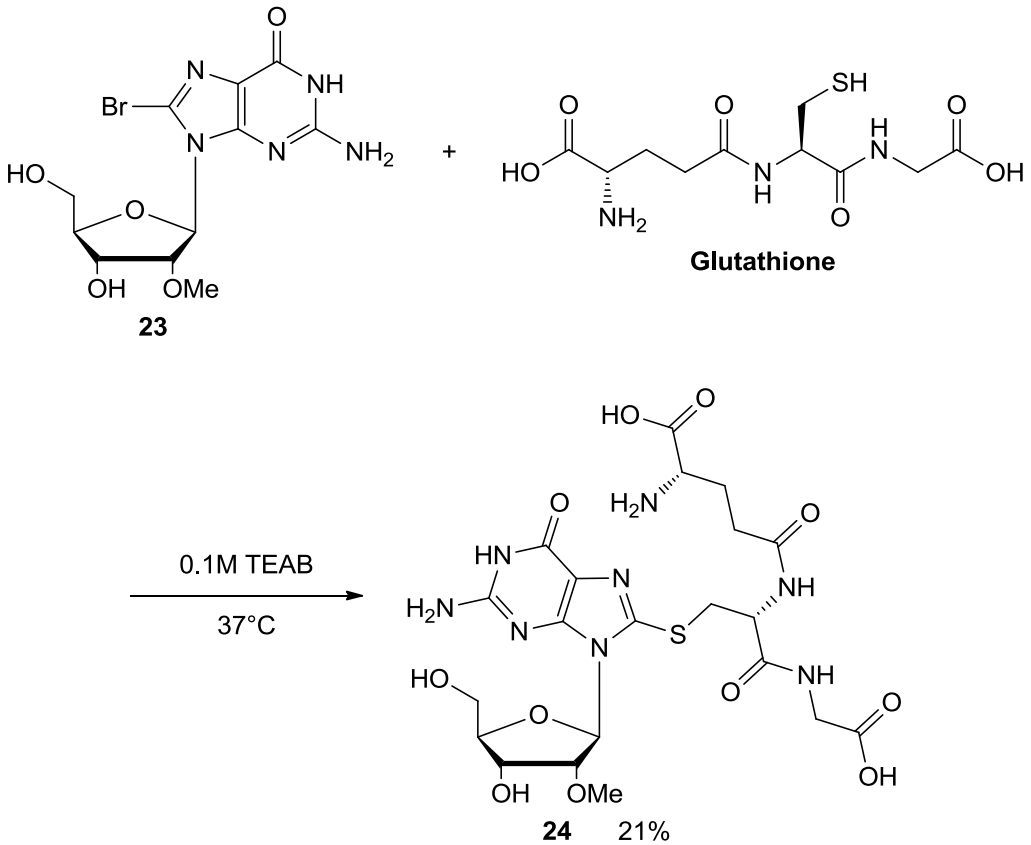

Scheme 3.8: Formation of the glutathione adduct of 2'-*O*-methylguanosine.

Complete structural characterisation was achieved using the same techniques and reasoning as employed for the ribose derivative. Confirmation of the displacement was seen from the ^{1}H NMR spectrum by the appearance of a peak at 4.51-4.56ppm corresponding to the proton directly attached to the glutathione chiral centre in the molecule. Once again the position by which glutathione was covalently bonded to the C8 position was verified using a HMBC experiment. The long range ^{1}H-^{13}C correlation between C8 and the diastereotopic protons adjacent to the sulfur atom was apparent and confirmed that the sulfur atom was acting as the nucleophile.

Following these positive results, the reaction was attempted utilising the site 1 oligodeoxynucleotide consisting of 13 nucleotides with a single modification located in the central position. The reaction was carried out by treating the site 1 oligodeoxynucleotide (~26μM) with a large excess of glutathione at pH 9 and 37°C.

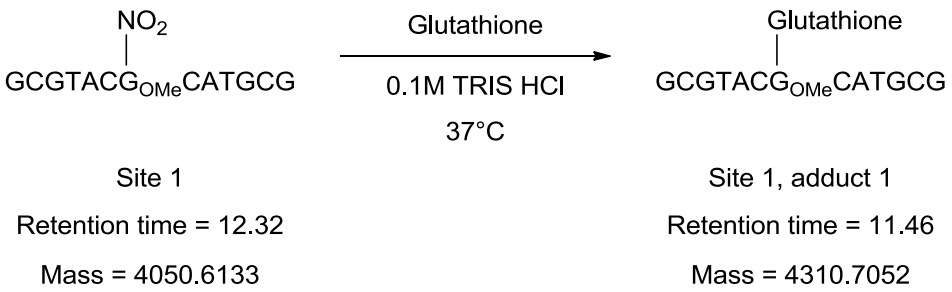

Scheme 3.9: Formation of the site 1, adduct 1 oligodeoxynucleotide. Note G_{OMe} = 2'-*O*-methylguanosine.

The course of the reaction was monitored by RP-HPLC for 18 hours after which no further changes were detectible. Interestingly, the strong yellow colour which is typical of all 8-nitroguanine containing derivatives was discharged as the reaction proceeded. With regards to the RP-HPLC analysis, a new peak (11.46 minutes) was detected which was marginally more polar than the starting material (12.32 minutes) and was not visible at 350nm where only nitro derivatives are detected. The similar mobilities of the two oligodeoxynucleotides on RP-HPLC was unsurprising as taking into consideration the size and composition of sequences it is reasonable that the addition of a glutathione substituent would not dramatically affect the polarity. This complicated the RP-HPLC purification to a certain extent however the desired product (site 1, adduct 1) was isolated.

The main technique for characterisation of the purified site 1, adduct 1 oligodeoxynucleotide was negative mode ESMS which has been discussed previously (Chapter 2 Section 6.4). The

identity of the product was confirmed by ESMS which showed a mass of 4310.7052 for the glutathione adduct.

These results successfully demonstrated that sulfur nucleophiles produced the desired effect of displacing the nitro group in oligodeoxynucleotides, thus verifying the feasibility of the concept. Following this proof of principle, the development of a fluorescent thiol analogue was investigated.

3.8 Development of fluorescent thiol analogue

Polycyclic aromatic compounds are an extensively used class of fluorescent dyes. The first fluorescent dye fluorescein, derived from xanthene, was synthesised by Baeyer in 1871[258,259]. Despite its long history, fluorescein remains one of the most extensively utilised fluorophores in modern biochemical research[260].

For the purpose of this research 5(6)-carboxyfluorescein was considered an appropriate fluorophore as the carboxylic acid provided a versatile means to derivatise it with the required thiol nucleophile through amide bond formation. The formation of amide bonds is an important reaction in organic chemistry and many different strategies have been devised for this objective[261]. The synthesis of an amide bond is formally the condensation of a carboxylic acid and an amine; however this reaction does not occur spontaneously. Consequently it is first necessary to activate the carboxylic acid towards nucleophilic substitution[261]. This can be achieved by converting the OH of the carboxylic acid group into a good leaving group, for example an acyl chloride or an ester[17]. The most commonly used coupling reagents for amide bond formation include; carbodiimide, phosphonium and uronium derived reagents[261].

The strategy developed in this case was to functionalise both amine groups of cystamine with two equivalents of the fluorophore and subsequently cleave the disulfide bond to generate the required thiol nucleophile (Scheme 3.10). Upon reviewing the literature it was apparent that only one other example of formation of the fluorescent disulfide had been attempted and unfortunately there was no characterisation data available[262]. Nevertheless, this provided the basis upon which the synthesis was developed.

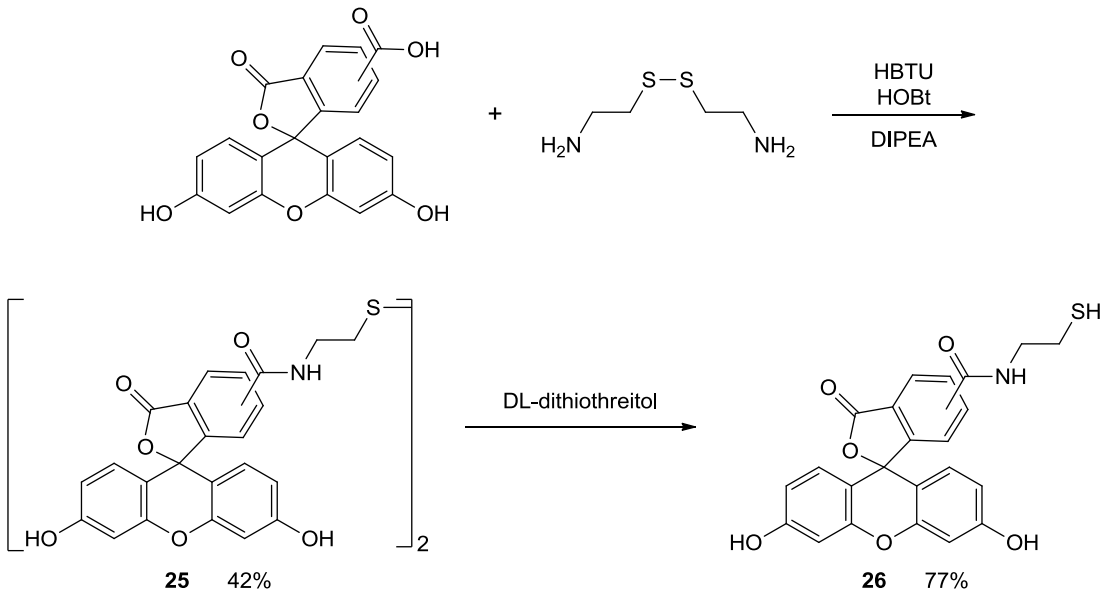

Scheme 3.10: Synthetic route to the fluorescent thiol.

The procedure as originally published utilised a combination of benzotriazol-1-yl-oxytripyrrolidinophosphonium hexafluorophosphate (PyBOP) and 1-hydroxybenzotriazole (HOBt) as the coupling reagents[262]. However as the coupling agent *N,N,N′,N′*-tetramethyl-*O*-(1*H*-benzotriazol-1-yl)uronium hexafluorophosphate (HBTU) was readily available and is often considered more stable than phosphonium reagents, this reagent was judged to be a suitable substitute for PyBOP.

The reaction was carried out by activating 2 equivalents of 5(6)-carboxyfluorescein (this is a mixture of regioisomers with the carboxylic acid at either the 5 or 6 position) in DMF by treatment with a combination of HBTU, HOBt and DIPEA followed by the addition of cystamine dihydrochloride. Purification of the crude material by flash column chromatography afforded the desired compound (**25**) as a mixture of isomers. The complexity of the product, a result of the starting material being a mixture of isomers, permitted only a tentative assignment of ^{1}H NMR and ^{13}C NMR spectrum. Consequently characterisation primarily replied upon mass spectrometry. A good high resolution mass spectrum was obtained finding a mass of 891.1291 compared to the calculated mass of 891.1289.

The next stage in the synthesis was cleavage of the disulfide bond of the cystamine moiety. Initially we envisaged the use of sodium borohydride for this purpose[263]; however following several failed small scale attempts at the reaction, an alternative reducing agent was sought.

Dithiothreitol, also known as Cleland's reagent, is the most popular reagent utilised for the reduction of disulphide bonds in biological molecules[264–266]. This suggested an alternative route for generation of the nucleophilic thiol molecule. Therefore reduction of the disulphide was performed using dithiothreitol (Scheme 3.10). Initially the reaction was extremely slow and low yielding, but increasing the temperature to 37°C generated the fluorescent thiol (**26**) in a vastly improved yield of 77%. Characterisation of the compound was again complicated due to the product being a mixture of isomers; however the ^{13}C NMR chemical shift corresponding to the α carbon indicates the presence of a thiol as opposed to a disulfide. An upfield shift in the resonance signal, from 38.27ppm to 22.89ppm, is observed upon conversion to the thiol. This is consistent with results observed in the literature when distinguishing between disulfides and thiols, although the magnitude of the shift difference was somewhat larger than expected[267].

The fluorescent thiol adduct was then prepared by treating 8-nitro-2'-*O*-methylguanosine (**27**) with 1.5 equivalents of the fluorescent thiol (**26**) at 37°C in TEAB buffer (0.1M) (Scheme 3.11). Whilst monitoring the reaction using RP-HPLC, it was established that oxidation of the thiol starting material to the disulfide was competing with the displacement reaction. Therefore a further 1.5 equivalents of the fluorescent thiol (**26**) were added to the reaction to ensure that enough of the nucleophile was present for the displacement reaction to occur. Although consumption of the starting material was completed in 2 hours, there were multiple peaks in the HPLC trace which were not attributable to the desired product. The luminescent yellow colour of the product simplified purification and flash column chromatography afforded the desired product (**28**) as a mixture of isomers in a 45% yield. The complexity of the isomers means that only a tentative assignment of ^{1}H NMR spectrum could be carried out and other methods were used for the characterisation of these compounds. Therefore in order to characterise these compounds, HPLC analysis and mass spectrometry were utilised. HPLC analysis was recorded at both 260nm and 350nm. Despite the compound being a mixture of isomers, only one peak was observed for the product at 260nm. As there was no observable peak corresponding to the product at 350nm, which specifically reveals 8-nitroguanine derivatives, it could be concluded that the nitro group was displaced during the reaction. Characterisation by mass spectrometry provided additional confirmation of the generation of the C8 substituted fluorescent nucleoside, as a mass of 729.1636 was observed compared to the calculated mass of 729.1615.

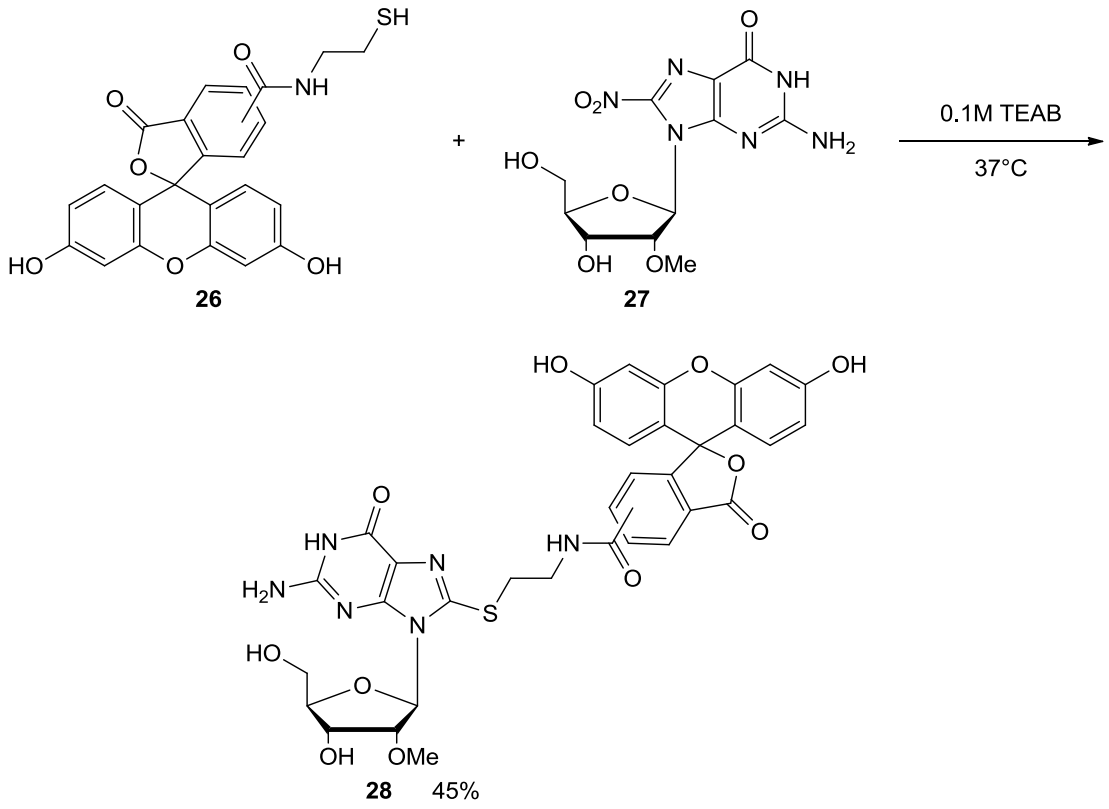

Scheme 3.11: Formation of the fluorescent adduct of 2'-*O*-methylguanosine.

The reaction was then adapted for the displacement of the nitro group within an oligonucleotide (Scheme 3.12). The reaction was carried out by treating a solution of the site 1 oligodeoxynucleotide (~26μM) in TRIS HCl buffer (pH 9, 0.1M) with a large excess of the fluorescent thiol nucleophile (**26**) at 37°C. The use of a pH 9 buffer was anticipated to facilitate the reaction by increasing the concentration of the reactive thiolate and by reducing depurination. The reaction was monitored by RP-HPLC over a 24 hour period. During this time the peak corresponding to the starting oligodeoxynucleotide decreased in intensity and a number of new peaks developed which did not have absorbances at 350nm. The complicated nature of the chromatograph recorded for this reaction made determining which peak corresponded to the desired product challenging. However, based upon retention times and co-injections of known compounds, for example the thiol nucleophile and the disulfide, it was established that there were four peaks present which could represent the product. Therefore isolation of these peaks by RP-HPLC yielded four compounds which were subsequently analysed by mass spectrometry in order to ascertain which peak corresponded to the fluorescent oligodeoxynucleotide. It was established that the desired fluorescent yellow product eluted at 18.63 minutes compared to the starting material which had a retention time of 11.55

minutes. The isolated product (site 1, adduct 2) was obtained in 1% yield, this is less than expected however as identification and isolation proved problematic, this was acceptable. Characterisation by ESMS verified that the displacement reaction had been successful as a mass of 4438.7090 was recorded compared to the calculated mass of 4438.7810

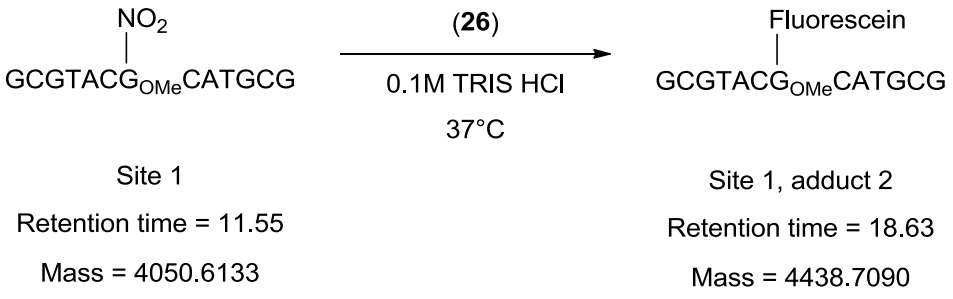

Scheme 3.12: Formation of the site 1, adduct 2 oligodeoxynucleotide. Note G_{OMe} = 2'-*O*-methylguanosine.

3.9 Displacement reactions using a fully protected cysteine derivative

Whilst it has been shown that both glutathione and the fluorescent thiol can replace the nitro group in nucleosides and oligodeoxynucleotides, neither are ideal reagents for studying and optimising this reaction. The glutathione product (site 1, adduct 1) has a retention time on HPLC that is very close to the nitrated site 1 oligodeoxynucleotide starting material and analysis of reactions with the fluorescent thiol are complicated by the mixture of isomers. As an alternative, a simple partially protected cysteine derivative was chosen, which due to the lipophilicity of the protecting groups was expected to increase the HPLC retention time of the product oligodeoxynucleotide. Conveniently cysteine also has a low extinction coefficient and therefore HPLC analysis will not be complicated by absorbances resulting from the nucleophile.

With the aforementioned in mind, a route to a partially protected cysteine nucleophile was developed starting from the readily available *N,N'*-bis(*tert*-butoxycarbonyl)cysteine (Scheme 3.13). Protection of the carboxylic acid group was performed according to a protocol previously described in the literature[268]. The reactive carboxylic acid groups were simultaneously protected by the sequential addition of ethanol, DMAP and *N,N'*-dicyclohexylcarbodiimide. The fully protected diethyl ester (**29**) was isolated in an 80% yield following purification by flash column chromatography. The emergence of signals in the ^{1}H NMR corresponding to the CH_3 and CH_2 groups of the ester at 1.28-1.32 and 4.20-4.26 respectively confirmed the recovery of the desired product.

Reduction of the disulphide bond was performed using dithiothreitol as previously described. The reaction was heated at 37°C for 18 hours to obtain the crude fully protected cysteine thiol. Purification by flash column chromatography afforded the pure product as a white solid in a 73% yield. Although NMR experiments produced spectra which were largely consistent with that of the starting material, the presence of a single set of peaks and characteristic chemical shifts in the ^{13}C NMR conclusively proved the structure of the product. An upfield shift, from 41.46ppm to 27.49ppm, in the signal corresponding to the carbon α to the thiol group again confirmed that the disulfide bond was reduced[267].

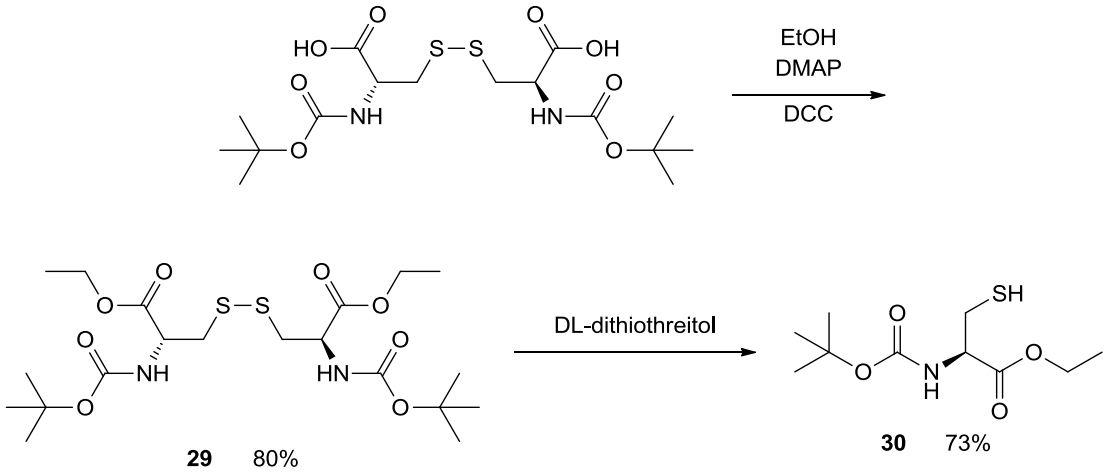

Scheme 3.13: Synthetic route to the protected cysteine nucleophile.

Displacement reactions were then carried out on both 8-nitroguanosine and 2'-*O*-methyl-8-nitroguanosine utilising the cysteine derivative **30** (Scheme 3.14). The reaction progress was monitored by TLC and in both cases conversion to a single nucleoside product was achieved in 2 to 4 hours. Following purification by flash column chromatography, the substituted guanosine (**31**) and 2'-*O*-methylguanosine (**32**) analogues were isolated in a 69% and 72% yield respectively.

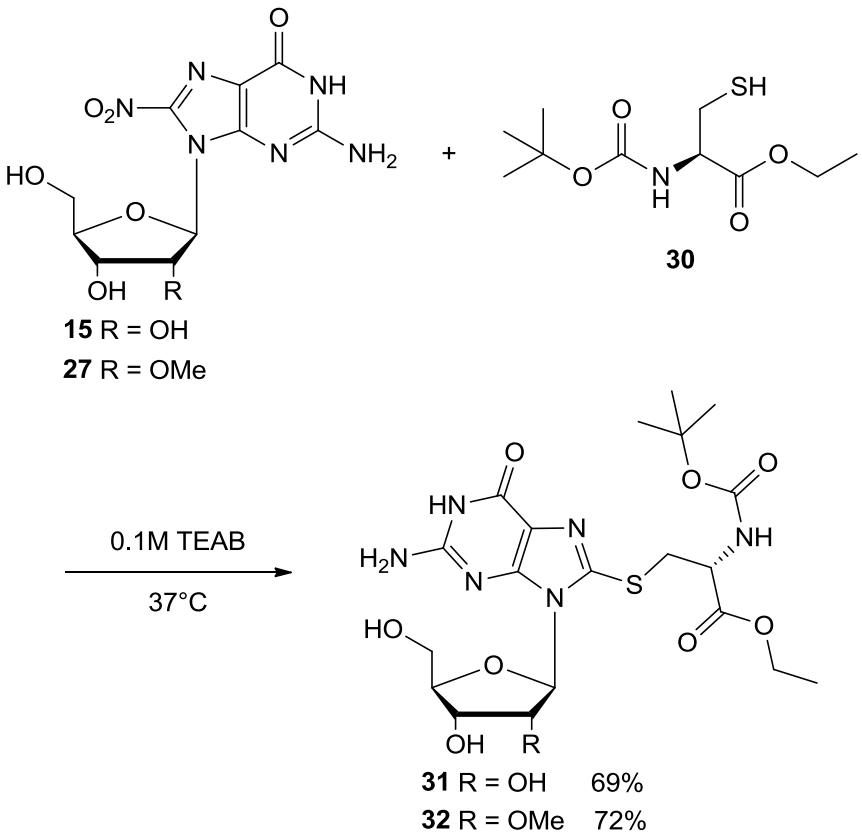

Scheme 3.14: Displacement of the nitro group with the fully protected cysteine derivative.

Complete structural characterisation was accomplished using the same techniques and reasoning as employed previously. The position by which the cysteine nucleophile was covalently attached to the nucleoside was verified using a HMBC experiment. Analysis of ^{1}H-^{13}C HMBC contour map revealed a long range ^{1}H-^{13}C correlation between the C8 resonance and the protons adjacent to the sulfur atom, thus confirming that the sulfur atom had displaced the nitro group in addition-elimination type reaction. The 2'-*O*-methyl analogue generated was a suitable standard for comparison purposes following enzymatic digestion of the DNA.

Since the displacement reactions were successful when utilising the 8-nitroguanine nucleosides, the reaction was applied to oligodeoxynucleotides containing the lesion. Thus the site 1 oligodeoxynucleotide (~26μM) in TRIS HCl buffer (pH 9, 0.1M) was treated with a large excess of protected cysteine thiol at 37°C (Scheme 3.15).

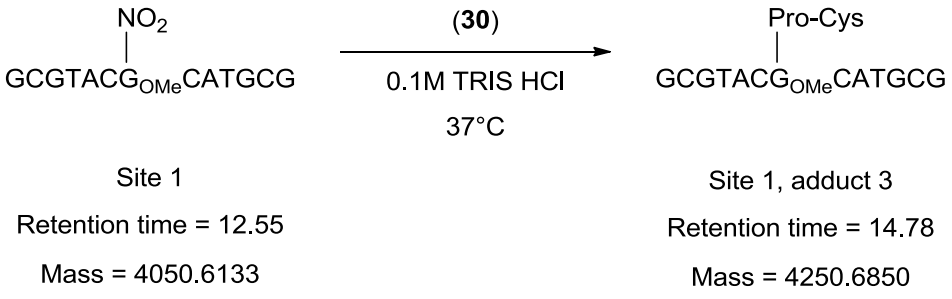

Scheme 3.15: Formation of the site 1, adduct 3 oligodeoxynucleotide. Note G_{OMe} = 2'-*O*-methylguanosine and Pro-Cys = Boc-Cys-OEt.

The progress of the reaction was closely monitored by RP-HPLC. It was evident the reaction proceeded more rapidly than those previously investigated. HPLC analysis indicated that there was approximately a 58% conversion of the starting material to a single product after 2.5 hours and the reaction appeared to go to completion within 6 hours (Figure 3.4). The HPLC analysis was also monitored at 350nm and upon complete conversion, the chromatograph showed no observable peak corresponding to 8-nitroguanine derivatives which absorb at this wavelength. The HPLC trace was considerably cleaner than those obtained previously; it appeared that a single product was exclusively formed. The product (site 1, adduct 3), which had a retention time of 14.78 minutes in comparison to the starting material which eluted at 12.55 minutes, was isolated using RP-HPLC. The site 1, adduct 3 oligodeoxynucleotide was obtained in 85% yield, which represents an excellent conversion from the starting material.

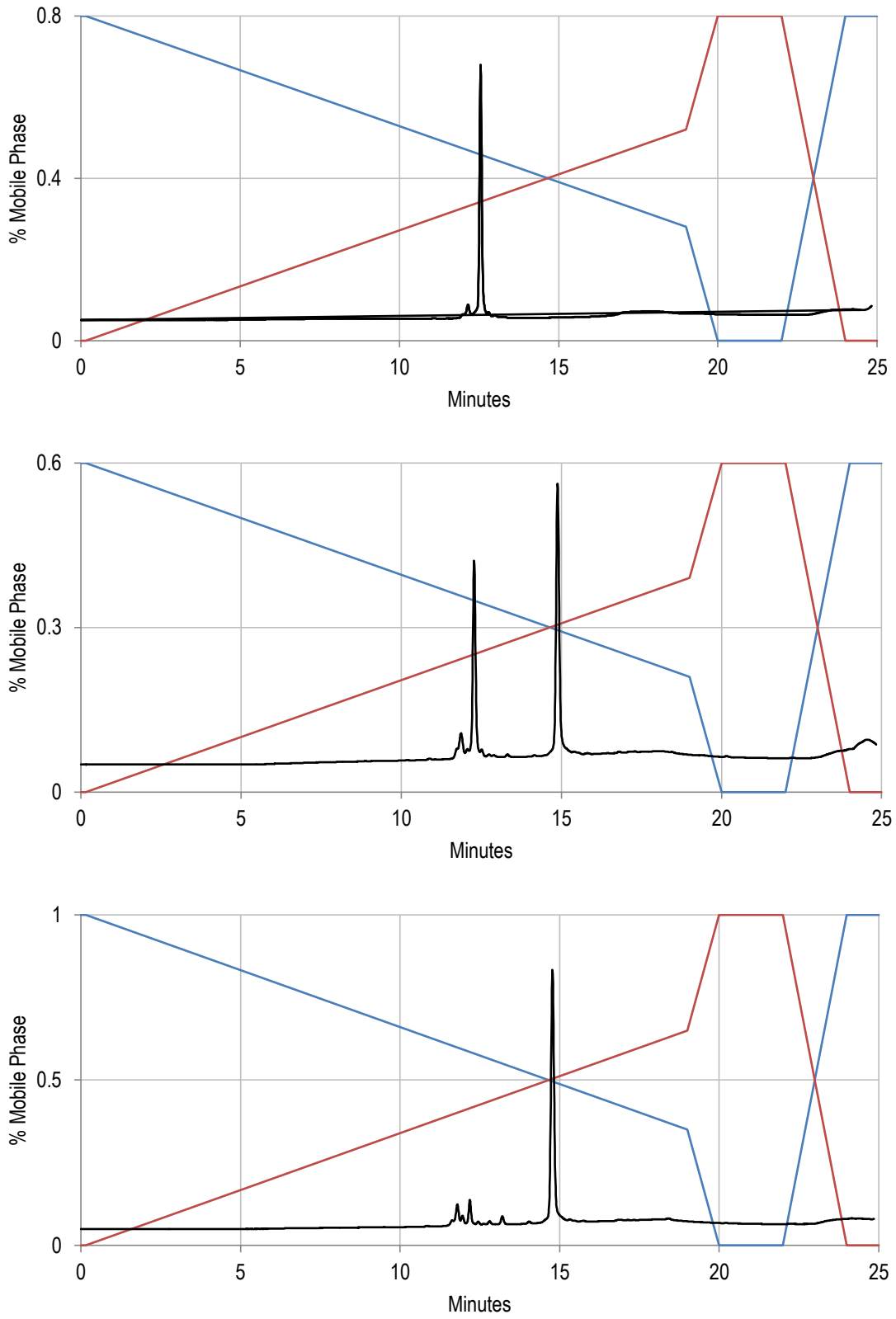

Figure 3.4: Chromatographs documenting the conversion from the site 1 oligodeoxynucleotide (retention time = 12.55 minutes) to the site 1, adduct 3 oligodeoxynucleotide (retention time = 14.78 minutes). Top = 0 hours, middle = 2.5 hours, bottom = 6 hours (Control method 0-65, page 140).

Characterisation of the oligodeoxynucleotide was carried out using negative mode ESMS. Replacement of the nitro group on the modified 2-*O*-methylguanosine in the site 1 oligodeoxynucleotide with the protected cysteine derivative (**30**) caused an increase in molecular weight of 200.0717, thus obtaining an accurate mass of 4250.6850 for the product compared to the calculated mass of 4250.7996.

Given the simplicity of the reaction with the protected cysteine derivative and the exclusive formation of the desired product, displacement of the nitro group within longer oligodeoxynucleotides was investigated. Typically, longer length oligodeoxynucleotide sequences are more representative of naturally occurring DNA as they often feature some degree of secondary structure formation. Therefore utilising longer sequences synthesised previously for biological applications would support the principle of detecting 8-nitroguanine within DNA.

The displacement reactions of both the site 2 (37mer) and site 3 (27mer) oligodeoxynucleotides with the cysteine nucleophile were carried out using the same conditions as discussed previously for the preparation of site 1, adduct 3. Although the reactions were considerably slower when compared with that of site 1, they were completed in 11 hours. The site 2 and site 3 oligodeoxynucleotides were both predominantly converted to a single product with retention times of 13.74 and 14.13 minutes respectively compared to the starting materials which eluted at 12.52 and 12.82 minutes.

Unfortunately the high molecular weight of these oligonucleotides meant that analysis of the product using ESMS was not feasible. It was considered that the oligodeoxynucleotides would be better suited to analysis by the matrix-assisted laser desorption/ionization (MALDI) technique, unfortunately this service was not available within the department. Thus inquiries have been made about the possibility of submitting these samples to external analytical service departments.

Consequently, to date characterisation of the longer oligodeoxynucleotide sequences has primarily relied upon HPLC analysis. The increased retention time is indicative of incorporation of the cysteine nucleophile into the oligodeoxynucleotides. The possible generation of an oligodeoxynucleotide containing an abasic site could be disregarded as it had been established within the group that the depurinated species has a shorter retention than that of the staring material[194]. Confirmation of the displacement of the nitro group is also apparent due to the disappearance of the absorbance in the HPLC chromatograph at 350nm corresponding

to the 8-nitroguanine nucleoside. This analysis provided convincing evidence that the generation of the desired oligodeoxynucleotides was successful, but more conclusive evidence was sort.

3.10 Characterisation of oligodeoxynucleotide adducts by enzymatic digestion

Given the problems associated with characterising the site 2, adduct 3 and site 3, adduct 3 oligodeoxynucleotides, the presence of the cysteine adduct could be established by enzymatic hydrolysis to the constituent nucleosides and subsequent analysis by HPLC. Phosphodiesterases are responsible for catalysing the hydrolysis of phosphodiesters to monophosphate esters. Intracellular phosphodiesterases play a role in signal transduction while extracellular phosphodiesterases are present in venoms and their mechanism of action is through the stepwise removal of nucleoside 5'-monophosphates from the 3'-end of oligodeoxynucleotides[269,270]. Alkaline phosphatase is then responsible for catalysing the hydrolysis of nucleoside 5'-monophosphates to produce inorganic phosphate and the nucleoside[271]. These enzymatic processes generate a hydrolysate which can be analysed by HPLC to determine the base composition of DNA. This is achieved by comparing the constituent nucleoside retention times to those of natural and synthetically prepared standards.

Enzymatic digestion of the site 1, adduct 3 sequence was performed using phosphodiesterase I from *Crotalus Atrox* and alkaline phosphatase from bovine intestinal mucosa. The reaction was heated at 37ºC for 2 hours to ensure complete hydrolysis of the oligodeoxynucleotide. The proteins were precipitated with ice cold ethanol and the heterogeneous mixture was separated using centrifugation.

The relative amounts of deoxyadenosine, deoxycytidine, deoxyguanosine, thymidine and the modified 2'-*O*-methylguanosine in the hydrolysate were analysed using RP-HPLC. The nucleoside composition analysis for the enzymatic digestion is shown in Figure 3.5. The chromatograph was recorded at 280nm as both the standard and modified nucleosides have acceptable extinction coefficients and hence absorbances at this wavelength. By comparing the retention times of the remaining unidentified peaks to various reagents and the standards which have previously been synthesised, assignments for the key peaks were achieved.

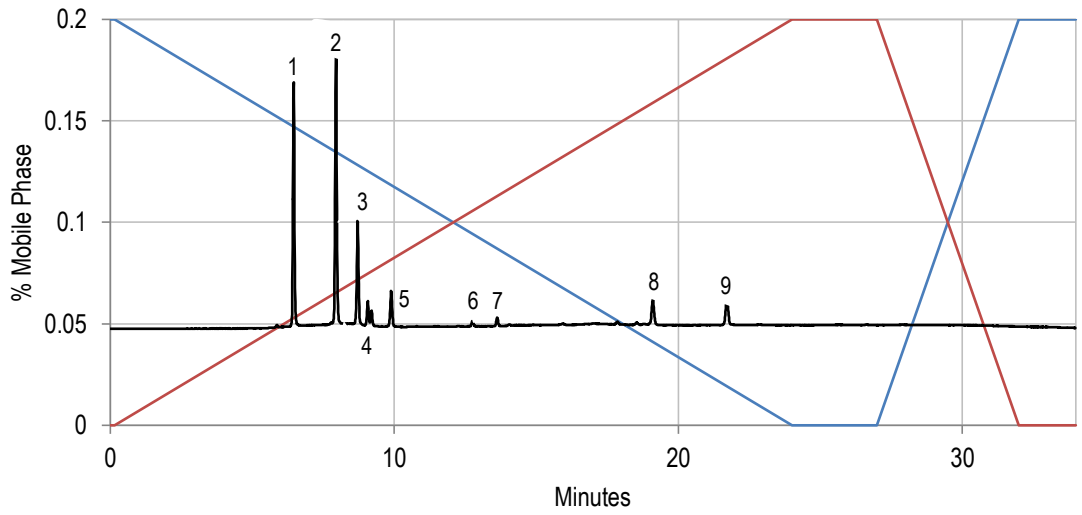

Figure 3.5: Chromatograph showing the RP-HPLC nucleoside composition analysis of the site 1, adduct 3 oligodeoxynucleotide at 280nm. Peaks 1, 2, 3, and 5 correspond to deoxycytidine, deoxyguanosine, thymidine and deoxyadenosine respectively. The UV properties of peak 4 indicated that this was also nucleoside derived. Peaks 6 and 7 were as a result of residual phophodiesterase and alkaline phosphatase enzymes (Control method 0-100B, page 139).

Displacement of the nitro group with the cysteine nucleophile resulted in nucleoside (**32**) which was considerably less polar than those which are naturally occurring. Accordingly, the retention time of adduct **32** was increased to 21.69 minutes on RP-HPLC and it was identified as corresponding to peak 9. The integration of the peaks can be used to determine the relative amount of each constituent nucleoside in an oligonucleotide and hence establish its composition. However, the integration for peak 9 was lower than expected. Interestingly peak 8 at 19.07 minutes corresponded to the retention time of the cysteine nucleophile (**30**). This was not evident in the chromatograph of the oligodeoxynucleotide prior to enzymatic hydrolysis. Therefore the possibility of the thiol substituent being displaced during the reaction was investigated.

To examine this, initially the cysteine substituted nucleoside (**32**) was treated with phosphodiesterase and alkaline phosphatase to determine if the enzymes were not compatible with this substrate; however no significant changes were identified. In order to test the remaining variable of the enzymatic hydrolysis, the cysteine substituted nucleoside was dissolved in TRIS HCl buffer and heated overnight. It was apparent upon analysis that decomposition of the nucleoside generated a species which eluted with a retention time comparable to peak 4.

It was considered that the C8 cysteine substituted nucleoside was possibly being hydrolysed in the aqueous buffer to generate 8-oxo-2'-*O*-methylguanosine and the cysteine derivative (**30**). Consequently, synthesis of an 8-oxo-2'-*O*-methylguanosine standard (**33**) was carried out in order to confirm this hypothesis. The 8-oxoguanine derivative was generated according to a protocol previously described in the literature (Scheme 3.16)[272]. Briefly, 8-bromo-2'-*O*-methylguanosine (**23**) was heated with sodium benzyloxide in DMSO to produce the 8-benzyloxy-2'-*O*-methylguanosine. Following isolation by flash column chromatography, direct treatment of the intermediate with 1M HCl in methanol generated the crude 8-oxo-2'-*O*-methylguanosine (**33**). Careful trituration of the residue afforded the desired product as a pale yellow sold in a 42% yield. The proton environments of the starting material and product are essentially identical in MeOD; therefore characterisation relied principally on ^{13}C NMR and mass spectrometry. A downfield shift from 117.44ppm to 152.30ppm was observed for the signal corresponding to C8, which is consistent with the literature value and therefore confirming the structure of the 8-oxo-2'-*O*-methylguanosine (**33**).

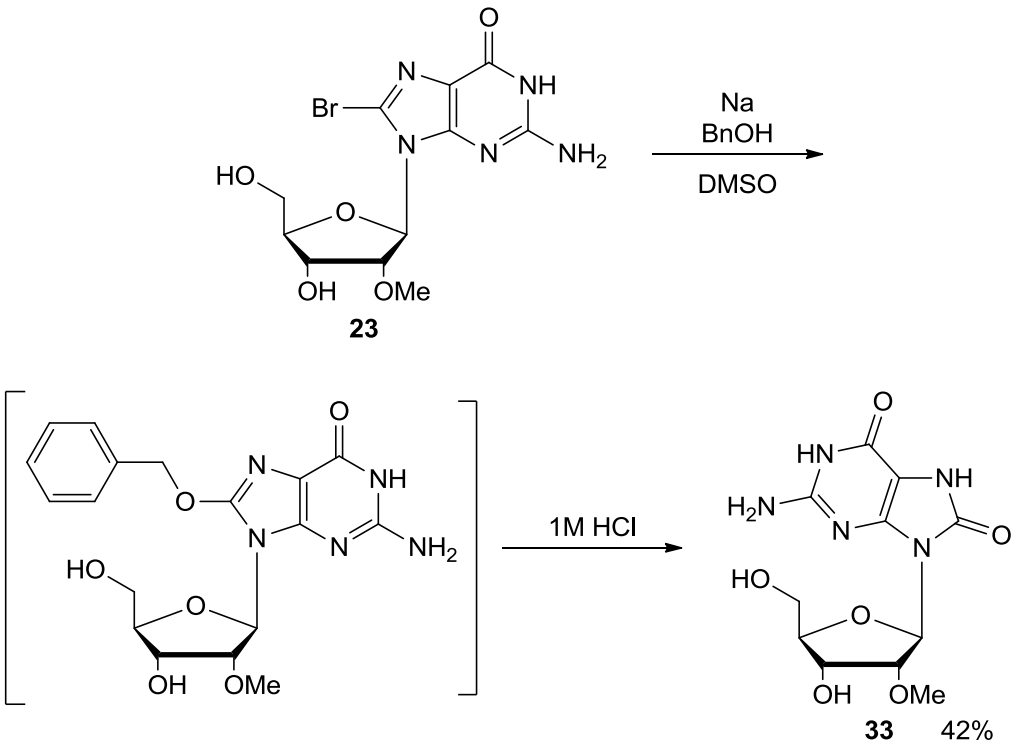

Scheme 3.16: Synthetic route for the synthesis of 8-oxo-2'-*O*-methylguanosine.

RP-HPLC comparison of 8-oxo-2'-*O*-methylguanosine and peak 4 (Figure 3.5) revealed them to co-elute thereby suggesting that the unidentified peak in the chromatograph was as a result of decomposition of the cysteine adduct. Although the presence of the C8 cysteine derivative

was established using enzymatic hydrolysis and subsequent HPLC analysis of the hydrolysate, quantitative analysis was not feasible.

3.11 Conclusion

The concept of displacing the nitro group from an 8-nitroguanine derivative within an oligodeoxynucleotide using nucleophilic thiols has been demonstrated. The covalent attachment of an extrinsic fluorophore, with the specificity to covalently modify the lesion would provide a method to directly detect the levels of 8-nitroguanine in DNA. Additionally, displacement of the nitro group using this method would prevent depurination, thereby stabilising the adduct for further analysis; although further investigation would be required in order to study the hydrolytic stability of the thiol adduct. Thus these derivatives could become useful chemical probes for monitoring levels of 8-nitroguanine derivatives *in vivo* and act as a biomarker for inflammation related cancers. Future work will need to investigate the stability of the 8-thioguanine adducts to hydrolysis.

Chapter 4

Results and Discussion 3:

Detection of the 8-nitroguanine lesion using surface enhanced Raman spectroscopy

4 Results and Discussion 3

4.1 A brief overview of SERS

The research presented in this chapter was carried out by Susan Dick, supervised by Professor Steven Bell at Queen's University, Belfast. In order to discuss the sensitive detection techniques utilised in this application, it is first appropriate to give a brief overview of the principles regarding Raman scattering.

Raman spectroscopy is a technique which can provide insight into the structure of a molecule by analysing its vibrational transitions; in this respect it is related to infra-red spectroscopy[273]. An important distinction between these two techniques is while the intensity of an IR absorbance is determined by changes in the dipole moment during vibration, Raman signals are dependent on a change in polarisability, that is how easily the electrons are distorted in response to an external field[274].

The principle of Raman scattering is based upon the premise that upon the interaction of light with a substrate, in addition to being transmitted or reflected, a small proportion of the photons are scattered. The majority of photons emerge having the same frequency as the incident radiation, this is known as elastic or Raleigh scattering. A small quantity of the light scattered following a collision with the molecule has a different frequency than that of the incident radiation. When energy is transferred from the incident photon to a molecule, excitation of the vibrational bonds within the molecule occurs[274,275]. Essentially, the molecule is promoted to a virtual excited state, the molecule then emits a photon of a lower energy (longer wavelength) than that which was absorbed. The loss of the photon causes the molecule to decay to a lower vibrational state, but as some of the incident photons energy has been transferred to the molecule, the energy level is above the initial ground state[276]. This is defined as stokes scattering.

The alternative is also possible, thus if the molecule is initially in a higher vibrational state, the photon may gain energy from the vibration. This causes the molecule to decay to the ground state and the scattered light to be of a higher energy (shorter wavelength) than the incident radiation. This is defined as anti-stokes scattering; this situation is less frequent and is often associated with an increase in temperature of the system[274–276].

The applications of Raman spectroscopy are limited due to it being an inherently weak process. For this reason, surface-enhanced Raman scattering (SERS) and surface-enhanced

resonance Raman scattering (SERRS) are more frequently utilised as these processes amplify the Raman signals.

SERS is a process that occurs following adsorption of a substrate onto a metal surface. The surface electrons of the metal absorb energy from the incident laser. This interaction induces collective oscillations of the surface electrons known as plasmons[273,277]. Smooth surfaces are not effective for this enhancement as the plasmon energy is bound to the surface. Utilising a roughened metal surface or aggregated metal nanoparticles gives rise to the scattering process, as the irregular morphology generates plasmons which are not restricted to movement parallel to the surface[278]. This creates an enhanced localised field at the surface of the metal, thus electromagnetic radiation of the same frequency as the laser interacts with the substrate adsorbed to the surface. The energy transferred to the molecule gives rise to the Raman process. The energy is then returned to the surface plasmon and the scattering process ensues. The difference in energy between the incident and scattered radiation is consistent with the vibrational transitions within the molecule[277,279]. The magnitude of the enhancement of the Raman signal can vary considerably; values are typically amplified by several orders of magnitude using the SERS technique[273].

The weak signal of a Raman emission can also be enhanced using resonance Raman spectroscopy. This occurs when the energy of the incident radiation is close to the energy of an electronic transition within the molecule. Resonance Raman spectroscopy is often exploited when the molecule has a visible chromophore; by utilising a laser wavelength which is resonant with this absorption band, considerable enhancement in the intensity of the relevant signals may occur. Since only the chromophore is accountable for the scattering observed at this wavelength this technique proves particularly useful for identifying unique components within a species. This effect produces an enhancement of the Raman signals associated with the absorbing chromophore by a factor of 10^3 to 10^4, thus presenting a method for introducing electronic selectivity[273,280,281].

The SERRS technique combines SERS and resonance Raman spectroscopy in order to obtain synergistic enhancements resulting from both metal surface plasmons and a resonant chromophore[277,282]. The laser wavelength must be tuned to the resonance frequency of the surface plasmons of the metal, therefore the application of SERRS is limited to molecules which have chromophoric components absorbing within these regions[281]. Although maximum enhancements are to be expected when these wavelengths are equivalent, SERRS can be

effective even with approximately a 250nm separation between the resonance frequencies[277,283].

4.2 Background relevant to the detection of DNA using SERS

Our collaborators in Belfast have previously shown that surface enhanced Raman spectroscopy (SERS) can detect single nucleotide exchanges in DNA. This was achieved by absorption of oligodeoxynucleotides on to a suitably enhancing metal surface and subsequent acquisition of SERS spectra using appropriate experimental conditions. The SERS spectra obtained, display identifiable bands which are characteristic of the constituent bases present in an oligodeoxynucleotide, therefore variation of these distinctive bands can be exploited to detect polymorphisms in short strands of DNA[284].

Interestingly, studies indicate that specificity as well as enhanced sensitivity can be obtained when the SERS technique is applied to the detection of nitro aromatic compounds[280,285,286]. Consequently, this technology is currently being utilised in the development of a real time method for trace level detection of nitro based explosives.

Given this sensitivity, it is an interesting prospect to explore whether SERS is a valid method for detection of this naturally occurring biomarker. In view of the unique UV absorption profile of the 8-nitroguanine derivatives, it was envisaged that SERRS experiments could selectively detect signals corresponding to the chromophore, providing a method to detect the prevalence of the lesion in DNA. This approach eliminates the additional processes required to label and prepare the sample of DNA which are necessary when using alternative methods for detection[287]. It would allow for the levels of a lesion with a unique chromophore to be monitored within a biological system in real time.

4.3 SE(R)RS experiments on 8-nitroguanine substrates

For the SE(R)RS experiments the following compounds were prepared: 8-nitroguanine (**16**), a dimer containing only the 8-nitroguanine base (**9**, for structure see page 68) and site 1 and site 3 oligodeoxynucleotides (for sequences see page 61) which both contain a single 8-nitroguanine modification together with the four standard DNA bases. In all cases the 8-nitroguanine base was associated with the 2'-*O*-methyl ribose sugar to increase the stability of the glycosidic bond. The corresponding control compounds were also prepared in which guanine replaced 8-nitroguanine. This gave a series of compounds which presented the 8-

nitroguanine base in an increasingly complex set of oligonucleotide sequences which aided assignment of resonance bands.

Initial proof of principle was achieved by comparing the experimental data obtained for 8-nitroguanine to guanine. As the free base is the simplest model of the lesion, this provided a suitable foundation on which to develop the approach, where complications arising due to the presence of the 2'-*O*-methyl sugar would not factor in its viability.

Figure 4.1 shows representative data for the 8-nitroguanine and guanine bases. When using a laser wavelength of 785nm, the relative band intensities of the signals in both spectra are quite similar. Although 8-nitroguanine shares some bands with those present in the guanine sample, there are additional peaks which are exclusive to the modified base. In order to investigate whether resonance enhancement of the signals associated with the absorbing chromophore could be achieved, the laser wavelength was lowered to 532nm; this was significantly closer to the absorption of 8-nitroguanine at approximately 400nm. As is evident in Figure 4.1, the signals corresponding to 8-nitroguanine are considerably greater in intensity than those of guanine. Furthermore, the signals resulting exclusively from the nitrated base, for example the band at approximately 1280cm^{-1}, are more prominent at this wavelength.

The positions of the peaks observed in the experiments are consistent with density functional theory (DFT) calculations also performed by our collaborators in Belfast. These calculations enabled the assignment of the identified bands to specific vibrations within the molecules. For example, the DFT calculations predict a band at 1282cm^{-1} representing the symmetrical stretching vibration of the nitro group which is evident in the experimental data. Encouraged by these preliminary results, the complexity of the system being examined was increased.

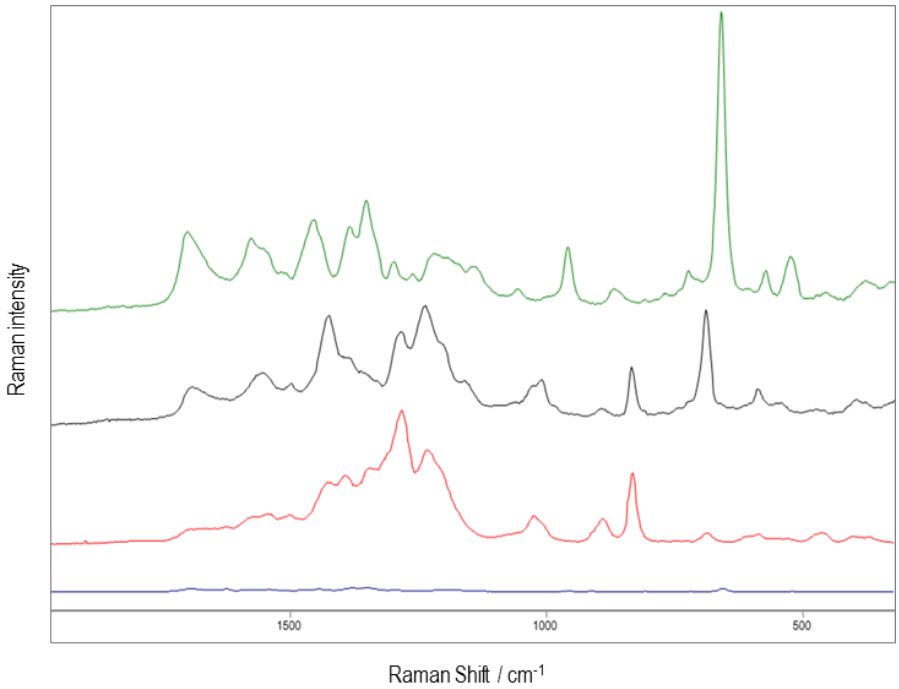

Figure 4.1: SERS spectra of 5 x 10^{-6}M solutions showing comparison of guanine and 8-nitroguanine at 785nm and 532nm on the same absolute scale. Green line = guanine (785nm), black line = 8-nitroguanine (785nm), red line = 8-nitroguanine (532nm), blue line = guanine (532nm).

In a previous study evaluating single nucleotide exchanges in oligodeoxynucleotides, the SERS spectrum of dGMP was recorded for use as a reference spectrum in order to aid the analysis of the DNA spectra[284]. As the corresponding 8-nitro-2'-*O*-methylguanosine monophosphate was not accessible, a dinucleotide containing two modified residues (**9**) was envisaged as a suitable alternative.

The spectra of the 8-nitroguanine dimer, site 3 oligodeoxynucleotide and site 3 control oligodeoxynucleotide are somewhat different as shown in Figure 4.2. This can be attributed to differences in the relative band intensities of identifiable spectral features and the presence of additional bands. These inconsistencies were to be expected as the acquired spectra for the oligodeoxynucleotide is comprised of bands representative of all the nucleobases present, each of which produce varying degrees of Raman scattering[287]. Notably, the intense broad peak at approximately 1238cm^{-1} is present in the compounds containing the 8-nitroguanine base but not in the control samples.

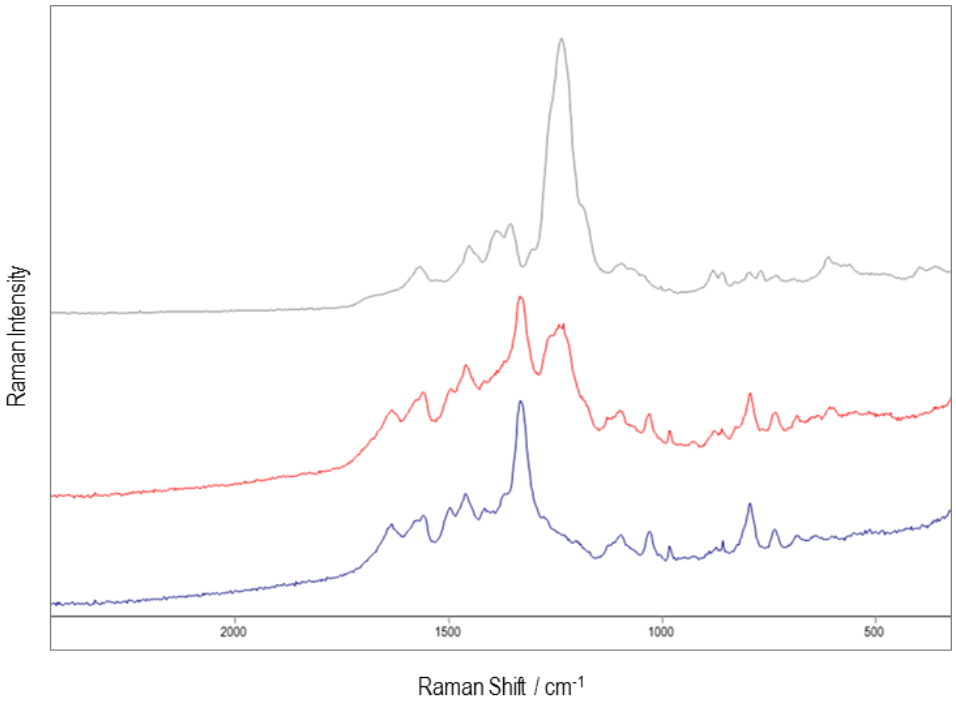

Figure 4.2: SERS spectra of 10^{-5}M solutions showing comparison of the 8-nitroguanine dimer (top), site 3 oligodeoxynucleotide (middle) and site 3 control oligodeoxynucleotide (bottom) at 785nm.

Despite the varying intensities, it is evident that the characteristic band pattern recorded for the 8-nitroguanine dimer is distinguishable when analysing the representative data of the mixed sequence site 3 oligodeoxynucleotide. The absence of analogous signals in the spectra obtained for the site 3 control oligodeoxynucleotide, confirmed that these bands could be assigned exclusively to the 8-nitroguanine residue.

The same series of spectra were then obtained using the 532nm laser, substantial enhancement of the signals associated with the 8-nitroguanine modification were apparent (Figure 4.3). The difference in the absolute intensities of the sequences containing the 8-nitroguanine modification and the control sequence is the key aspect of the spectra. The band patterns observed for the site 3 oligodeoxynucleotide were consistent with those obtained for the 8-nitroguanine dimer and previously for the 8-nitroguanine base. This suggests that the Raman scattering observed at this wavelength is predominantly due to contributions resulting from the 8-nitroguanine modification.

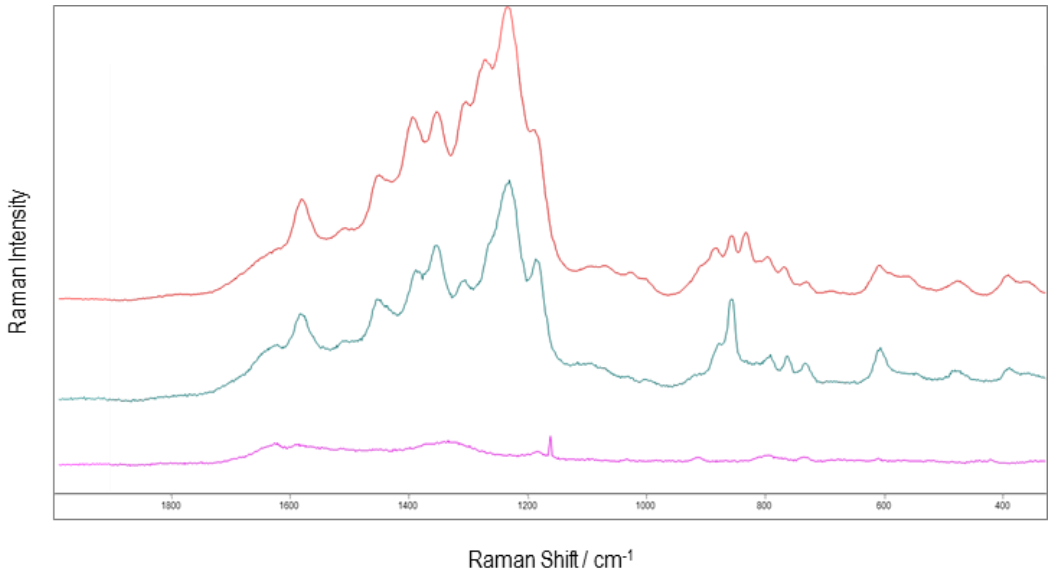

Figure 4.3: SERS spectra of 5 x 10^{-6}M solutions showing comparison of the 8-nitroguanine dimer (top), site 3 oligodeoxynucleotide (middle) and site 3 control oligodeoxynucleotide (bottom) at 532nm. Note the peak at ~1170cm^{-1} in the bottom trace is considered to be an experimental artefact.

While the spectra presented to date show that the 8-nitroguanine base has a unique scattering pattern that distinguish it from the four natural DNA bases, it was of interest to analyse samples in which the 8-nitroguanine lesion was only a very minor constituent of the DNA sample. This would be a closer analogy to the analysis of biological DNA samples containing the 8-nitroguanine lesion. As a means to accomplish this, samples were analysed in which the site 3 oligodeoxynucleotide was diluted with its control sequence.

In order to increase the selectivity and specificity for the signal associated with the unique absorbing chromophore of 8-nitroguanine, in these diluted samples the excitation wavelength was lowered again to 488nm shifting it closer to the λ_{max} for this base at ~400nm. It is evident from the representative data shown in Figure 4.4 that doping a site 3 control sample with as little as 2% of the site 3 oligodeoxynucleotide containing a single 8-nitroguanine modification generated bands diagnostic of the lesion. Unsurprisingly, as the quantity of the site 3 oligodeoxynucleotide in the experiment was increased, the intensity of the signal at 1248cm^{-1} resulting from the 8-nitroguanine residue was enhanced accordingly; this scattering was not seen in the control sequence.

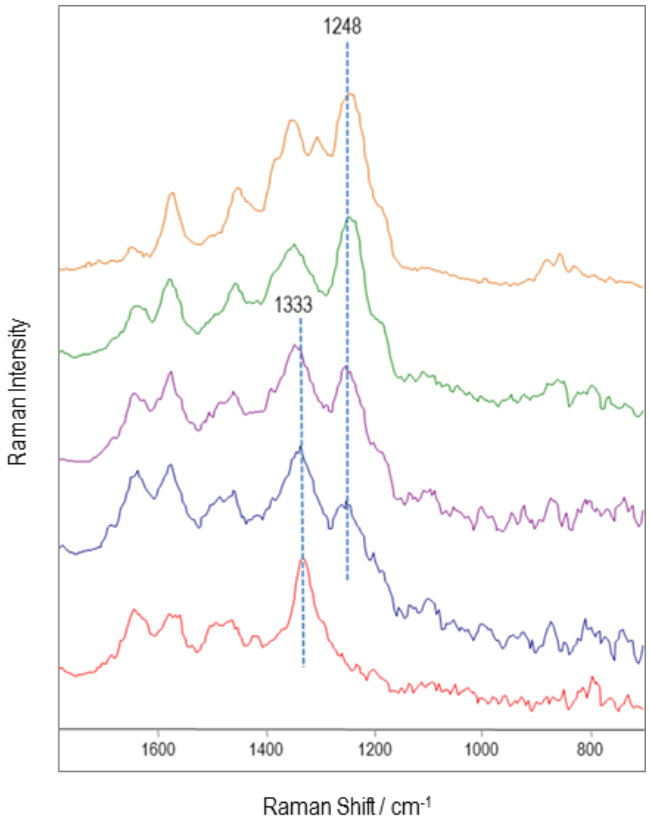

Figure 4.4: SERS spectra showing doping experiments whereby a small amount of the site 3 oligodeoxynucleotide was introduced to a bulk sample of the site 3 control oligodeoxynucleotide at 488nm. Red = site 3 control (scale enhanced for comparison purposes), blue = 2% site 3, purple = 5% site 3, green = 10% site 3, yellow = 100% site 3. All samples measured at 10^{-5}M.

Finally, experiments were conducted in order to definitively establish that the bands that are observed in the spectra are representative of the 8-nitroguanine modification within an oligonucleotide as opposed to the free base resulting from depurination (Figure 4.5). Notably the peak at ~830cm^{-1} which is characteristic of the 8-nitroguanine base but not the modified oligodeoxynucleotides, was absent from the site 3 spectra. An equimolar mixture of the site 3 oligonucleotide and 8-nitroguanine was examined to ascertain whether this signal was distinguishable from the background in the presence of the signals representing the natural nucleobases. The band at ~830cm^{-1} was easily observed in the mixed spectra, therefore it was determined that the results demonstrated were not due to depurination of the labile 8-nitroguanine base.

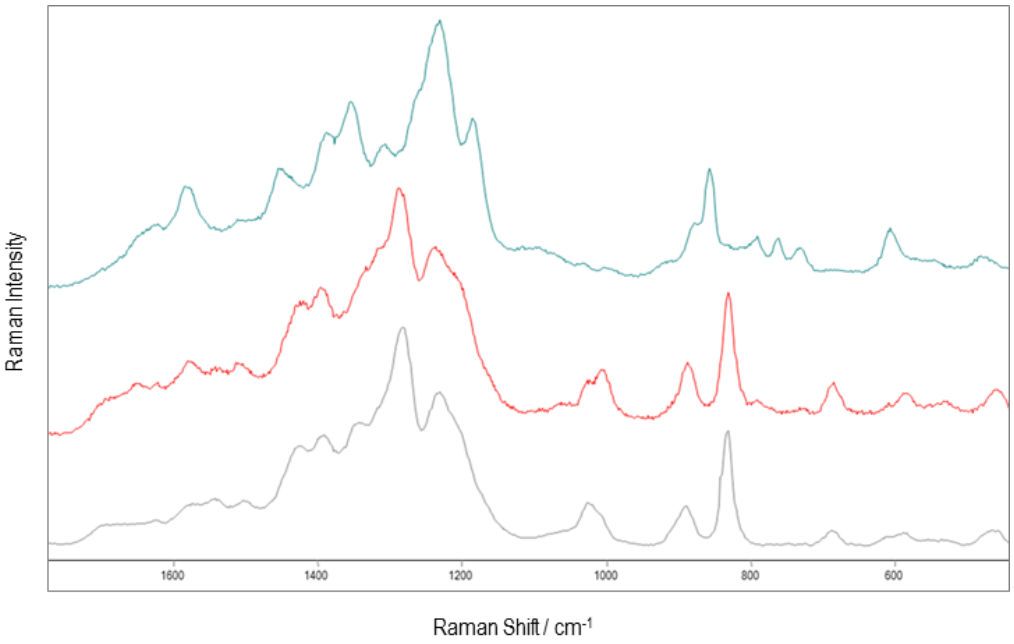

Figure 4.5: SERS spectra of 5 x 10^{-6}M solutions showing comparison of site 3 (top), equimolar mixture of site 3 control and 8-nitroguanine base (middle) and 8-nitroguanine base (bottom).

4.4 Conclusion

This work demonstrates a simple method for detecting the prevalence of the 8-nitroguanine lesion within DNA using the SE(R)RS technique. The unique scattering profile of the 8-nitroguanine derivatives provides a valuable method by which electronic selectivity can be achieved. The SERS signals observed for the modification in the free base, dimer and oligodeoxynucleotide were enhanced considerably upon lowering the excitation wavelength from 785nm to 532nm and 488nm. Thus SE(R)RS is a viable method for the real-time detection of this naturally occurring biomarker. The technique is highly sensitive and selective for the lesion enabling identification of trace amounts within a bulk sample of DNA.

Chapter 5

Results and Discussion 4:

Studies towards the synthesis of 8-nitroguanosine triphosphate

5 Results and Discussion 4

5.1 Nucleoside triphosphates

Nucleoside triphosphates are of fundamental importance within biological systems. They act as substrates for polymerase-mediated DNA and RNA replication, regulators of signal transduction, cofactors of metabolic pathways and adenosine triphosphate (ATP) acts as the 'molecular currency' for intracellular energy transfer[288]. The hydrolysis of the high energy phosphate groups in ATP and other nucleoside triphosphates, results in the release of a large amount of free energy. Therefore nucleoside triphosphates play a central role in many energetically unfavourable processes within biological systems[289].

With regard to DNA replication, DNA polymerases have evolved to be highly accurate, with polymerases α, δ, ε and γ generating less than 1 error for every 10,000 correct incorporations[290,291]. While oxidative DNA damage can be as a result of direct reactions between reactive oxygen and nitrogen species and DNA, oxidation products generated within the nucleoside pool can act as substrates for DNA polymerases and be incorporated into the nascent strand. Accordingly there are enzymes functioning to reduce the mutagenic potential of the oxidised nucleotide triphosphates within the nucleotide pool.

As previously discussed, valuable information regarding the repair mechanisms against the mutagenesis caused by 8-oxoguanine has been gathered by studying the fidelity of replication in the presence of the modified nucleoside triphosphates[165]. Of particular interest with regards to sanitising the nucleotide pool of oxidised nucleoside triphosphates is the enzyme MutT (MTH1). The enzyme is a triphosphatase that is responsible for hydrolysing 8-oxo-dGTP in the nucleotide pool to the corresponding monophosphate and pyrophosphate, thus eliminating it as a potential substrate for replication by DNA polymerases[166]. MutT efficiently hydrolyses a number of oxidised triphosphates including 8-oxo-dGTP and 2-OH-dATP and the corresponding ribonucleotides in nucleotide pools[292,293].

The aim of this part of the project was to synthesise 8-nitroguanosine triphosphate in order to investigate its behaviour both as a template for polymerase mediated replication and as a substrate for the triphosphatase MutT. Since MutT catalyses the hydrolysis of both ribo- and deoxyribo-triphosphates we opted to synthesise the ribonucleotide analogue 8-nitroguanosine triphosphate. In addition to the starting material being cheap and readily available, the labile glycosidic bond is sufficiently stabilised by the 2'-hydroxyl group and as the sugar functionality

is identical to that of the natural triphosphate any results would be as consequence of the nitro group alone.

5.2 Synthetic approaches to nucleoside triphosphates

The biological significance of nucleoside triphosphates and their involvement in a host of biochemical processes has led to the development of a number of methods for their synthesis. Early synthetic procedures were based upon the use of natural nucleoside 5'-monophosphates as precursors[294,295]. In 1964 Moffat reported that the conversion of a monophosphate to its morpholidate followed by displacement by pyrophosphate afforded the corresponding triphosphate in a 76% yield (Scheme 5.1)[294].

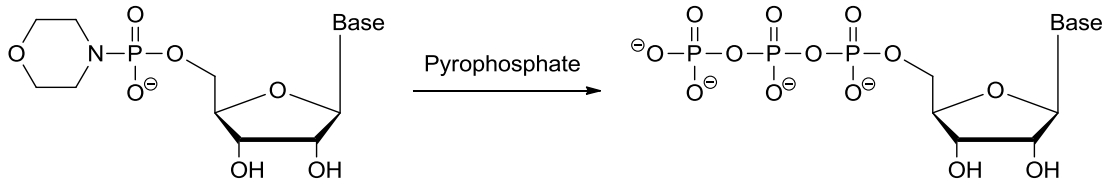

Scheme 5.1: Triphosphate synthesis using an activated monophosphate.

In order to generate synthetic triphosphates containing modified sugars or bases there became an increasing demand for procedures suitable for the 5'-phosphorylation of modified nucleosides.

A lack of regioselectivity of reagents for the 5'-position made synthesis of monophosphates problematic; primarily due to the production of a mixture of 2'-, 3'- and 5'-phosphorylated compounds and the difficulty in their identification and isolation[296]. The approach developed by Yoshikawa *et al.* in 1967 which lead, not only to accelerated reactions rates but also to selectivity at the 5'-position, was a noteworthy development and still remains the basis of one of the most popular methods for synthesising nucleoside triphosphates today[297]. The use of a trialkylphosphate as a solvent was the defining feature of this method. In addition to forming a homogeneous solution with the nucleoside, trialkylphosphates are believed to form an activated intermediate with the phosphorylating reagent giving rise to an increased rate of reaction[298].

Some of the early studies were carried out on 2',3'-*O*-isopropylidene nucleosides to prevent side reactions at these positions. However it was soon established that protection of the 2'- and 3'-hydroxyl groups was not necessary to phosphorylate selectively at the 5'-hydroxyl group

in good yields[297]. Ludwig then adapted this procedure in 1981 to generate nucleoside triphosphates in a 'one pot, three step procedure'. The initial methodology developed by Yoshikawa was retained to generate nucleoside 5'-dichlorophosphates which were then transformed into triphosphates by a short, *in situ* treatment with tri-*n*-butylammonium pyrophosphate followed by neutral hydrolysis (Scheme 5.2)[299].

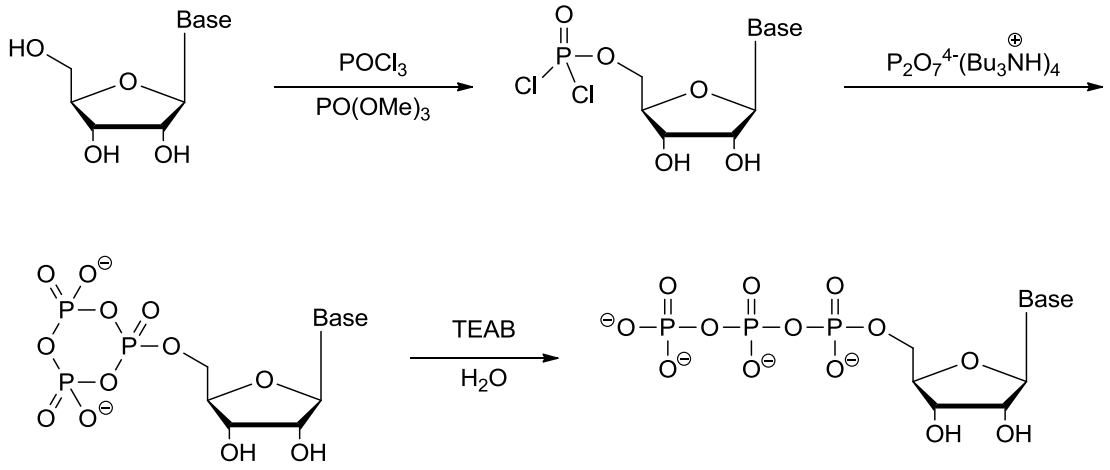

Scheme 5.2: One pot, three step formation of nucleoside triphosphates.

In 1986 the use of salicyl chlorophosphite was reported as a method to introduce a 3'-5'-phosphodiester linkage between nucleosides[300]. Ludwig and Eckstein utilised the multifunctionality of the cyclic phosphite intermediate in the synthesis of 5'-nucleoside triphosphates. The reaction initially gave rise to an activated phosphite that was reacted, in a double displacement process, with pyrophosphate to form the cyclic intermediate that was oxidized to give the corresponding triphosphate (Scheme 5.3)[298,301].

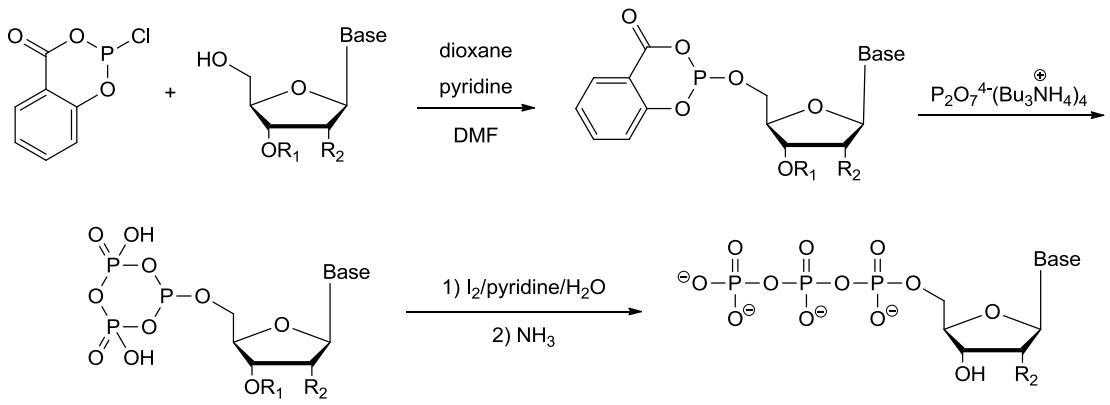

Scheme 5.3: The Ludwig and Eckstein approach to nucleoside triphosphate synthesis. Note R_1 = protecting group and R_2 = H or protected OH.

The procedure is carried out in one pot; hence the intermediates shown in Scheme 5.3 were not isolated. There is however evidence for their formation, as Ludwig and Eckstein followed the course of the reaction using ^{31}P NMR[298]. While protection of the exocylic amino groups of the nucleobases was not necessary, protection of the 2'- and 3'-hydroxyl groups is required. Consequently, this route to the synthesis of nucleoside triphosphates is lengthier due to the additional steps in preparing the nucleoside for the reaction, but is certainly valuable due to the reduced quantity of undesired by-products which can be generated in alternative routes.

Other strategies include; a solid-phase approach involving phosphorylation of the suitably protected nucleoside derivative anchored to a resin, direct nucleophilic substitution of leaving groups at the 5'-hydroxyl position by a triphosphate analogues and biocatalytic methods[298]. Of these additional strategies, biocatalysis is arguably the most successful approach to date. Whilst enzymatic method can be ideal for the synthesis of standard nucleoside triphosphates, modified nucleoside triphosphates present a more complex challenge. The potential for a lack of base specificity with regard to the modified nucleoside substrate renders this method less attractive than the chemical based approaches.

There is no method that is universally applicable for the synthesis of triphosphates; while some approaches will produce excellent yields with certain substrates, others are not tolerated[288,298]. Ideally to produce the 8-nitroguanosine triphosphate, the approach adopted would not require the lengthy protection and deprotection of multiple functional groups and would produce a high yield of the desired product. With this in mind, we initially focused our efforts on the phosphorylation procedure developed by Yoshikawa and modified by Ludwig.

5.3 Initial route towards the synthesis of 8-nitroguanosine triphosphate

The Yoshikawa approach modified by Ludwig was attractive as it does not require selective protection of the 2'- and 3'-hydroxyl groups, thus reducing the length of the overall synthesis considerably. With the aim of enhancing solubility, which would in turn make the compounds easier to handle, we intended carrying out the monophosphorylation on the *N2*-DMT protected nucleoside, even though it would undoubtedly be removed on addition of the phosphorus oxychloride ($POCl_3$). In order to confirm that this was the case, trial reactions were carried out using both guanosine and *N2*-DMT protected guanosine (Scheme 5.4).

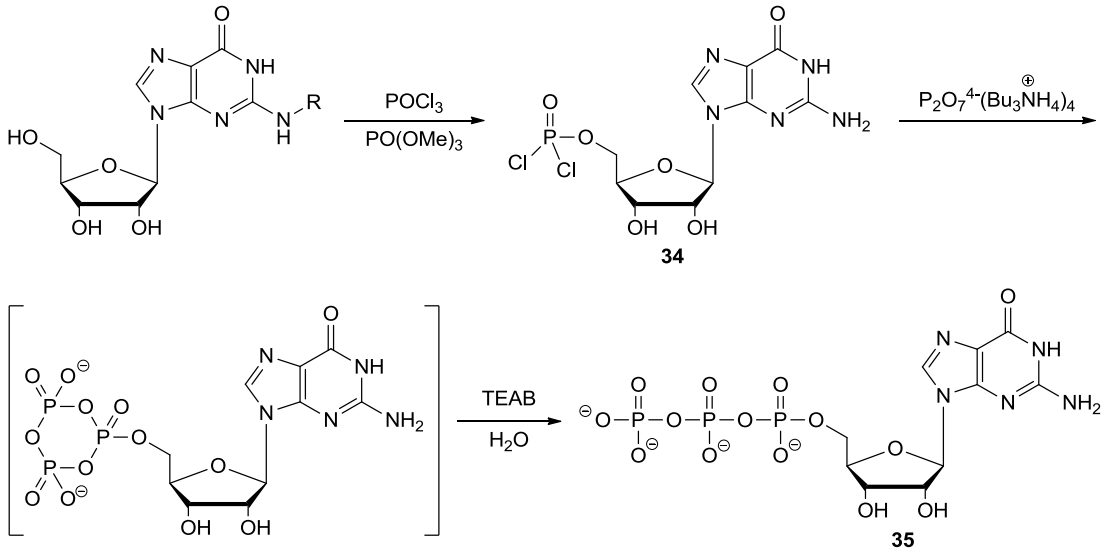

Scheme 5.4: Synthetic route to guanosine triphosphate. Note R = H or DMT.

The Yoshikawa phosphorylation was conducted utilising a published protocol[302]. After meticulous drying of the reagents, solvents and equipment, a 0.2mmol solution of the nucleoside in trimethylphosphate ($PO(OMe)_3$) was treated with 1.2 equivalents of $POCl_3$ to generate a highly reactive phosphorodichloridate intermediate. Upon sufficient conversion to the corresponding monophosphate (as monitored by HPLC, see below), the intermediate was reacted with tri-*n*-butylammonium pyrophosphate and subsequent hydrolysis with aqueous TEAB afforded the nucleoside triphosphate[302].

Both stages of the phosphorylation reaction were monitored directly by HPLC using a Dionex ion exchange (IE) column. To aid the interpretation of the chromatograms, standards of guanosine, guanosine monophosphate and guanosine triphosphate were analysed by IE-HPLC and gave retention times of 1.15, 4.46 and 10.79 minutes respectively.

Interpretation of the HPLC chromatographs from the reactions of guanosine indicated that the deprotected mono- and tri-phosphates were formed. The monophosphate (**34**) eluted at 4.71 minutes with an optimal conversion of 68% within 1.5 hours. The triphosphate (**35**) which had a retention time of 10.88 minutes was subsequently generated in a 40% yield. Very similar results were obtained when the reaction was repeated using *N2*-DMT-protected guanosine with conversions of 59% and 38% for the mono- and tri-phosphates, respectively. As anticipated these results confirmed that the addition of $POCl_3$ removed the DMT protecting group but notably also suggests that the presence of a DMT group does not affect the phosphorylation reaction. Isolation was not carried out at this point, though this is necessary to

unambiguously assign these compounds as 5'-phosphates. The purification of nucleoside triphosphates remains to be intricate and extensive[288]; therefore, it was reasoned that attempted purification and its optimisation would be delayed until we had the desired 8-nitroguanosine triphosphate in hand.

Following this positive result, phosphorylation of *N2*-dimethoxytrityl-8-nitroguanosine (**36**) was attempted using the same conditions. However in this case, the reaction proved unsuccessful as following addition of $POCl_3$ and stirring for 3 hours, no monophosphate could be seen in the HPLC trace (Scheme 5.5).

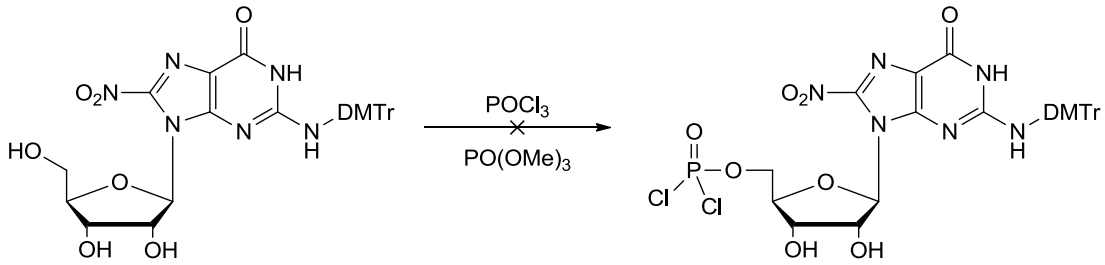

Scheme 5.5: Unsuccessful Yoshikawa approach to *N2*-dimethoxytrityl-8-nitroguanosine monophosphate.

Taking into account the considerable difference between the two nucleosides, particularly in terms of their conformation, it was considered that the DMT group may not affect the reaction whilst using unhindered guanosine, but have a deleterious effect when using the 8-nitro derivative as a substrate. Therefore detritylation of the compound was carried out. Treatment of *N2*-dimethoxytrityl-8-nitroguanosine with 0.25 equivalents of *p*-toluenesulfonic acid dissolved in methanol, in order to remove the *N2*-DMT protecting group, proceeded smoothly and after optimisation of the purification conditions afforded the detritylated nucleoside in a good yield. The formation of 8-nitroguanosine (**15**) was confirmed by ^{1}H NMR through the loss of 13 aromatic proton signals. The complete deprotection of the modified nucleoside dramatically reduced its solubility in the majority of organic solvents, complicating its handling considerably.

The conformational bias imposed on the nucleoside by the 8-nitro substituent is also largely present in 8-bromoguanosine. Therefore to address the effect of steric bulk at the C8 position on the phosphorylation, the reaction was now performed using 8-bromoguanosine (**37**) as a substrate. Introduction of the bromine group at the C8 position was achieved by the reaction of guanosine with bromine water. Confirmation of the addition was seen in the ^{1}H NMR, with the disappearance of the signal at 7.94ppm corresponding to H8.

Optimisation of the triphosphate synthesis was then carried out using 8-bromoguanosine. HPLC analysis indicated a 43% conversion to the monophosphate (**38**), which eluted at 5.37 minutes, after a reaction time of 1 hour. It was established that contrary to the 10 minutes suggested for pyrophosphate coupling, the optimal time for this step was in fact 40 minutes, with a 23% conversion to the triphosphate (**39**) (retention time = 11.15 minutes). The procedure was then repeated using the modified nucleoside 8-nitroguanosine.

The monophosphorylation reaction initially appeared to be successful as an intermediate containing the 8-nitroguanine analogue was detected in the HPLC trace eluting at 4.17 minutes and with a 50% conversion. The species containing the nitro modification was easily identifiable due to its distinctive UV profile. However on addition of the pyrophosphate, despite the formation of several compounds with longer retention times visible in the HPLC trace, no peaks characteristic of the triphosphate were observed. There seems to be two possible reasons for the failure of this reaction:

- The required phosphorodichloridate intermediate was not formed and the peak at 4.17 minutes was due to a decomposition product rather than the monophosphate.
- The phosphorodichloridate did not subsequently react with the pyrophosphate.

The guanosine-TMP complex[303] (Figure 5.1) is suggested to be an active intermediate formed between the nucleoside and the trimethylphosphate solvent in this reaction. This may go some way in explaining why the reaction with 8-nitroguanosine does not proceed. The complex forces the nucleoside into a *high-anti* conformation to allow *N7* to interact with the phosphorus atom, and the sp^2 oxygen forms a hydrogen bond with the 5'-hydroxyl group. This activates the 5'-hydroxy group to preferentially react with the phosphorus oxychloride[303]. If this complex is in fact the reactive intermediate, the conformation adopted by 8-nitroguanosine may affect the reaction.

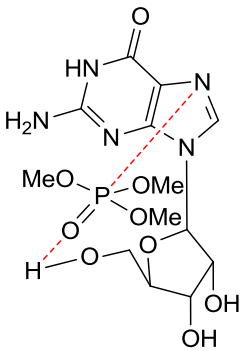

Figure 5.1: Guanosine-TMP complex, adapted from reference 303[303].

NMR shifts are diagnostic of a change in the conformation of a nucleoside from *anti* to *syn*. A comparison of 8-nitroguanosine and guanosine showed that not all of the chemical shifts indicative of the *syn* conformation were observed. The signals corresponding to H1', H2', and C1' experienced downfield shifts as would be expected for the *syn* nucleoside, likewise the peak corresponding to C2' showed the anticipated upfield shift. However the peaks corresponding to C3' and C4' did not behave as expected. For these signals, the direction of the shift in the chemical signals changes from an upfield shift which would be expected in a *syn* nucleoside to a downfield shift, as shown in Table 5.1. This is in contrast to that which was observed for the 8-nitro-2'-*O*-methyl derivative, which suggests the conformation of the two species differs[194,200].

Nucleoside	H1'	H2'	C1'	C2'	C3'	C4'
Guanosine	5.73	4.45	87.34	74.72	71.40	86.23
8-Nitroguanosine	6.27	4.92	90.46	71.08	70.10	85.67
2'-*O*-Methylguanosine	5.82	4.28	85.85	82.73	68.66	84.32
8-Nitro-2'-*O*-methylguanosine	6.32	4.68	89.12	80.88	69.55	86.20

Table 5.1: ^{1}H and ^{13}C NMR shifts of the sugar protons and carbons of guanosine, 8-nitroguanosine, 2'-*O*-methylguanosine and 8-nitro-2'-*O*-methylguanosine[194] measured in D_6-DMSO.

Computational modelling of guanosine and 8-nitroguanosine was carried out in order to support this conclusion. Molecular modelling calculations were performed using Spartan '10 version 1.1.0. The molecular mechanics model was considered suitable for a conformation distribution calculation to determine the lowest energy conformer of each nucleoside. The lowest energy conformations generated for guanosine and 8-nitroguanosine show considerable differences (Figure 5.2). Whilst guanosine exists in the *syn* conformation due to internal hydrogen bonds within the free nucleoside, 8-nitroguanosine adopts the *anti* conformation. Furthermore, 8-nitroguanosine can form two intramolecular hydrogen bonds in comparison to guanosine which forms only one. The contrasting orientation of the two lowest energy conformers may account for the different reactivities of the two species. It is possible that formation of the guanosine-TMP complex does not occur in this conformation, thus preventing the phosphorylation reaction. However this suggestion is speculative and further investigation would be required to determine if this was in fact the case.

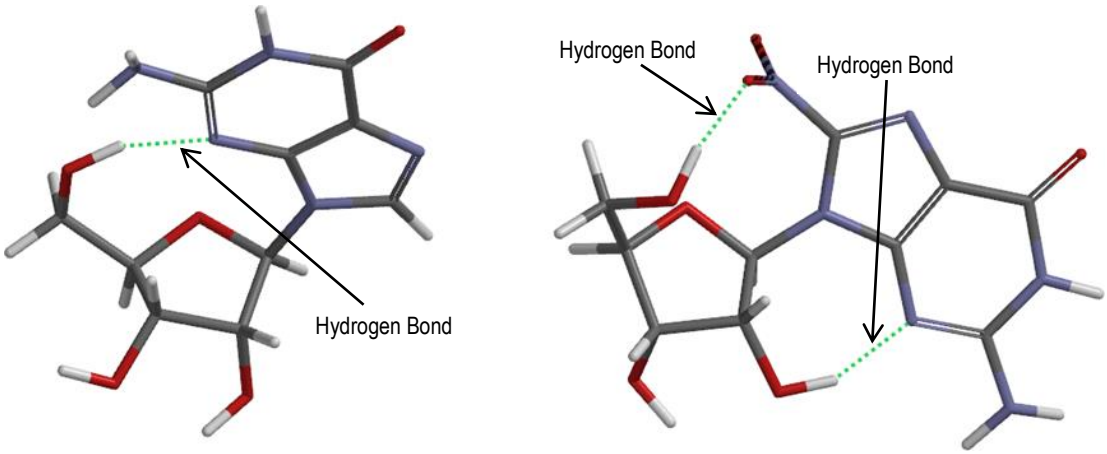

Figure 5.2: Lowest energy conformation of guanosine (left) and 8-nitroguanosine (right) calculated using Spartan. Note hydrogen bonds are represented by green dashed lines.

Based on previous studies of the 8-nitro-2'-*O*-methylguanosine[194] the observation that 8-nitroguanosine adopted the *anti* conformation was somewhat unexpected, hence the validity of the computational methods were questioned. In order to determine the accuracy of the model, computational modelling of 8-nitro-2'-*O*-methylguanosine was carried out. As shown in Figure 5.3, 8-nitro-2'-*O*-methylguanosine assumes a *syn* orientation and is consistent with results previously established. Therefore the model was considered to be valid.

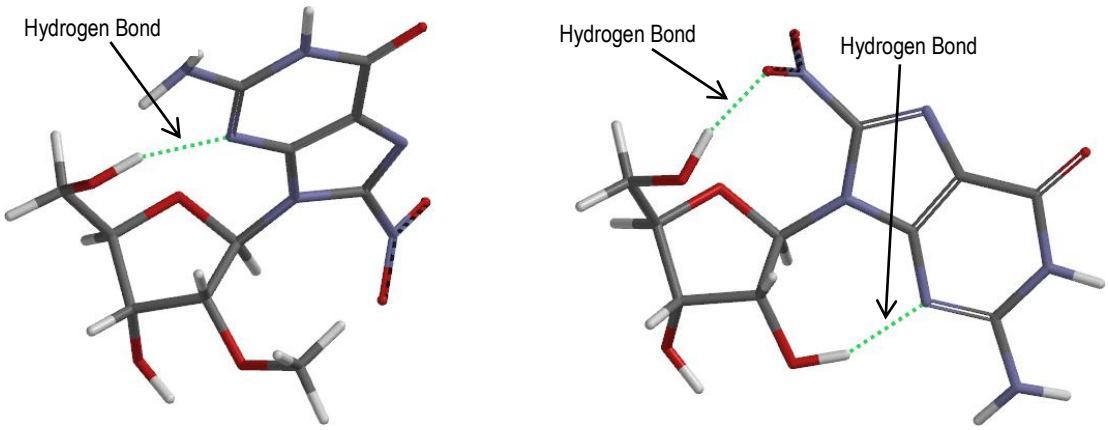

Figure 5.3: Lowest energy conformation of 8-nitro-2'-*O*-methylguanosine (left) and 8-nitroguanosine (right) calculated using Spartan. Note hydrogen bonds are represented by green dashed lines.

We concluded that the Yoshikawa procedure was not suitable for the phosphorylation of 8-nitroguanosine. It was evident that a more reliable method where complications arising from unprotected hydroxyl groups need not be considered would be advantageous. Therefore our efforts were focused on a synthetic pathway where the 2'- and 3'-hydroxyl groups are protected and a more reactive P(III) reagent is used to effect phosphorylation. In this approach

the trialklyphosphate solvent is not needed to give selectivity for the 5'-hydroxyl group and the guanosine-TMP complex will not form.

5.4 Ludwig and Eckstein phosphorylation: selective deprotection

With the aforementioned in mind, an efficient route was sought for the preparation of a 2'-, 3'-selectively protected 8-nitroguanosine analogue. It had been observed during previous syntheses, that deprotection of the acetyl protecting groups of fully protected 8-nitroguanine nucleosides proceeded in a stepwise manner. In general reaction at the primary 5'-position occurs more readily when compared to that of the secondary 2'- and 3'-positions, this suggests that the relative reactivity is a consequence of steric control. Therefore it is reasonable to assume that upon treatment with ammonia, deacetylation of the 5'-hydroxyl group would occur first. Based upon this reasoning, the generation of a regioselectively protected derivative *via* selective deprotection of the primary hydroxyl group was envisioned.

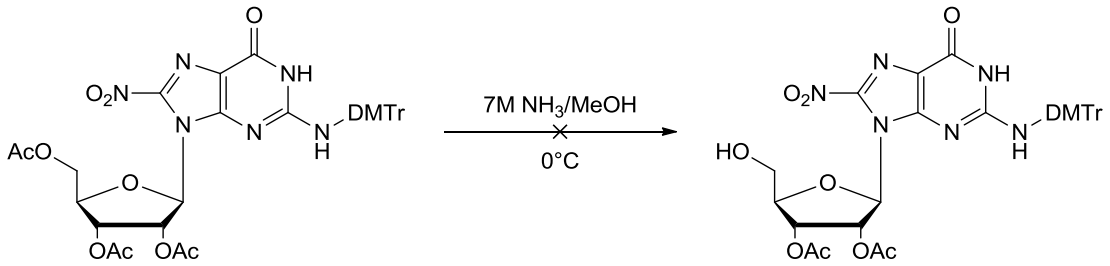

Scheme 5.6: Attempted regioselective deacetylation reaction.

Unfortunately despite numerous attempts transformation of the fully protected nucleoside to the corresponding 5'-hydroxyl derivative was unsuccessful. A balance was required between adequate formation of the 5'-hydroxyl derivative; that is disappearance of the starting material and limiting the generation of the 2'- and 3'-deprotected nucleosides. Although during the deacetylation, a slower running compound was initially formed on TLC that was presumed to be the 5'-deacetylated nucleoside, isolation of a sufficient quantity of material prior to further reaction was unfeasible. Thus it was evident that this route was not viable and exploration of alternative routes to prepare the suitably protected 8-nitroguanosine was necessary.

5.5 Ludwig and Eckstein phosphorylation: orthogonal protection (route A)

Scheme 5.7 demonstrates the alternative procedure proposed to generate the appropriately protected 8-nitroguanosine derivative. This route features some steps common to syntheses

outlined previously in this thesis and despite the additional steps, suggests a seemingly reliable approach.

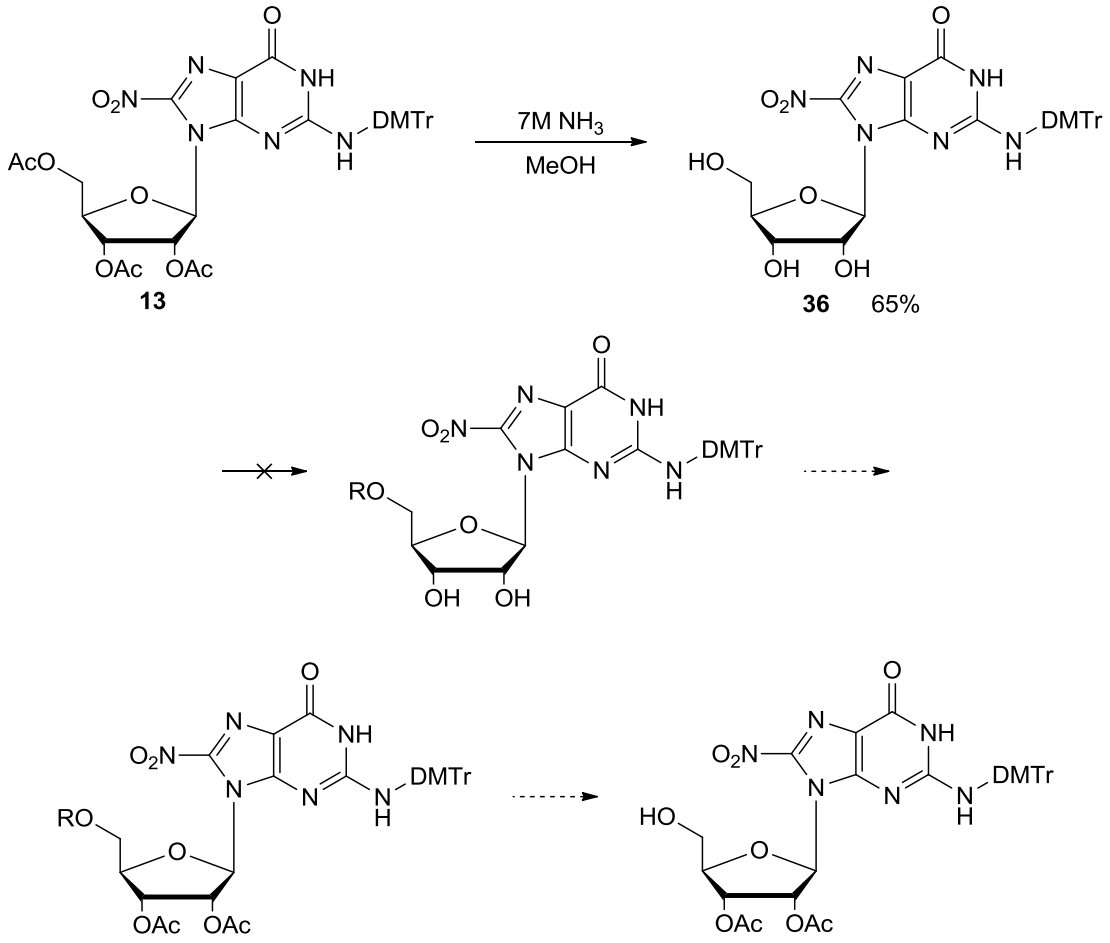

Scheme 5.7: Proposed synthetic route to *N*2- dimethoxytrityl-8-nitro-2'-3'-di-*O*-acetylguanosine. Note R = DMT or TBDMS.

The first step involved standard acetyl deprotection, carried out using methanolic ammonia to afford unprotected hydroxyl groups at the 2'-, 3'- and 5'-positions. It is essential that the temporary protecting group on the 5'-position of the nucleoside is orthogonal to that of the 2'- and 3'-protecting groups as these must be preserved during the phosphorylation reaction. For this purpose it was anticipated that selective protection of the 5'-hydroxyl group with the acid labile DMT or *tert*-butyldimethylsilyl (TBDMS) protecting groups would be suitable. The greater nucleophilicity of the primary 5'-hydroxyl group and the steric bulk of these protecting groups favour formation of the desired compound.

Unexpectedly, attempts to introduce both the DMT and TBDMS groups using standard reaction conditions were unsuccessful. This is in contrast to the 2'-*O*-methyl derivative whereby

functionalisation of the 5'-hydroxyl group occurs readily. It is feasible that the altered electronic and stereochemical properties of the 8-nitroguanosine derivative may result in difference in the reactivity of the 5'-hydroxyl group towards electrophiles. Taking these results into consideration, it seemed appropriate to selectively protect the nucleoside prior to the nitration reaction. Moreover, this would prove advantageous as it would avoid unnecessary waste of the valuable nitrated nucleoside. Alternative methods for the dimethoxytritylation such as those based on tetrafluoroborate salts were not investigated[304].

5.6 Ludwig and Eckstein phosphorylation: orthogonal protection (route B)

A second strategy for the synthesis of a suitably protected 8-nitroguanosine derivative for use as a substrate in the Ludwig and Eckstein phosphorylation procedure was developed, route B (Scheme 5.8). This involved manipulation of the protecting groups prior to functionalisation of the C8 position with a nitro group.

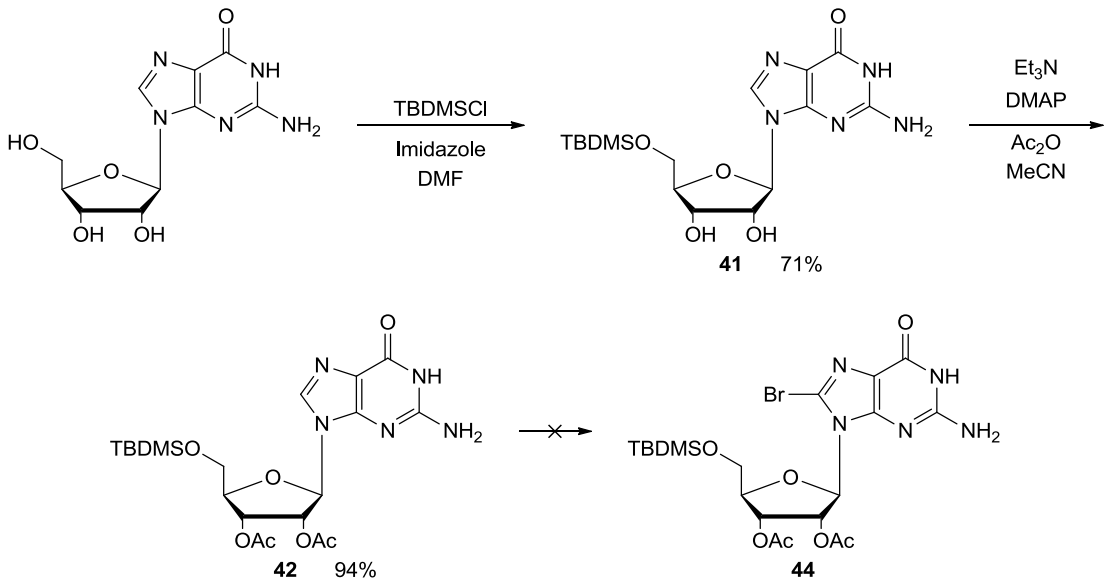

Scheme 5.8: Synthetic route B.

The first step in the route B approach was to introduce a silyl protecting group at the 5'-hydroxyl position. The use of TBDMS is favourable, as silyl protecting groups can be selectively removed using a source of fluoride ions; hence the protecting group can be removed without treating the compound with either acid or base. Consequently it is possible to retain both an acid labile DMT group on the base, to improve solubility of the nucleoside, and the base labile acetyl protecting groups on the 2'- and 3'-hydroxyls, to prevent phosphorylation at this position in subsequent steps. Introduction of the 5'-*O*-TBDMS group was achieved by

the addition of a small excess of TBDMSCl to a solution of guanosine and imidazole in anhydrous DMF. The protection proceeded smoothly in a 71% yield; some 2'- and 3'-protection was also observed which accounted for the loss of yield in this reaction. This is in marked contrast to the previous attempt to silylate the 8-nitroguanosine derivative. The appearance of characteristic singlets in the ^{1}H NMR at 0.04ppm and 0.87ppm indicated the presence of the silyl protecting group in the product; these peaks correspond to the 6 protons of the methyl and 9 protons of the *t*-butyl group respectively.

Protection of the 2'- and 3'-hydroxyl groups with acetyl groups was completed using a similar method to that used previously. However a slight modification of the purification procedure was required, as due to the enhanced solubility of the TBDMS-protected nucleoside recrystallization from propan-2-ol was not feasible. Consequently the desired product (**42**) was obtained in a 94% yield by partitioning the residue obtained between DCM and water. Diagnostic peaks in the ^{1}H NMR spectrum at 2.00ppm and 2.11ppm corresponding to the methyl ester protons indicated the presence of the acetyl protecting groups.

Following this, electrophilic bromination at the C8 position was attempted; unfortunately the reaction conditions lead to untimely desilylation of the 5'-hydroxyl group. Regrettably, the generation of hydrogen bromide during the reaction was not given due consideration whilst developing the route to the suitably protected nucleoside. However it was apparent that the quantity of hydrogen bromide produced was sufficient to remove the TBDMS protecting group. This was confirmed by the disappearance of the peaks at 0.07ppm and 0.88ppm in ^{1}H NMR indicative of the silyl group. Upon re-evaluation of the approach, it was evident that electrophilic bromination must be performed prior to introduction of the silyl protecting group.

5.7 Ludwig and Eckstein phosphorylation: orthogonal protection (route C)

In order to circumvent the complications which arose during the electrophilic bromination step in the initial strategy, the steps in the synthetic pathway were reordered to present an alternative approach, route C (Scheme 5.9). Incorporating the bromine functionality at the outset removes the incompatibility of the TBDMS group with the bromination conditions.

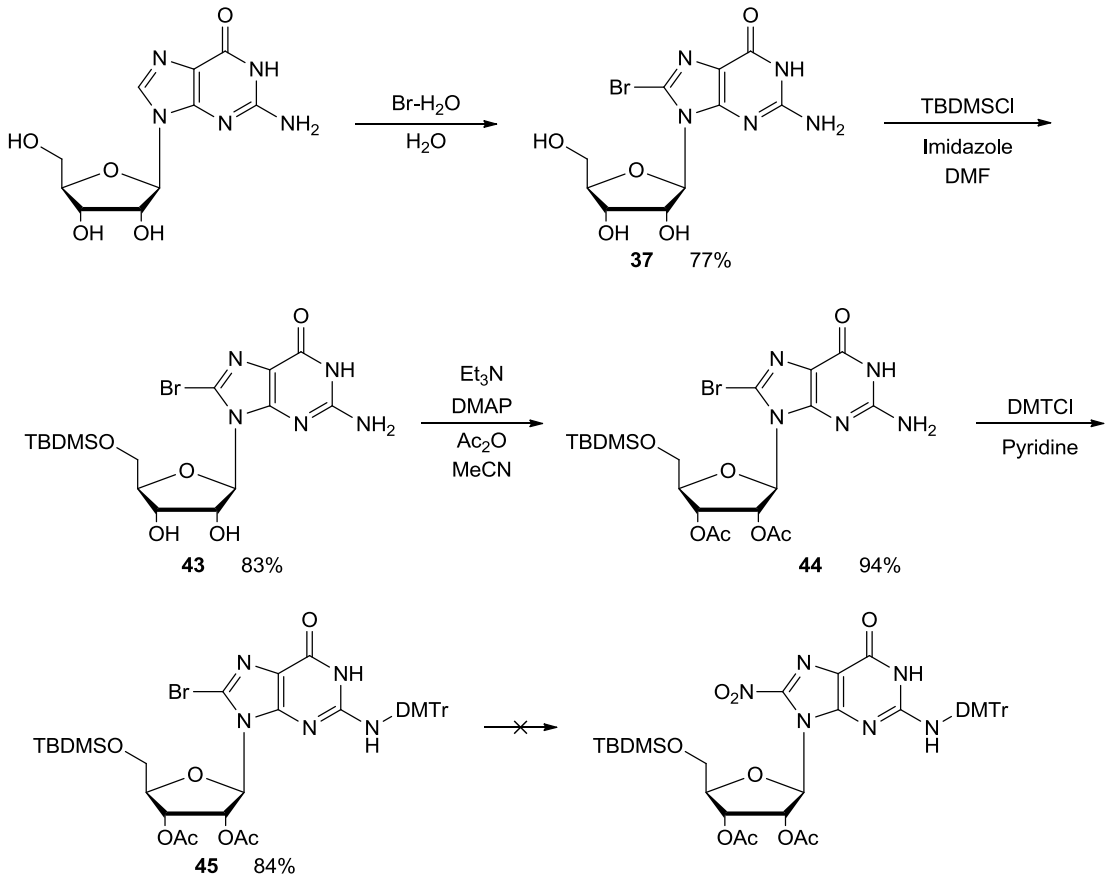

Scheme 5.9: Synthetic route C.

Although route B was ultimately unsuccessful, the initial steps are common to this route, thus the section below describes only the reactions that were attempted exclusively in route C. With the nucleobase brominated and the sugar suitably protected, the exocyclic amine moiety was then protected using DMTCl to give the fully protected nucleoside (**45**) in an 84% yield. The identity of the product was confirmed by the presence of diagnostic peaks in the ^{1}H NMR at 3.71ppm corresponding to the six methoxy protons and the appearance of aromatic protons at 7.12-7.36ppm.

The nitration reaction was carried out on the fully protected 8-bromoguanosine using the optimised conditions established for the 2'-*O*-methyl derivative which used a concentration of 0.01mM. The reaction was monitored closely by RP-HPLC and TLC in order to follow the conversion to the nitro compound; however no reaction was observed. The absence of peaks in the HPLC absorbing at 350nm where only 8-nitroguanine derivatives have a significant absorbance was testament to this. Analysis of the major decomposition products identified the detritylated, desilylated and the depurinated species. Taking into consideration the sensitivity

of the reaction and that the use of alternative protection schemes has previously led to failure to convert these compounds through to the nitro derivatives, it was concluded that the presence of the silyl protecting group is detrimental to the reaction[194]. Steric hindrance resulting from the relatively bulky TBDMS group may additionally factor in the lack of success of the reaction.

Theoretically, removal of the silyl protecting group ahead of nitration would prevent these complications. As previously mentioned, the affinity of silicon for fluoride ions makes the protecting group particularly susceptible to treatment with tetra-*n*-butylammonium fluoride (TBAF) (Scheme 5.10). In order to supress the undesirable side reactions which can occur due the basicity of the fluoride ion, the reaction was buffered with acetic acid[305]. However this proved unsuccessful and concurrent removal of the acetyl protecting groups was also observed.

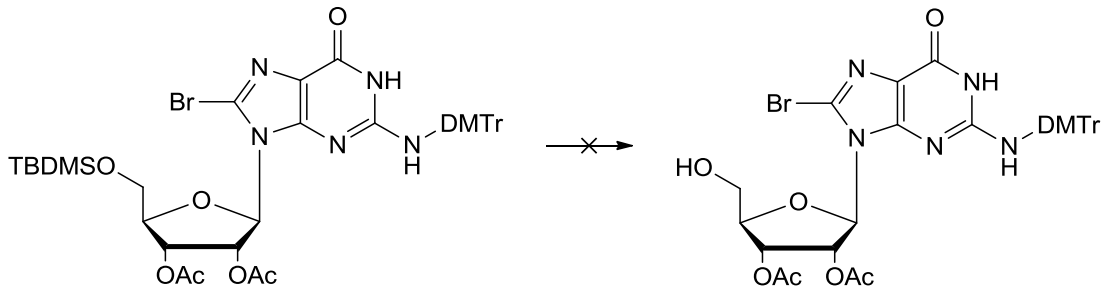

Scheme 5.10: Failed attempt at desilylation reaction.

5.8 Molecular modelling

In order to gain a better insight into the differences in reactivity and behaviour of the *N2*-dimethoxytrityl-8-nitroguanosine and *N2*-dimethoxytrityl-8-nitro-2'-*O*-methylguanosine we focused upon the application of molecular modelling. It was envisioned that by using computational methods it would be possible to identify factors that may have resulted in the unsuccessful reactions encountered in this route and how this differs from the 2'-*O*-methyl analogue. As the molecular mechanics model had been successfully used previously to produce a global energy minima conformer, it was again considered a suitable model. Conformer distribution calculations were utilised to find the energetically preferred conformations of the molecules; shown in Figure 5.4.

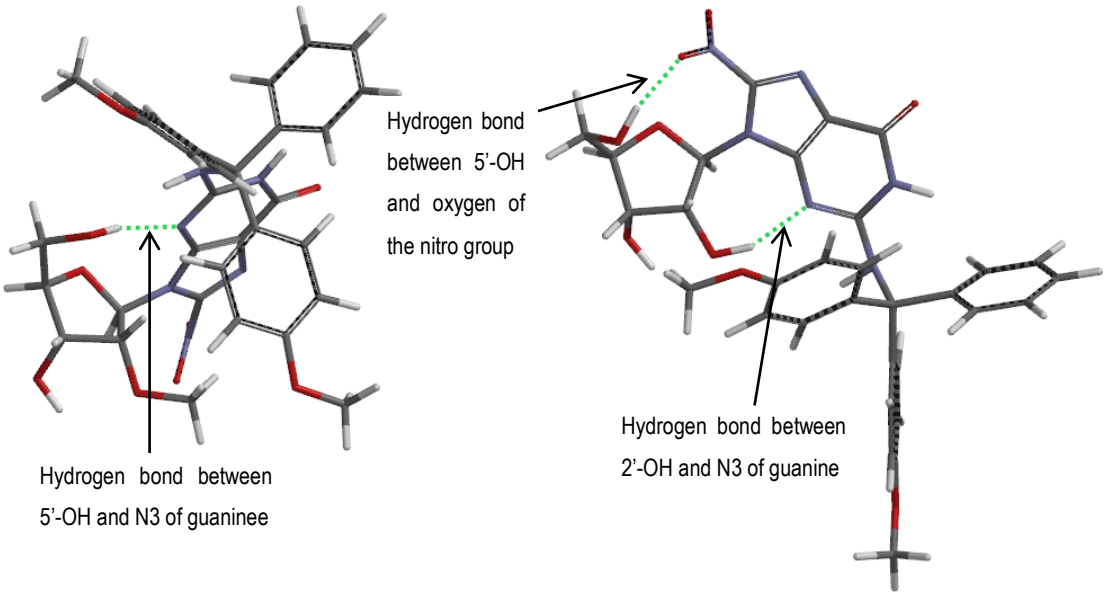

Figure 5.4: Lowest energy conformation of *N2*-dimethoxytrityl-8-nitro-2'-*O*-methylguanosine (left) and *N2*-dimethoxytrityl-8-nitroguanosine (right) calculated using Spartan. Note hydrogen bonds are represented by green dashed lines.

The lowest energy conformations of *N2*-dimethoxytrityl-8-nitroguanosine and *N2*-dimethoxytrityl-8-nitro-2'-*O*-methyguanosine vary considerably with respect to the orientation of the functionalised base with respect to the sugar moiety. Furthermore the number and nature of hydrogen bonds within the molecules also differs. In order to explain how these differences may affect the reactivity of the molecules, it is first necessary to consider the properties of hydrogen bonds.

A good hydrogen bond acceptor is characterised as having a larger electronegativity relative to hydrogen and a lone pair of electrons. A good hydrogen bond donor has a hydrogen atom covalently bonded to a small highly electronegative atom. The electronegative atom draws electron density away from the hydrogen atom, resulting in a partial positive charge. Therefore an electrostatic interaction between the partially positive hydrogen atom and the electronegative acceptor atom leads to the formation of a hydrogen bond[17]. The electron density between the hydrogen donor and hydrogen acceptor is rearranged upon formation of a hydrogen bond. The electron density flows from the lone pair of the proton acceptor to the proton donor which in turn induces a negative charge on the hydrogen atom and a more positive charge on the electronegative atom[306]. Moreover, as the difference in electronegativity between oxygen and hydrogen (1.24) is greater than that of nitrogen and hydrogen (0.84), it stands to reason that the hydrogen bond that is formed in the ribose derivative is stronger than that formed in the 2'-*O*-methyl derivative (Figure 5.5)[17]. Taking these factors into consideration

it is possible that reactivity of the 5'-hydroxyl group towards electrophiles is reduced in the ribonucleoside as compared to the 2'-*O*-methyl derivative.

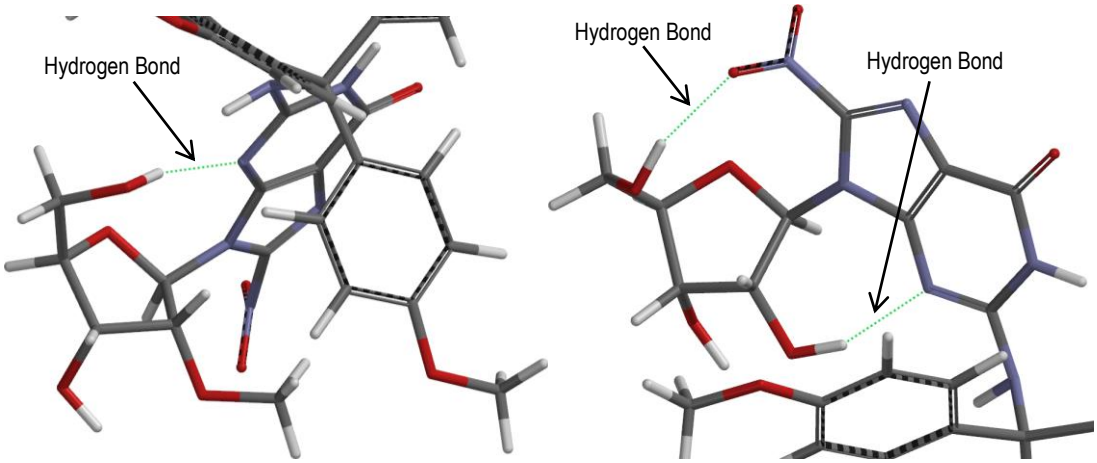

Figure 5.5: Enlarged image of the hydrogen bonding regions of *N*2-dimethoxytrityl-8-nitro-2'-*O*-methylguanosine (left) and *N*2-dimethoxytrityl-8-nitroguanosine (right) predicted using Spartan. Note hydrogen bonds are represented by green dashed lines.

5.9 Conclusion

Although the initial aim of synthesising 8-nitroguanosine triphosphate has not been successful, the principles for the phosphorylation of a nucleoside have been shown. It should be noted that computational studies suggest that the preferred conformation of the ribose derivative is dissimilar to that of the 2'-*O*-methyl derivative and this may account for the different reactivities of the two species. On account of functionalization of the 5'-hydroxyl group having being demonstrated using the 2'-*O*-methyl derivative following nitration, it is possible that this may prove to be a better substrate for the phosphorylation reaction. In general, the synthesis of 8-nitroguanosine triphosphate derivative remains a work in progress and further studies should include the use of 2'-*O*-methylguanosine as the starting material and the investigation of alternative protecting group schemes.

Chapter 6

Future Work

6 Future work

Two collaborations are currently in progress that start to address whether there are processes that can repair the 8-nitroguanine lesion.

In collaboration with Professor Andy Bates (University of Liverpool, Biological Sciences) investigations into the miscoding potential of the 8-nitroguanine lesion incorporated into bacterial plasmid DNA are currently being undertaken.

The basic principle of this experiment is that an oligodeoxynucleotide containing the stabilised lesion is annealed to its analogous sequence in a 300 nucleotide single-stranded gap within a plasmid. The site 2 and site 3 sequences, synthesised for this purpose correspond to specific sequences within the *lacZ* gene of the *lac* operon. The *lacZ* gene encodes the cytoplasmic enzyme β-galactosidase, which catalyses the hydrolysis of lactose into glucose and galactose in *Escherichia coli*[307]. Following introduction of the modified plasmid to the bacterial cells, constituent enzymes carry out gap filling DNA synthesis. The double-stranded plasmid can then be completely replicated in a series of reactions catalysed by innate bacterial enzymes and subsequently colonies of the bacteria grown.

The indicator of lacZ activity which will be utilised in these studies is the chromogenic substrate bromochloroindolygalactoside (Xgal). This compound is colourless but upon hydrolysis by *lacZ*, dimerization of the resulting compound forms the insoluble dye indigo[307]. Therefore if the lesion is faithfully copied in replication, that is, it is recognised as a guanine base paired with cytosine, the lacZ enzyme will be active and a blue colony will be formed. However any misincorporations opposite the lesions will result in inactivation of the gene and the colonies generated will be white.

Hence screening colonies which do not produce a blue colour and subsequent sequence analysis enables identification of the specific substitutions involved. Performing these replication experiments in bacteria either containing or deficient in specific DNA repair enzymes that are of particular interest with regards to oxidative DNA lesions, should enable us to establish whether these enzymes are involved in a repair system directed against 8-nitroguanine in DNA.

A second collaboration with Professor Aidan Doherty (University of Sussex, Genome Damage and Stability Centre) is aimed at studying a protein with the potential to remove the 8-nitroguanine lesion by direct reduction back to guanine. The enzyme is a deazaflavin (F_{420})

dependent nitroreductase (Ddn). Reduction of nitroimidazole using Ddn has been demonstrated and the suggested mechanism proceeds *via* hydride transfer from the enzyme complex to the imidazole ring followed by protonation of the C2 position and elimination of the nitrous acid (Scheme 6.1)[308].

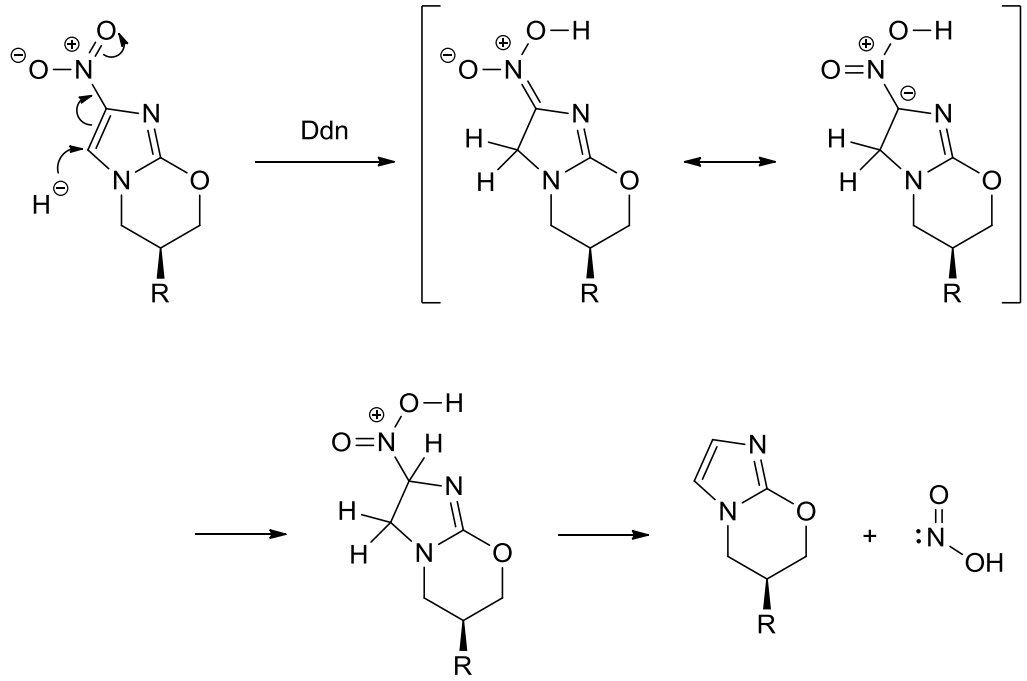

Scheme 6.1: Suggested mechanism for the reduction of nitroimidazole with Ddn[308].

Based on this research it was proposed that a related enzyme that binds to DNA could be responsible for replacement of the nitro group in 8-nitroguanine with hydride, effectively regenerating guanine. Thus, evaluation of the site 1, site 2 and site 3 sequences as substrates for this putative repair enzyme are currently being carried out, however this remains a work in progress. In preliminary chemical model studies that are not described in this thesis, sodium borohydride was shown to reduce 8-nitroguanine back to guanine, suggesting that a hydride type reducing agent could carry out the repair.

Chapter 7

Experimental

7 Experimental

7.1 General techniques, protocols, solvents and reagents

7.1.1 General techniques

Analytical thin layer chromatography (TLC)

TLC was performed on UV_{254} sensitive, silica gel coated, aluminium TLC plates purchased from Merck. The developed chromatographs were visualised using a UV lamp (254nm). Most TLC plates were stained with *p*-anisaldehyde with spots turning blue upon heating with the exception of those compounds containing a DMT group which produced an orange colour on contact becoming darker upon heating. Ellman's reagent was used to identify compounds containing a thiol or disulfide group, this turned the respective compounds bright yellow upon heating. Compounds containing the ribose or 2'-*O*-methylribose moiety could be distinguished by treatment with the sugar stain which upon heating, the spots were observed at black spots.

Flash column chromatography

The required quantity of silica gel (particle size 40-63μM supplied by Sigma Aldrich) was made into a homogeneous slurry with the column eluent and applied to the column over a base layer of sand. The material to be purified was then introduced to the column in a minimum volume of eluent or as a powder by pre-absorption onto silica. All eluted fractions were collected and analysed by TLC.

Nuclear magnetic resonance (NMR) spectroscopy

All NMR spectra were recorded on either a Bruker AMX-400 MHz or 500 MHz spectrometer. Chemical shifts are reported in ppm and coupling constants (*J*) in hertz. ^{13}C NMR and ^{31}P NMR spectra were all proton decoupled. For all samples ran in deuterated chloroform ($CDCl_3$) and deuterated dimethyl sulfoxide (D_6-DMSO) ^{1}H NMR and ^{13}C NMR spectra are relative to an internal standard of tetramethylsilane (TMS).

Mass spectrometry

All electrospray and chemical ionisation mass spectra were recorded by Ms Moya McCarron at the University of Liverpool using a Micromass LCT mass spectrometer. All samples were recorded using the ionisation mode specified and were injected using a direct infusion syringe pump. All purified and fully deprotected oligodeoxynucleotides were diluted with distilled water

and analysed using negative mode electrospray ionisation. Mass spectra of the site 3 oligodeoxynucleotides were obtained using a Bruker UltrafleXtreme MALDI-TOF/TOF mass spectrometer (Bruker Daltonics, UK) using 3-hydroxypicolinic acid as a matrix and recorded by Dr. Phillip Brownridge (University of Liverpool, Biological Sciences).

pH Measurements

pH Measurements were carried out using a Metrohm 691 pH meter. This was calibrated prior to use with buffers purchased from Thermo Russell (pH 4.00, 7.00 and 10.00 ± 0.01 at 25°C).

Solid-phase oligodeoxynucleotide synthesis

All oligodeoxynucleotides and dinucleotides were synthesised on a Mermade® 4 column DNA synthesiser purchased from BioAutomation™, equipped with Mermade 12© v2.3.2 software. All 1μM, 500Å controlled pore glass (CPG) columns, standard phosphoramidite monomers and synthesis reagents were purchased from Link Technologies. Sensitive reagents were stored over DNA Moisture Traps supplied by ChemGenes. Modified phosphoramidites were synthesised as outlined in Chapter 2 Section 3 and stored under nitrogen at -22°C.

UV spectrophotometry

The UV absorbance of the oligodeoxynucleotides, dinucleotides and nucleosides were measured at 260nm, unless otherwise stated, on a PerkinElmer LAMBDA Bio+ spectrophotometer. A Hellma® Traycell™ was used as an alternative to making the serial dilutions of oligodeoxynucleotide stock solutions required when using standard quartz cuvettes of 1cm pathlength. UV absorbance measurements were made on 5μl of the stock oligodeoxynucleotide solution using either a TrayCell-0.2 mm (Factor 50) Cap or an TrayCell-0.1 mm (Factor 100) Cap. The pathlength compensation factor was then applied to the absorbance obtained in order to adjust the values to that of a 1cm cuvette.

High performance liquid chromatography (HPLC)

HPLC was performed on an automated Gilson HPLC system equipped with a 234 Autoinjector, a 170 Photodiode Array Detector and a 231 Dual Hydraulic Pump. Chromatographic data was handled using UniPoint Version 3.0.

Reverse Phase (RP) HPLC was performed on a Gemini® 5 μm C18 110Å, LC Column 250 x 4.6 mm which was supplied from phenomenex®. A two buffer system, with differing eluent

compositions and control methods, were used depending on the relative polarity of the compounds being analysed. A flow rate of 1ml/min was used in all protocols. The RP-HPLC column was stored in HPLC grade MeCN.

Ion Exchange (IE) HPLC was performed on a DNA Pac® PA-100, Analytical Column 4 x 250mm which was supplied by Dionex using a two buffer system. A flow rate of 1ml/min was used in all protocols. The IE-HPLC column was stored in distilled H_2O.

7.1.2 HPLC solvents

Acetonitrile HPLC gradient grade was purchased from Fisher Scientific

1M Aqueous triethylammonium bicarbonate (TEAB) was prepared by bubbling CO_2 gas through a solution of triethylamine and distilled water until a pH between 7.50 and 7.70 was obtained. This was then diluted to give a final concentration of 1M which was then further diluted as necessary.

RP-HPLC Buffer A (0.1M aqueous TEAB solution, 1L) was prepared by diluting 100ml of the 1M TEAB solution with 900ml distilled water.

RP-HPLC Buffer B (0.1M aqueous TEAB containing 40% MeCN, 1L) was prepared by diluting 100ml of the 1M aqueous TEAB solution with 500ml distilled water and 400ml MeCN.

1M Aqueous triethylammonium acetate (TEAA) was prepared by the addition of triethylamine to a solution of acetic acid and distilled water until a pH of 4 was obtained. This was then diluted to give a final concentration of 1M.

RP-HPLC Buffer C (23mM TEAA) was prepared by diluting 23ml of the 1M aqueous triethylammonium acetate solution with 977ml distilled water.

1M Aqueous potassium phosphate pH 6.6 was prepared by dissolving 87.78g potassium phosphate monobasic and 61.84g potassium phosphate dibasic in distilled water to give a final volume of 1L.

IE-HPLC Buffer 1 (10mM aqueous potassium phosphate) was prepared by diluting 10ml of the 1M aqueous potassium phosphate solution with 990ml distilled water.

IE-HPLC Buffer 2 (500mM aqueous potassium phosphate) was prepared by diluting 500ml of the 1M aqueous potassium phosphate solution with 500ml distilled water.

7.1.3 HPLC protocols

Control method 0-100

The eluent was gradually changed from 100% buffer A to 100% buffer B over 25 minutes and held at 100% buffer B for 5 minutes before being gradually changed back to 100% buffer A over 5 minutes.

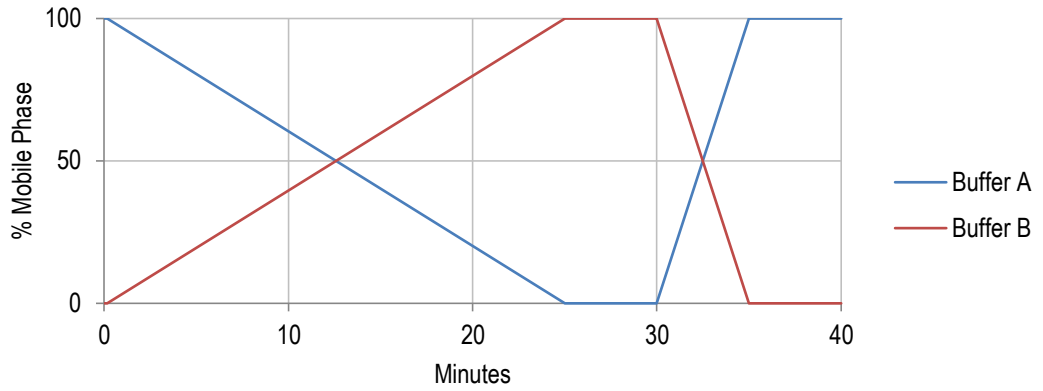

Figure 7.1: Control method 0-100.

Control method 0-100B

The eluent was gradually changed from 100% buffer A to 100% buffer B over 24 minutes and held at 100% buffer B for 3 minutes before being gradually changed back to 100% buffer A over 5 minutes.

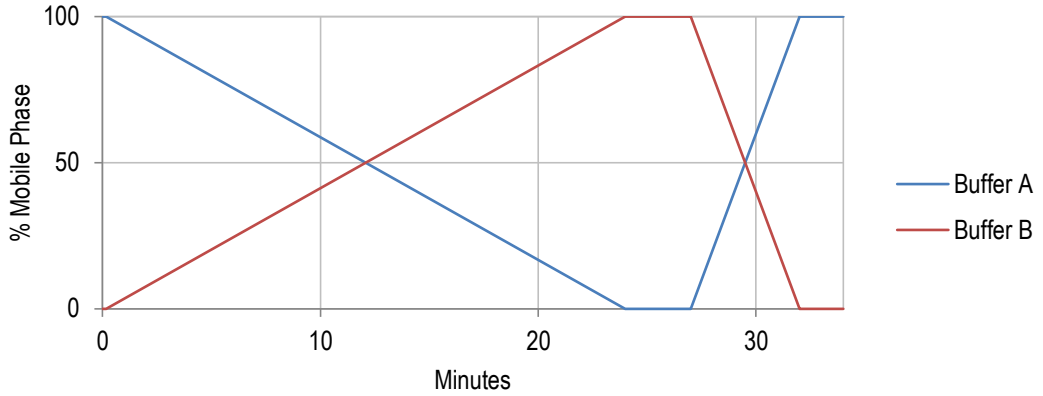

Figure 7.2: Control method 0-100B.

Control method 0-65

The eluent was gradually changed from 100% buffer A (0% buffer B) to 35% buffer A (65% buffer B) over 19 minutes, and then to 100% buffer B in the following 1 minute. After holding buffer B for 2 minutes the eluent was changed back to 100% buffer A over 2 minutes.

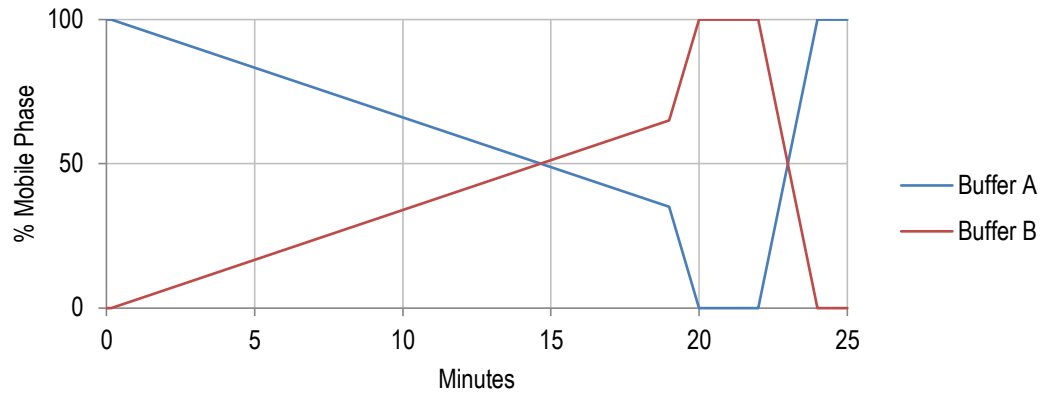

Figure 7.3: Control method 0-65.

Control method 0-50

The eluent was gradually changed from 0% MeCN (100% buffer B) to 50% MeCN (50% buffer B) over 20 minutes, and then to 100% MeCN in the following 2 minutes. After holding MeCN for 5 minutes the eluent was changed back to 100% buffer B over 2 minutes.

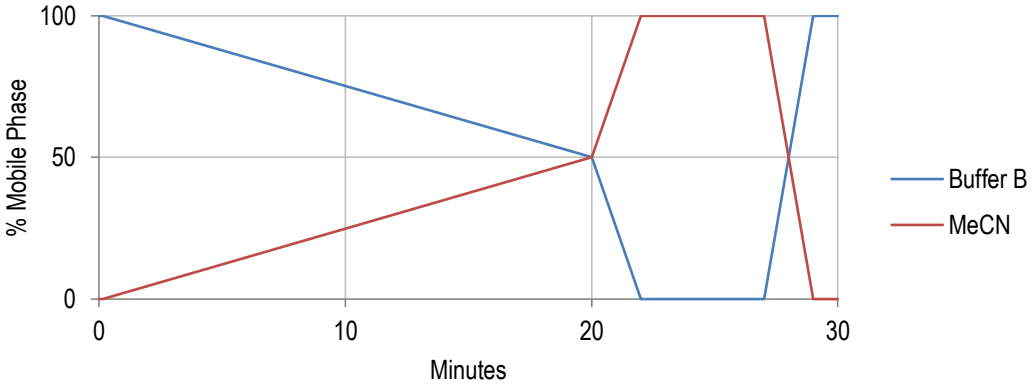

Figure 7.4: Control method 0-50.

Control method 0-22

The eluent was gradually changed from 0% MeCN (100% buffer B) to 22% MeCN (78% buffer B) over 20 minutes and then to 100% MeCN in the following 2 minutes. The eluent was held at

100% buffer B for 5 minutes before being gradually changed back to 100% buffer A over 2 minutes.

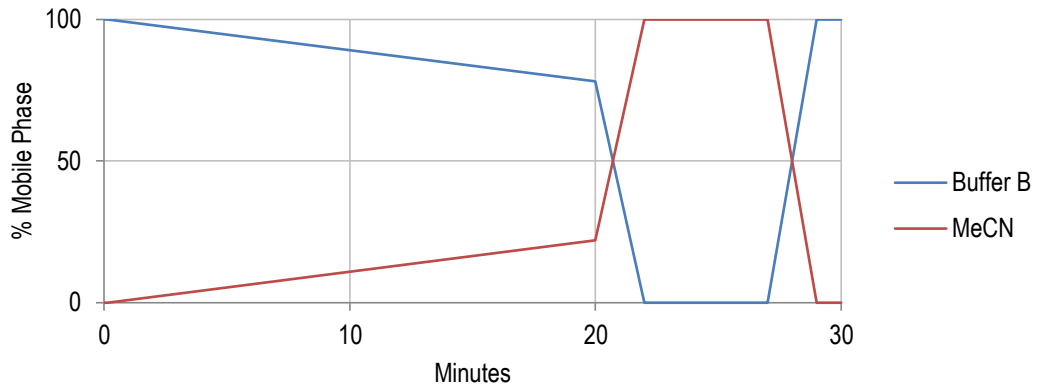

Figure 7.5: Control Method 0-22.

Control method 65/35

The composition of the mobile phase was kept constant with isocratic elution of 65% buffer B and 35% MeCN for 12 minutes. The eluent was then changed to 100% MeCN over the following 3 minutes. After holding the buffer at 100% MeCN for 1 minute the eluent was gradually changed back to its original composition over 3 minutes.

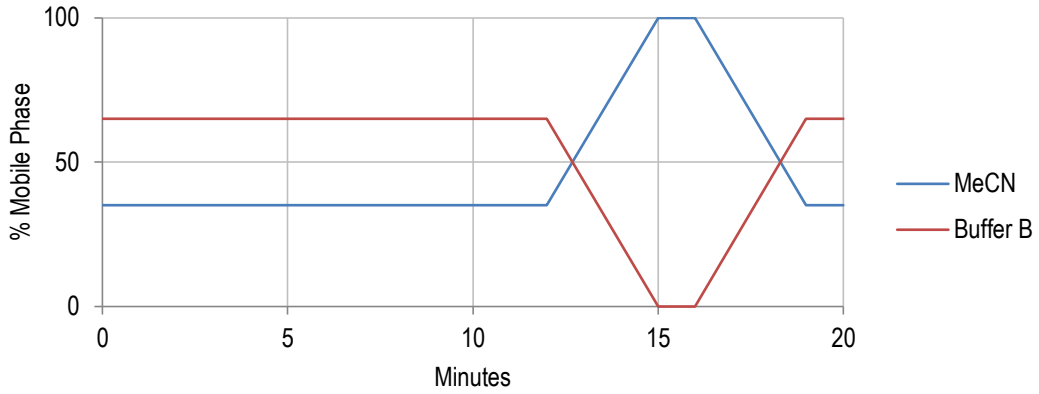

Figure 7.6: Control method 65/35.

Control method 65/35B

The composition of the mobile phase was kept constant with isocratic elution of 65% buffer C and 35% MeCN for 12 minutes. The eluent was then changed to 100% MeCN over the following 3 minutes. After holding the buffer at 100% MeCN for 11 minutes the eluent was gradually changed back to its original composition over 3 minutes.

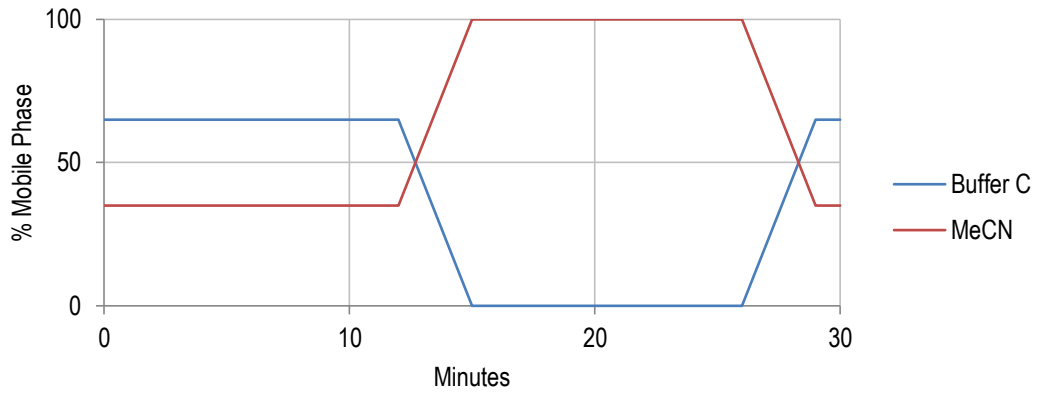

Figure 7.7: Control method 65/35B.

Control method IE 0-100

The eluent was gradually changed from 100% buffer 1 to 100% buffer 2 over 20 minutes and held at 100% buffer 2 for 5 minutes before being gradually changed back to buffer 1 over 5 minutes.

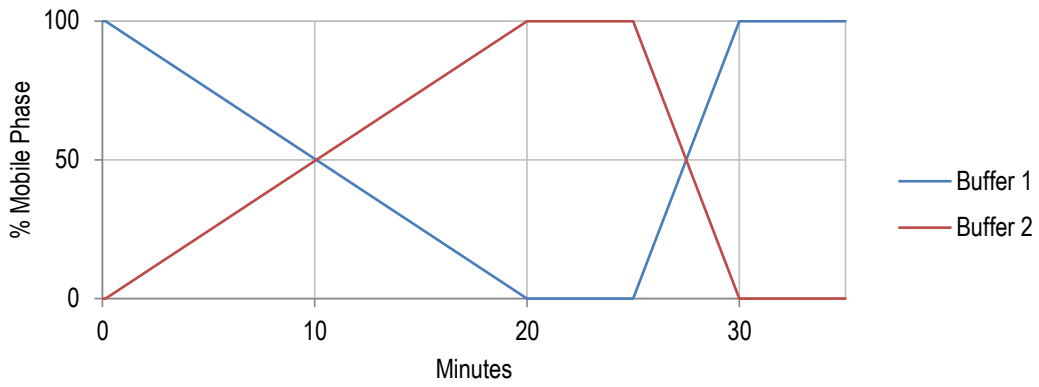

Figure 7.8: Control method IE 0-100.

7.1.4 Solvents

Unless otherwise stated, solvents were purchased from Fisher Scientific. Anhydrous solvents were obtained at follows:

Acetonitrile: Pre-dried DNA synthesis grade purchased from Link Technologies.

Dichloromethane: distilled from calcium hydride.

N,N-Dimethylformamide: Sure-Seal™ anhydrous solvent purchased from Sigma Aldrich or fractionally distilled from calcium hydride.

Dimethyl sulfoxide: Sure-Seal™ anhydrous solvent purchased from Sigma Aldrich or fractionally distilled from calcium hydride.

Pyridine: Sure-Seal™ anhydrous solvent purchased from Sigma Aldrich.

7.1.5 General Reagents

Unless otherwise stated general reagents were purchased from Sigma Aldrich, Acros Organics or Chemgenes.

1M TRIS.HCl: Tris(hydroxymethyl)aminoethane (Tris) was dissolved in distilled water and concentrated hydrochloric acid was added until the desired pH was achieved. The volume was adjusted to achieve a final concentration of 1M.

p-Anisaldehyde Stain: *p*-Anisaldehyde (3ml) was mixed with sulfuric acid (4ml), acetic acid (1.2ml) and ethanol (114ml).

Ellman's Reagent (0.1% w/v): 5,5'-dithiobis(2-nitrobenzoic acid) (0.15g) was dissolved in ethanol (75ml) and 0.45M TRIS.HCl (75ml).

Sugar Stain: Phenol (3g) was dissolved in a solution of ethanol (95ml) and sulfuric acid (5ml).

*N*2-Dimethoxytritylguanosine was previously prepared by Dr. I. Bhamra.

Tri-*N*-butylammonium pyrophosphate was prepared according to a published protocol[302].

7.2 Experimental procedures for results and discussion 1

3',5'-Di-*O*-acetyl-2'-*O*-methylguanosine (1)[194]

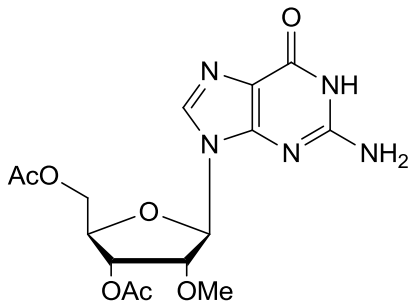

To a stirred solution of 2'-*O*-methylguanosine (5.00g, 16.80mmol) in MeCN (50ml) was added Et_3N (9.38ml, 67.28mmol) and DMAP (0.14g, 1.11mmol), the solution was cooled to 0°C prior to addition of Ac_2O (3.17ml, 33.60mmol). The mixture was allowed to warm to room temperature and was stirred for a further 2 hours. The reaction was quenched with MeOH (6ml) and the solvent removed *in vacuo.* The white solid formed was recrystallised from boiling ^{i}PrOH which yielded the title product as a white solid (6.04g, 94%). HRMS (ES^+) (m/z): 404.1196 ($[M+Na]^+$); $C_{15}H_{19}N_5O_7Na$ requires 404.1182 (+3.4643 ppm). ^{1}H NMR (400 MHz, D_6-DMSO): δ (ppm) 10.77 (1H, bs, N*H*); 7.98 (1H, s, H8); 6.57 (2H, s, NH_2); 5.80-5.82 (1H, d, *J* 7.0 Hz, H1'); 5.38-5.39 (1H, d, *J* 5.2, H3'); 4.60-4.63 (1H, dd, *J* 6.9 and 5.3, H3'); 4.23-4.31 (3H, m, H4', H5' and H5''); 3.28 (3H, s, 2'OC*H*$_3$); 2.13 (3H, s, COC*H*$_3$); 2.07 (3H, s, COC*H*$_3$). ^{13}C NMR (100 MHz, DMSO): δ (ppm) 170.66 (CO), 170.09 (CO), 157.19 (C6), 154.51 (C2), 151.86 (C4), 135.59 (C8) 117.16 (C5), 84.62 (C1'), 80.26 (C2') 80.21 (C4'), 71.16 (C3'), 63.84 (C5'), 58.72 (2'O*C*H$_3$'), 21.11 (CO*C*H$_3$).

8-Bromo-3',5'-di-*O*-acetyl-2'-*O*-methylguanosine (2)[194]

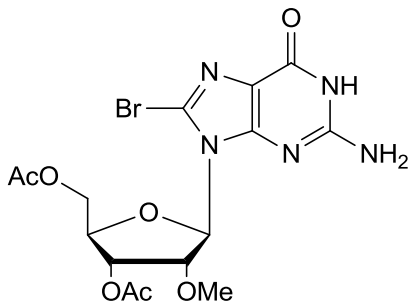

To a solution of 3',5'-di-*O*-acetyl-2'-*O*-methylguanosine (**1**, 6.35g, 13.01mmol) suspended in distilled H_2O (40ml) was added aliquots of saturated bromine water (ca. 25ml) with vigorous

stirring. Once the solution was permanently yellow, the mixture was filtered and washed with cold ^{i}PrOH, before drying in a vacuum dessicator for 12 hours, to yield the product as a pale orange solid (7.07g, 88%). R_f = 0.31 (15% MeOH, 85% DCM). HRMS (ES$^-$) (m/z): 458.0301 and 460.0304 ([M-Na]$^-$); $C_{15}H_{17}N_5O_7Br$ requires 458.0311 and 460.0291 (-2.1833 and +2.826 ppm). ^{1}H NMR (400 MHz, D$_6$-DMSO): δ (ppm) 10.93 (1H, s, N*H*), 6.61 (2H, s, N*H*$_2$), 5.77-5.78 (1H, d, *J* 5.5, H1'), 5.48-5.51(1H, dd, *J* 5.5 and 4.7, H3'), 5.01-5.04 (1H, ap t, *J* 5.7, H2'), 4.37-4.41 (1H, dd, *J* 11.0 and 3.3, H5'), 4.20-4.28 (2H, m, H4 and H5'') 3.28 (3H, s, 2'OC*H*$_3$), 2.13 (3H, s, COC*H*$_3$), 2.02 (3H, s, COC*H*$_3$). ^{13}C NMR (100 MHz, DMSO): δ (ppm) 170.64 (CO), 170.09 (CO), 155.92 (C6), 154.18 (C2), 152.56 (C4), 120.62 (C8), 117.74 (C5), 88.26 (C1'), 80.05 (C2'), 78.61 (C4'), 71.29 (C3'), 63.59 (C5'), 58.76 (2'O*C*H$_3$), 21.04 (CO*C*H$_3$), 21.02 (CO*C*H$_3$).

_N2_-Dimethoxytrityl-8-bromo-3',5'-di-_O_-acetyl-2'-_O_-methylguanosine (3)[194]

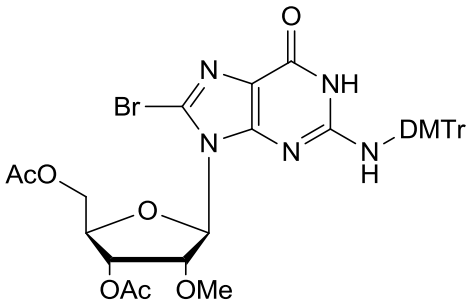

8-Bromo-3',5'-di-*O*-acetyl-2'-*O*-methylguanosine (**2**, 6.35g, 13.80mmol) was co-evaporated to dryness with anhydrous pyridine before re-dissolving in anhydrous pyridine (40ml). The resultant solution was stirred under an atmosphere of N_2 at 0°C and DMTCl (7.01g, 20.70mmol) was added in ca. 0.5g portions over 5 minutes. The mixture was allowed to warm to room temperature and stirred for a further 16 hours. The pyridine was removed *in vacuo* and the resultant oil partitioned between DCM (50ml) and H_2O (50ml), the organic layer was further washed with H_2O (2 x 50ml) and saturated aqueous $NaHCO_3$ (50ml), dried over Na_2SO_4, filtered and evaporated to give the crude material. Purification by flash column chromatography (100% DCM - 5% MeOH, 95% DCM) gave the product as a white solid (8.52g, 81%). R_f = 0.21 (40% EtOAc, 60% DCM). HRMS (ES$^+$) (m/z): 784.1584 and 786.1576 ([M+Na]$^+$); $C_{36}H_{36}N_5O_9BrNa$ requires 784.1594 and 786.1574 (-1.2753 and +0.2544 ppm). ^{1}H NMR (400 MHz, D$_6$-DMSO): δ (ppm) 10.97 (1H, s, N*H*), 7.72 (1H, s, N*H*), 7.14-7.34 (9H, m, DMT Ar-H), 6.87-6.90 (4H, m, DMT C*H*COCH$_3$), 5.40-5.42 (1H, d, *J* 6.7, H1'), 4.80-4.82 (1H, dd, *J* 6.1 and

4.0, H3'), 3.98-4.02 (1H, ap t, *J* 6.7, H2'), 3.88-3.92 (1H, dd, *J* 11.2 and 6.23, H5'), 3.71-3.72 (7H, m, Ar-OC*H*$_3$ and H4'), 3.48-3.52 (1H, dd, *J* 11.7 and 7.1, H5''), 2.74 (1H, s, 2'OC*H*$_3$), 2.07 (3H, s, COC*H*$_3$), 2.00 (3H, s, COC*H*$_3$). ^{13}C NMR (100 MHz, D_6-DMSO): δ (ppm) 170.15 (CO), 169.92 (CO), 158.41 (Ar-C), 158.35 (Ar-C), 155.60 (C6), 151.78 (C4), 151.15 (Ar-C), 130.63 (Ar-C), 129.97 (Ar-C), 128.63 (Ar-C), 128.33 (Ar-C), 127.27 (Ar-C), 121.60 (C8), 118.69 (C5), 113.63 (Ar-C), 113.56 (Ar-C), 88.20 (C2'), 79.56 (C1'), 76.10 (C4'), 70.75 (NH*C*), 69.77 (C3'), 62.77 (C5'), 57.95 (2'O*C*H$_3$), 55.42 (Ar-OC*H*$_3$), 55.39 (Ar-O*C*H$_3$), 20.96 (CO*C*H$_3$).

_N2_-Dimethoxytrityl-8-nitro-3',5'-di-_O_-acetyl-2'-_O_-methylguanosine (4)[194]

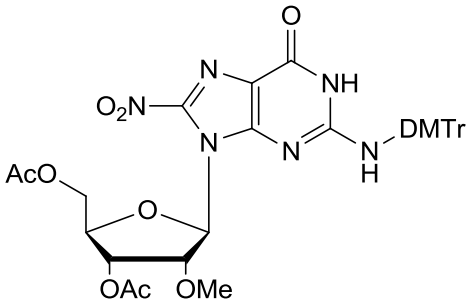

To a solution of *N*2-dimethoxytrityl-8-bromo-3',5'-di-*O*-acetyl-2'-*O*-methylguanosine (**3**, 1.50g, 1.97mmol) in anhydrous DMF (150ml) under an inert atmosphere was added 18-crown-6 (5.20g, 19.67mmol) and KNO_2 (1.67g, 19.67mmol). The resultant mixture was heated to 100°C and stirred for 6 hours before being cooled to room temperature. The solution was poured into saturated $NaHCO_3$ (50ml), extracted with EtOAc (3 x 50ml), dried over Na_2SO_4, filtered and concentrated *in vacuo*. Flash column chromatography of the crude material (50% EtOAc, 50% hexane – 80% EtOAc, 20% hexane) afforded the title product as a yellow amorphous solid (0.52g, 36%). R_f = 0.46 (40% EtOAc, 60% DCM). HRMS (ES$^+$) (m/z): 751.2313 ([M+Na]$^+$); $C_{36}H_{36}N_6O_{11}Na$ requires 751.2340 (-3.7272 ppm). ^{1}H NMR (400 MHz, D_4-MeOD): δ (ppm) 7.23-7.31 (9H, m, DMT Ar-H), 6.86-6.89 (4H, m, DMT C*H*COCH$_3$), 5.60-5.61 (1H, d, *J* 4.5, H1'), 5.06-5.09 (1H, ap t, *J* 6.9, H3'), 4.27-4.30 (1H, dd, *J* 6.9 and 4.6, H2'), 4.10-4.14 (1H, m, H5'), 3.99-4.03 (1H, m, H4'), 3.94-3.98 (1H, dd, *J* 11.6 and 5.4, H5''), 3.78 (6H, s, 2 x Ar-OC*H*$_3$), 2.84 (3H, s, 2'OC*H*$_3$), 2.09 (3H, s, COC*H*$_3$), 2.05 (3H, s, COC*H*$_3$). ^{13}C NMR (100 MHz, MeOD): δ (ppm) 170.87 (CO), 170.15 (CO), 158.72 (CO), 157.41 (C4), 153.14 (C6), 151.48 (C8), 144.78 (C2), 143.66 (Ar-C), 136.46 (Ar-C), 135.79 (Ar-C), 129.92 (Ar-C), 129.77 (Ar-C), 128.41 (Ar-C), 127.66 (Ac-C), 126.81 (Ac-C), 115.03 (C5), 112.95 (Ar-C), 89.75 (C1'), 78.71

(C2'), 78.66 (C4'), 70.50 (NH*C*), 70.35 (C3'), 61.81 (C5'), 57.49 (2'O*C*H$_3$), 54.39 (Ar-O*C*H$_3$), 19.24 (CO*C*H$_3$),19.06 (CO*C*H$_3$).

_N2_-Dimethoxytrityl-8-nitro-2'-_O_-methylguanosine (5)[194]

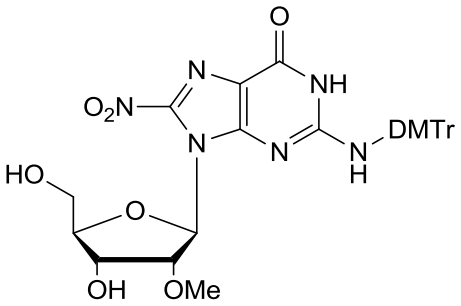

N2-Dimethoxytrityl-8-nitro-3',5'-di-*O*-acetyl-2'-*O*-methylguanosine (**4**, 1.74g, 2.39mmol) was dissolved in NH_3 (7M) in MeOH (15ml) and stirred in a sealed vessel for 48 hours. The solvent was removed *in vacuo* and purified by flash column chromatography (50% EtOAc, 50% DCM) to yield the deacetylated nucleoside as a yellow amorphous solid (1.47g, 95%). R_f = 0.27 (50% EtOAc, 50% DCM). HRMS (ES$^+$) (m/z): 667.2131 ([M+Na]$^+$); $C_{32}H_{32}N_6O_9Na$ requires 667.2128 (+0.4496 ppm). ^{1}H NMR (400 MHz, D_4-MeOD): δ (ppm) 7.20-7.31 (9H, m, DMT Ar-H), 6.85-6.88 (4H, m, DMT C*H*COCH$_3$), 5.82-5.82 (1H, d, *J* 3.2, H1'), 3.79-3.81 (1H, dd, *J* 7.0 and 3.2, H2'), 3.73-3.77 (6H ,s, 2x Ar-OC*H*$_3$), 3.76 (1H, ap t, *J* 7.1, H3'), 3.58-3.62 (1H, dt, *J* 7.2 and 2.9, H4'), 3.52-3.55 (1H, dd, *J* 12.2 and 2.9, H5'), 3.36-3.41 (1H, dd, *J* 12.2 and 7.2, H5''), 3.03 (3H, s, 2'OC*H*$_3$). ^{13}C NMR (100 MHz, MeOD): δ (ppm) 160.13 (Ar-C), 160.08 (Ar-C), 158.95 (C4), 154.42 (C6), 152.65 (C8), 146.10 (C2), 145.24 (Ar-C), 137.90 (Ar-C), 137.31 (Ar-C), 131.20 (Ar-C), 131.11 (Ar-C), 129.81 (Ar-C), 129.11 (Ar-C), 128.20 (Ar-C), 116.52 (C5), 114.41 (Ar-C), 114.37 (Ar-C), 91.14 (C1'), 85.44 (C2'), 81.28 (C3), 71.90 (C4), 70.58 (NH*C*), 63.49 (C5'), 58.50 (2'O*C*H$_3$), 55.77 (Ar-C), 54.80 (Ar-C).

5'-*O*,*N*2-bis-dimethoxytrityl-8-nitro-2'-*O*-methylguanosine (6)[194]

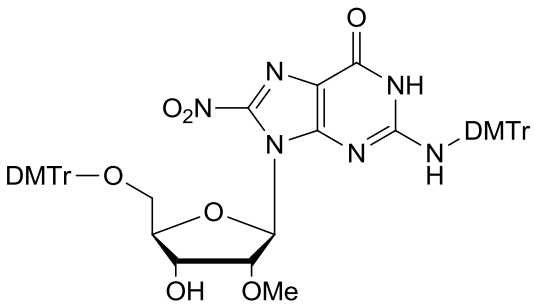

*N*2-Dimethoxytrityl-8-nitro-2'-*O*-methylguanosine (**5**, 1.45g, 2.25mmol) was dried by co-evaporation of anhydrous pyridine before re-dissolving in anhydrous pyridine (15ml) and adding DMTCl (1.02g, 3.00mmol) in portions. The solution was stirred for 16 hours at room temperature under an inert atmosphere. The pyridine was removed *in vacuo* and the residue was subjected to flash column chromatography (20% EtOAc, 80% Hexane) to afford the title compound as a yellow solid (1.66g, 78%). R_f = 0.66 (40% EtOAc, 60% DCM). HRMS (ES^+) (m/z): 969.3444 ($[M+Na]^+$); $C_{53}H_{50}N_6O_{11}Na$ requires 969.3435 (+0.9285 ppm). ^1H NMR (400 MHz, D_6-DMSO): δ (ppm) 11.22 (1H, br s, N*H*), 8.10 (1H, br s, N*H*), 7.13-7.31(18H, m, DMT Ar-H), 6.80-6.87 (8H, m, DMT C*H*COCH$_3$), 5.70 (1H, d, *J* 1.8, H1'), 4.55-4.57 (1H, d, *J* 8.5, H3'), 3.86-3.87 (1H, m, H4') 3.68-3.73 (13H, 4 x Ar-OC*H*$_3$ and H2'), 3.03-3.05 (1H, d, *J* 9.73, H5'), 2.93- 2.95 (4H, m, 2'OC*H*$_3$ and H5''). ^{13}C NMR (100 MHz, DMSO): δ (ppm) 158.03 (Ar-C), 157.88 (Ar-C), 157.91 (Ar-C), 157.86 (Ar-C), 156.11 (C4), 153.06 (C6), 150.02 (C8), 144.79 (Ar-C), 144.28 (Ar-C), 143.21 (C2), 136.89 (Ar-C), 135.82 (Ar-C), 135.82 (Ar-C), 135.50 (Ar-C), 129.76 (Ar-C), 129.66 (Ar-C), 129.58 (Ar-C), 128.23 (Ar-C), 127.81 (Ar-C), 127.68 (Ar-C), 127.62 (Ar-C), 115.40 (C5), 113.21 (Ar-C), 113,12 (Ar-C), 113.05 (Ar-C), 113.02 (Ar-C), 89.57 (C1'), 85.26 (NH*C*), 81.83 (C2'), 79.63 (C4'), 69.70 (NH*C*), 69.36 (C3'), 63.57 (C5'), 57.04 (2'OCH$_3$), 55.05 (Ar-C), 55.02 (Ar-C), 54.99 (Ar-C), 54.97 (Ar-C).

5'-*O*,*N*2-bis-dimethoxytrityl-8-nitro-2'-*O*-methylguanosine-3'-*O*-[(2-cyanoethyl)-(*N*,*N*-diisopropyl)]-phosphoramidite (7)[194]

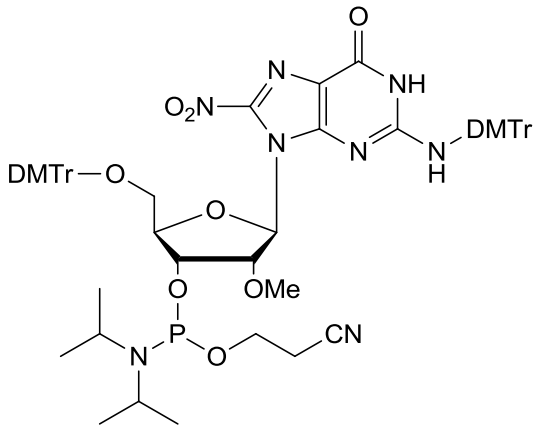

5'-*O*,*N*2-bis-dimethoxytrityl-8-nitro-2'-*O*-methylguanosine (**6**, 1.00g, 1.06mmol) was dissolved in anhydrous DCM (10ml), and cooled to 0°C under an inert atmosphere. *N*,*N*-Diisopropylethylamine (2.30ml, 13.20mmol) was added followed by dropwise addition of 2-cyanoethy-*N*,*N*-diisopropyaminochlorophosphoramidite (0.47ml, 2.11mmol). The solution was allowed to warm to room temperature and stirred for 3 hours before adding H_2O (20ml) and DCM (40ml). The phases were separated and the organic solution was dried with Na_2SO_4, filtered and concentrated *in vacuo* to give a pale brown solid. Purification by flash column chromatography (30% EtOAc, 70% DCM) resulted in a yellow amorphous solid containing both diastereoisomers (a) and (b) (0.55g, 45%). R_f = 0.81 (75% EtOAc, 25% DCM). HRMS (ES^+) (m/z): 1169.4540 ($[M+Na]^+$); $C_{62}H_{67}N_8O_{12}PNa$ requires 1169.4514 (+2.2233 ppm). ^{31}P NMR (160 MHz, $CDCl_3$): δ (ppm) 152.06, 150.57. ^1H NMR (400 MHz, $CDCl_3$): δ (ppm) 7.10-7.44 (36H, m, DMT Ar-H), 6.73-6.80 (16H, m, DMT C*H*COCH$_3$), 6.67-6.69 (1H, d, *J* 8.89, H1' (a)), 6.63-6.66 (1H, d, *J* 8.9, H1' (b)) 5.66-5.72 (2H, br peak, H4' (a) and (b)), 4.48-4.54 (2H, br peak, H2'(a) and H2'(b)), 4.02-4.04 (2H, br peak, H3' (a) and (b)), 3.80-3.87 (2H, m, C*H*$_2$CH$_2$CN), 3.71-3.71 (13H, m, Ar-OC*H*$_3$ (a) and (b), H3'), 3.57-3.65 (12H, br peak, Ar-OC*H*$_3$ (a) and (b)), 3.41-3.49 (4H, m, N(C*H*(CH$_3$)$_2$)$_2$ (a) and (b)), 3.12-3.23 (4H, m, H5' (a) and (b)), 3.03-3.08 (2H, br peak, H2' (a) and (b)), 3.06 (3H, br peak, 2'OC*H*$_3$ (a) and (b)), 2.61-2.65 (2H, t, *J* 6.5, CH$_2$C*H*$_2$CN (a)), 2.32-2.36 (2H, t, *J* 6.4, CH$_2$C*H*$_2$CN (b)),1.09-1.15 (18H, m, N(CH(*C*H$_3$)$_2$)$_2$ (a) and (b)), 0.88.0.90 (6H, d, *J* 6.73, N(CH(*C*H$_3$)$_2$)$_2$ (a) and (b)).

7.2.1 General procedure for the solid-phase synthesis of unmodified and modified oligodeoxynucleotides

All oligodeoxynucleotides were synthesised on a 1µmol scale using either SynBase™ CPG Functionalised supports or Universal Q SynBase™ CPG supports both of which were 1µmol, 500Å CPG columns. Synthesis was carried out using a MerMade® 4 DNA/RNA synthesiser. All commercially supplied 5'-*O*-(4,4'-dimethoxytrityl)-2'-deoxynucleoside-3'-[(2-cyanoethyl)-*N,N*-diisopropyl]-phosphoramidite derivatives were diluted with anhydrous MeCN to the recommended concentration of 0.1M and loaded at ports 1-4 on the synthesiser. 5'-*O*-(4,4'-dimethoxytrityl)-2'-*O*-methylguanosine-3'-[(2-cyanoethyl)-*N,N*-diisopropyl]-phosphoramidite was also used at the recommended 0.1M concentration and loaded into port 6 on the synthesiser.

The modified phosphoramidite monomer was dissolved in anhydrous MeCN (0.12M) and loaded at position 5 on the synthesiser. In order to prevent the modified phosphoramidite from crystallising inside the reagent lines, the solution was loaded into the port immediately prior to the start of the X cycle. This required a soft pause of the synthesiser and manual priming of the line 5.

1	START TRITYL
2	DEBLOCK
3	DEBLOCK
4	END TRITYL
5	MeCN WASH
6	MeCN WASH
7	COUPLING
8	COUPLING
9	MeCN WASH
10	CAPPING
11	MeCN WASH
12	OXIDATION
13	MeCN WASH
14	MeCN WASH

Table 7.1: Generalised cycle corresponding to the standard Mermade® 4 1µmol protocol.

Prior to oligodeoxynucleotide synthesis the reagent lines were primed accordingly. All unmodified and modified oligodeoxynucleotides using a functionalised support were synthesised according to the standard Mermade ® 4 1µmol protocol (Table 7.1). Dimers synthesised on a non nucleosidic universal support were treated with an initial extended detritylation pre-cycle (Table 7.2) to ensure complete detritylation of the support.

A	MeCN WASH
B	MeCN WASH
C	MeCN WASH
D	DEBLOCK

Table 7.2: Pre-cycle employed when using universal supports.

Standard 3'-5' synthesis procedures and reagents were used for detritylations, capping and oxidations steps (Table 7.3). Coupling settings with extended coupling times for 2'-*O*-methyl phosphoramidites and modified 2'-*O*-methyl phosphoramidites were employed as shown in Table 7.4. Coupling efficiencies were measured using an integrated spectrophometer. In all cases the final 5'-DMT group was left on the 5'-terminus of the oligodeoxynucleotide strand at the end of the synthesis and the oligodeoxynucleotide was left attached to the solid-support.

Function	**Reagent**	**Injection volume (µl)**
DEBLOCK	3% Trichloroacetic acid in dichloromethane	240
MeCN WASH	Anhydrous acetonitrile	275
ACTIVATOR	ETT (0.25M): 5-thylthio-1*H*-tetrazole in acetonitrile, anhydrous	50
CAPPING	CAP A: Acetic anhydride in THF/pyridine (1:8:1)	110
	CAP B: 10% N-methylimidazole in THF	125
OXIDISER	0.2M Iodine in THF/pyridine/water (7:2:1)	150

Table 7.3: General reagents used for standard DNA synthesis and modified DNA synthesis.

Phosphoramidite	Standard	2'-*O*-methyl		Modified 2'-*O*-methyl	
CPG support	**Function-alised**	**Function-alised**	**Universal**	**Function-alised**	**Universal**
Number of amidite primes	3	3	3	1	1
Amidite injection volume (µl)	40	40	40	40	40
Activator injection volume (µl)	50	50	50	50	50
Wait time (s)	30	70	70	70	80

Table 7.4: Coupling settings for all phosphoramidites and supports.

7.2.2 General procedure for the cleavage of oligodeoxynucleotide strands from the functionalised CPG support and removal of base labile protecting groups

After the synthesis was complete the support bound oligodeoxynucleotides were transferred to a Wheaton V-Vial®, and H_2O (0.50ml) and concentrated aqueous ammonia (1.00ml) were added. The vial was sealed and the resulting mixture was heated at 55°C for 8 hours until cleavage of the oligodeoxynucleotides from the linker and removal of the base labile protecting groups was achieved. The ammonium hydroxide solution was then transferred into eppendorf vials (1.5ml). Care was taken to avoid transferring any of the CPG support as it can prove problematic during purification. The remaining solid was washed with H_2O (0.5ml) and the supernatant was transferred into an eppendorf vial. The eppendorfs were then centrifuged for 10 minutes to ensure that any residual solid was not present.

7.2.3 General procedure for the cleavage of oligodeoxynucleotides strands from the Universal Q CPG support and removal of base labile protecting groups

After the synthesis was complete the support bound oligodeoxynucleotides were transferred to a Wheaton V-Vial®, and H_2O (0.25ml), concentrated aqueous ammonia (0.50ml) and 40% methylamine (0.75ml) were added. The vial was sealed and the resulting mixture was heated at 55°C for 17 hours until cleavage of the oligodeoxynucleotides from the linker and removal of the base labile protecting groups was achieved. The supernatant was then transferred into eppendorf vials (1.5ml). Care was taken to avoid transferring any of the CPG support as it can prove problematic during purification. The remaining solid was washed with H_2O (0.5ml) and

the solution was transferred into an eppendorf vial. The eppendorfs were then centrifuged for 10 minutes to ensure that any residual solid was not present.

7.2.4 Procedure for the removal of the DMT groups on the modified dinucleotide prior to purification

Removal of the 5'-DMT and 2 x *N*2-DMT was achieved by treatment of the unpurified dinucleotide with 3% trichloroacetic acetic acid in dichloromethane (0.5ml, 0.09mmol) and the resulting mixture was left to stand at room temperature for 10 minutes. The acidic solution was neutralized with triethylamine (0.026ml, 0.18mmol) and then concentrated *in vacuo*. The yellow solid was dissolved in H_2O (0.5ml), extracted with EtOAc (3 x 0.5ml) and the aqueous layer concentrated *in vacuo.* The resulting residue was resuspended in distilled water (1ml) and the fully deprotected dinucleotide was purified by the general procedure for fully deprotected oligodeoxynucleotides described below (section 2.7).

7.2.5 General procedure for RP-HPLC analysis and purification of the crude 5'-DMT oligodeoxynucleotides

Analytical scale

Analytical, RP-HPLC was performed with a sample injection of 15µl. The composition of the eluent was controlled by the control method 0-100 as shown in Figure 7.1 (page 139). Full length oligonucleotides with the 5'-DMT group present have a retention time of greater than 19 minutes. Eluted compounds were detected by UV absorbance at both 254 and 350nm.

Preparative scale

Preparative RP-HPLC was performed with sample injections of up to 400µl using the control method 0-100 (Figure 7.1, page 139). The fractions collected containing the desired 5'-DMT protected oligonucleotides were combined and concentrated *in vacuo*. The resulting residue was co-evaporated with water (1ml) and concentrated under reduced pressure. The solid that remained was resuspended in distilled H_2O to afford the pure 5'-DMT protected oligodeoxynucleotide. The 5'-DMT group was then removed by treatment with acid as described in the following procedure.

7.2.6 General procedure for the removal of the 5'-DMT group

Removal of the 5'-DMT was achieved by treatment of the purified 5'-DMT oligodeoxynucleotide with 20% aqueous acetic acid solution (1ml) and the resulting solution was left to stand at room

temperature for 20 minutes. The aqueous acid was removed *in vacuo* and the remaining residue was washed with distilled water (1ml) and reconcentrated.

7.2.7 General procedure for the RP-HPLC analysis and purification of the fully deprotected oligodeoxynucleotides

Analytical scale

Analytical, RP-HPLC was performed with a sample injection of 15µl using the control method 0-100 described previously (page 139). Fully deprotected oligodeoxynucleotides eluted between ~11-14 minutes and were detected by UV absorbance at both 254 and 350nm.

Preparative scale

Preparative RP-HPLC was performed on up to 400µl sample injections using the control method 0-100 (page 139). The fractions containing the desired oligonucleotides were collected, combined and concentrated *in vacuo*. The resulting residue was co-evaporated with water (1ml), concentrated under reduced pressure to afford the pure full length oligonucleotides.

7.2.8 Quantification of oligodeoxynucleotides

The fully deprotected, dried oligodeoxynucleotide samples were dissolved in 1.0ml of distilled water to give the oligodeoxynucleotide stock solution. The concentration and final yield of the purified oligodeoxynucleotides were calculated using the values obtained for the UV absorbance at 260nm.

The pathlength compensation factor was applied to the absorbance obtained from 5µl of the stock solutions using the TrayCell™ in order to adjust the values to that of a 1cm cuvette (Equation 7.1).

$$\text{Absorbance}_{(\text{stock})} = \text{Absorbance}_{(260)} \times \text{Pathlength compensation factor}$$

Equation 7.1: Calculation of the absorbance of the stock solution.

The Beer-Lambert law was utilized to calculate the concentrations of the oligodeoxynucleotides. As there is no molar extinction coefficient (ε) value for the modified oligodeoxynucleotides, the ε value for the analogous unmodified sequence was used.

$$\text{Concentration} = \frac{\text{Absorbance}_{(stock)}}{\varepsilon \times \text{Pathlength}} \times 10^6$$

Equation 7.2: Beer-Lambert Law.

Equation 7.3 is used to calculate the optical density (OD) from the absorbance. Since the stock solution was generally in 1ml, the optical density and the absorbance of the stock solution were often equivalent.

$$\text{Optical Density}_{(260)} = \text{Absorbance}_{(stock)} \times \text{Volume (ml)}$$

Equation 7.3: Calculation of optical density.

In order to determine the overall yield it was necessary calculate the theoretical optical density at 260nm. The calculation is based on a 1μmole scale and assumes that each coupling step is quantitative.

$$\text{Theoretical optical density}_{(260)} = \varepsilon \times \text{Moles} \times 1000$$

Equation 7.4: Calculation of theoretical optical density.

The percentage yield of the purified oligodeoxynucleotide was then calculated using Equation 7.5.

$$\text{Percentage yield of oligodeoxynucleotide} = \frac{\text{Optical density}_{(260)}}{\text{Theoretical optical density}_{(260)}}$$

Equation 7.5: Calculation of the % yield of the purified oligodeoxynucleotide.

7.2.9 HPLC and UV analysis of all oligodeoxynucleotide synthesised

The HPLC analysis obtained for all oligonucleotide syntheses is shown in Table 7.5

	HPLC analysis (Control method 0-100)		
	Retention time (minutes)		Purity (%)
Oligodeoxynucleotide	**DMT-on**	**DMT-off**	
Site 1 control	21.45	11.35	97
Site 1	21.69	10.95	95
Site 2 Control	18.15	11.54	86
Site 2	19.51	11.46	87
Site 3 Control	20.28	11.67	95
Site 3	19.88	11.71	90
Dimer (**8**)	19.16	13.80	97
Dimer (**9**)	-	13.83	74

Table 7.5: All oligodeoxynucleotides prepared together with their retention times and purity as determined by HPLC. For sequences see table 2.1 or abbreviations section.

As aforementioned the typical loading of the CPG solid-support is in the range of 30-60μmol g^{-1}. Therefore the yields calculated for oligodeoxynucleotide synthesis are an approximation rather than accurate calculation.

	UV Analysis		
Oligodeoxynucleotide	**ε (260nm)***	**OD_{260} units**	**Yield (%)**
Site 1 control	122100	31.65	26
Site 1	122100	39.02	32
Site 2 Control	361200	25.72	7
Site 2	361200	66.60	18
Site 3 Control	254400	51.04	20
Site 3	254400	29.21	11
Dimer (**8**)	21600	14.65	68
Dimer (**9**)	21600	0.97	4

Table 7.6: The yields of the purified oligodeoxynucleotides as determined by UV analysis. * ε was calculated using the IDT Biophysics website[309].

7.2.10 Mass spectrometry data for all oligodeoxynucleotides

Table 7.7 and Table 7.8 show the theoretical and experimental molecular weights of all oligodeoxynucleotides synthesised.

	Mass spectrometry analysis		
Oligodeoxynucleotide	**Charge**	**Theoretical mass**	**Experimental mass**
Site 1 Control	-3	1324.2277	1324.2203
Site 1	-4	1011.6678	1011.6455

Table 7.7: Theoretical and experimental molecular weights for the mass to charge ratio (m/z) for electrospray spectra. For sequences see table 2.1 or abbreviations section.

The $[M-nH]^{n-}$ peaks were then used to give experimental average masses for the parent ions of each oligodeoxynucleotide product.

	Parent ion molecular weight		
Oligodeoxynucleotide	**Theoretical mass**	**Experimental mass**	**Error (ppm)**
Site 1 Control	3975.7066	3975.6844[a]	-5.6033
Site 1	4050.7025	4050.6133[a]	-22.1026
Site 2 Control	nd	nd	Nd
Site 2	nd	nd	Nd
Site 3 Control	8311.42	8314.74[b]	Nd
Site 3	8460.31[c]	8460.64[b]	Nd
Dimer (**8**)	655.1626	655.1617[a]	-1.3737
Dimer (**9**)	745.1327	745.1313[a]	-1.8789

Table 7.8: Theoretical and experimental average molecular weights of the parent ion for all oligodeoxynucleotides synthesised. Note the experimental masses of the dimers were obtained directly from the spectra. Note nd = not determined, [a] determined by electrospray ionisation, [b] determined by MALDI and [c] corresponds to (M-4H)+3Na+K. For sequences see table 2.1 or abbreviations section.

7.3 Experimental procedures for results and discussion 2

2',3',5'-Tri-*O*-acetylguanosine (10)[310]

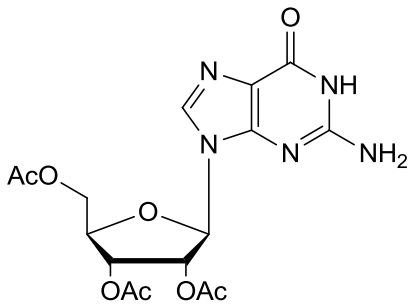

Acetic anhydride (1.00ml, 10.6mmol) was added dropwise to an ice cooled mixture of guanosine (1.00g, 3.5mmol), triethylamine (2.95ml, 21.1mmol) and DMAP (0.043g, 0.35mmol) in MeCN (10ml). The reaction mixture was then allowed to warm to room temperature. There was complete solubilisation when the reaction had gone to completion. The reaction was quenched with MeOH. The solvent was removed *in vacuo* to give a cloudy gel. The product was then isolated by recrystallisation from the minimum amount of hot ^{i}PrOH. The white solid was then co-evaporated with Et_2O to remove excess triethylamine. This yielded the product as a white solid (1.24g, 86%). HRMS (ES^+) (m/z): 432.1115 ($[M+Na]^+$); $C_{16}H_{19}N_5O_8Na$ requires 432.1131 (-3.7027 ppm). ^{1}H NMR (400 MHz, D_6-DMSO): δ (ppm) 10.83 (1H, br s, N*H*), 7.94 (1H, s, C8), 6.59 (2H, br s, NH_2), 5.98-6.00 (1H, d, *J* 6.1, H1'), 5.78-5.81 (1H, ap t, *J* 6.1, H2'), 5.48-5.51 (1H, dd *J* 5.9 and 4.1, H3'), 4.36-4.40 (1H, dd *J* 11.2 and 3.7, H5'), 4.30-4.34 (1H, m, H4'), 4.24-4.27 (1H, dd *J* 11.2 and 5.7, H5''), 2.12 (3H, s, COCH_3), 2.05 (3H, s, COCH_3), 1.90 (3H, s, COCH_3). ^{13}C NMR (100 MHz, DMSO): δ (ppm) 170.47 (CO), 169.82 (CO), 169.65 (CO), 157.03 (C6), 154.30 (C2), 151.48 (C4), 135.97 (C8), 117.150 (C5), 84.70 (C1'), 79.89 (C2'), 72.39 (C4'), 70.66 (C3'), 63.44 (C5'), 21.70 (CO*C*H_3), 20.75 (CO*C*H_3), 20.56 (CO*C*H_3).

8-Bromo-2',3',5'-tri-*O*-acetylguanosine (11)[311]

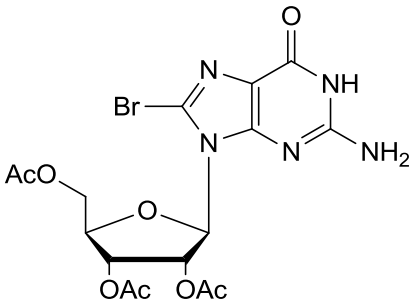

To a stirred solution of 2',3',5'-tri-*O*-acetylguanosine (**10**, 1.20g, 2.9mmol) suspended in distilled H_2O (10ml), was added bromine water in aliquots (3ml) with vigorous stirring until the solution remained permanently yellow. The mixture was filtered and washed with cold ^{i}PrOH leaving the product as a pale orange solid (1.36g, 89%). HRMS (ES^+) (m/z): 510.0227 and 512.0200 ($[M+Na]^+$); $C_{16}H_{18}N_5O_8BrNa$ requires 510.0236 and 512.0216 (-1.7646 and -3.1249 ppm). ^{1}H NMR (400 MHz, D_6-DMSO): δ (ppm) 10.95 (1H, br s, N*H*), 6.63 (2H, br s, NH_2), 5.99-6.02 (1H, dd, *J* 6.4 and 4.5, H3'), 5.88-5.89 (1H, d, *J* 4.4, H1'), 5.54-5.66 (1H, ap t, *J* 6.3, H2'), 4.36-4.4 (1H, dd, *J* 11.8 and 3.7, H5'), 4.31-4.35 (1H, ddd, *J* 6.2, 6.1 and 3.8, H4'), 4.19-4.23 (1H, dd, *J* 11.8 and 6.2, H5''), 2.12 (3H, s, COCH_3), 2.08 (3H, s, COCH_3), 2.00 (3H, s, COCH_3). ^{13}C NMR (100 MHz, DMSO): δ (ppm) 170.47 (CO), 169.86 (CO), 169.78 (CO), 155.78 (C6), 154.16 (C2), 152.27 (C4), 120.50 (C8), 117.53 (C5), 87.99 (C1'), 79.65 (C2'), 71.64 (C3'), 70.27 (C4'), 63.13 (C5'), 20.84 (COCH_3), 20.67 (COCH_3), 20.61 (COCH_3).

***N*2-Dimethoxytrityl-8-bromo-2',3',5'-tri-*O*-acetylguanosine (12)**[194]

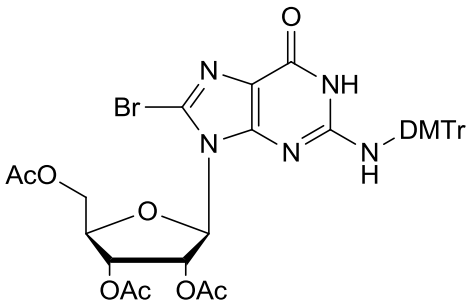

8-Bromo-2'-3'-5'-tri-*O*-acetylguanosine (**11**, 1.10g, 2.3mmol) was co-evaporated with anhydrous pyridine (3 x 10ml) and subsequently dissolved in anhydrous pyridine (10ml). DMTCl (1.5g, 4.5mmol) was added over 5 minutes to the solution under a nitrogen atmopshere. The reaction mixture was stirred overnight and then partitioned between H_2O (10ml) and $CHCl_3$ (20ml). The aqueous layer was washed with $CHCl_3$ (3 x 20ml) and the combined organic extracts were dried over Na_2SO_4. The solvent was then removed *in vacuo* to give a brown oil. The crude product was purified by column chromatography (100% $CHCl_3$ - 2% MeOH, 98% $CHCl_3$) to give the desired product as a yellow amorphous solid (1.78g, 90%). R_f = 0.50 (10% MeOH, 90% DCM). HRMS (ES^+) (m/z): 812.1520 and 814.1494 ($[M+Na]^+$); $C_{37}H_{36}N_5O_{10}BrNa$ requires 812.1543 and 814.1523 (-2.8320 and -3.5620 ppm). λ_{max} (H_2O) 236 and 274nm. ^{1}H NMR (400 MHz, D_4-MeOD): δ (ppm) 7.21-7.30 (9H, m, DMT Ar-H), 6.84-6.87 (4H, ap d, DMT C*H*COCH$_3$), 5.58-5.60 (1H, d, *J* 6.1, H1'), 5.22-5.25 (2H, ap t, *J* 6.4, H2'), 4.97-

5.00 (1H, dd, *J* 6.4 and 4.7, H3'), 4.00-4.04 (1H, dd, *J* 11.2 and 6.1, H5'), 3.83-3.92 (2H, m, H4' and H5''), 3.78 (6H, s, Ar-OC*H*$_3$), 2.11 (3H, s, COC*H*$_3$), 2.03 (3H, s, COC*H*$_3$), 1.96 (3H, s, COC*H*$_3$). ^{13}C NMR (100 MHz, MeOD): δ (ppm) 172.00 (CO), 170.97 (CO), 170.79 (CO), 160.03 (Ar-C), 159.98 (Ar-C), 158.14 (C6), 153.02 (C2), 152.87 (C4), 146.73 (Ar-C), 137.40 (Ar-C) 131.14 (Ar-C), 131.02 (Ar-C), 129.72 (Ar-C), 129.08 (Ar-C), 128.11 (Ar-C), 123.23 (C8) 119.18 (C5), 114.31 (Ar-C), 114.25 (Ar-C), 89.31 (C1'), 80.64 (C2'), 71.89 (C3'), 71.76 (NH*C*), 71.35 (C4'), 64.19 (C5'), 55.68 (Ar-O*C*H$_3$), 20.70 (CO*C*H$_3$), 20.45 (CO*C*H$_3$), 20.16 (CO*C*H$_3$).

_N2_-Dimethoxytrityl-8-nitro-2',3',5'-tri-_O_-acetylguanosine (13)[194]

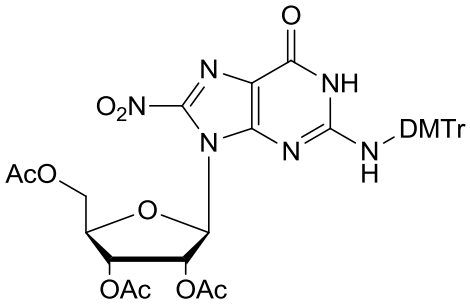

N2-Dimethoxytrityl-8-bromo-2',3',5'-tri-O-acetylguanosine (**12**, 1.50g, 1.90mmol) was dissolved in anhydrous DMF (150ml). To this solution was added KNO_2 (1.61g, 19.0mmol) and 18-crown-6 (5.01g, 19.0mmol). The resulting mixture was then heated at 100°C for 6 hours under an inert atmosphere before cooling to room temperature and pouring directly into H_2O (50ml). The aqueous solution was extracted with EtOAc (3 x 50ml), and the combined organic extracts were washed with $NaHCO_3$ (50ml), dried with Na_2SO_4, filtered and concentrated to an oil. The crude product was purified by flash column chromatography (50% EtOAc, 50% Hexane – 70% EtOAc, 30% Hexane). This gave the product as a yellow amorphous solid (0.46, 32%). R_f = 0.48 (40% EtOAc, 60% DCM). HRMS (ES$^+$) (m/z): 779.2302 ([M+Na]$^+$); $C_{37}H_{36}N_6O_{12}Na$ requires 779.2289 (+1.6683 ppm). λ_{max} (H_2O) 237, 274 and 398. ^{1}H NMR (400 MHz, D_6-DMSO): δ (ppm) 11.20 (1H, br s, 1H, N*H*), 8.08 (2H, br s, N*H*$_2$), 7.12-7.35 (9H, m, DMT Ar-H), 6.86-6.91 (4H, m, DMT C*H*COCH$_3$), 5.58-5.59 (1H, d, *J* 4.8, H1'), 5.44-5.47 (1H, dd, *J* 6.7 and 5.1, H2') 5.14-5.18 (1H, ap t, *J* 6.9, H3'), 4.12-4.16 (1H, dd, *J* 11.9 and 2.8, H5'), 3.97-4.01 (1H, ddd, *J* 6.6, 6.2 and 3.3, H4'), 3.83-3.88 (1H, dd, *J* 12.0 and 6.0, H5''), 3.73 (6H, s, Ar-O*C*H$_3$),2.06 (3H, s, COC*H*$_3$), 2.00 (3H, s, COC*H*$_3$), 1.79 (3H, s, COC*H*$_3$). ^{13}C NMR (100 MHz, DMSO): δ (ppm) 169.89 (CO), 169.16 (CO), 168.85 (CO), 157.98 (Ar-C), 157.92 (Ar-C), 156.05 (C6), 153.33 (C4), 151.29 (C8), 144.68 (C2), 142.92 (Ar-C), 135.98 (Ar-C), 129.70 (Ar-

C), 129.66 (Ar-C), 128.26 (Ar-C), 127.92 (Ar-C), 126.85 (Ar-C), 115.26 (C5), 113.18 (Ar-C), 113.11 (Ar-C), 82.27 (C1'), 78.25 (C2'), 70.90 (C3'), 70.00 (NH*C*), 68.63 (C4'), 61.85 (C5'), 55.03 (Ar-O*C*H_3), 55.02, 20.41 (CO*C*H_3), 20.24 (CO*C*H_3), 19.87 (CO*C*H_3).

8-Nitro-2',3',5'-tri-*O*-acetylguanosine (14)

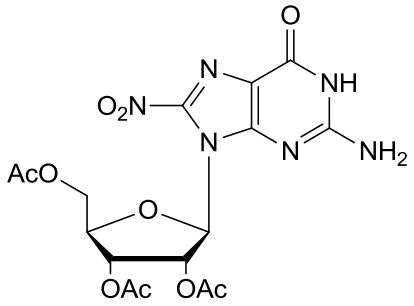

N2-Dimethoxytrityl-8-nitro-2',3',5'-tri-*O*-acetylguanosine (**13**, 0.25g, 0.33mmol) was dissolved in $CHCl_3$ (5ml) before adding a solution of *p*TsOH (0.028g, 0.17mmol) in MeOH (1ml). After 20 minutes the solvent was removed *in vacuo*. The orange solid was the triturated with Et_2O to afford the detritylated nucleoside (0.1259g, 84%). HRMS (ES^-) (m/z): 453.1014 ($[M-H]^-$); $C_{16}H_{17}N_6O_{10}$ requires 453.1006 (+1.7656 ppm). ^{1}H NMR (400 MHz, D_6-DMSO): δ (ppm) 11.34 (1H, br s, N*H*), 7.18 (1H, br s, NH_2), 6.54 (1H, d, *J* 3.0, H1'), 5.90-5.93 (1H, d, *J* 6.3 and 3.2, H2'), 5.71-5.74 (1H, t, *J* 7.0, H3'), 4.41-4.44 (1H, dd, *J* 11.8 and 2.7, H5'), 4.30-4.33 (1H, ap dt, *J* 2.8 and 6.9, H4'), 4.19-4.23 (1H, dd, *J* 6.5 and 11.9, H5''), 2,08 (3H, s, COCH_3), 2.05 (3H, s, COCH_3), 1.98 (3H, s, COCH_3). ^{13}C NMR (100 MHz, DMSO): δ (ppm) 170.46 (*C*OCH$_3$), 169.80 (*C*OCH$_3$), 169.63 (*C*OCH$_3$), 157.20 (C4), 156.26 (C6), 152.67 (C8), 142.98 (C2), 115.33 (C5), 88.73 (C1'), 79.52 (C2'), 72.78 (C3'), 69.99 (C4'), 63.26 (C5'), 20.81 (CO*C*H_3), 20.64 (CO*C*H_3), 20.60 (CO*C*H_3).

8-Nitroguanosine (15)[194]

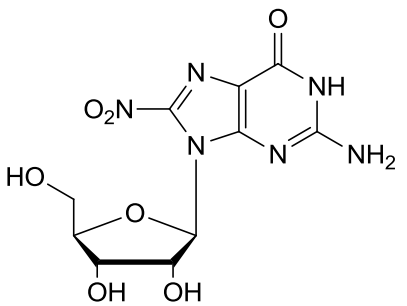

N2-Dimethoxytrityl-8-nitro-2',3',5'-tri-*O*-acetylguanosine (**13**, 0.12g, 0.2mmol) was dissolved in $CHCl_3$ (3ml) before adding a solution of *p*TsOH (6.8mg, 0.04mmol) in MeOH (0.5ml). After 20 minutes the solvent was removed *in vacuo.* The resulting orange solid was triturated with Et_2O three times to afford the crude base deprotected nucleoside. This was then dissolved in NH_3 (7M) in MeOH (3ml) and stirred in a sealed vessel for 36 hours. The precipitate was isolated by drawing off the solution with a syringe followed by trituration of the solid with Et_2O three times to afford the desired compound as an orange solid (40mg, 77%). HRMS (ES^-) (m/z): 327.0700 ($[M-H]^-$); $C_{10}H_{11}N_6O_7$ requires 327.0689 (+3.3632 ppm). ^1H NMR (400 MHz, D_6-DMSO): δ (ppm) 9.60 (1H, br s, NH), 7.18 (2H, br s, NH_2), 6.26-6.28 (1H, d, J 5.3, H1'), 5.41 (1H, br s, OH), 5.07 (1H, br s, OH), 4.91-4.93 (1H, ap t, J 5.5, H2'), 4.19-4.21 (1H, ap t, J 5.3, H3'), 3.83-3.87 (1H, ap q, J 4.9, H4'), 3.65-3.70 (1H, dd, J 11.8 and 4.4, H5'), 3.50-3.55 (1H, dd, J 11.8 and 5.9, H5''). ^{13}C NMR (100 MHz, DMSO): δ (ppm) 157.69 (C4), 156.06 (C6), 152.59 (C8), 143.40 (C2), 115.24 (C5), 90.46 (C1'), 85.67 (C4'), 71.08 (C2'), 70.10 (C3'), 61.85 (C5').

8-Nitroguanine (16)

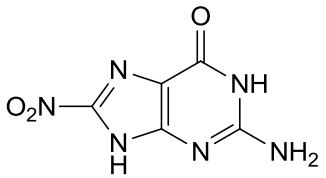

8-Nitroguanosine (**15**, 0.20g, 0.61mmol) was dissolved in 1M HCl and heated at 60°C for 6 hours. The solution was then neutralised with 1M NaOH taking care that the pH did not fall below 7 to avoid formation of salts. The resulting precipitate was isolated by filtration, washed with ice cold H_2O and triturated with EtOAc to give the product as an orange solid (94mg, 79%). λ_{max} (H_2O) 254 and 400nm; ^1H NMR (400 MHz, D_6-DMSO): δ (ppm) 11.28 (1H, br s, N*H*), 6.75 (2H, br s, NH_2), 3.62 (1H, br s, N*H*). 13C NMR (100 MHz, DMSO): δ (ppm) 158.47 (C4), 156.76 (C6), 153.83 (C2), 153.44 (C8), 119.84 (C5).

***N1*-(3,5-di-tert-butyl-4-hydroxybenzyl)-2'3'5'-tri-*O*-acetyl-8-nitroguanosine (17)**

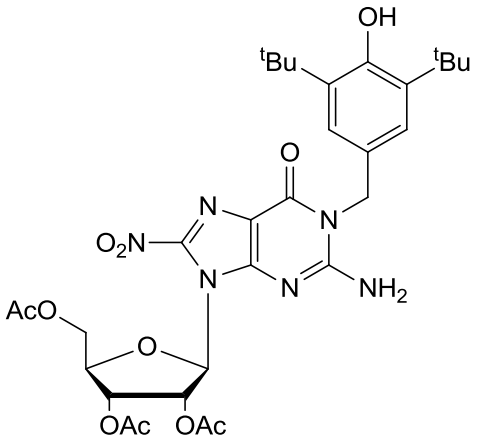

To a solution of butylated hydroxytoluene (24mg, 0.11mmol) in hexane (10ml) was added Ag_2O (0.77g, 3.30mmol), the resulting mixture was stirred in the dark for 20 minutes to generate 2,6-di-*tert*-butyl-4-methylidenecyclohexa-2,5-dien-1-one. The mixture was filtered into a flask containing DMF (1ml), the hexane was removed *in vacuo* and the remaining solution was heated to 37°C. A solution of 8-nitro-2',3',5'-tri-*O*-acetylguanosine (**14**, 0.05g 0.11mmol) in DMF (1ml) was added and the resulting mixture was stirred at 37°C for 1 hour. Upon complete conversion, as indicated by TLC and RP-HPLC (Control method 65/35B, page 141), the reaction was diluted with EtOAc (15ml) and washed with H_2O (3 x 15ml). The combined organic extracts were dried under ($MgSO_4$) and concentrated to an orange residue. Purification by flash column chromatography (70% Hexane, 30% EtOAc) isolated the title compound (24mg, 68%). HRMS (ES^+) (m/z): 695.2678 ($[M+Na]^+$); $C_{31}H_{40}N_6O_{11}Na$ requires 695.2653 (+3.5957 ppm). ^1H NMR (400 MHz, D_3-CD_3CN): δ (ppm) 7.14 (2H, s, Ar-H), 6.60-6.61 (1H, d, *J* 3.2, H1'), 6.08-6.10 (1H, dd, *J* 6.2 and 3.2, H2'), 6.06 (2H, br s, NH_2), 5.86-5.90 (1H, dd, *J* 7.2 and 6.4, H3'), 5.50 (1H, br s, O*H*), 5.11 (2H, s, NCH_2), 4.47-4.51 (1H, dd, *J* 12.0 and 3.7, H5'), 4.33-4.35 (1H, ddd, *J* 6.8, 6.6 and 3.7, H4'), 4.20-4.24 (1H, dd, *J* 12.0 and 6.1, H5''), 2.07 (3H, s, COCH_3), 2.05 (3H, s, COCH_3), 1.90 (3H, s, COCH_3), 1.37 (18H, s, C(CH_3)$_3$).). ^{13}C NMR (100 MHz, CD_3CN): δ (ppm) 171.41 (CO), 170.79 (CO), 158.01 (C4), 156.60 (C2), 154.47 (C6), 151.18 (C8), 138.70 (Ar-C), 126.87 (Ar-C), 125.07 (Ar-C), 118.31 (C5), 89.93 (C1'), 80.41 (C2), 73.62 (C3), 71.06 (C4), 63.73 (C5'), 45.64 (NCH_2), 35.21 (C(CH$_3$)$_3$), 30.44 (C(CH_3)$_3$), 20.84 (COCH_3), 20.69 (COCH_3).

O-tert-butyldimethylsilyl-2-methylphenol (18)[249]

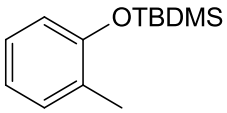

ortho-Cresol (3g, 27.74 mmol) was dissolved in DCM (12ml) and cooled to 0°C. To the solution was added imidazole (3.78g, 55.48mmol) and *tert*-butyldimethylsilyl chloride (5.02g, 33.29mmol) over 10 minutes. The reaction was allowed to warm to room temperature and stirred for a further 18 hours. The mixture was then diluted with DCM (100ml) and washed with 5% $NaHCO_3$ (50ml), before drying with $MgSO_4$, filtering and evaporating to give the product as a colourless oil (5.99g, 97%). HRMS (CI^+) (m/z): 223.1516 ($[M+H]^+$); $C_{13}H_{22}OSi$ requires 223.1513 (+1.3444 ppm). ^1H NMR (400 MHz, $CDCl_3$): δ (ppm) 7.10-7.11 (1H, d, *J* 7.4, Ar-H3), 7.01-7.05 (1H, ap t, *J* 7.7**,** Ar-H5), 6.81-6.85 (1H, ap t, *J* 7.4, Ar-H4), 6.74-6.76 (1H, d, *J* 8.1, Ar-H6), 2.19 (3H, s, C*H*$_3$), 1.00 (9H, s, SiC(C*H*$_3$)$_3$), 0.20 (6H, s, Si(C*H*$_3$)$_2$). ^{13}C NMR (100 MHz, $CDCl_3$): δ (ppm) 154.02 (Ar-C1), 131.09 (Ar-C3), 129.07 (Ar-C2), 126.72 (Ar-C5), 121.12 (Ar-C4), 118.65 (Ar-C6), 25.93 (Si*C*(CH$_3$)$_3$), 18.41 (SiC(*C*H$_3$)$_3$), 17.00 (*C*H$_3$), -4.05 (Si(*C*H$_3$)$_2$).

2-Bromomethyl-_O-tert_-butyldimethylsilylphenol (19)[249]

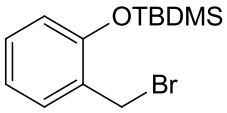

To a solution of *O-tert*-butyldimethylsilyl-2-methylphenol (**18**, 2.00g, 8.99mmol) dissolved in $CHCl_3$ (30ml) was added *N*-bromosuccinimide (1.76g, 9.89mmol) and AIBN (0.15g, 0.89mmol). The resulting mixture was heated to reflux for 6 hours before cooling to room temperature and removing the solvent *in vacuo*. Hexane (100ml) was added and the precipitate formed was removed by filtration. The solvent was removed under reduced pressure and the crude product was purified by flash column chromatography (100% Hexane – 1% EtOAc, 99% Hexane) to give the title compound as a colourless oil (2.47g, 91%). HRMS (CI^+) (m/z): 301.0622 and 303.0604 ($[M+H]^+$); $C_{13}H_{22}OBrSi$ requires 301.0618 and 303.0603 (+1.3286 and +0.330 ppm). ^1H NMR (400 MHz, $CDCl_3$): δ (ppm) 7.18-7.20 (1H, dd, *J* 7.6 and 1.7, Ar-H3), 7.02-7.06 (1H, ddd, *J* 9.1, 7.5 and 1.8, Ar-H5), 6.76-6.80 (1H, ddd, *J* 8.6, 7.5 and 1.1, Ar-H4), 6.66-6.68 (1H, dd, *J* 8.2 and 0.9, H6), 4.39 (2H, s, C*H*$_2$Br), 0.92 (9H, s, SiC(C*H*$_3$)$_3$), 0.15 (6H, s, Si(C*H*$_3$)$_2$). ^{13}C NMR (100 MHz, $CDCl_3$): δ (ppm) 154.04 (Ar-C1), 131.34 (Ar-C3), 130.05 (Ar-C2), 128.56 (Ar-

C6), 121.41 (Ar-C4), 118.77 (Si*C*$(CH_3)_3$), 29.46 (*C*H_2Br), 25.94 (Si*C*$(CH_3)_3$), 18.43 (SiC(*C*$H_3)_3$), -3.97 (Si(*C*$H_3)_3$).

***N1*-2-hydroxybenzyl-2'3'5'-tri-*O*-acetyl-8-nitroguanosine (20) and *O6*,*N2*-bis-(2-hydroxybenzyl)-2'3'5'-tri-*O*-acetyl-8-nitroguanosine (21)**

A solution of 2-bromomethyl-O-*tert*-butyldimethylsilylphenol (**19**, 0.27g, 0.88mmol) dissolved in DMF (0.3ml) was added to a stirred solution of 8-nitro-2',3',5'-tri-*O*-acetylguanosine (**14**, 0.10g, 0.22mmol) in DMF (1.00ml). The mixture was warmed to 37°C followed by addition of 2.64M $KF_{(aq)}$ (0.36ml, 0.92mmol). The red solution which formed turned pale orange over the course of 10 minutes when the reaction reached completion as confirmed by RP-HPLC (Control method 65/35B, page 141) and TLC analysis. The solution was partitioned between EtOAc (30ml) and H_2O (30ml), the organic layer was further washed with H_2O (2 x 30ml) before drying over Na_2SO_4, filtering and evaporating to give the crude product. Purification by flash column chromatography (40% Hexane, 60% EtOAc – 20% Hexane, 80% EtOAc) isolated the di-alkylated (R_f = 0.69 in 80% EtOAc, 20% Hexane) (0.040g, 27%) and mono-alkylated (R_f = 0.29 in 80% EtOAc, 20% Hexane) (0.049g, 40%) products.

***N1*-2-hydroxybenzyl-2'3'5'-tri-*O*-acetyl-8-nitroguanosine (20)**

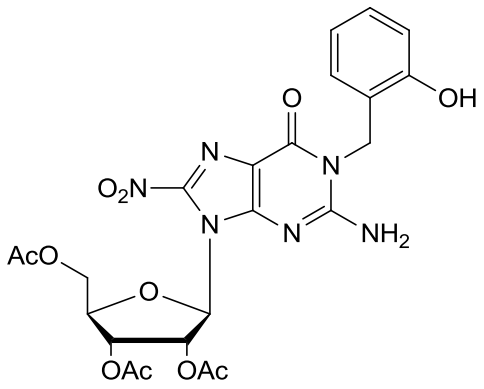

HRMS (ES$^+$) (m/z): 583.1398 ([M+Na]$^+$); $C_{23}H_{24}N_6O_{11}$ requires 583.1401 (-0.5144 ppm). ^{1}H NMR (400 MHz, CD_3CN): δ (ppm) 7.25-7.28 (1H, dd, *J* 7.7 and 1.4, CH_2CCH aromatic), 7.16-7.21 (1H, ap t, *J* 7.7, COHCHC*H* aromatic), 6.92-6.94 (1H, d, *J* 8.07, COHC*H* aromatic), 6.85-6.88 (1H, ap t, *J* 7.5, CH_2CCHCH aromatic), 6.6 (1H, d, *J* 3.0, H1'), 6.52 (1H, bs, OH), 6.06-6.08 (1H, dd, *J* 6.2 and 3.0, H2'), 5.88 and 5.92 (1H, dd, *J* 7.5 and 6.3, H3') 5.17 (2H, s, NCH_2Ph), 4.46- 4.50 (1H, dd, *J* 12.0 and 3.6, H5'), 4.32-4.36 (1H, ddd, *J* 7.5 and 6.0 and 3.6, H4'), 4.12-4.22 (1H, dd, *J* 6.0 and 12.0, H5''), 2.06 (3H, s, $COCH_3$), 2.05 (3H, s, $COCH_3$), 1.90 (3H, s, $COCH_3$). ^{13}C NMR (100 MHz, CD_3CN): δ (ppm) 170.10 (CO), 169.50 (CO), 169.48

(CO), 156.93 (C4), 155.19 (C6), 153.39 (C8), 149.89 (COH), 142.98 (C2), 129.32 (NCH_2C), 129.21 (C*C*H), 121.14 (COHCH*C*H), 120.63 (CCH*C*H), 115.05 (C5), 114.70 (COH*C*H), 88.60 (C1'), 78.97 (C2'), 72.30 (C3'), 69.64 (C4'), 62.30 (C5'), 39.54 (NCH_2), 19.45 ($COCH_3$), 19.36 ($COCH_3$).

***O6*,*N2*-bis-(2-hydroxybenzyl)-2'3'5'-tri-O-acetyl-8-nitroguanosine (21)**

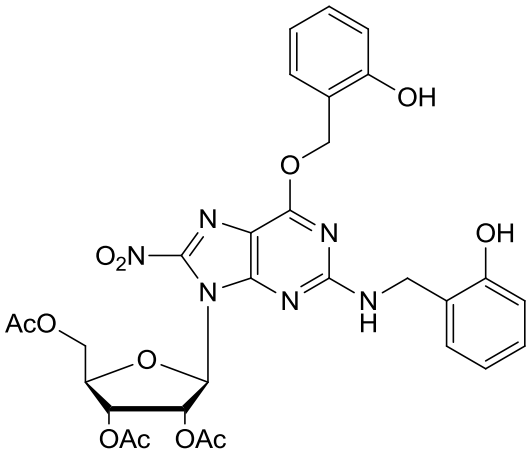

HRMS (ES^+) (m/z): 689.1823 ($[M+Na]^+$); $C_{30}H_{30}N_6O_{12}$ requires 689.1819 (+0.5804 ppm). ^1H NMR (400 MHz, CD_3CN): δ (ppm) 7.51 (1H, bs, N*H*), 7.39-7.41 (1H, dd, *J* 7.4 and 1.5, Ar-H) 7.29-7.33 (1H, dt, *J* 7.8 and 1.64, Ar-H), 7.21-7.25 (2H, m, Ar-H), 7.15-7.17 (1H, d, *J* 8.4, Ar-H), 6.89-6.95 (3H, ap dq, 8.4, 7.6 and 7.4, Ar-H), 6.61 (1H, d, *J* 3.0, H1), 6.36 (2H, bs, O*H*), 6.06-6.08 (1H, dd, *J* 6.2and 3.0, H2'), 5.87-5.91 (1H, dd, *J* 7.4 and 6.2, H3'), 5.18 (2H, s, OCH_2), 5.17 (2H, s, $NHCH_2$), 4.47-4.50 (1H, dd, *J* 12.0 and 3.6, H5'), 4.32-4.36 (1H, ddd, *J* 7.4, 5.9 and 3.6, H4'), 4.18-4.22 (1H, dd, *J* 12.0 and 6.0, H5''), 2.07 (3H, s, $COCH_3$), 2.05 (3H, s, $COCH_3$), 1.88 (3H, s, $COCH_3$). ^{13}C NMR (100 MHz, CD_3CN); δ (ppm) 171.43 ($COCH_3$), 170.78 ($COCH_3$), 170.74 ($COCH_3$), 158.00 (C6), 156.67 (*C*OH), 156.40 (C2), 156.06 (C4), 151.12 (C8), 131.26 (OCH_2CCH), 130.86 ($OCH_2CCHCHCH$), 130.45 (OCH_2C), 129.85 ($NHCH_2CCHCHCH$), 124.19 (OCH_2CCHCH), 123.44 ($NHCH_2C$), 122.46 ($NHCH_2CCHCH$), 121.00 ($NHCH_2CCH$), 116.44 (COH*C*H), 115.95 (COH*C*H), 113.39 (C5), 89.95 (C1'), 80.23 (C2'), 73.58 (C3'), 70.94 (C4'), 67.25 (OCH_2), 63.59 (C5'), 39.89 ($NHCH_2$), 20.74 ($COCH_3$), 20.63 ($COCH_3$).

g-Glutamyl-*S*-(2-amino-6-oxo-9-pentofuranosyl-6,9-dihydro-1*H*-purin-8-yl)cysteinylglycine (22)

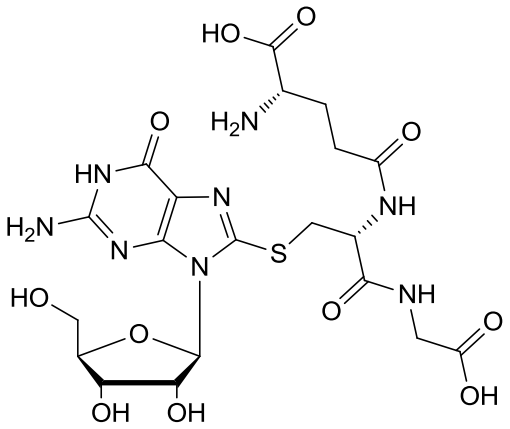

To a solution of 8-nitroguanosine (**15**, 10mg, 0.03mmol) in 0.1M (pH 9) TRIS HCl (5ml) heated to 37°C was added glutathione (46mg, 0.15mmol). The resulting mixture was allowed to stir for 1 hour during which time the reactions progress was monitored by RP-HPLC (Control method 0-50, page 140). Purification was carried out by RP-HPLC with the product eluting at 10.34 minutes. Removal of the solvent *in vacuo* gave the title compound as an off white solid (11mg, 61%). HRMS (ES^-) (m/z): 587.1511 ($[M-H]^-$); $C_{20}H_{27}N_8O_{11}S$ requires 587.1520 (-1.5328 ppm). λ_{max} (H_2O) 271nm. ^1H NMR (400 MHz, D_2O): δ (ppm) 5.86-5.88 (1H, d, *J* 6.8, H1'), 4.78-4.81 (1H, dd, *J* 6.6 and 5.9, H2'), 4.51-4.56 (1H, dd, *J* 8.8 and 4.3, SCH_2CH) 4.27-4.29 (1H, dd, *J* 5.6 and 2.9, H3'), 4.06-4.08 (1H, ddd, *J* 6.4, 3.5 and 3.1, H4'), 3.74-3.78 (1H, dd, *J* 12.7 and 2.9, H5'), 3.67-3.71 (1H, dd, *J* 12.7 and 3.9, H5''), 3.61-3.62 (1H, d, *J* 4.9, SCH_2CH), 3.57-3.58 (2H, d, *J* 4.3 $NHCH_2$), 3.49-3.52 (1H, t, *J* 6.3, $CHCH_2CH_2$) 3.21-3.26 (1H, dd, *J* 14.4 and 8.8, SCH_2CH), 2.28-2.32 (2H, t, *J* 7.6, $CHCH_2CH_2$), 1.87-1.93 (2H, dt, *J* 7.6 and 6.3, $CHCH_2CH_2$). ^{13}C NMR (100 MHz, D_2O): δ (ppm) 176.19 (CO), 174.81 (CO), 171.08 (CO), 155.61 (C6), 153.51 (C2)), 148.12 (C4), 144.52 (C8), 119.92 (C5), 88.83 (C1'), 85.81 (C4'), 71.83 (C2'), 70.61 (C3'), 61.88 (C5'), 54.19 (SCH_2CH), 52.97 ($CHNH_2$), 43.34 (CH_2COOH), 34.81 (SCH_2), 31.49 (CH_2CH_2CH), 26.16 (CH_2CH_2CH).

8-Bromo-2'-*O*-methylguanosine (23)

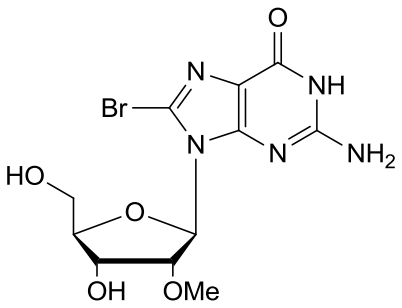

To a suspension of 2'-*O*-methylguanosine (0.50g, 1.68mmol) in H_2O (5ml) was added bromine water (10ml) with vigorous stirring for 2 hours. The mixture was filtered and washed with cold ^{i}PrOH before drying in a vacuum dessicator for 12 hours, to yield the product as a pale orange solid (0.55g, 84%). HRMS (ES^+) (m/z): 398.0073 and 400.0061 ($[M+Na]^+$); $C_{11}H_{14}N_5O_5NaBr$ requires 398.0076 and 400.0056 (-0.7538 and -1.2500 ppm). ^{1}H NMR (400 MHz, D_6-DMSO): δ (ppm) 10.86 (1H, s, N*H*), 6.55 (2H, s NH_2), 5.77 (1H, d, *J* 6.3, H1'), 4.76 (1H, ap t, *J* 5.83, H2'), 4.35 (1H, dd, *J* 5.2 and 3.7, H3'), 3.88 (1H, dd, *J* 8.8 and 5.2, H4'), 3.64-3.68 (1H, dd, *J* 11.8 and 5.1, H5'), 3.50-3.55 (1H, dd, *J* 11.8 and 5.7, H5''), 3.31 (3H, s, 2'OCH_3). ^{13}C NMR (100 MHz, DMSO): δ (ppm) 155.39 (C6), 153.53 (C2), 152.03 (C4), 120.71 (C5), 117.44 (C8), 87.60 (C1'), 86.22 (C4'), 79.38 (C2'), 68.85 (C3'), 61.79 (C5'), 57.53 (2'OCH_3).

g-Glutamyl-*S*-[2-amino-9-(2-*O*-methylpentafuranosyl)-6-oxo-6,9-dihydro-1*H*-purin-8-yl]cysteinylglycine (24)

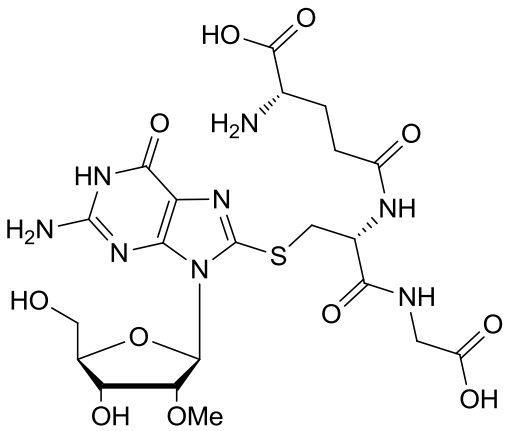

To a solution of 8-bromoguanosine (**23**, 30mg, 0.08mmol) in 0.1M TEAB (5ml) heated to 37°C was added glutathione (0.12g, 0.40mmol). The resulting mixture was allowed to stir for 22 hours during which time the reactions progress was monitored by RP-HPLC (Control method

0-22, page 140). Purification was carried out by RP-HPLC with the product eluting at 17.27 minutes. Removal of the solvent *in vacuo* yielded the title compound as a white solid (10mg, 21%). HRMS (ES^-) (m/z): 601.1683 ($[M-H]^-$); $C_{21}H_{29}N_8O_{11}S$ requires 601.1677 (+0.9981 ppm). ^1H NMR (400 MHz, D_2O): δ (ppm) 5.97-5.99 (1H, d, *J* 7.1, H1'), 4.44-4.51 (2H, m, H2' and SCH_2CH), 4.12-4.13 (1H, dd, *J* 4.6 and 2.5, H4'), 3.76-3.79 (1H, dd, *J* 12.9 and 2.3, H5'), 3.67-3.71 (1H, dd, *J* 12.9 and 2.8, H5''), 3.60-3.64 (1H, dd, *J* 10.8 and 3.8, H3'), 3.53-3.59 (3H, m, $NHCH_2$ and SCH_2), 3.15-3.23 (4H, m, 2'OCH_3 and CH_2CH_2CH), 3.08-3.14 (1H, ap q, *J* 7.2, SCH_2), 2.17-2.21 (2H, t, *J* 7.8, CH_2CH_2CH), 1.70-1.76 (2H, m, CH_2CH_2CH). ^{13}C NMR (100 MHz, D_2O): δ (ppm) 179.25 (CO), 176.19 (CO), 175.61 (CO), 171.28 (CO), 159.01 (C6), 158.83 (C2), 151.47 (C4), 142.18 (C8), 118.73 (C5), 87.42 (C1'), 86.81 (C4'), 80.85 (C2'), 69.41 (C3'), 62.13 (C5'), 58.08 (2'OCH_3), 55.04 (SCH_2CH), 53.32 ($CHNH_2$), 43.37 (CH_2COOH), 35.49 (SCH_2), 31.87 (CH_2CH_2CH), 29.10 (CH_2CH_2CH).

***N,N'*-(Disulfanediyldiethane-2,1-diyl)bis(3',6'-dihydroxy-3-oxo-3*H*-spiro[2-benzofuran-1,9'-xanthene]-5(6)-carboxamide) (25)[262] (Prepared as a mixture of the 3 isomers shown below)**

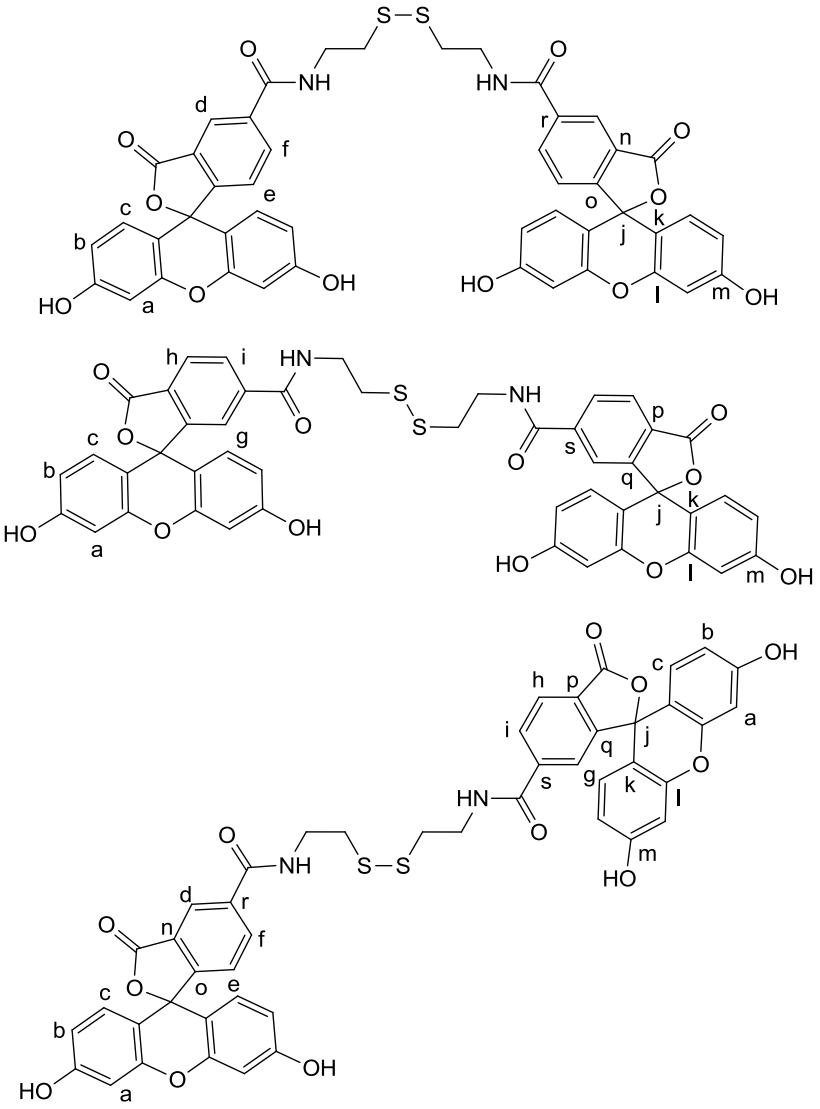

To a solution of 5(6)-carboxyfluorescein (0.20g, 0.53mmol), *N,N,N',N'*-tetramethyl-*O*-(1*H*-benzotriazol-1-yl)uronium hexafluorophosphate (0.34g, 0.88mmol), 1-hydroxybenzotriazole hydrate (0.6g, 0.44mmol) and diisopropylethylamine (0.15ml, 0.88mmol) in DMF (5ml) was added cystamine dihydrochloride (0.50g, 0.22mmol) and the solution was stirred at room temperature for 18 hours. The reaction mixture was concentrated and the crude residue was triturated with Et_2O and $CHCl_3$. Purification by flash column chromatography (R_f = 0.55 in 90% DCM, 8% MeOH, 2% AcOH) isolated the title compound as a mixture of isomers (81mg, 42%). HRMS (ES^+) (m/z): 891.1291 ($[M+Na]^+$); $C_{46}H_{32}N_2O_{12}S_2Na$ requires 891.1289 (-0.2244 ppm). ^1H NMR (400 MHz, D_6-DMSO) The number of hydrogens corresponding to each peak is not

given due to the compound being a mixture of 3 isomers: δ (ppm) 10.19 (br s, O*H*), 9.02-9.07 (m, N*H*), 8.87-8.91 (m, N*H*), 8.46-8.49 (m, g), 8.22-8.28 (m, f), 8.13-8.20 (m, h), 8.04-8.13 (m, d), 7.68-7.75 (m, i), 7.38-7.45 (m, e), 6.70 (m, a), 6.57-6.61 (m, b and c), 3.46-3.66 (m, NHCH_2), 2.83-3.16 (m, CH_2SH). ^{13}C NMR (100 MHz, DMSO): δ (ppm) 168.21 (CO), 168.06 (CO), 164.76 (CO), 164.63 (CO), 159.64 (Cm), 154.81 (Co), 152.73 (Cq), 151.85 (Cl), 140.43 (Cs), 136.00 (Cf), 134.72 (Cr), 129.44 (Cp) 129.32 (Cc) 129.24 (Cc), 128.33 (Ch), 126.53 (Cd), 124.98 (Ce), 124.36 (Cn), 123.29 (Cg), 122.25 (Ci), 112.78 (Cb), 112.71 (Cb), 109.14 (Ck), 109.07 (Ck), 102.28 (Ca), 83.32 (Cj), 53.61 (NH*C*H$_2$), 38.27 (*C*H$_2$S).

3',6'-Dihydroxy-3-oxo-*N*-(2-sulfanylethyl)-3*H*-spiro[2-benzofuran-1,9'-xanthene]-5(6)-carboxamide (26) (Prepared as a mixture of 2 isomers shown below)

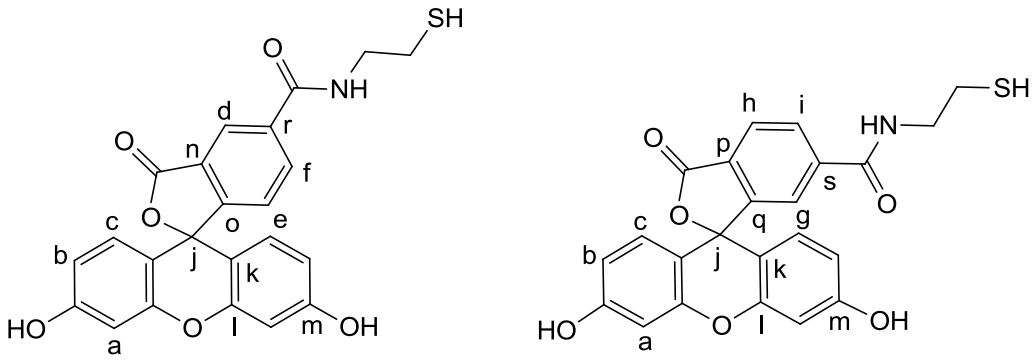

To a solution of *N,N'*-(disulfanediyldiethane-2,1-diyl)bis(3',6'-dihydroxy-3-oxo-3*H*-spiro[2-benzofuran-1,9'-xanthene]-5(6)-carboxamide) (**25**, 0.11g, 0.12mmol) in degassed MeOH (5ml) was added DL-dithiothreitol (0.11g, 0.73mmol) and the resulting solution was heated at 37°C for 24 hours. Flash column chromatography (1% MeOH, 99% DCM, 0.1% AcOH - 6% MeOH, 94% DCM, 0.1% AcOH) afforded the yellow product as mixture of isomers (0.81g, 77%). HRMS (ES$^+$) (m/z): 436.0849 ([M+H]$^+$); $C_{23}H_{18}NO_6S$ requires 436.0855 (-1.3759 ppm). ^{1}H NMR (400 MHz, D$_6$-DMSO): δ (ppm) 10.32 (4H, br s, 4 x O*H*), 8.45-8.48 (1H, d, *J* 11.9, g), 8.78-8.85 (1H, m, N*H*), 8.93-8.90 (1H, m, N*H*), 8.23-8.26 (1H, m, f), 8.14-8.21 (1H, m, h), 8.07-8.09 (1H, m, i), 7.67-7.70 (1H, m, d), 7.37-7.39 (1H, d, *J* 7.6, e), 6.56-6.69 (12H, m, 4 x a, 4 x b and 4 x c), 3.68-3.64 (1H, dd, *J* 12.1 and 6.2, NHCH_2), 3.57-3.62 (1H, dd, *J* 12.5 and 6.4, NHCH_2), 3.51-3.56 (1H, dd, *J* 12.9 and 6.4, NHCH_2), 3.45-3.50 (1H, dd, *J* 13.6 and 6.6, NHCH_2), 3.00-3.04 (1H, ap t, *J* 6.8, CH_2SH), 2.90-2.96 (1H, dd, *J* 13.3 and 6.5, CH_2SH), 2.83-2.86 (1H, ap t, *J* 6.7, CH_2SH), 2.71-2.78 (1H, m, CH_2SH) 1.24 (2H, br s, 2 x S*H*). ^{13}C NMR (100 MHz, DMSO): δ (ppm) 168.10 (CO), 164.68 (CO), 164.55 (CO), 161.58 (Cm), 151.96 (Co), 151.92 (Cl),

147.39 (Cq), 140.89 (Cs), 140.22 (Cf) 136.03 (Cr), 134.43 (Cp), 129.33 (Ch), 129.31 (Cc), 129.29 (Ce), 129.23 (Cd), 129.15 (Cn), 129.11 (Cg), 124.34 (Ci), 113.54 (Cb), 112.86 (Cb), 109.22 (Ck), 109.15 (Ck), 102.26 (Ca), 63.20 (Cj), 58.10 (Cj), 48.56 (CH_2CH_2SH), 42.87 (CH_2CH_2SH), 23.20 (CH_2SH), 22.89 (CH_2SH).

8-Nitro-2-*O*-methylguanosine (27)[194]

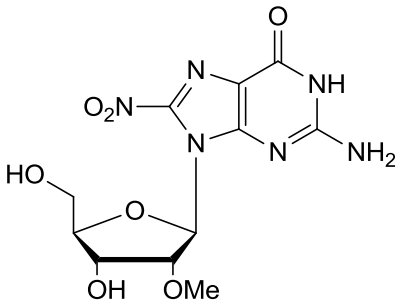

5'-*O,N2*-bis-dimethoxytrityl-8-nitro-2'-*O*-methylguanosine (**6**, 0.20g, 0.21mmol) was dissolved in $CHCl_3$ (3ml) before adding a solution of *p*TsOH (18mg, 0.11mmol) in MeOH (0.5ml). After 20 minutes the solvent was removed *in vacuo* leaving an orange solid which was triturated with Et_2O three times and EtOAc three times to afford the nucleoside as an orange solid (0.57mg, 79%). HRMS (ES^-) (m/z): 341.0847 ($[M-H]^-$); $C_{11}H_{13}N_6O_7$ requires 341.0846 (+0.2932 ppm). λ_{max} (H_2O) 233 and 408nm. ^1H NMR (400 MHz, D_6-DMSO): δ (ppm) 11.27 (1H, br s, N*H*), 7.02-7.20 (2H, br s, NH_2), 6.30-6.31 (1H, d, *J* 4.6, H1'), 4.86-5.19 (2H, br s, O*H*), 4.62-4.64 (1H, ap t, *J* 5.3, H2'), 4.36-4.39 (1H, ap t, *J* 5.9, H3'), 3.78-3.82 (1H, dd, *J* 10.1 and 6.1, H4'), 3.63-3.67 (1H, dd, *J* 11.9 and 3.9, H5'), 3.46-3.51 (1H, dd, *J* 11.9 and 6.4, H5''), 3.36 (3H, s, 2'OCH_3). ^{13}C NMR (100 MHz, DMSO): δ (ppm) 156.58 (C4), 155.55 (C6), 152.55 (C8), 143.28 (C2), 115.19 (C5), 88.87 (C1'), 85.61 (C4'), 80.57 (C2'), 69.21 (C3'), 61.67 (C5'), 57.97 (2'OCH_3).

8-[(2-{[(3',6'-dihydroxy-3-oxo-3*H*-spiro[2-benzofuran-1,9'-purin-6-one-xanthen]-5(6)-yl)carbonyl]amino}ethyl)sulfanyl]-2'-*O*-methylguanosine (28) (Prepared as a mixture of 2 isomers shown below)

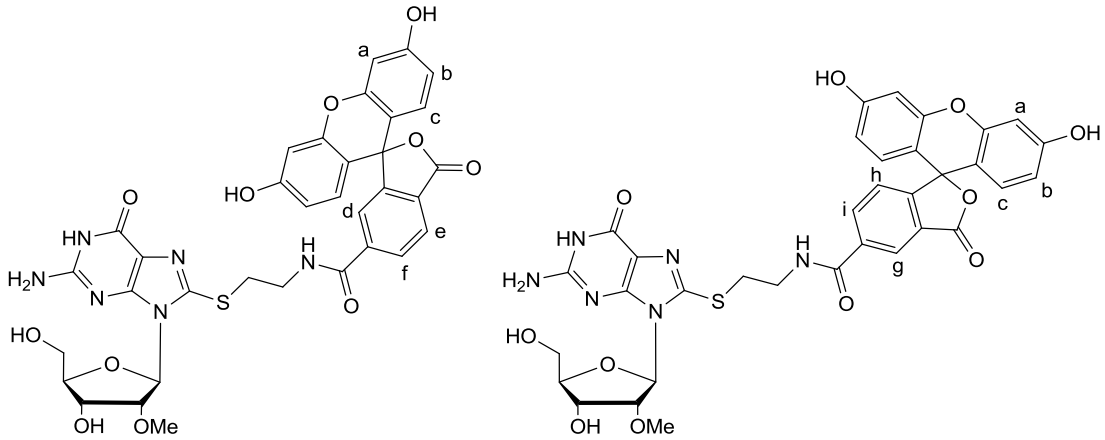

To a solution of 8-nitro-2'-*O*-methylguanosine (**27**, 12mg, 0.034mmol) in 0.1M TEAB was added 3',6'-dihydroxy-3-oxo-*N*-(2-sulfanylethyl)-3*H*-spiro[2-benzofuran-1,9'-xanthene]-5(6)-carboxamide (**26**, 22mg, 0.050mmol). The reaction mixture was stirred at 37°C for 2 hours. The reaction progress was monitored by RP-HPLC (Control method 0-65, page 140) with the product eluting at 14.04 minutes. Purification by flash column chromatography (15% MeOH, 85% DCM) gave the title compound as a bright yellow solid as a mixture of isomers (11mg, 45%). HRMS (ES^-) (m/z): 729.1636 ($[M-H]^-$); $C_{34}H_{29}N_6O_{11}S$ requires 729.1615 (+2.8800 ppm). ^1H NMR (500 MHz, D_2O): δ (ppm) 7.96 (1H, d, *J* 1.9, Hi), 7.95 (1H, d, *J* 1.7, Hf), 7.93 (1H, s, d), 7.91 (1H, s, g), 7.18 (1H, s, c), 7.16 (1H, s, c), 7.11-7.12 (2H, m, e and h), 7.09 (1H, s, c), 7.07 (1H, s, c), 6.87-6.89 (4H, m, a), 8.61-6.82 (1H, d, *J* 2.3, b), 6.79-6.80 (1H, d, *J* 2.3, b), 6.77-6.78 (1H, d, *J* 2.1, b), 6.74-6.75 (1H, d, *J* 2.1, b), 5.84-5.86 (2H, d, *J* 6.1, H1'), 4.51-4.53 (2H, ap t, *J* 4.8, H3'), 4.31-4.34 (2H, ap t, *J* 5.9, H2'), 4.04-4.07 (2H, dd, *J* 7.6 and 4.0, H4'), 3.87-3.92 (2H, m, H5'), 3.77-3.80 (2H, m, H5''), 3.70-3.72 (4H, m, C*H*$_2$S), 3.22 (6H, s, 2'OC*H*$_3$), 2.96-3.02 (4H, m, C*H*$_2$CH$_2$S).

Diethyl *N,N'*-bis(*tert*-butoxycarbonyl)cystinate (29)[268]

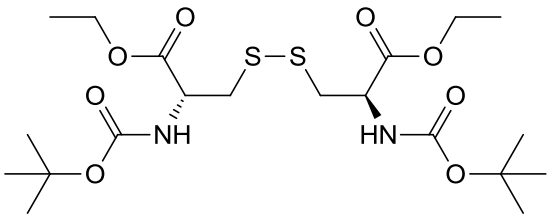

To a solution of *N,N'*-bis(*tert*-butoxycarbonyl)cystine (0.50g, 1.13mmol) in DCM (5ml) was added DMAP (25mg, 0.23mmol) and EtOH (0.38ml). The solution was allowed to stir for 10 minutes before addition of *N,N'*-dicyclohexylcarbodiimide (0.70g, 3.40mmol) over 30 minutes. The reaction was monitored by TLC and upon completion the solid precipitate was removed by filtration and the solvent removed *in vacuo*. Purification by flash column chromatography (70% Hexane, 30% EtOAc) isolated the title compound as a white solid (0.45g, 80%). R_f = 0.49 (70% EtOAc, 30% DCM). HRMS (ES^+) (m/z): 519.1807 ($[M+Na]^+$); $C_{20}H_{36}N_2O_8S_2Na$ requires 519.1811 (-0.7704 ppm). ^1H NMR (400 MHz, $CDCl_3$): δ (ppm) 5.39-5.41 (2H, d, *J* 6.6, N*H*), 4.56-4.58 (2H, dd, *J* 6.7 and 5.9, NHC*H*CH_2), 4.21-4.26 (2H, q, *J* 7.1, C*H*$_2$$CH_3$), 4.20-4.25 (2H, q, *J* 7.1, C*H*$_2$$CH_3$), 3.17-3.18 (4H, d, *J* 3.1, SC*H*$_2$), 1.45 (18H, s, 2 x C(C*H*$_3$)$_3$), 1.28-1.32 (6H, t, *J* 7.1, 2 x C*H*$_3$). ^{13}C NMR (100 MHz, $CDCl_3$): δ (ppm) 170.64 (*C*O), 155.06 (CO), 80.19 (*C*$(CH_3)_3$), 61.84 (O*C*H_2), 53.01 (*C*HCH_2), 41.46 (*C*H_2S), 28.30 (C(*C*H_3)*3*), 14.11 (CH_2*C*H_3).

Ethyl *N*-(*tert*-butoxycarbonyl)cysteinate (30)

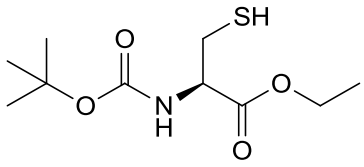

To a stirred solution of diethyl *N,N'*-bis(*tert*-butoxycarbonyl)cystinate (**29**, 0.18g, 0.36mmol) in degassed MeOH (5ml) was added DL-dithiothreitol (82mg, 1.42mmol) and the resulting mixture was heated to reflux for 18 hours. The progress of the reaction was monitored by TLC (30% EtOAc, 70% Hexane), using $KMnO_4$ in order to visualise the product, and upon completion the solvent was removed *in vacuo*. Purification by flash column chromatography (10% EtOAc, 90% Hexane) gave the title compound as a white solid (0.13g, 73%). R_f = 0.74 (70% EtOAc, 30% Hexane). HRMS (ES^+) (m/z): 272.0929 ($[M+Na]^+$); $C_{10}H_{19}NO_4SNa$ requires 272.0932 (-1.1026 ppm). ^1H NMR (400 MHz, $CDCl_3$): δ (ppm) 5.43-5.45 (1H, d, *J* 6.61, N*H*), 4.57-4.60 (1H, dt, *J* 7.6 and 3.8, C*H*CH_2SH), 4.22-4.28 (1H, dq, *J* 7.2 and 4.6, C*H*$_2$$CH_3$), 4.22-4.28 (1H, dq, *J* 10.8 and 7.2, C*H*$_2$$CH_3$), 4.21-4.27 (1H, dq, *J* 10.8 and 7.1, C*H*$_2$$CH_3$), 2.97-3.01 (2H, dd, 8.7 and 4.3, CHC*H*$_2$SH), 1.46 (9H, s, C(C*H*$_3$)$_3$), 1.37-1.41 (1H, t, *J* 8.9, S*H*), 1.29-1.32 (3H, t, *J* 7.1, CH_2C*H*$_3$). ^{13}C NMR (100 MHz, $CDCl_3$): δ (ppm) 170.42 (CO), 155.26 (CO), 80.33 (*C*$(CH_3)_3$), 61.99 (O*C*H_2), 54.93 (*C*HCH_2), 28.41 (C(*C*H_3)$_3$), 27.49 (*C*H_2S), 14.34 (CH_2*C*H_3).

Ethyl *S*-(guanosine)-*N*-(*tert*-butoxycarbonyl)cysteinate (31)

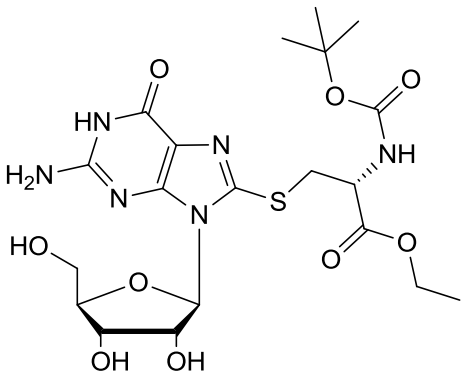

To a solution of 8-nitroguanosine (**15**, 30mg, 0.09mmol) in 0.1M TEAB (4ml) was added ethyl *N*-(*tert*-butoxycarbonyl)cysteinate (**30**, 34mg, 0.14mmol). The reaction mixture was stirred at 37°C for 4 hours. The reaction progress was monitored by TLC and upon completion the solvent was removed *in vacuo.* Purification by flash column chromatography (5% MeOH, 95% DCM) gave the title compound as a yellow solid (33mg, 69%). HRMS (ES^+) (m/z): 553.1711 ($[M+Na]^+$); $C_{20}H_0N_6O_9SNa$ requires 553.1693 (+3.2540 ppm). ^1H NMR (500 MHz, D_6-DMSO): δ (ppm) 13.26 (1H, br s, N*H*), 8.87-8.89 (1H, d, *J* 10.3, N*H*CH), 7.70 (2H, br s, NH_2), 6.53-6.55 (1H, d, *J* 8.2, H1'), 6.18-6.19 (1H, d, *J* 7.21, 2'O*H*), 5.83 (1H, br s, 3'O*H*), 5.68-5.70 (1H, ap t, *J* 6.3, 4'O*H*), 5.52-5.53 (1H, dd, *J* 7.5 and 6.8, H2'), 4.74-4.81 (1H, dt, *J* 10.6 and 6.2, C*H*CH_2S), 4.54-4.60 (3H, m, H3' and CH_2CH_3), 4.20-4.24 (1H, dd, *J* 10.3 and 5.9, H4'), 3.92-4.00 (2H, m, H5' and CH_2S), 3.77-3.84 (1H, dd, *J* 15.1 and 7.4, H5''), 3.50-3.54 (1H, m, CH_2S), 1.05 (9H, s, C(CH_3)$_3$), 0.78-0.83 (3H, t, *J* 9.1, CH_2CH_3). ^{13}C NMR (125 MHz, DMSO): δ (ppm) 170.84 (*C*OOCH_2CH_3), 155.80 (O*C*ONH), 155.49 (C6), 153.42 (C1), 152.76 (C4), 142.57 (C8), 117.36 (C5), 88.49 (C1'), 85.95 (C4'), 78.76 (*C*$(CH_3)_3$), 70.85 (C3'), 70.78 (C2'), 62.26 (C5'), 61.11 (CH_2CH_3), 53.35 (C*H*CH_2S), 33.61 (CH_2S), 28.32 (C(CH_3)$_3$), 14.25 (CH_3).

Ethyl *S*-(2'-*O*-methylguanosine)-*N*-(*tert*-butoxycarbonyl)cysteinate (32)

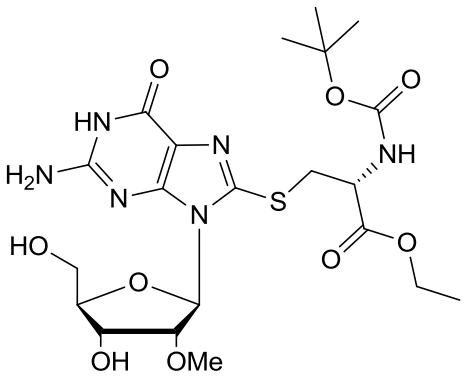

To a solution of 8-nitro-2'-*O*-methylguanosine (**27**, 36mg, 0.11mmol) in 0.1M TEAB (4ml) was added ethyl *N*-(*tert*-butoxycarbonyl)cysteinate (**30**, 32mg, 0.13mmol). The reaction mixture was stirred at 37°C for 2 hours. The reaction progress was monitored by TLC (8% MeOH, 92% DCM) and upon completion the solvent was removed *in vacuo*. Purification by flash column chromatography (6% MeOH, 94% DCM) gave the title compound as a pale yellow solid (41mg, 72%). HRMS (ES^+) (m/z): 567.1848 ($[M+Na]^+$); $C_{21}H_{32}N_6O_9SNa$ requires 567.1849 (-0.1763 ppm). λ_{max} (H_2O) 275nm. ^1H NMR (400 MHz, D_4-MeOD): δ (ppm) 6.04-6.06 (1H, d, *J* 6.39, H1'), 4.66-4.69 (1H, ap t, *J* 5.8, H2'), 4.53-4.55 (1H, dd, *J* 5.1 and 3.0, H3'), 4.42-4.45 (1H, dd, *J* 7.6 and 4.6, SCH_2CH), 4.16-4.21 (2H, q, *J* 7.1, OCH_2CH_3), 4.10-4.12 (1H, dd, *J* 3.2, H4'), 3.86-3.90 (1H, dd, *J* 12,3 and 3.0, H5'), 3.75-3.79 (1H, dd, *J* 12.3 and 3.8, H5''), 3.70-3.75 (1H, dd, *J* 13.9 and 4.5, SCH_2), 3.44-3.50 (1H, dd, *J* 14.2 and 8.3, SCH_2), 3.43 (3H, s, $2'OCH_3$), 1.40 (9H, s, $C(CH_3)_3$), 1.26-1.30 (3H, t, *J* 7.1, OCH_2CH_3). ^{13}C NMR (100 MHz, MeOD): 170.47 (*C*OOEt), 156.94 (*C*OO^tBu), 156.04 (C6), 153.44 (C2), 152.26 (C4), 143.95 (C8),117.66 (C5), 87.87 (C3'), 86.71 (C1'), 81.05 (C2'), 79.33 ($C(CH_3)_3$), 69.61 (C4'), 62.36 (C5'), 61.36 (OCH_2CH_3), 57.41 ($2'OCH_3$), 53.69 (SCH_2CH),35.11 (SCH_2),27.24 ($C(CH_3)_3$), 13.05 (OCH_2CH_3).

8-Oxo-2'-*O*-methylguanosine (33)[272]

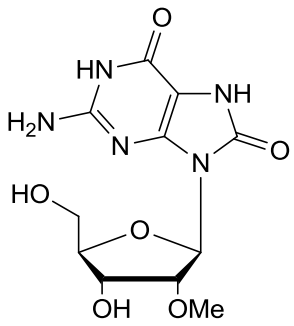

Sodium benzylate was prepared by addition of sodium (6mg) to a stirred freshly distilled benzyl alcohol (0.21ml, 17.25mmol) at 60°C in an inert atmosphere until the solution was homogeneous. To the solution was added anhydrous DMSO (1ml) and 8-bromo-2'-*O*-methylguanosine (**23**, 60mg, 0.16mmol) in anhydrous DMSO (1.5ml) and the mixture was heated at 65°C for 18 hours and then cooled to room temperature. The solvent was removed *in vacuo* and the crude residue was purified by flash column chromatography (10% MeOH, 90% DCM, 0.01% Et_3N) to give 8-benzyloxy-2'-*O*-methlguanosine. The white solid (30mg) dissolved in MeOH (3ml) was treated with 1M HCl (0.3ml) and allowed to stir for 1 hour. Removal of the solvents *in vacuo* followed by trituration of the residue with $CHCl_3$/EtOAc afforded the title compound as a pale yellow solid (21mg, 42%). HRMS (ES^+) (m/z): 336.0922 ($[M+Na]^+$); $C_{11}H_{15}N_5O_6Na$ requires 336.0920 (+0.5951 ppm). λ_{max} (H_2O) 248 and 290nm. ^1H NMR (400 MHz, D_4-MeOD): δ (ppm) 5.89-5.90 (1H, d, *J* 5.7, H1'), 4.56-4.59 (1H, ap t, *J* 5.4, H2'), 4.50-4.52 (1H, dd, *J* 5.2 and 3.7, H3'), 4.01-4.04 (1H, ap q, *J* 3.6, H4'), 3.82-3.86 (1H, dd, *J* 12.2 and 2.8, H5'), 3.70-3.73 (1H, dd, *J* 12.2 and 3.9, H5''), 3.45 (3H, s, 2'OC*H*$_3$). ^{13}C NMR (100 MHz, MeOD): δ (ppm) 153.47 (C4), 152.50 (C6), 152.30 (C8), 147.47 (C4), 99.46 (C5), 85.66 (C1'), 84.79 (C2'), 80.69 (C3'), 69.76 (C4'), 62.36 (C5'), 57.28 (2'O*C*H_3).

7.3.1 Oligodeoxynucleotide Reactions

Site 1, adduct 1

GCGTACG$^{(glut)}$CATGCG

To a solution of the site 1 oligodeoxynucleotide (3.1 OD units) dissolved in distilled H_2O (100µl) was added 1M TRIS.HCl (10µl) and 0.26M glutathione (15µl). The resulting mixture was stirred at 37°C for 18 hours during which time the solution changed from yellow to

colourless. Monitoring the progress of the reaction and purification of product was carried out by RP-HPLC. The composition of the eluent was controlled by the control method 0-65 as shown in Figure 7.3 (page 140). Eluted compounds were detected by UV absorbance at both 254 and 350nm.

Site 1, adduct 2

GCGTACG$^{(fluor)}$CATGCG

To a solution of the site 1 oligodeoxynucleotide (3.1 OD units) dissolved in distilled H_2O (100µl) was added 1M TRIS.HCl (10µl) and 3',6'-dihydroxy-3-oxo-*N*-(2-sulfanylethyl)-3*H*-spiro[2-benzofuran-1,9'-xanthene]-5(6)-carboxamide (**26**, 1.7mg). The resulting mixture was stirred at 37°C for 24 hours during which time the progress of the reaction was monitored by RP-HPLC. Purification of the product by RP-HPLC using control method 0-65 (page 140) afforded the title compound.

Site 1, adduct 3

GCGTACG$^{(Pro\text{-}Cys)}$CATGCG

To a solution of the site 1 oligodeoxynucleotide (3.1 OD units) dissolved in distilled H_2O (100µl) was added 1M TRIS.HCl (10µl) and ethyl *N*-(*tert*-butoxycarbonyl)cysteinate (**30**, 0.80mg, 100eq). The resulting mixture was stirred at 37°C for 6 hours during which time the progress of the reaction was monitored by RP-HPLC. Purification by RP-HPLC using control method 0-65 (page 140) afforded the title compound.

Site 2, adduct 3

5'-d(GCGCAACGCAATTAATGTG$^{(Pro\text{-}Cys)}$AGTTAGCTCACTCATTAG)-3'

To a solution of the site 2 oligodeoxynucleotide (5.0 OD units) dissolved in distilled H_2O (100µl) was added 1M TRIS.HCl (10µl) and ethyl *N*-(*tert*-butoxycarbonyl)cysteinate (**30**, 0.34mg, 100eq). The resulting mixture was stirred at 37°C for 11 hours during which time the

progress of the reaction was monitored by RP-HPLC. Purification by RP-HPLC using control method 0-65 (page 140) afforded the title compound.

Site 3, adduct 3

5'-d(GTGACTGGG$^{(Pro\text{-}Cys)}$AAAACCCTGGCGTTACCC)-3'

To a solution the site 3 oligodeoxynucleotide (2.9 OD units) dissolved in distilled H_2O (100µl) was added 1M TRIS.HCl (10µl) and ethyl *N*-(*tert*-butoxycarbonyl)cysteinate (**30**, 0.28mg, 100eq). The resulting mixture was stirred at 37°C for 11 hours during which time the progress of the reaction was monitored by RP-HPLC. Purification by RP-HPLC using control method 0-65 (page 140) afforded the title compound.

7.3.2 Oligonucleotide reactions characterization

The RP-HPLC analysis obtained for all oligodeoxynucleotide reactions is shown in Table 7.9

		HPLC analysis (Control method 0-65)	
Oligodeoxynucleotide reactions		**Retention time (minutes)**	
Starting material	**Product**	**Starting Material**	**Product**
Site 1	Site 1, adduct 1	12.32	11.46
Site 1	Site 1, adduct 2	11.55	18.63
Site 1	Site 1, adduct 3	12.55	14.78
Site 2	Site 2, adduct 3	12.52	13.74
Site 3	Site 3, adduct 3	12.82	14.13

Table 7.9: HPLC retention times corresponding to the starting materials and products from all oligodeoxynucleotide reactions.

The UV analysis obtained for the purified oligodeoxynucleotide reaction products is shown in Table 7.10.

	UV analysis		
Product	**OD_{260} units**	**ε (260nm)**	**Conc. in 1ml H_2O (μM)**
Site 1, adduct 1	0.057	122100	0.47
Site 1, adduct 2	0.022	122100	0.18
Site 1, adduct 3	2.79	122100	22.05
Site 2, adduct 3	0.67	361200	1.82
Site 3, adduct 3	1.06	254400	4.17

Table 7.10: Data obtained from UV analysis of the oligodeoxynucleotide reaction products.

Table 7.11 shows the theoretical and experimental molecular weights recorded for all of the oligodeoxynucleotide reaction products

	Mass spectrometry analysis		
Product	**Charge**	**Theoretical mass**	**Experimental mass**
Site 1, adduct 1	-3	1435.9145	1435.8939
Site 1, adduct 2	-6	738.7889	738.7769
Site 1, adduct 3	-3	1416.5937	1416.5312
Site 2, adduct 3	nd	nd	nd
Site 3, adduct 3	nd	nd	nd

Table 7.11: Theoretical and experimental molecular weights for all of the products of the oligodeoxynucleotide reactions. Note nd = not determined.

The $[M-nH]^{n-}$ peaks were then used to give experimental average masses for the parent ions of each oligodeoxynucleotide product.

	Average molecular weight (Parent ion)		
Product	**Theoretical mass**	**Experimental mass**	**Error (ppm)**
Site 1, adduct 1	4310.7670	4310.7052	-14.3047
Site 1, adduct 2	4438.7810	4438.7090	-16.1618
Site 1, adduct 3	4250.7996	4250.6850	-44.1360
Site 2, adduct 3	nd	nd	nd
Site 3, adduct 3	nd	nd	nd

Table 7.12: Theoretical and experimental average molecular weights corresponding to the parent free acid of each oligodeoxynucleotide product. Note nd = not determined.

7.3.3 Enzymatic digestion

The site 1 oligodeoxynucleotide (1 OD unit), phosphodiesterase I from *Crotalus atrox* (10mg, 0.1U) and aqueous bovine intestinal alkaline phosphatase (2 µl, 40 U) were dissolved in 0.1 M TRIS.HCl pH 8.5 (100 µl total volume) and incubated at 37°C for 2 hours. The mixture was diluted with water (100 µl) and the protein precipitated with ice cold ethanol (100 µl) prior to centrifugation. The supernatant was concentrated *in vacuo* and dissolved in 0.1 M TEAB (100 µl) prior to analysis by RP-HPLC.

7.4 Experimental procedures for results and discussion 4

General method for the Yoshikawa phosphorylation[302]

The pre-dried nucleoside (0.22mmol) was placed in a dried 2-neck flask, and dissolved in trimethylphosphate (2.0 mL). The solution was cooled to 0°C before dropwise addition of $POCl_3$ (30 microlitres, 0.33 mmol). The reaction mixture was stirred for 90 minutes during which time the progress was monitored by IE-HPLC (Control method IE 0-100, page 142). A suspension of tri-*N*-butylammonium pyrophosphate in anhydrous DMF (0.5M, 2ml) and tributylamine (0.16 mL) was added. After 40 min, the reaction mixture was combined with TEAB (0.1M, 20 mL). The composition of the reaction mixture was then analysed by IE-HPLC (Table 7.13 and 7.14).

Compound	Retention time (minutes)	Conversion (%)
Guanosine monophosphate (**34**)	4.71	68
8-Bromoguanosine monophosphate (**38**)	5.37	43
8-Nitroguanosine monophosphate (**40**)	4.17	50

Table 7.13: Showing the nucleoside monophosphates prepared together with their retention times and percentage conversions as determined by HPLC.

Compound	Retention time (minutes)	Conversion (%)
Guanosine triphosphate (**35**)	10.88	40
8-Bromoguanosine triphosphate (**39**)	11.15	23

Table 7.14: Showing the nucleoside triphosphates prepared together with their retention times and percentage conversions as determined by HPLC.

N2-Dimethoxytrityl-8-nitroguanosine (36)

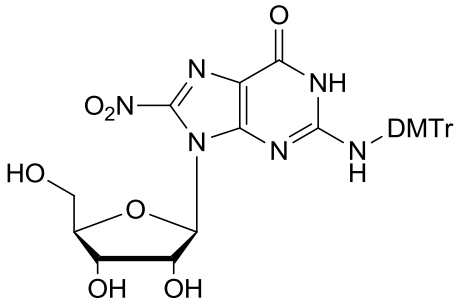

N2-Dimethoxytrityl-8-nitro-2',3',5'-tri-*O*-acetylguanosine (**13**, 0.37g, 0.5mmol) was dissolved in NH_3 (7M) in MeOH (5ml) and the solution was stirred in a sealed vessel for 36 hours. The

reaction mixture was then concentrated *in vacuo*. Purification by flash column chromatography (30% EtOAc, 70% DCM - 60% EtOAc, 40% DCM) gave the desired product as a yellow solid (0.20g, 65%). HRMS (ES$^+$) (m/z): 653.1956 ([M+Na]$^+$); $C_{31}H_{30}N_6O_9Na$ requires 653.1972 (-2.4495 ppm). ^{1}H NMR (400 MHz, D_6-DMSO): δ (ppm) 7.17-7.32 (9H, m, DMT Ar-H), 6.84-6.86 (4H, m, DMT C*H*COCH$_3$), 5.94-5.95 (1H, d, *J* 5.0, H1'), 3.99-4.03 (1H, dd, *J* 6.3 and 5.1, H2'), 3.76 (6H, s, Ar-OC*H*$_3$), 3.64-3.69 (1H, *J* 10.5, 6.6 and 4.6, H4'), 3.51-3.54 (1H, ap t, *J* 6.1, H3'), 3.25-3.31 (2H, m, H5'). ^{13}C NMR (100 MHz, DMSO): δ (ppm) 160.14 (Ar-C), 158.94 (C4), 154.33 (C6), 152.20 (C8), 146.00 (C2), 145.74 (Ar-C), 137.76 (Ar-C), 137.57 (Ar-C), 131.10 (Ar-C), 131.06 (Ar-C), 129.75 (Ar-C), 129.15 (Ar-C), 128.26 (Ar-C), 116.17 (C5), 114.41 (Ar-C), 91.99 (C1'), 86.10 (C4'), 72.03 (NH*C*), 71.15 (C2'), 70.99 (C3'), 63.73 (C5'), 55.75 (Ar-C).

8-Bromoguanosine (37)

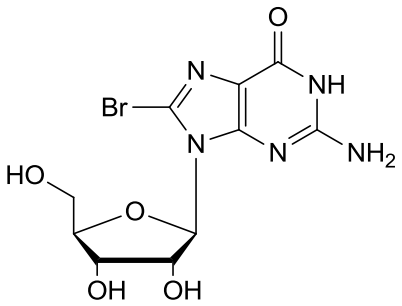

To a solution of guanosine (5.00g, 17.65mmol) suspended in distilled H_2O (30ml) was added aliquots of saturated bromine water (ca. 60ml) with vigorous stirring. Once the solution was permanently yellow, the mixture was filtered and washed with cold ^{i}PrOH, before drying in a vacuum dessicator for 12 hours, to yield the product as a pale orange solid (6.39g, 77%). HRMS (ES$^+$) (m/z): 383.9924 and 385.9915 ([M+Na]$^+$); $C_{10}H_{12}N_5O_5NaBr$ requires 383.9919 and 385.9899 (+1.3021 and +4.1452 ppm). ^{1}H NMR (400MHz, D_6-DMSO): δ (ppm) 10.84 (1H, s, N*H*), 6.52 (2H, br s, N*H*$_2$), 5.68-5.70 (1H, d, *J* 6.4, H1'), 5.48-5.45 (1H, d, *J* 6.2, 2'O*H*), 5.11-5.13 (1H, d, *J* 5.2, 3'O*H*), 4.99-5.04 (1H, dd, *J* 11.9 and 6.1, H2'), 4.93-4.96 (1H, dd ,*J* 6.4 and 5.7, 5'O*H*), 4.12-4.16 (1H, ddd, *J* 8.6, 5.1 and 3.6, H3'), 3.84-3.88 (1H, ddd, *J* 8.6, 5.2 and 3.9, H4'), 3.63-3.69 (1H, ddd, *J* 11.8, 5.2 and 4.9 H5'), 3.49-3.55 (1H, ddd, *J* 12.0, 6.0 and 5.8, H5''). ^{13}C NMR (100 MHz, DMSO): δ (ppm) 154.86 (C6), 153.66 (C2), 151.94 (C4), 121.55 (C5), 117.63 (C8), 90.02 (C1'), 86.22 (C4'), 70.87 (C3'), 70.65 (C2'), 62.36 (C5').

5'-*tert*-Butyldimethylsilylguanosine (41)

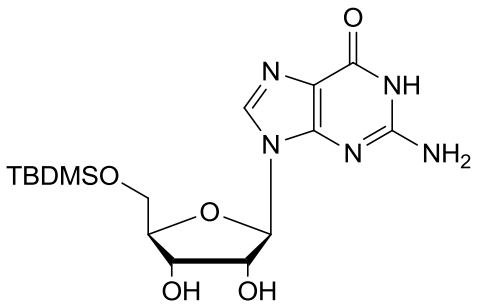

To a stirred solution of guanosine (5.00g, 17.7mmol) in anhydrous DMF (50ml) was added imidazole (2.40g, 35.3mmol) and TBDMSCl (5.32g, 35.3mmol). The reaction was stirred at room temperature under an atmosphere of N_2 for 18 hours before being cooled to 0°C and quenched with ice cold H_2O. The resulting precipitate was then filtered and washed with H_2O (50ml) and acetone (50ml) to afford the title compound as a white solid (4.98g, 71%). HRMS (ES^+) (m/z): 420.1680 ($[M+Na]^+$); $C_{16}H_{27}N_5O_5SiNa$ requires 420.1679 (+0.2380 ppm). ^1H NMR (400 MHz, D_6-DMSO): δ (ppm) 10.66 (1H, br s, N*H*), 7.85 (1H, s, H8), 6.51 (2H, br s, NH_2), 5.70-5.71 (1H, d, *J* 5.4, H1'), 5.49-5.50 (1H, d, *J* 5.7, 2'OH), 5.17-5.19 (1H, d, *J* 4.8, 3'OH), 4.31-4.35 (1H, dd, *J* 10.4 and 5.3, H2'), 4.07-4.11 (1H, dd, *J* 8.7 and 4.4, H3'), 3.88-3.90 (1H, dd, *J* 7.8 and 3.9, H4'), 3.78-3.82 (1H ,dd, *J* 11.4 and 3.7, H5'), 3.69-3.73 (1H, dd, *J* 11.4 and 4.1, H5''), 0.87 (9H, s, C(CH_3)$_3$), 0.04 (6H, s, Si(CH_3)$_2$). ^{13}C NMR (100 MHz, DMSO): δ (ppm) 156.77 (C6), 153.76 (C2), 151.38 (C4), 134.91 (C8), 116.57 (C5), 86.72 (C1'), 84.33 (C4'), 73.85 (C2'), 69.99 (C3'), 63.03 (C5'), 25.87 (C(*C*H_3)$_3$), 18.08 (*C*(CH_3)$_3$), -5.39 (Si*C*H_3), -5.44 (Si*C*H_3).

5'-*tert*-butyldimethylsilyl-2'-3'-di-*O*-acetylguanosine (42)

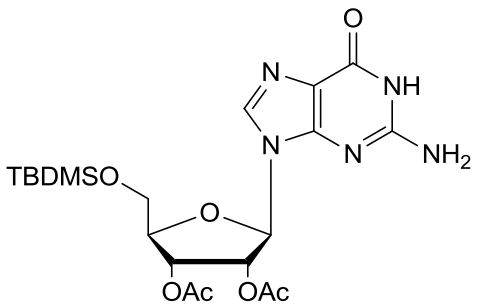

Acetic anhydride (2.08ml, 22.0mmol) was added dropwise to an ice cooled mixture of 5'-*tert*-butyldimethylsilylguanosine (**41**, 4.39g, 11.0mmol), triethylamine (6.16ml, 44.2mmol) and

DMAP (0.135g, 1.10mmol) in MeCN (50ml). The reaction mixture was then allowed to warm to room temperature. There was complete solubilisation when the reaction had gone to completion. The reaction was quenched with MeOH and the solvent removed *in vacuo*. The residue was then re-dissolved in DCM (50ml) and washed with H_2O (3 x 50ml) before drying over $MgSO_4$, filtering and concentrated to yield the product as a white solid (5.02g, 94%). HRMS (ES^+) (m/z): 504.1907 ($[M+Na]^+$); $C_{20}H_{31}N_5O_7SiNa$ requires 504.1890 (+3.3718 ppm). ^1H NMR (400 MHz, D_6-DMSO): δ (ppm) 10.74 (1H, br s, N*H*), 7.84 (1H, s, H8), 6.58 (2H, br s, NH_2), 5.97-5.99 (1H, d, *J* 7.1, H1'), 5.66-5.69 (1H, dd, *J* 7.1 and 5.5, H2'), 5.40-5.42 (1H, dd, *J* 5.4 and 2.6, H3'), 4.20-4.21 (1H, dd, *J* 6.2 and 3.4, H4'), 3.83-3.85 (2H, m, H5'), 2.11 (3H, s, COCH_3), 2.00 (3H, s, COCH_3), 0.88 (9H, s, C(CH_3)$_3$), 0.07 (6H, s, Si(CH_3)$_2$). ^{13}C NMR (100 MHz, DMSO): δ (ppm) 169.52 (CO), 169.27 (CO), 156.66 (C6), 154.06 (C2), 151.36 (C4), 134.38 (C8), 116.56 (C5), 83.38 (C1'), 82.87 (C4'), 72.25 (C2'), 70.94 (C3'), 62.90 (C5'), 25.76 (C(*C*H_3)$_3$), 20.47 (COCH$_3$), 20.18 (CO*C*H$_3$), 17.98 (*C*(CH$_3$)$_3$), -5.53 (Si*C*H$_3$), -5.58 (Si*C*H$_3$).

5'-*tert*-Butyldimethylsilyl-8-bromoguanosine (43)

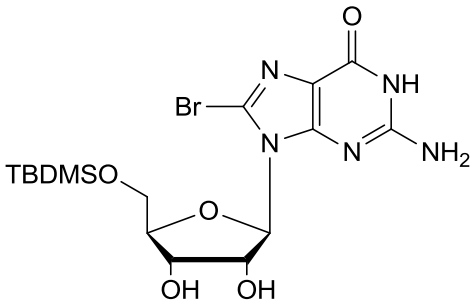

To a solution of 8-bromoguanosine (**37**, 10.80g, 29.8mmol) in anhydrous DMF (60ml) was added imidazole (4.06g, 59.6mmol) and TBDMSCl (8.98g, 59.6mmol). The reaction was stirred at room temperature under an atmosphere of N_2 until the reaction reached completion (18 hours) before being cooled to 0°C and quenched with ice cold H_2O. The resulting precipitate was then washed with H_2O (100ml) and acetone (100ml) to afford the title compound as a pale orange solid (11.79g, 83%). HRMS (ES^+) (m/z): 498.0786 and 500.0768 ($[M+Na]^+$); $C_{16}H_{26}N_5O_5NaSiBr$ requires 498.0784 and 500.0764 (+0.4015 and +0.7999 ppm). ^1H NMR (400 MHz, D_6-DMSO): δ (ppm) 10.83 (1H, s, N*H*), 6.56 (2H, br s, NH_2), 5.70-5.71(1H, d, *J* 5.7, H1), 5.53 (1H, d, *J* 5.9, 2'O*H*), 5.08-5.10 (1H, d, *J* 5.8, 3'O*H*), 5.06-5.08 (1H, dd, *J* 5.7, H2') 4.24 (1H, dd, *J* 9.8 and 5.1, H4'), 3.81-3.86 (2H, m, H4' and H5'), 3.71-3.76 (1H, dd, *J* 12.4 and 7.7, H5''), 0.84 (9H, s, SiC(CH_3)$_3$), 0.00 (3H, s, SiCH_3), -0.01 (3H, s, SiCH_3). ^{13}C NMR (100

MHz, DMSO): δ (ppm) 155.86 (C6), 153.84 (C2), 152.65 (C4), 121.24 (C8), 117.16 (C5), 90.17 (C1'), 85.25 (C4'), 70.57 (C2'), 70.31 (C3'), 63.77 (C5'), 26.14 (Si*C*$(CH_3)_3$), 18.34 (SiC(*C*$H_3)_3$), -4.96 (Si*C*H_3), -5.01 (Si*C*H_3).

5'-*tert*-Butyldimethylsilyl-2'-3'-di-*O*-acetyl-8-bromoguanosine (44)

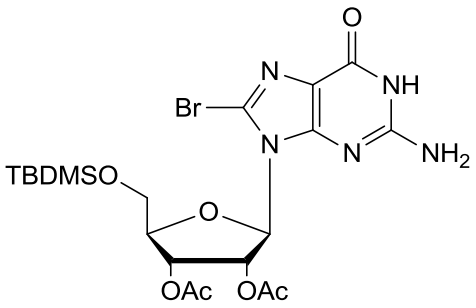

Acetic anhydride (2.08ml, 22.0mmol) was added dropwise to an ice cooled mixture of 5'-*tert*-butyldimethylsilyl-8-bromoguanosine (**43**, 4.39g, 11.0mmol), triethylamine (6.16ml, 44.2mmol) and DMAP (0.135g, 1.10mmol) in MeCN (50ml). The reaction mixture was then allowed to warm to room temperature. There was complete solubilisation when the reaction had gone to completion. The reaction was quenched with MeOH and the solvent removed *in vacuo*. The residue was then redissolved in DCM (50ml) and washed with H_2O (3 x 50ml) before drying over $MgSO_4$, filtering and concentrated to yield the product as a white solid (5.02g, 94%). HRMS (ES^+) (m/z): 582.1003 and 584.0950 ($[M+Na]^+$); $C_{20}H_{30}N_5O_7BrSiNa$ requires 582.0996 and 584.0975 (+1.2025 and -4.2801 ppm). ^{1}H NMR (400 MHz, D_6-DMSO): δ (ppm) 10.95 (1H, br s, N*H*), 6.56 (2H, br s, NH_2), 6.14-6.17 (1H, dd, *J* 6.1 and 5.0, H2'), 5.88-5.89 (1H, d, *J* 4.9, H1'), 5.58-5.62 (1H, ap t, *J* 5.9, H3'), 4.11-4.15 (1H, dd, *J* 10.2 and 5.5, H4'), 3.81-3.91 (2H, m, H5'), 2.10 (3H, s, COCH_3), 2.05 (3H, s, CO*C*H_3), 0.80 (9H, s, SiC(C$H_3)_3$), -0.04 (6H, s, 2 x Si*C*H_3). ^{13}C NMR (100 MHz, DMSO); δ (ppm) 169.41 (CO), 169.36 (CO), 155.47 (C6), 153.75 (C2), 152.06 (C4), 120.10 (C8), 117.16 (C5), 87.17 (C1'), 82.26 (C4'), 70.86 (C2'), 69.89 (C3'), 62.48 (C5'), 25.67 (Si*C*$(CH_3)_3$), 20.34 (CO*C*H_3), 20.24 (CO*C*H_3), 17.90 (SiC(*C*$H_3)_3$), -5.52 (Si(*C*$H_3)_2$).

N2-Dimethoxytrityl-5'-tert-butyldimethylsilyl-2'-3'-di-O-acetal-8-bromoguanosine (45)

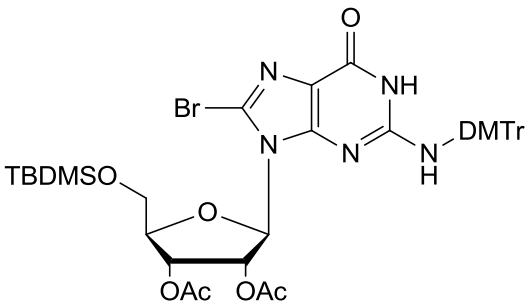

5'-*tert*-Butyldimethylsilyl-2'-3'-di-*O*-acetyl-8-bromoguanosine (**44**, 3.34g, 5.96mmol) was co-evaporated to dryness with anhydrous pyridine before re-dissolving in anhydrous pyridine (25ml). 4,4'-Dimethoxytrityl chloride (3.03g, 8.94mmol) was added slowly over 5 minutes to the stirred solution of the nucleoside under an atmosphere of N_2. The reaction was warmed to room temperature and stirred for 18 hours. The solution was concentrated *in vacuo* and the resulting orange residue was partitioned between DCM and H_2O. The organic extracts were then washed with $NaHCO_3$, dried under $MgSO_4$, filtered and concentrated to give the crude product as an orange solid. Purification by flash column chromatography eluting 2% MeOH in DCM yielded the title compound as a white solid (4.36g, 84%). HRMS (ES^-) (m/z): 860.2345 and 862.2327 ($[M-H]^-$); $C_{41}H_{47}N_5O_9BrSi$ requires 860.2326 and 862.2306 (+2.2087 and +2.4355 ppm). ^1H NMR (400 MHz, D_6-DMSO): δ (ppm) 7.77 (1H, br s, N*H*), 7.12-7.36 (9H, m, DMT Ar-H), 6.83-6.86 (4H, m, C*H*COCH$_3$), 6.76-6.78 (1H, m, H1'), 5.38-5.42 (2H, m, H2' and H3'), 4.88-4.92 (1H, m, H4'), 3.84-3.88 (1H, dd, *J* 10.8 and 5.3, H5'), 3.71 (6H, s, Ar-OC*H*$_3$), 3.64-3.66 (1H, d, *J* 5.1, H5''), 2.05 (3H, s, COC*H*$_3$), 1.89 (3H, s, COC*H*$_3$), 0.84 (9H, s, C(C*H*$_3$)$_3$), 0.00 (6H, s, Si(C*H*$_3$)$_2$). ^{13}C NMR (100 MHz, DMSO): δ (ppm) 168.97 (CO), 168.79 (CO). 157.76 (Ar-C), 157.77 (Ar-C), 155.11 (C6), 151.52 (C2), 151.23 (C4), 144.59 (Ar-C), 135.29 (Ar-C), 129.63 (Ar-C), 129.59 (Ar-C), 128.26 (Ar-C), 127.83 (Ar-C), 127.66 (Ar-C), 126.54 (Ar-C), 120.87 (C8), 117.39 (C5), 112.96 (Ar-C), 113.19 (Ar-C), 112.92 (Ar-C), 87.18 (C1'), 81.23 (C4'), 69.67 (NH*C*), 69.36 (C2'), 69.24 (C3'), 62.36 (C5'), 54.93 (Ar-C), 54.91 (Ar-C), 25.64 (Si*C*(CH$_3$)$_3$), 20.14 (CO*C*H$_3$), 19.90 (CO*C*H$_3$), 17.85 (SiC(*C*H$_3$)$_3$), -5.45 (Si*C*H$_3$), -5.51 (Si*C*H$_3$).

Chapter 8

Bibliography

8 Bibliography

1. R. Dahm, *Hum. Genet.*, 2008, **122**, 565–581.

2. G. M. Blackburn and M. J. Gait, *Nucleic Acids in Chemistry and Biology*, Oxford University Press Inc, 2nd edn., 1996.

3. O. T. Avery, C. M. MacLeod, and M. McCarty, *J. Exp. Med.*, 1944, **79**, 137–158.

4. E. Chargaff, *Experientia*, 1950, **6**, 201–240.

5. R. G. Franklin, Rosalind E.Gosling, *Nature*, 1953, **171**, 740–741.

6. M. H. F. Wilkins, A. R. Stokes, and H. R. Wilson, *Nature*, 1953, **171**, 738–740.

7. J. D. Watson and F. H. C. Crick, *Nature*, 1953, **171**, 737–738.

8. J. D. Watson and F. H. C. Crick, *Nature*, 1953, **171**, 964–967.

9. R. W. Holley, J. Apgar, G. A. Everette, J. T. Madison, M. Marquisee, S. H. Merrill, J. R. Penswick, and A. Zamir, *Science (80-.).*, 1965, **147**, 1462–1465.

10. J. C. Venter, M. D. Adams, E. W. Myers, P. W. Li, R. J. Mural, G. G. Sutton, H. O. Smith, M. Yandell, C. A. Evans, R. A. Holt, *et al.*, *Science*, 2001, **291**, 1304–1351.

11. B. Alberts, A. Johnson, J. Lewis, M. Raff, K. Roberts, and P. Walter, in *Molecular Biology of the Cell*, Garland Science, New York, 4th edn., 2002, p. Chapter 4.

12. A. Rich, *Nat. Struct. Mol. Biol.*, 2003, **10**, 247–249.

13. W. Saenger, *Principles of Nucleic Acid Structure*, Springer-Verlag, 1984.

14. W. Saenger, *Angew. Chemie*, 1973, **12**, 591–682.

15. C. Altona and M. Sundaralingam, *J. Am. Chem. Soc.*, 1972, **4377**, 8205–8212.

16. K. Bondensgaard, M. Petersen, S. K. Singh, V. K. Rajwanshi, R. Kumar, J. Wengel, and J. P. Jacobsen, *Chem. - A Eur. J.*, 2000, **6**, 2687–2695.

17. J. Clayden, N. Greeves, S. Warren, and P. Wothers, *Organic Chemistry*, Oxford University Press, 1st edn., 2001.

18. J. Plavec, W. Tong, and J. Chattopadhyaya, *J. Am. Chem. Soc.*, 1993, **115**, 9734–9746.

19. W. K. Olson and J. L. Sussman, *J. Am. Chem. Soc.*, 1982, **104**, 270–278.

20. J. Plavec, C. Thibaudeau, and J. Chattopadhyaya, *J. Am. Chem. Soc.*, 1994, **116**, 6558–6560.

21. NC-IUB, *Eur. J. Biochem.*, 1985, **150**, 1–5.

22. J. E. Sokoloski, S. A. Godfrey, S. E. Dombrowski, and P. C. Bevilacqua, *RNA*, 2011, **17**, 1775–1787.

23. N. Foloppe, B. Hartmann, L. Nilsson, and A. D. MacKerell, *Biophys. J.*, 2002, **82**, 1554–1569.

24. M. L. Hamm, S. Rajguru, A. M. Downs, and R. Cholera, *J. Am. Chem. Soc.*, 2005, **127**, 12220–12221.

25. A. M. Michelson, C. Monny, and A. M. Kapuler, *Biochim. Biophys. Acta*, 1970, **217**, 7–17.

26. S. S. Tavale and H. M. Sobell, *J. Mol. Biol.*, 1970, **48**, 109–123.

27. R. B. Corey and L. Pauling, *Arch. Biochem. Biophys.*, 1956, **65**, 164–181.

28. K. Hoogsteen, *Acta Crystallogr.*, 1959, **12**, 822–823.

29. E. N. Nikolova, H. Zhou, F. L. Gottardo, H. S. Alvey, I. J. Kimsey, and H. M. Al-Hashimi, *Biopolymers*, 2013, **99**, 955–968.

30. P. Belmont, J. F. Constant, and M. Demeunynck, *Chem. Soc. Rev.*, 2001, **30**, 70–81.

31. E. T. Kool, *Annu. Rev. Biophys. Biomol. Struct.*, 2001, **30**, 1–22.

32. E. T. Kool, *Chem. Rev.*, 1997, **97**, 1473–1488.

33. P. Yakovchuk, E. Protozanova, and M. D. Frank-Kamenetskii, *Nucleic Acids Res.*, 2006, **34**, 564–574.

34. T. J. Matray and E. T. Kool, *J. Am. Chem. Soc.*, 1998, **120**, 6191–6192.

35. V. N. Potaman and R. R. Sinden, in *DNA Conformation and Transcription*, ed. T. Ohyama, Springer, 1st edn., 2005, pp. 1–16.

36. R. M. Roat-Malone, *Bioinorganic Chemistry: A Short Course*, Wiley-Blackwell, 2nd edn., 2007.

37. R. E. Dickerson, H. R. Drew, B. N. Conner, R. M. Wing, a V Fratini, and M. L. Kopka, *Science*, 1982, **216**, 475–485.

38. I. Brovchenko, A. Krukau, A. Oleinikova, and A. Mazur, *Phys. Rev. Lett.*, 2006, **97**, 137801.

39. X. J. Lu, Z. Shakked, and W. K. Olson, *J. Mol. Biol.*, 2000, **300**, 819–840.

40. A. H. J. Wang, G. J. Quigley, F. J. Kolpak, J. L. Crawford, J. H. Van Boom, G. Van Der Marel, and R. Alexander, *Nature*, 1979, **282**, 680–686.

41. A. Rich and Z. Shuguang, *Nat. Rev. Genet.*, 2003, **4**, 566–572.

42. A. Rich, A. Nordheim, and A. H. Wang, *Annu. Rev. Biochem.*, 1984, **53**, 791–846.

43. A. Ghosh and M. Bansal, *Acta Crystallogr. D. Biol. Crystallogr.*, 2003, **59**, 620–626.

44. X. J. Lu and W. K. Olson, *Nucleic Acids Res.*, 2003, **31**, 5108–5121.

45. R. V Brown and L. H. Hurley, *Biochem. Soc. Trans.*, 2011, **39**, 635–640.

46. P. Murat and S. Balasubramanian, *Curr. Opin. Genet. Dev.*, 2014, **25**, 22–29.

47. Y. Xu, *Chem. Soc. Rev.*, 2011, **40**, 2719–2740.

48. J. L. Huppert and S. Balasubramanian, *Nucleic Acids Res.*, 2005, **33**, 2908–2916.

49. S. Burge, G. N. Parkinson, P. Hazel, A. K. Todd, and S. Neidle, *Nucleic Acids Res.*, 2006, **34**, 5402–5415.

50. G. Biffi, D. Tannahill, J. McCafferty, and S. Balasubramanian, *Nat. Chem.*, 2013, **5**, 182–186.

51. A. Ambrus, D. Chen, J. Dai, T. Bialis, R. a Jones, and D. Yang, *Nucleic Acids Res.*, 2006, **34**, 2723–2735.

52. V. L. Makarov, Y. Hirose, and J. P. Langmore, *Cell*, 1997, **88**, 657–666.

53. C. B. Harley, B. A. Futcher, and C. W. Greider, *Nature*, 1990, **345**, 458–460.

54. S. Neidle, *FEBS J.*, 2010, **277**, 1118–1125.

55. S. Balasubramanian, L. H. Hurley, and S. Neidle, *Nat. Rev. Drug Discov.*, 2011, **10**, 261–275.

56. L. Yuan, T. Tian, Y. Chen, S. Yan, X. Xing, Z. Zhang, Q. Zhai, L. Xu, S. Wang, X. Weng, *et al.*, *Nat. Sci. reports*, 2013, **3**, 1811.

57. E. Y. N. Lam, D. Beraldi, D. Tannahill, and S. Balasubramanian, *Nat. Commun.*, 2013, **4**, 1796.

58. A. U. Ahmed, *Front. Biol. (Beijing).*, 2011, **6**, 274–281.

59. R. Medzhitov, *Nature*, 2008, **454**, 428–435.

60. M. E. Bianchi, *J. Leukoc. Biol.*, 2007, **81**, 1–5.

61. R. Medzhitov and C. A. Janeway Jr, *Curr. Opin. Immunol.*, 1997, **9**, 4–9.

62. D. Okin and R. Medzhitov, *Curr. Biol.*, 2012, **22**, R733–R740.

63. L. M. Coussens and Z. Werb, *Nature*, 2002, **420**, 860–867.

64. R. Medzhitov, *Cell*, 2010, **140**, 771–776.

65. E. N. Hatada, D. Krappmann, and C. Scheidereit, *Curr. Opin. Immunol.*, 2000, **12**, 52–58.

66. H. Lu, W. Ouyang, and C. Huang, *Mol. Cancer Res.*, 2006, **4**, 221–233.

67. N. T. Ashley, Z. M. Weil, and R. J. Nelson, *Annu. Rev. Ecol. Evol. Syst.*, 2012, **43**, 385–406.

68. M. Karin, Y. Cao, F. R. Greten, and Z.-W. Li, *Nat. Rev. Cancer*, 2002, **2**, 301–310.

69. A. Mantovani, P. Allavena, A. Sica, and F. Balkwill, *Nature*, 2008, **454**, 436–444.

70. C. N. Serhan and J. Savill, *Nat. Immunol.*, 2005, **6**, 1191–1197.

71. T. Lawrence and D. W. Gilroy, *Int. J. Exp. Pathol.*, 2007, **88**, 85–94.

72. C. S. Stevenson, L. A. Marshall, and D. W. Morgan, *In Vivo Models of Inflammation Volume 1*, Birkhauser Verlag, 2nd edn., 2006.

73. G. Cirino, E. Distrutti, and J. L. Wallace, *Inflamm. Allergy Drug Targets*, 2006, **5**, 115–119.

74. D. A. Wink, Y. Vodovotz, J. Laval, F. Laval, M. W. Dewhirst, and J. B. Mitchell, *Carcinogenesis*, 1998, **19**, 711–721.

75. D. M. Dudzinski, J. Igarashi, D. Greif, and T. Michel, *Annu. Rev. Pharmacol. Toxicol.*, 2006, **46**, 235–276.

76. M. A. Marletta, *Cell*, 1994, **78**, 927–930.

77. A. Pautz, J. Art, S. Hahn, S. Nowag, C. Voss, and H. Kleinert, *Nitric Oxide*, 2010, **23**, 75–93.

78. P. C. Dedon and S. R. Tannenbaum, *Arch. Biochem. Biophys.*, 2004, **423**, 12–22.

79. W. K. Alderton, C. E. Cooper, and R. G. Knowles, *Biochem. J.*, 2001, **357**, 593–615.

80. K. Kilinc, *Indoor Built Environ.*, 2005, **14**, 503–512.

81. P. Lirk, G. Hoffmann, and J. Rieder, *Curr. Drug Targets. Inflamm. Allergy*, 2002, **1**, 89–108.

82. U. Förstermann and W. C. Sessa, *Eur. Heart J.*, 2012, **33**, 829–837.

83. C. Giroud, M. Moreau, T. a Mattioli, V. Balland, J.-L. Boucher, Y. Xu-Li, D. J. Stuehr, and J. Santolini, *J. Biol. Chem.*, 2010, **285**, 7233–7245.

84. H. Li, J. Igarashi, J. Jamal, W. Yang, and T. L. Poulos, *J. Biol. Inorg. Chem.*, 2006, **11**, 753–768.

85. D. Li, M. Kabir, D. J. Stuehr, and D. L. Rousseau, *J. Am. Chem. Soc.*, 2007, **129**, 6943–6951.

86. J. Sabat, T. Egawa, C. Lu, D. J. Stuehr, G. J. Gerfen, D. L. Rousseau, and S.-R. Yeh, *J. Biol. Chem.*, 2013, **288**, 6095–6106.

87. L. J. Ignarro, G. M. Buga, K. S. Wood, R. E. Byrns, and G. Chaudhuri, *Proc. Natl. Acad. Sci. U. S. A.*, 1987, **84**, 9265–9269.

88. R. M. J. Palmer, A. G. Ferrige, and S. Moncada, *Nature*, 1987, **327**, 524–526.

89. S. Burney, J. L. Caulfield, J. C. Niles, J. S. Wishnok, and S. R. Tannenbaum, *Mutat. Res.*, 1999, **424**, 37–49.

90. J. S. Beckman and W. H. Koppenol, *Am. J. Physiol.*, 1996, **271**, C1424–C1437.

91. M. N. Hughes, *Methods Enzymol.*, 2008, **436**, 3–19.

92. S. H. Francis, J. L. Busch, and J. D. Corbin, *Pharmacol. Rev.*, 2010, **62**, 525–563.

93. J. R. Lancaster, *Nitric Oxide Biol. Chem.*, 1997, **1**, 18–30.

94. E. S. Underbakke, A. T. Iavarone, M. J. Chalmers, B. D. Pascal, S. Novick, P. R. Griffin, and M. A. Marletta, *Structure*, 2014, **22**, 602–611.

95. F. Balkwill and A. Mantovani, *Lancet*, 2001, **357**, 539–545.

96. M. Rosselli, P. J. Keller, and R. K. Dubey, *Hum. Reprod. Update*, 1998, **4**, 3–24.

97. H. H. H. W. Schmidt and U. Walter, *Cell*, 1994, **78**, 919–925.

98. K. L. Davis, E. Martin, I. V. Turko, and F. Murad, *Annu. Rev. Pharmacol. Toxicol.*, 2001, **41**, 203–236.

99. M. Freitas, J. L. F. C. Lima, and E. Fernandes, *Anal. Chim. Acta*, 2009, **649**, 8–23.

100. Y. Chen and W. G. Junger, in *Leucocytes: Methods and Protocols*, Springer, 2012, pp. 115–124.

101. M. C. Martínez and R. Andriantsitohaina, *Antioxid. Redox Signal.*, 2009, **11**, 669–702.

102. P. Pacher, J. S. Beckman, and L. Liaudet, *Physiol. Rev.*, 2007, **87**, 315–424.

103. R. Kissner, T. Nauser, C. Kurz, and W. Koppenol, *IUBMB Life*, 2003, **55**, 567–572.

104. R. Radil, J. S. Beckman, K. M. Bush, and B. A. Freeman, *J. Biol. Chem.*, 1991, **266**, 4244–4250.

105. K. Takakura, J. S. Beckman, L. A. Macmillan-Crow, and J. P. Crow, *Arch. Biochem. Biophys.*, 1999, **369**, 197–207.

106. N. K. Tonks, *Nat. Rev. Mol. Cell Biol.*, 2006, **7**, 833–846.

107. J. P. Crow, J. S. Beckman, and J. M. McCord, *Biochemistry*, 1995, **34**, 3544–3552.

108. C. E. Richeson, P. Mulder, V. W. Bowry, and K. U. Ingold, *J. Am. Chem. Soc.*, 1998, **120**, 7211–7219.

109. M. Wörle, P. Latal, R. Kissner, R. Nesper, and W. H. Koppenol, *Chem. Res. Toxicol.*, 1999, **12**, 305–307.

110. B. Liang and L. Andrews, *J. Am. Chem. Soc.*, 2001, **123**, 9848–9854.

111. W. H. Koppenol, J. J. Moreno, W. A. Pryor, H. Ischiropoulos, and J. S. Beckman, *Chem. Res. Toxicol.*, 1992, **5**, 834–842.

112. J. P. Crow, C. Spruell, J. Chen, C. Gunn, H. Ischiropoulos, M. Tsai, C. D. Smith, R. Radi, W. H. Koppenol, and J. S. Beckman, *Free Radic. Biol. Med.*, 1994, **16**, 331–338.

113. G. Merényi, J. Lind, S. Goldstein, and G. Czapski, *Chem. Res. Toxicol.*, 1998, **11**, 712–713.

114. G. Merényi and J. Lind, *Chem. Res. Toxicol.*, 1998, **11**, 243–246.

115. J. S. Beckman, T. W. Beckman, J. Chen, P. A. Marshall, and B. A. Freeman, *Proc. Natl. Acad. Sci. U. S. A.*, 1990, **87**, 1620–1624.

116. H. Ohshima, T. Sawa, and T. Akaike, *Antioxid. Redox Signal.*, 2006, **8**, 1033–1045.

117. R. Radi, *Chem. Res. Toxicol.*, 1998, **11**, 720–721.

118. R. M. Uppu and W. A. Pryor, *Biochem. Biophys. Res. Commun.*, 1996, **229**, 764–769.

119. J. K. Kundu and Y. J. Surh, *Free Radic. Biol. Med.*, 2012, **52**, 2013–2037.

120. D. Kidane, W. J. Chae, J. Czochor, K. a Eckert, P. M. Glazer, A. L. M. Bothwell, and J. B. Sweasy, *Crit. Rev. Biochem. Mol. Biol.*, 2014, **49**, 116–139.

121. S. Bjelland, *Mutat. Res. Mol. Mech. Mutagen.*, 2003, **531**, 37–80.

122. S. Steenken and S. V Jovanovic, *J. Am. Chem. Soc.*, 1997, **119**, 617–618.

123. C. E. Crespo-Hernandez, D. M. Close, L. Gorb, and J. Leszczynski, *J. Phys. Chem. B*, 2007, **111**, 5386–5395.

124. S. Kanvah and G. B. Schuster, *Nucleic Acids Res.*, 2005, **33**, 5133–5138.

125. B. Giese, *Curr. Opin. Chem. Biol.*, 2002, **6**, 612–618.

126. W. L. Neeley and J. M. Essigmann, *Chem. Res. Toxicol.*, 2006, **19**, 491–505.

127. S. I. Grivennikov, F. R. Greten, and M. Karin, *Cell*, 2010, **140**, 883–899.

128. A. Mantovani, *Nature*, 2009, **457**, 36–37.

129. G. Multhoff, M. Molls, and J. Radons, *Front. Immunol.*, 2011, **2**, 98.

130. D. Hanahan and R. A. Weinberg, *Cell*, 2000, **100**, 57–70.

131. F. Colotta, P. Allavena, A. Sica, C. Garlanda, and A. Mantovani, *Carcinogenesis*, 2009, **30**, 1073–1081.

132. F. R. Balkwill and A. Mantovani, *Semin. Cancer Biol.*, 2012, **22**, 33–40.

133. S. P. Hussain and C. C. Harris, *Int. J. cancer*, 2007, **121**, 2373–2380.

134. J. R. Warren, *Lancet*, 1983, **321**, 1273–1275.

135. IARC, *World Heal. Organ. IARC Monogr. Eval. Carcinog. Risks to Humans. Schistosomes, Liver flukes Helicobacter pylori*, 1994, **61**, 177–240.

136. H. W. Chung and J. B. Lim, *World J. Gastroenterol.*, 2014, **20**, 1667–1680.

137. J. Ferlay, I. Soerjomataram, M. Ervik, R. Dikshit, S. Eser, C. Mathers, M. Rebelo, D. Parkin, D. Forman, and F. Bray, *IARC CancerBase No.11*, 2012, Population Fact Sheets.

138. O. Handa, Y. Naito, and T. Yoshikawa, *Inflamm. Res.*, 2010, **59**, 997–1003.

139. E. Touati, *Mutat. Res.*, 2010, **703**, 66–70.

140. K. Nagata, H. Yu, M. Kashiba, E. F. Sato, T. Tamura, and M. Inoue, *J. Biol. Chem.*, 1998, **273**, 14071–14073.

141. H. Kuwahara, Y. Miyamoto, T. Akaike, T. Kubota, T. Sawa, S. Okamoto, and H. Maeda, *Infect. Immun.*, 2000, **68**, 4378–4383.

142. N. Ma, M. Murata, S. Ohnishi, R. Thanan, Y. Hiraku, and S. Kawanishi, in *Biomarker*, ed. T. Khan, InTech, 2012, pp. 201–224.

143. S. Kawanishi, Y. Hiraku, S. Pinlaor, and N. Ma, *Biol. Chem.*, 2006, **387**, 365–372.

144. G. Castello, S. Scala, G. Palmieri, S. a Curley, and F. Izzo, *Clin. Immunol.*, 2010, **134**, 237–250.

145. S. L. Chen and T. R. Morgan, *Int. J. Med. Sci.*, 2006, **3**, 47–52.

146. N. S. Reyes De Mochel, S. Seronello, S. H. Wang, C. Ito, J. X. Zheng, T. J. Liang, J. D. Lambeth, and J. Choi, *Hepatology*, 2010, **52**, 47–59.

147. S. Horiike, S. Kawanishi, M. Kaito, N. Ma, H. Tanaka, N. Fujita, M. Iwasa, Y. Kobayashi, Y. Hiraku, S. Oikawa, *et al.*, *J. Hepatol.*, 2005, **43**, 403–410.

148. T. Walser, X. Cui, J. Yanagawa, J. M. Lee, E. Heinrich, G. Lee, S. Sharma, and S. M. Dubinett, *Proc. Am. Thorac. Soc.*, 2008, **5**, 811–815.

149. R. Talhout, T. Schulz, E. Florek, J. van Benthem, P. Wester, and A. Opperhuizen, *Int. J. Environ. Res. Public Health*, 2011, **8**, 613–628.

150. S. S. Hecht, *J. Natl. Cancer Inst.*, 1999, **91**, 1194–1210.

151. Y. S. Hsieh, B. C. Chen, S. J. Shiow, H. C. Wang, J. D. Hsu, and C. J. Wang, *Chem. Biol. Interact.*, 2002, **140**, 67–80.

152. R. Cueto and W. A. Pryor, *Vib. Spectrosc.*, 1994, **7**, 97–111.

153. J. Lee, V. Taneja, and R. Vassallo, *J. Dent. Res.*, 2012, **91**, 142–149.

154. K. S. Ahn and B. B. Aggarwal, *Ann. N. Y. Acad. Sci.*, 2005, **1056**, 218–233.

155. T. Sawa, M. Tatemichi, T. Akaike, A. Barbin, and H. Ohshima, *Free Radic. Biol. Med.*, 2006, **40**, 711–720.

156. B. D. Preston, T. M. Albertson, and A. J. Herr, *Semin. Cancer Biol.*, 2010, **20**, 281–293.

157. H. Kasai and S. Nishimura, *Nucleic Acids Res.*, 1984, **12**, 2137–2146.

158. F. Altieri, C. Grillo, M. Maceroni, and S. Chichiarelli, *Antioxid. Redox Signal.*, 2008, **10**, 891–937.

159. D. Venkateswarlu and J. Leszczynski, *J. Comput. Aided. Mol. Des.*, 1998, **12**, 373–382.

160. B. Van Loon, E. Markkanen, and U. Hübscher, *DNA Repair (Amst).*, 2010, **9**, 604–616.

161. X. Cheng, C. Kelso, V. Hornak, C. D. L. Santos, A. P. Grollman, and C. Simmerling, *J. Am. Chem. Soc.*, 2005, **127**, 13906–13918.

162. G. E. Plum, A. P. Grollman, F. Johnson, and K. J. Breslauer, *Biochemistry*, 1995, **34**, 16148–16160.

163. S. S. David, V. L. O. Shea, and S. Kundu, *Nature*, 2007, **447**, 941–950.

164. D. Wang, D. A. Kreutzer, and J. M. Essigmann, *Mutat. Res.*, 1998, **400**, 99–115.

165. S. K. Singh, M. W. Szulik, M. Ganguly, I. Khutsishvili, M. P. Stone, L. A. Marky, and B. Gold, *Nucleic Acids Res.*, 2011, **39**, 6789–6801.

166. T. Paz-Elizur, Z. Sevilya, Y. Leitner-Dagan, D. Elinger, L. C. Roisman, and Z. Livneh, *Cancer Lett.*, 2008, **266**, 60–72.

167. T. Nakamura, S. Meshitsuka, S. Kitagawa, N. Abe, J. Yamada, T. Ishino, H. Nakano, T. Tsuzuki, T. Doi, Y. Kobayashi, *et al.*, *J. Biol. Chem.*, 2010, **285**, 444–452.

168. A. A. Kuznetsova, N. A. Kuznetsov, A. A. Ishchenko, M. K. Saparbaev, and O. S. Fedorova, *Biochim. Biophys. Acta*, 2014, **1840**, 387–395.

169. C. M. Crenshaw, K. Nam, K. Oo, P. S. Kutchukian, B. R. Bowman, M. Karplus, and G. L. Verdine, *J. Biol. Chem.*, 2012, **287**, 24916–24928.

170. J. C. Fromme, A. Banerjee, S. J. Huang, and G. L. Verdine, *Nature*, 2004, **427**, 652–656.

171. C. Kairupan and R. J. Scott, *Hered. Cancer Clin. Pract.*, 2007, **5**, 199–209.

172. M. Christmann, M. T. Tomicic, W. P. Roos, and B. Kaina, *Toxicology*, 2003, **193**, 3–34.

173. L. G. Brieba, B. F. Eichman, R. J. Kokoska, S. Doublié, T. A. Kunkel, and T. Ellenberger, *EMBO J.*, 2004, **23**, 3452–3461.

174. G. W. Hsu, M. Ober, T. Carell, and L. S. Beese, *Nature*, 2004, **431**, 217–221.

175. K. E. Zahn, S. S. Wallace, and S. Doublié, *Curr. Opin. Struct. Biol.*, 2011, **21**, 358–369.

176. A. J. Atkinson, W. G. Magnuson, W. A. Colburn, V. G. DeGruttola, D. L. DeMets, G. J. Downing, D. F. Hoth, J. A. Oates, C. C. Peck, R. T. Schooley, *et al.*, *Clin. Pharmacol. Ther.*, 2001, **69**, 89–95.

177. D. Ziech, R. Franco, A. G. Georgakilas, S. Georgakila, V. Malamou-Mitsi, O. Schoneveld, A. Pappa, and M. I. Panayiotidis, *Chem. Biol. Interact.*, 2010, **188**, 334–339.

178. B. Pesch, T. Brüning, G. Johnen, S. Casjens, N. Bonberg, D. Taeger, A. Müller, D. G. Weber, and T. Behrens, *Biochim. Biophys. Acta*, 2014, **1844**, 874–883.

179. M. Valko, C. J. Rhodes, J. Moncol, M. Izakovic, and M. Mazur, *Chem. Biol. Interact.*, 2006, **160**, 1–40.

180. O. Keiki and D. Wang, *Acta Med. Okayama*, 2007, **61**, 181–189.

181. V. Yermilov, J. Rubio, and H. Ohshima, *FEBS Lett.*, 1995, **376**, 207–210.

182. M. Masuda, H. Nishino, and H. Ohshima, *Chem. Biol. Interact.*, 2002, **139**, 187–197.

183. N. Suzuki, M. Yasui, N. E. Geacintov, V. Shafirovich, and S. Shibutani, *Biochemistry*, 2005, **44**, 9238–9245.

184. Y. W. Kow, G. Bao, B. Minesinger, S. Jinks-Robertson, W. Siede, Y. L. Jiang, and M. M. Greenberg, *Nucleic Acids Res.*, 2005, **33**, 6196–6202.

185. G. L. Dianov, K. M. Sleeth, I. I. Dianova, and S. L. Allinson, *Mutat. Res. Mol. Mech. Mutagen.*, 2003, **531**, 157–163.

186. D. M. Wilson and D. Barsky, *Mutat. Res.*, 2001, **485**, 283–307.

187. L. A. Loeb and B. D. Preston, *Annu. Rev. Genet.*, 1986, **20**, 201–230.

188. L. Haracska, I. Unk, R. E. Johnson, E. Johansson, P. M. Burgers, S. Prakash, and L. Prakash, *Genes Dev.*, 2001, **15**, 945–954.

189. M. Murata, R. Thanan, N. Ma, and S. Kawanishi, *J. Biomed. Biotechnol.*, 2012, **2012**, 623019.

190. P. Cuniasse, G. V Fazakerley, W. Guschlbauer, B. E. Kaplan, and L. C. Sowers, *J. Mol. Biol.*, 1990, **213**, 303–314.

191. Y. Hiraku, *Environ. Health Prev. Med.*, 2010, **15**, 63–72.

192. T. Akaike, S. Okamoto, T. Sawa, J. Yoshitake, F. Tamura, K. Ichimori, K. Miyazaki, K. Sasamoto, and H. Maeda, *Proc. Natl. Acad. Sci. U. S. A.*, 2003, **100**, 685–690.

193. T. Sawa, T. Akaike, K. Ichimori, T. Akuta, K. Kaneko, H. Nakayama, D. J. Stuehr, and H. Maeda, *Biochem. Biophys. Res. Commun.*, 2003, **311**, 300–306.

194. I. Bhamra, P. Compagnone-Post, I. A. O'Neil, L. A. Iwanejko, A. D. Bates, and R. Cosstick, *Nucleic Acids Res.*, 2012, **40**, 11126–11138.

195. V. Shafirovich, S. Mock, A. Kolbanovskiy, and N. E. Geacintov, *Chem. Res. Toxicol.*, 2002, **15**, 591–597.

196. Y. Saito, H. Taguchi, S. Fujii, T. Sawa, E. Kida, C. Kabuto, T. Akaike, and H. Arimoto, *Chem. Commun.*, 2008, **45**, 5984–5986.

197. E. A. Lesnik, C. J. Guinosso, A. M. Kawasaki, H. Sasmor, M. Zounes, L. L. Cummins, D. J. Ecker, P. D. Cook, and S. M. Freier, *Biochemistry*, 1993, **32**, 7832–7838.

198. W. Guschlbauer and K. Jankowski, *Nucleic Acids Res.*, 1980, **8**, 1421–1433.

199. L. L. Cummins, S. R. Owens, L. M. Risen, E. A. Lesnik, S. M. Freier, D. McGee, C. J. Guinosso, and P. D. Cook, *Nucleic Acids Res.*, 1995, **23**, 2019–2024.

200. S. Uesugi and M. Ikehara, *J. Am. Chem. Soc.*, 1977, **99**, 3250–3253.

201. P. M. Gannett and T. P. Sura, *Chem. Res. Toxicol.*, 1993, **6**, 690–700.

202. P. Acharya, P. Cheruku, S. Chatterjee, S. Acharya, and J. Chattopadhyaya, *J. Am. Chem. Soc.*, 2004, **126**, 2862–2869.

203. J. Chen, M. A. Mcallister, J. K. Lee, and K. N. Houk, *J. Org. Chem.*, 1998, **63**, 4611–4619.

204. V. Verdolino, R. Cammi, B. H. Munk, and H. B. Schlegel, *J. Phys. Chem. B*, 2008, **112**, 16860–16873.

205. J. Mergny and L. Lacroix, *Oligonucleotides*, 2003, **13**, 515–537.

206. S. Creighton, L. B. Bloom, and M. F. Goodman, *Methods Enzymol.*, 1995, **262**, 232–256.

207. L. A. Loeb and R. J. Monnat, *Nat. Rev. Genet.*, 2008, **9**, 594–604.

208. T. Kurahashi, T. Mizutani, and J. Yoshida, *J. Chem. Soc. Perkin Trans. 1*, 1999, **4**, 465–473.

209. C. J. Pedersen, *J. Am. Chem. Soc.*, 1967, **89**, 7016–7036.

210. J. S. Bradshaw and R. M. Izatt, *Acc. Chem. Res.*, 1997, **30**, 338–345.

211. R. B. Merrifield, *J. Am. Chem. Soc.*, 1963, **85**, 2149–2154.

212. A. R. Mitchell, *Biopolymers*, 2008, **90**, 175–184.

213. C. B. Reese, *Org. Biomol. Chem.*, 2005, **3**, 3851–3868.

214. S. L. Beaucage and P. I. Radhakrishnan, *Tetrahedron*, 1992, **48**, 2223–2311.

215. S. L. Beaucage and M. H. Caruthers, *Tetrahedron Lett.*, 1981, **22**, 1859–1862.

216. R. L. Letsinger and W. B. Lunsford, *J. Am. Chem. Soc.*, 1976, **98**, 3655–3661.

217. R. L. Letsinger, J. L. Finnan, G. A. Heavner, and W. B. Lunsford, *J. Am. Chem. Soc.*, 1975, **97**, 3278–3279.

218. T. Wagner and W. Pfleiderer, *Helv. Chim. Acta*, 2000, **83**, 2023–2035.

219. C. D. Claeboe, R. Gao, and S. M. Hecht, *Nucleic Acids Res.*, 2003, **31**, 5685–5691.

220. M. Smith, D. H. Rammler, I. H. Goldberg, and H. G. Khorana, *J. Am. Chem. Soc.*, 1962, **84**, 430–440.

221. H. Schaller, G. Weimann, B. Lerch, and H. G. Khorana, *J. Am. Chem. Soc.*, 1963, **85**, 3821–3827.

222. R. Hogrefe, *http://www.trilinkbiotech.com/tech/oligo_history.pdf*.

223. E. F. Fisher and M. H. Caruthers, *Nucleic Acids Res.*, 1983, **11**, 1589–1599.

224. R. T. Pon, *Artificial DNA: Methods and Applications*, CRC Press, 1st edn., 2002.

225. G. M. Tener, *J. Am. Chem. Soc.*, 1961, **83**, 159–168.

226. R. L. Letsinger and K. K. Ogilvie, *J. Am. Chem. Soc.*, 1969, **91**, 3350–3355.

227. D. C. Capaldi, H. Gaus, A. H. Krotz, J. Arnold, R. L. Carty, M. N. Moore, A. N. Scozzari, K. Lowery, D. L. Cole, and V. T. Ravikumar, *Org. Process Res. Dev.*, 2003, **7**, 832–838.

228. L. Bellon and F. Wincott, *Solid-Phase Synthesis: A Practical Guide*, CRC Press, 1st edn., 2000.

229. X. Wei, *Tetrahedron*, 2013, **69**, 3615–3637.

230. R. Welz and S. Müller, *Tetrahedron Lett.*, 2002, **43**, 795–797.

231. G. R. Gough, M. J. Brunden, and P. T. Gilham, *Tetrahedron Lett.*, 1983, **24**, 5321–5324.

232. W. T. Markiewicz and T. K. Wyrzykiewicz, *Nucleic Acids Res.*, 1989, **17**, 7149–7158.

233. M. H. Lyttle, D. Hudson, and R. M. Cook, *Nucleic Acids Res.*, 1996, **24**, 2793–2798.

234. A. V Azhayev and M. L. Antopolsky, *Tetrahedron*, 2001, **57**, 4977–4986.

235. R. T. Pon and Y. Shuyuan, *Tetrahedron Lett.*, 1997, **38**, 3327–3330.

236. A. P. Henderson, J. Riseborough, C. Bleasdale, W. Clegg, M. R. J. Elsegood, and B. T. Golding, *J. Chem. Soc. Perkin Trans. 1*, 1997, **22**, 3407–3413.

237. B. P. Fors and S. L. Buchwald, *J. Am. Chem. Soc.*, 2009, **131**, 12898–12899.

238. M. Breugst, F. Corral Bautista, and H. Mayr, *Chem. - A Eur. J.*, 2012, **18**, 127–137.

239. P. Pande, J. Shearer, J. Yang, W. A. Greenberg, and S. E. Rokita, *J. Am. Chem. Soc.*, 1999, **121**, 6773–6779.

240. L. P. Bignold, *Anticancer Res.*, 2006, **26**, 1327–1336.

241. D. Fu, J. A. Calvo, and L. D. Samson, *Nat. Rev. Cancer*, 2012, **12**, 104–120.

242. W. F. Veldhuyzen, Y. F. Lam, and S. E. Rokita, *Chem. Res. Toxicol.*, 2001, **14**, 1345–1351.

243. S. E. Rokita, J. Yang, P. Pande, and W. A. Greenberg, *J. Org. Chem.*, 1997, **62**, 3010–3012.

244. M. A. Lewis, D. G. Yoerg, J. L. Bolton, and J. A. Thompson, *Chem. Res. Toxicol.*, 1996, **9**, 1368–1374.

245. M. M. Toteva and J. P. Richard, *Adv. Phys. Org. Chem.*, 2011, **45**, 39–91.

246. S. E. Rokita, *Qunione Methides*, Wiley-Interscience, 2009.

247. S. R. Angle, D. Amaiz, J. P. Boyce, R. P. Frutos, M. S. Louie, H. L. Mattson-amaiz, J. D. Rainier, K. D. Turnbull, and W. Yang, *J. Org. Chem.*, 1994, **59**, 6322–6337.

248. J. L. Bolton, L. G. Valerio, and J. A. Thompson, *Chem. Res. Toxicol.*, 1992, **5**, 816–822.

249. T. Li and S. E. Rokita, *J. Am. Chem. Soc.*, 1991, **113**, 7771–7773.

250. R. Bruckner, *Organic Mechanisms: Reactions, Stereochemistry and Synthesis*, Springer, 2010.

251. J. Reinhard, W. E. Hull, C. W. Von Der Lieth, U. Eichhorn, H. C. Kliem, B. Kaina, and M. Wiessler, *J. Med. Chem.*, 2001, **44**, 4050–4061.

252. M. Freccero, R. Gandolfi, and M. Sarzi-Amadè, *J. Org. Chem.*, 2003, **68**, 6411–6423.

253. J. R. Lakowicz, *Principles of Fluorescence Spectroscopy*, Springer, 3rd edn., 2006.

254. M. Sauer, J. Hofkens, and J. Enderlein, in *Handbook of Fluorescence Spectroscopy and Imaging: From Single Molecules to Ensembles*, Wiley-VCH Verlag GmbH & Co, 2011, pp. 1–30.

255. L. M. Wilhelmsson, *Q. Rev. Biophys.*, 2010, **43**, 159–183.

256. Y. Fuchi and S. Sasaki, *Org. Lett.*, 2014, **16**, 1760–1763.

257. V. I. Lushchak, *J. Amino Acids*, 2012, **2012**, 736837.

258. A. Heinrichs, *Nat. Cell Biol.*, 2009, **11**, S7.

259. A. Baeyer, *Berichte der Dtsch. Chem. Gesellschaft*, 1871, **4**, 555–558.

260. T. Terai and T. Nagano, *Pflügers Arch. - Eur. J. Physiol.*, 2013, **465**, 347–359.

261. E. Valeur and M. Bradley, *Chem. Soc. Rev.*, 2009, **38**, 606–631.

262. J. Fernández-Carneado, M. Van Gool, V. Martos, S. Castel, P. Prados, J. De Mendoza, and E. Giralt, *J. Am. Chem. Soc.*, 2005, **127**, 869–874.

263. D. W. Brown, *Biochim. Biophys. Acta*, 1960, **44**, 365–367.

264. R. Singh and G. M. Whitesides, *Bioorg. Chem.*, 1994, **22**, 109–115.

265. W. W. Cleland, *Biochemistry*, 1964, **3**, 480–482.

266. J. C. Lukesh, M. J. Palte, and R. T. Raines, *J. Am. Chem. Soc.*, 2012, **134**, 4057–4059.

267. X. Li, D. M. Andrews, and R. Cosstick, *Tetrahedron*, 1992, **48**, 2729–2738.

268. M. D. Ward and J. D. Rimer, 2011, World Patent 2011/062640 A1.

269. J. K. Bentley and J. A. Beavo, *Curr. Opin. Cell Biol.*, 1992, **4**, 223–240.

270. S. S. Stoynov, A. T. Bakalova, S. I. Dimov, A. V Mitkova, and L. B. Dolapchiev, *FEBS Lett.*, 1997, **409**, 151–154.

271. B. Stec, K. M. Holtz, and E. R. Kantrowitz, *J. Mol. Biol.*, 2000, **299**, 1303–1311.

272. S. Nampalli and S. Kumar, *Bioorg. Med. Chem. Lett.*, 2000, **10**, 1677–1679.

273. E. C. Le Ru and P. G. Etchegoin, *Principles of Surface-Enhanced Raman Spectroscopy and Related Plasmonic Effects*, Elsevier, 2008.

274. T. E. Creighton, *Physical and Chemical Basis of Molecular Biology*, Helvetian Press, 2010.

275. A. Clark, in *Water Contamination Emergencies: Can We Cope?*, eds. K. C. Thompson and J. Gray, RSC, 2003, pp. 85–90.

276. L. G. Rodriguez, S. J. Lockett, and G. R. Holtom, *Cytometry*, 2006, **69A**, 779–791.

277. G. McNay, D. Eustace, W. E. Smith, K. Faulds, and D. Graham, *Appl. Spectrosc.*, 2011, **65**, 825–837.

278. G. Herrera, A. Padilla, and S. Hernandez-Rivera, *Nanomaterials*, 2013, **3**, 158–172.

279. E. C. Le Ru and P. G. Etchegoin, *MRS Bull.*, 2013, **38**, 631–640.

280. R. S. Das and Y. K. Agrawal, *Vib. Spectrosc.*, 2011, **57**, 163–176.

281. E. V Efremov, F. Ariese, and C. Gooijer, *Anal. Chim. Acta*, 2008, **606**, 119–134.

282. E. Smith and G. Dent, *Modern Raman Spectroscopy - A Practical Approach*, John Wiley & Sons, Ltd, 2004.

283. D. Cunningham, R. E. Littleford, W. E. Smith, P. J. Lundahl, I. Khan, D. W. McComb, D. Graham, and N. Laforest, *Faraday Discuss.*, 2006, **132**, 135–145.

284. E. Papadopoulou and S. E. J. Bell, *Angew. Chemie (International ed.)*, 2011, **50**, 9058–9061.

285. S. S. R. Dasary, A. K. Singh, D. Senapati, H. Yu, and P. C. Ray, *J. Am. Chem. Soc.*, 2009, **131**, 13806–13812.

286. S. Botti, S. Almaviva, L. Cantarini, A. Palucci, A. Puiu, and A. Rufoloni, *J. Raman Spectrosc.*, 2013, **44**, 463–468.

287. E. Papadopoulou and S. E. J. Bell, *Chem. - A Eur. J.*, 2012, **18**, 5394–5400.

288. M. Hollenstein, *Molecules*, 2012, **17**, 13569–13591.

289. G. M. Cooper, *The Cell: A Molecular Approach*, Sinauer Associates, 2nd edn., 2000.

290. S. D. McCulloch and T. A. Kunkel, *Cell Res.*, 2008, **18**, 148–161.

291. M. E. Arana and T. A. Kunkel, *Semin. Cancer Biol.*, 2010, **20**, 304–311.

292. Y. Nakabeppu, K. Kajitani, K. Sakamoto, H. Yamaguchi, and D. Tsuchimoto, *DNA Repair (Amst).*, 2006, **5**, 761–772.

293. Y. Nakabeppu, S. Oka, Z. Sheng, D. Tsuchimoto, and K. Sakumi, *Mutat. Res.*, 2010, **703**, 51–58.

294. J. G. Moffatt, *Can. J. Chem.*, 1964, **42**, 599–604.

295. J. G. Moffatt and H. G. Khorana, *J. Am. Chem. Soc.*, 1961, **83**, 649–658.

296. A. Lebedev, K. Aoki, E. De Clercq, S. Eriksson, G. H. McGall, J. Y. Feng, W. Abdel-Gawad, A. Johnson, I. Koukhareva, L. Wang, *et al.*, *Nucleoside triphosphates and their analogues*, CRC Press, 2005.

297. M. Yoshikawa, T. Kato, and T. Takenishi, *Tetrahedron Lett.*, 1967, **50**, 5065–5068.

298. K. Burgess and D. Cook, *Chem. Rev.*, 2000, **100**, 2047–2059.

299. J. Ludwig, *Acta Biochim. Biophys. Acad. Sci. Hung.*, 1981, **16**, 131–133.

300. J. E. Marugg, M. Tromp, E. Kuyl-Yeheshiely, G. A. Van der Marel, and J. H. Van Boom, *Tetrahedron Lett.*, 1986, **27**, 2661–2664.

301. J. Ludwig and F. Eckstein, *J. Org. Chem.*, 1989, **54**, 631–635.

302. D. M. Williams and V. H. Harris, in *Organophosphorus Reagents: A Practical Approach in Chemistry*, ed. P. J. Murphy, Oxford University Press, Oxford, 2004, pp. 237–272.

303. T. Ikemoto, A. Haze, H. Hatano, Y. Kitamoto, M. Ishida, and K. Nara, *Chem. Pharm. Bull. (Tokyo).*, 1995, **43**, 210–215.

304. C. Bleasdale, S. B. Ellwood, and B. T. Golding, *J. Chem. Soc. Perkin Trans. 1*, 1990, **3**, 803–805.

305. T. W. Greene and P. G. M. Wuts, *Protective Groups in Organic Synthesis*, Wiley-Interscience, 3rd edn., 1999.

306. E. S. Kryachko and F. Remacle, in *Theoretical Aspects of Chemical Reactivity*, ed. A. Toro-Labbe, Elsevier, 1st edn., 2006, pp. 222–224.

307. H. A. Shuman and T. J. Silhavy, *Nat. Rev. Genet.*, 2003, **4**, 419–431.

308. R. Singh, U. Manjunatha, H. I. M. Boshoff, Y. H. Ha, P. Niyomrattanakit, R. Ledwidge, C. S. Dowd, Y. I. Lee, P. Kim, L. Zhang, *et al.*, *Science (80-.).*, 2008, **322**, 1392–1395.

309. *http://biophysics.idtdna.com/UVSpectrum.html*.

310. A. Matsuda, M. Shinozaki, M. Suzuki, K. Watanabe, and T. Miyasaka, *Synthesis*, 1986, **5**, 385–386.

311. C. Sheu and C. S. Foote, *J. Am. Chem. Soc.*, 1995, **117**, 6439–6442.